UNIVERSIDAD NACIONAL AUTÓNOMA DE MÉXICO
Programa de Posgrado en Ciencias de la Tierra
Instituto de Geofísica

Reconstrucción paleoclimática cuantitativa durante el Cuaternario tardío en el registro del lago de Chalco, México.

T E S I S

que para optar por el grado de

Doctora en Ciencias de la Tierra

presenta

Diana Angélica Avendaño Villeda

Tutor Principal

Dra. Margarita Caballero Miranda Instituto de Geofísica

Comité Tutor

Dra. Socorro Lozano García Instituto de Geología

Dr. Lorenzo Vázquez Selem Instituto de Geografía

Jurado Examinador:

Dra. Elizabeth Solleiro Rebolledo Presidente

Dr. Lorenzo Vázquez Selem Vocal

Dra. Margarita Caballero Miranda Secretario

Dra. Elsa Arellano Torres Suplente

Dra. Claudia Magali Chávez Lara Suplente

Ciudad de México, 9 de abril de 2023.

Agradecimientos institucionales

Al Posgrado en Ciencias de la Tierra de la Universidad Nacional Autónoma de México, por brindarme la oportunidad de aprender a través de un programa con modalidad de doctorado directo.

A todos los miembros administrativos del posgrado en Ciencias de la Tierra por el apoyo en todos los trámites durante mis estudios de posgrado.

Al Consejo Nacional de Ciencia y Tecnología por otorgarme la beca con el número de CVU 854736, que me proveyó económicamente durante mis estudios de posgrado.

Al Programa de Apoyo a Proyectos de investigación e Innovación Tecnológica (PAPIIT) y a la Dirección General de Asuntos del Personal Académico (DGAPA) por el financiamiento para el desarrollo de mi investigación, a través de los proyectos: DGAPA-IV-100215 ‘‘Cambio Climático y Medio Ambiente en la historia del lago de Chalco’’, DGAPA-PAPIIT-IN103819 ‘‘Variabilidad climática y paleoambientes durante la terminación II (130 ka): el paso del penúltimo glacial (MIS 6) al penúltimo interglaciar (MIS 5)’’ y UNAM-PAPIIT 100820 “Registros Interglaciares del Centro de México”.

Al Programa de Apoyo a los Estudios de Posgrado (PAEP) por el financiamiento para participar en diferentes congresos internacionales, que me ayudaron a tener una visión más amplia e integrativa del cambio climático pasado, así como obtener una retroalimentación de los resultados obtenidos de mi trabajo.

A la Dra. Margarita Caballero, directora de tesis quien desde la licenciatura tuve la fortuna de conocer y me adentró al mundo de las diatomeas y los estudios paleoambientales. Le agradezco infinitamente por inspirarme constantemente y ayudarme a desarrollar nuevas ideas que consolidaran mi proyecto de investigación. Muchas gracias por todo el tiempo, paciencia, conocimiento brindado y guía que me ayudaron a ser una mejor estudiante, investigadora y persona. Todo mi respeto, admiración y cariño.

A los miembros del comité tutor, la Dra. Socorro Lozano y el Dr. Lorenzo Vázquez, por los comentarios y sugerencias para mejorar las ideas y las estrategias de mi trabajo científico.

A los miembros del comité de jurado: Dres. Elizabeth Solleiro, Lorenzo Vázquez, Margarita Caballero, Elsa Arellano y Claudia Chávez por ser parte importante en la culminación de mis estudios, gracias por sus observaciones y comentarios.

A las Dras. Gabriela Vázquez, Beatriz Ortega Guerrero y Socorro Lozano por las facilidades brindadas, comentarios y sugerencias en los artículos que colaboramos.

Al Dr. Alexander Correa y el M. en C. Margarito Álvarez por adentrarme al mundo de la estadística.

A las Dras. Cecilia Caballero y Ana María Soler por brindarme su apoyo durante mi trabajo de tesis.

A las chicas del laboratorio: Maripili, Alex, Johana, Wendy, Vianey Guadalupe y Monse con quienes pasé momentos de risas e hicieron más placenteros los largos periodos de trabajo en el microscopio y laboratorio.

A los colegas de los laboratorios: Marco Albarrán, Arnaldo Hérnandez, Alejandro Rosado, el Dr. Jorge Rivas y el Sr. Víctor Macías por las charlas y atenciones que hacían agradable el tiempo en el Instituto de Geofísica.

Agradecimientos a título personal

Gracias a Dios por permitirme vivir esta gran experiencia, porque estos cinco años y medio fueron de aprendizaje en todos los aspectos de mi vida, ayudaron a conocerme y ver de lo que soy capaz. La aplicación y enseñanza del conocimiento serán unas de las formas con las que seguiré desarrollando mi misión en la vida. Dios mío, gracias por enseñarme a disfrutar el viaje y no solo la meta durante este arduo, estresante, meticuloso y maravilloso proyecto de investigación.

A mi querida mamá, María Patricia, quien en todo momento me apoyó y motivó a seguir mis sueños y ser una mujer emprendedora. Gracias por estar siempre estar presente. Todo mi amor, respeto y admiración.

A mi querida hermana, Rocio Nayeli, gracias por escuchar todas mis ideas y teorías locas. Por entenderme y ser mi cómplice durante esos largos días sentadas en el estudio. Todo mi amor, respeto y admiración.

A mi papá, Miguel Ángel, quien siempre me incita a "echarle ganas" a todo lo que me proponga.

A mi abuelita "Conchita", mi segunda mamá quien siempre me escucha y tiene tiempo para mí.

A mi abuelita Ángela, quien me anima y mima en todo momento.

A mi abuelito Rodolfo†, quien siempre me alentó a ser mejor. Sé que desde el cielo esta orgulloso de mí y me echa porras.

A mi tío Luis, mi segundo papá, quien me alienta a su manera tan peculiar.

A todos mis tí@s y prim@s, quienes cerca o lejos están al pendiente de mí, brindándome su cariño.

A Francisco Charqueño, Araceli González y Paco, queridos amigos de la familia, quien siempre me han alentado en todas mis actividades académicas.

A Maripili Ramírez, gracias, querida amiga por los consejos y las experiencias que vivimos juntas en el laboratorio. Sin ti, mi doctorado no hubiera sido lo mismo.

A Rodrigo Martínez, quien a pesar de la distancia, sigue siendo un gran amigo y me incita a continuar en la vida científica.

A mis queridas amigas, Fernanda Rojas y Diana Carrillo, por su cariño constante.

A Kevin David Vázquez, gracias por confiar en mi propósito y siempre escucharme.

Dedicatoria

A mi mamá y mi hermana: Patricia y Rocio

Por ser mis dos grandes pilares y compañeras de aventuras, mi gran equipo.

Contenido

Relación de figuras y tablas

Resumen

La investigación realizada en esta tesis contribuye al estudio de las variaciones climáticas ocurridas durante los últimos 150 mil años en el centro de México. A través del uso de diatomeas tanto modernas como fósiles como indicadores (proxy), fue posible estudiar su distribución ecológica actual y utilizar estos datos para inferir de manera indirecta cambios en el pasado, principalmente de temperatura y evaporación. El trabajo de investigación se desarrolló en tres etapas, divido en cinco artículos científicos (Capítulos II-VI):

1. Análisis de las diatomeas fósiles del registro de Chalco por grupos ecológicos generales. Esta etapa permitió conocer de forma general el cambio de las asociaciones de diatomeas y a partir de un enfoque multiproxy inferir las variaciones climáticas pasadas. Los estudios previos de las diatomeas en el sitio de estudio constituyeron una línea base en el conocimiento de las afinidades ecológicas de algunas de las especies, destacando tres aspectos: i) correlación de la mineralogía magnética con las asociaciones de diatomeas (Capítulo II). ii) Se desarrolló la hipótesis de refugio glacial en el centro de México para la especie *Stephanodiscus niagarae* Ehrenberg (Capítulo III), a partir de analizar su distribución y ecología en el centro de México y en el resto de Norteamérica durante el Pleistoceno tardío y en la actualidad. Dado que en la actualidad se encuentra restringida en lagos de Estados Unidos y Canadá, se concluyó que la presencia de *S. niagarae* en el centro de México es favorecida por bajas temperaturas y ambientes ricos en nutrientes. ii) Se realizó un trabajo taxonómico de dos especies de *Cyclotella* y *Stephanocyclus* que fueron dominantes alternadamente en el registro de Chalco (Capítulo IV). Estas especies incluyen a *Stephanocyclus meneghinianus* (Kützing) Kulikovskiy, Genkal & Kociolek y *S. quillensis* Bailey, previamente reportadas en ambientes modernos y registros fósiles de México, así como dos nuevas especies: *Cyclotella poyeka* y *C. tlalocii* Avendaño & Caballero. Además, se discutió su afinidad ecológica, basada en reportes modernos (para *S. meneghinianus* y *S. quillensis*) y en las asociaciones de diatomeas con las cuales estaban presentes en los sedimentos (para *S. quillensis, C. poyeka* y *C. tlalocii*).
2. Estudio de la distribución ecológica de las especies de diatomeas del centro de México. Se analizó la diversidad y distribución de las asociaciones de diatomeas modernas en 49 muestras de sedimento superficial provenientes de 46 lagos de la Faja Volcánica Transmexicana

(FVTM) (Capítulo V). La FVTM como una zona altamente biodiversa permitió reflejar distintos gradientes ambientales como: salinidad, temperatura, pH, concentración de nutrientes; confirmando el potencial de las diatomeas en las reconstrucciones paleoambientales. Se resalta que la salinidad y la temperatura fueron las principales variables ambientales que controlan la distribución de las especies de diatomeas en la zona a nivel regional y que un grupo de ocho especies son las que tienen la mayor cobertura geográfica en la zona. Es decir, dos de ellas con afinidades hacia ambientes salobres (*Stephanocyclus meneghinianus* y *Nitzschia frustulum (*Kützing) Grunow) y las demás con preferencia por ambientes dulceacuícolas (*Aulacoseira ambigua* (Grunow) Simonsen, *A. granulata* (Ehrenberg) Simonsen, *A. granulata* var. *angustissima* (Müller) Simonsen, *Discostella stelligera* (Cleve & Grunow) Houk & Klee, *Fragilaria crotonensis* Kitton, *Achnanthidium minutissimum* (Kützing) Czarnecki.

3. Análisis paleoclimático de los últimos 150 mil años en el Lago Chalco, centro de México (Capítulo VI). Los datos de diatomeas fueron ordenados mediante un análisis de correspondencia sin tendencia (DCA por sus siglas en inglés) para explorar los cambios ecológicos de las asociaciones de diatomeas durante el penúltimo y último máximo glacial (Estadios Isotópicos (EI) 6 y 2), el último y presente interglacial (EI5e, EI1) así como la última glaciación. A partir del conocimiento de la ecología de las diatomeas (etapa 2), así como de otros estudios previos, se observaron cambios en las asociaciones de diatomeas a escala orbital y milenaria. Se concluyó a escala orbital, que los conjuntos de agua dulce: *Stephanodiscus* spp. – pequeñas Fragilariaceae spp. – *Cocconeis placentula* involucraron cambios durante los intervalos más fríos (final EI6, EI5d, EI2). Mientras que los taxones tolerantes a la concentración de sales son dominados por *Cyclotella* spp., en condiciones de mayor evaporación (EI5e, EI5c-a, EI4, EI3, principios del EI1). Por otro lado, las fluctuaciones climáticas a escala milenaria se identificaron como picos en agua dulce (principalmente por pequeñas Fragilariaecae spp.) o como picos en especies tolerantes a la concentración de sales.

Abstract

This thesis contributes to central Mexico's climatic fluctuations research over the last 150 thousand years. Using modern and fossil diatoms as a proxy, it was possible to study their current ecological distribution and use this information to infer past changes in temperature and evaporation. This study was developed in three stages, divided in five journal papers (Chapter II-VI):

1. Analysis of the fossil diatoms by studying the general ecological groups of modern species at Lake Chalco (Chapter II). This stage allowed use to know the main change in diatom assemblages. Based on the multiproxy approach, it was then possible to infer past climatic changes. Previous studies in diatoms on the study site helped to establish a baseline of the knowledge of the ecological affinities of the principal species, emphasizing three aspects: i) Relation of the magnetic mineralogy with diatom assemblages. ii) Developing the hypothesis of the glacial refugia in central Mexico for the freshwater diatom *Stephanodiscus niagarae* Ehrenberg (Chapter III), based on its distribution and ecology in central Mexico and the rest of North America during the Late Pleistocene and the present. Due to this species is dominant in lakes from the United States and Canada, it was concluded that *Stephanodiscus niagarae* in central Mexico is favoured by cold temperatures and high nutrients. ii) A taxonomic study of four species of *Stephanocyclus* and *Cyclotella* that were alternately dominant in the Chalco record (Chapter IV). The former species including *Stephanocyclus meneghinianus* (Kützing) Kulikovskiy, Genkal & Kociolek and *S. quillensis* Bailey, have been previously reported in modern and fossil records of Mexico, besides two new species: *Cyclotella poyeka* and *C. tlalocii* Avendaño & Caballero. Moreover, the ecological affinities are based on the modern distribution (for *S. meneghinianus* and *S. quillensis*) and the species' ecology coincident with the fossil assemblages (for *S. quillensis*, *C. poyeka* and *C. tlalocii*).
2. Studying the ecological distribution of the diatom species in central Mexico. Analysing the diversity and distribution of modern diatom assemblages in 49 surface sediment samples of 46 lakes of the Trans-Mexican Volcanic Belt (TMVB) (Chapter V). The TMVB, a zone with high biodiversity, allows different environmental gradients such as salinity, temperature, pH, and trophic level, confirming the potential of diatoms in paleoenvironmental reconstructions. It is highlighted that salinity and temperature were the main environmental variables controlling the distribution of diatom species in this region on a regional scale. Also, a group of eight

species had the most significant regional occupancy, two were associated with high salinity conditions (*Stephanocyclus meneghinianus* y *Nitzschia frustulum (*Kützing) Grunow) and the rest with freshwater environments (*Aulacoseira ambigua* (Grunow) Simonsen, *A. granulata* (Ehrenberg) Simonsen, *A. granulata* var. *angustissima* (Müller) Simonsen, *Discostella stelligera* (Cleve & Grunow) Houk & Klee, *Fragilaria crotonensis* Kitton, *Achnanthidium minutissimum* (Kützing) Czarnecki).

3. Paleoclimatic analysis over the last 150 thousand years in Lake Chalco, central Mexico (Chapter VI). A detrended correspondence analysis with the relative abundance of diatoms was performed to estimate changes in ecological assemblages during the penultimate and last glacial maximum (Marine Isotope Stage (MIS) 6 and 2), the last and present interglacial (MIS5e and MIS1) along with the last glaciation. Based on the diatom current ecological information (step 2) and other bibliographic references, changes in the diatom assemblages were observed to orbital and millennial scales. It was concluded that at the orbital scale freshwater assemblages: *Stephanodiscus* spp. – small Fragilariaceae spp. – *Cocconeis placentula* involved changes during cool intervals (late MIS6, MIS5d, MIS2) while salt-tolerant taxa, dominated by *Stephanocyclus* and *Cyclotella* spp., in high evaporation periods (MIS5e, MIS5c-a, MIS4, MIS3, early MIS1). On the other hand, millennial-scale climatic fluctuations were identified as peaks in freshwater (mostly from the presence of small Fragilariaceae spp.) or as peaks in salt-tolerant species.

Capítulo I

1. Introducción

1.1 Variabilidad climática del Cuaternario

El clima ha fluctuado a lo largo del tiempo en distintas escalas, en el orden de décadas hasta millones de años. A partir de los diferentes tipos de registros naturales ha sido posible conocer las fluctuaciones climáticas pasadas y proponer perspectivas para entender los forzamientos asociados con las respuestas del clima. Durante el Cuaternario (últimos 2.58 Ma) se han observado oscilaciones cíclicas en las que se desarrollan extensos glaciares (glaciaciones), que culminan con episodios cálidos (interglaciales) en los cuales el nivel del mar aumenta como consecuencia de una disminución en la extensión de los casquetes de hielo (Imbrie et al. 1984, Berger et al. 2016).

Las glaciaciones cuaternarias han tenido una periodicidad de aproximadamente 100 ka durante los últimos 800 ka (Lisiecki & Raymo 2005, Köhler et al. 2010). Estos ciclos están asociados con forzamientos continuos sobre la órbita de la Tierra, influenciados por la Luna, el Sol y otros planetas, denominados ciclos de *Milankovitch* (variaciones orbitales). Estos ciclos involucran cambios en tres parámetros de la órbita terrestre, la excentricidad (cambio en la elongación de órbita de la Tierra), oblicuidad (cambio del ángulo de inclinación del eje terrestre con respecto a la eclíptica) y precesión (cambio de la posición del eje de rotación de la Tierra, que no siempre señala a un mismo punto estelar) (Milankovitch 1941, Imbrie et al. 1984). Estos tres ciclos alteran la distribución latitudinal y estacional de la insolación sobre la superficie terrestre (Davis & Brewer 2009, Berger et al. 2012). Los parámetros orbitales no actúan por si solos, sino que involucran mecanismos de retroalimentación que provocan un ajuste de las interacciones océano-atmósfera (Hansen y Sato, 2012, Köhler et al. 2010).

Los ciclos glaciales se han identificado globalmente a partir del registro de isótopos de oxígeno (^{18}O, ^{16}O) en largas secuencias marinas y núcleos de hielo. Los cambios en la composición isotópica del oxígeno en los océanos reflejan un cambio en el volumen de hielo almacenado en los continentes (Emiliani 1955, Berger et al. 2016). Su funcionamiento consiste en la diferencia de la relación evaporación/condensación entre los dos isótopos, siendo el ^{16}O quien tiene una mayor facilidad de evaporarse, mientras que el ^{18}O tiene una mayor facilidad de condensarse y precipitar (Tiwari et al. 2015). Por ejemplo, durante una etapa fría como consecuencia de la disminución de la temperatura se forman glaciares de montaña y extensos casquetes de hielo, por lo que el nivel del mar disminuye debido a que el agua se encuentra retenida en los continentes. La facilidad de precipitar del isótopo pesado (^{18}O) ocasiona una diferencia en las proporciones entre los isótopos del oxígeno ($^{18}O/^{16}O$) en el hielo (enriquecido en isotopo ligero) y el océano (enriquecido en el isótopo pesado). Por el contrario, durante una etapa cálida al reestablecerse el ciclo del agua, la concentración del ^{16}O aumenta en el océano.

Los cambios en la relación $^{18}O/^{16}O$ se definen mediante la notación $\delta^{18}O$ ($\delta = \left[\left({}^{18}O/{}^{16}O_{muestra}/{}^{18}O/{}^{16}O_{estandar}\right) - 1\right] * 10^3$) y las variaciones en este parámetro han permitido identificar fases o estadios isotópicos (EI) con condiciones contrastantes en el clima global. Los estadios con número par corresponden con eventos fríos (glaciales), mientras que los números impares corresponden con eventos cálidos (interglaciales) (Fig. 1a). La delimitación temporal de los EI depende de la resolución temporal con que se logren apreciar las variaciones del $\delta^{18}O$, los estadios se pueden subdividir en subestadios, variaciones climáticas de menor intensidad y duración dentro del mismo estadio, que se identifican con letras en orden alfabético (Shackleton y Opdyke 1973). Un ejemplo es el EI5, subdividido por Shackleton (1969) en cinco subestadios (5a-5e) (Fig. 1). Además, los momentos en que se observa un máximo cambio en el $\delta^{18}O$ se conocen como terminaciones (Fig. 1), los cuales marcan la transición de un periodo glacial a un interglacial. Por ejemplo, la Terminación I (TI) marca el final del E2 (18-11.7 ka), mientras que la Terminación II ocurrió al final del EI6 (135 – 130 ka) (Raymo 1997, Stern & Lisiecki 2014, Lisiecki & Stern 2016, Barker & Knorr 2021).

Es importante distinguir la diferencia entre el término interglacial e interestadial, ya que involucra un contexto climático distinto. El interglacial representa a los episodios de clima cálido que reflejan un gran contraste respecto a la extensión de los glaciares, donde la extensión de hielo en los hemisferios norte y sur es mínima, como es el caso del EI5e o último interglacial. Mientras que los interestadios están asociados a condiciones templadas a frías dentro de la glaciación, donde hay un exceso de hielo en el hemisferio norte fuera de Groenlandia. Los interestadios reflejan avances secundarios (EI4, subestadios 5d, 5b) o recesiones (EI3, subestadios 5c, 5a) dentro del ciclo glacial (Berger et al. 2016). Considerando la distinción entre interestadial e interglacial, la última glaciación engloba los subestadios 5d, 5c, 5b, 5a, así como los estadios isotópicos 4, 3 y 2 (EI5d-2) (Fischer et al. 1999, Lisiecki & Raymo 2005, Vázquez Riveiros et al. 2022).

Además de las variaciones a escala orbital, otro tipo de oscilaciones climáticas que se han observado en la señal del $\delta^{18}O$ de registros de hielo en Groenlandia (Fig. 1b) son los ciclos Dansgaard-Oeschger (DO), enfriamientos y calentamientos rápidos en escalas de tiempo milenarias (Dansgaard et al. 1984), esto es, de menor duración que los ciclos glaciales. Asimismo se han observado eventos de enfriamiento intensos entre los D/O que coinciden con capas de detritos glaciales en secuencias marinas al norte del océano Atlántico identificados como eventos Heinrich (HS) (Heinrich 1988) (Fig. 1b). Los eventos milenarios están asociados con una inestabilidad de la circulación oceánica y atmosférica en altas y bajas latitudes generando una variabilidad climática global tanto en registros marinos como terrestres (Harrison & Sanchez Goñi 2010, Sanchez Goñi & Harrison 2010).

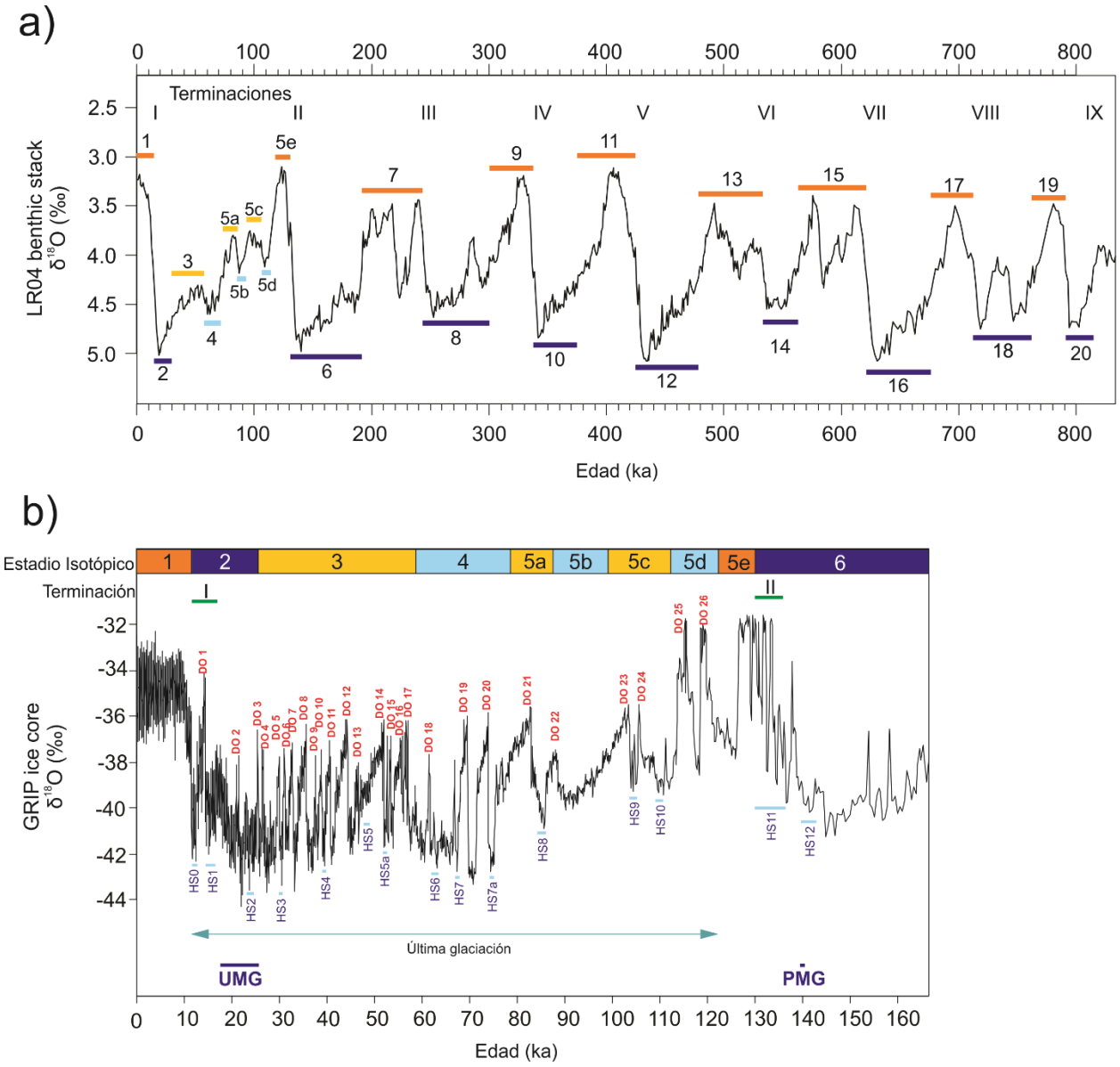

Fig. 1 Variabilidad climática durante los últimos 800 ka. a) Ciclos glaciales-interglaciales. Periodos glaciales (color azul marino), periodos interglaciales (color naranja), interestadiales (color azul claro y amarillo). b) Eventos milenarios durante la última glaciación. Eventos Henrich (HS, color azul) y eventos Dansgaard-Oescher (DO, color rojo). Datos obtenidos de Lisiecki & Raymo (2005) y Johnsen et al. (1997). UMG = último máximo glacial, PMG = penúltimo máximo glacial.

1.2 Planteamiento del problema

Los sedimentos de los lagos, como un tipo de registro natural continuo, permiten conocer las fluctuaciones climáticas pasadas con un alcance temporal desde decenas a millones de años. En México, las secuencias incluyen desde la última glaciación por ejemplo el lago de Pátzcuaro, Michoacán de 48 ka AP (Bradbury 2000), Tecocomulco, Hidalgo de 50 ka (Caballero et al. 1999), Zacapu, Michoacán de 52 ka (Ortega et al. 2002), Babícora, Chihuahua de 65 ka (Metcalfe et al. 2002), Laguna Seca de San Felipe, Baja California de 70 ka (Ortega-Guerrero et al. 1999), Cuitzeo, Michoacán de 120 ka (Israde-Alcántara et al. 2002, 2010), Xochimilco, Ciudad de México *ca.* 18 ka (Ortega-Guerrero *et al.*, 2018). La mayoría de estos trabajos son cualitativos, y tratan de revelar las condiciones del clima determinando de una manera general algunas de las variables climáticas, sin embargo, solo se puede indicar sí las condiciones eran cálidas o frías, húmedas o secas. En cambio, los modelos numéricos como promedios ponderados, análogos modernos, modelos lineares y aditivos generalizados, etcétera, se han usado para reconstruir distintas variables ambientales (estado trófico, pH, salinidad, temperatura, precipitación) del pasado dando un valor numérico estimado con buena precisión (Caballero-Rodríguez & Correa-Metrio 2017, Birks 2012).

A partir de utilizar a las diatomeas como paleoindicadores, con modelos numéricos basados en la ecología moderna de los organismos y las condiciones actuales de los sitios, se reconstruyeron de forma semicuantitativa distintas variables ambientales del lago de Chalco (pH, salinidad) y su entorno (temperatura, precipitación) para lograr una mejor resolución de las condiciones climáticas a lo largo de los distintos cambios que se registraron durante los últimos *ca.*150 ka (los primeros 122.5 m de profundidad de la secuencia sedimentaria en Chalco). Como se ha mencionado en secciones anteriores, ya se cuenta con una gran variedad de hallazgos paleoclimáticos de la secuencia maestra CHA08 (Ortega-Guerrero et al. 2017). El presente trabajo de tesis forma parte de esta secuencia maestra. No obstante, además de los estudios previos, el registro de diatomeas que se desarrolló en este trabajo permitió detallar las fluctuaciones climáticas a escala orbital y escala milenaria. Además, el desarrollo de modelos matemáticos proporcionó información de los cambios en el nivel del lago y la salinidad, los cuales están indirectamente asociados con variables climáticas como la temperatura y el balance de evaporación/precipitación.

1.3 Objetivos y premisas de la investigación

Objetivo general:

Este trabajo busca ofrecer información sobre la respuesta de las especies de diatomeas a las variaciones climáticas contrastantes de los ciclos glaciales-interglaciales, analizando el recambio ecológico de las diatomeas durante las fluctuaciones climáticas ocurridas en los últimos *ca.* 150 ka, un intervalo que abarca desde el EI6 hasta el EI1.

Para alcanzar esta meta, la tesis se dividió en tres partes que obedecieron a los siguientes objetivos particulares, además en algunas de las etapas se plantean premisas que ayudaron a establecer un marco de referencia general para la presente investigación. Los cinco artículos presentados en esta tesis contribuyen para conseguir cada objetivo particular.

Primera parte: Establecer un marco paleoclimático de la secuencia de Chalco a través de la mineralogía magnética y de documentar la diversidad taxonómica de las diatomeas.

Objetivos particulares:

→ Relacionar las principales asociaciones de diatomeas a parámetros geoquímicos del registro de Chalco, permitiendo una reconstrucción más clara y objetiva de los cambios ambientales y climáticos en la Cuenca de México. Este objetivo se cumplió en los Capítulo II, artículo Ortega-Guerrero et al. (2020).

→ Documentar la diversidad taxonómica del registro de diatomeas de los últimos 150 ka del lago de Chalco, identificando la existencia de taxones hoy extintos en la zona y la presencia de comunidades no análogas. Este objetivo se cumplió en los capítulos III y IV (Avendaño et al. 2021, 2022). Para lograr esta meta, se plantearon las siguientes premisas.

Premisas:

- Durante las glaciaciones del Cuaternario se han observado desplazamientos latitudinales de diferentes especies de plantas, insectos y mamíferos del Pleistoceno que han migrado al sur por medio de corredores biológicos (Jackson et al. 2000, Waltari et al. 2007, Ceballos et al. 2010, Pardi & Graham 2019) entre el sur de Estados Unidos hacia climas adecuados en el centro de México. Reportes modernos de la especie *Stephanodiscus niagarae* sitúan su distribución al norte de Estados Unidos y sur de Canadá, mientras que los registros paleoambientales del Cuaternario tardío indican que esta especie tuvo una amplia distribución en lagos del centro de México (Valadez et al. 2005). Por lo que se sugiere que

el centro de México fue un refugio para *Stephanodiscus niagarae* durante los periodos glaciales pasados.
Este supuesto se comprobó en el capítulo III, a través del artículo Avendaño et al. (2021).

- Debido a los contrastantes cambios climáticos glaciales-interglaciales durante el Cuaternario, se ha observado la existencia de climas no análogos a los modernos, por lo tanto, también la presencia de comunidades no análogas (Graham 2005, Williams & Jackson 2007, Keith et al. 2009). En diferentes registros se ha observado la evolución de diferentes especies de diatomeas (Khursevich et al. 2001, Paillès et al. 2020), por lo que en el registro de Chalco se espera encontrar comunidades no análogas durante los momentos de más intensa variabilidad ambiental, como en el EI5.
  Esta proposición se comprobó en el capítulo IV, a través del artículo Avendaño & Caballero (2022).

Segunda parte: Analizar la distribución ecológica de las especies de diatomeas del centro de México.

Objetivo particular:

→ Ampliar el conocimiento sobre la distribución ecológica de las especies de diatomeas en lagos modernos del centro de México, caracterizando a la distribución de las especies a lo largo de los principales gradientes ambientales. Se empleará la técnica de promedios ponderados para establecer los óptimos de la distribución de las especies de diatomeas respecto a las diferentes variables ambientales (salinidad, pH, temperatura, nutrientes). Este objetivo particular se cumplió en el capítulo V, artículo Avendaño et al. (2023a).

Tercera parte: Integrar con una visión multiproxy el registro fósil de diatomeas para obtener una reconstrucción de la dinámica climática de los últimos 150 ka en el lago de Chalco.

Objetivo particular:

→ Realizar una correlación del registro de diatomeas de la secuencia CHA08 (este estudio) con los datos de diatomeas ya publicados del núcleo ChaB (Caballero & Ortega Guerrero 1998, Caballero et al. 2019) (40-5 ka cal AP, EI3-EI1), permitiendo la comparación de los dos últimos interglaciales (EI5e vs. EI1) y los dos últimos máximos glaciales (UMG vs PMG). Este objetivo se cumplió en el capítulo V, en el artículo Avendaño et al. (2023b). Para lograr este objetivo particular, se plantearon las siguientes premisas.

Premisas:

- En estudios previos del lago de Chalco (Caballero & Ortega Guerrero 1998, Ortega-Guerrero et al. 2017, Avendaño-Villeda et al. 2018, Caballero et al. 2019) se ha observado que durante los episodios de enfriamiento del EI 2 y EI 6 las condiciones del lago fueron de agua dulce, mientras que durante el periodo de calentamiento a principios del EI 1 y EI 5 las condiciones del lago presentaron un nivel bajo y salobre, por lo que se espera que condiciones similares se registren en el resto de la secuencia de Chalco, identificando como eventos agua dulce a los periodos más fríos (por ejemplo el EI 4) y como eventos someros y salobres durante los intervalos más cálidos (por ejemplo el EI 3).

- Existe una gran controversia en cuanto a la intensidad de los dos últimos máximos glaciales. Masson-Delmonte et al. (2010) indican que hubo un mayor enfriamiento durante EI2 comparado con el EI6 en registros de la Antártida, aunque estos autores también sugieren que el cambio del nivel del mar en ambos periodos puede ser comparable. Por lo que se espera que a partir de las asociaciones de diatomeas presentes durante los EI6 y EI2 permitan indicar si estos periodos glaciales son o no análogos.

- El último interglacial (EI5e) se reconoce como el último periodo más cálido que ha tenido el planeta (Anderson et al. 2006, Masson-Delmotte et al. 2010), con estimaciones de temperatura que sugieren entre 1 a 2º C más que en la actualidad en los trópicos (Cárdenes-Sandí et al. 2019). Por lo que se espera que a partir de las asociaciones de diatomeas presentes durante los EI5e y EI1 permitan indicar una diferencia climática entre ambos interglaciales.

  Estas premisas se desarrollaron en el capítulo IV, a través del artículo Avendaño & Caballero (2022).

A continuación, se presenta una breve recopilación de la historia ambiental del planeta durante los últimos 150 ka. Además, se ofrece una descripción del clima actual en México y un resumen de diferentes trabajos paleoclimáticos del país que abarcan desde finales del EI6 a principios del EI1, incluyendo al sitio de estudio.

1.4 Historia ambiental del planeta de los últimos 150 ka.

Los últimos 150 ka corresponden con los primeros seis estadios isotópicos, que incluyen los dos últimos periodos fríos que ha tenido el planeta: el penúltimo máximo glacial (PMG ≈ 140 ka, al final del EI6) y el último máximo glacial (UMG ≈ 21 ka A. P., durante el EI2), así como los últimos dos periodos cálidos: el último interglacial (EI5e = 130-116 ka) y el presente interglacial (11.7-0 ka) (Shackleton et al. 2003, Lisiecki & Stern 2016).

El EI5e es reconocido a nivel mundial como el periodo más cálido de los últimos 800 ka (Anderson et al. 2006, Masson-Delmotte et al. 2010, Turney & Jones 2010). Durante este periodo los casquetes de hielo de la Antártida y Groenlandia fueron mínimos y el nivel del mar alcanzó 4 a 9 m por arriba del nivel actual (Blanchon et al. 2009, Dutton & Lambeck 2012, Aburto-Oropeza et al. 2021). Además, las estimaciones de temperatura también sugieren valores por arriba del actual, siendo 2-5º C mayores al actual en latitudes altas y medias del hemisferio Norte (Anderson et al. 2006) y 1-2º C en los trópicos (Cárdenes-Sandí et al. 2019).

Sin embargo, hay una gran controversia en cuanto a la intensidad de los dos últimos máximos glaciales. Masson-Delmonte et al. (2010) indican que hubo un mayor enfriamiento durante EI2 comparado con el EI6 en registros de la Antártida, aunque estos autores también sugieren que el cambio del nivel del mar en ambos periodos puede ser comparable. En el PMG, las reconstrucciones del nivel del mar sugieren una disminución de 92 m en latitudes medias (Rabineau et al. 2006) y un descenso de 130 m en los trópicos (Chappell & Shackleton 1986). Mientras que en el UMG, los cambios del nivel del mar sugieren una disminución de 107 m en latitudes medias (Rabineau et al. 2006) y un descenso 130-140 m en los trópicos (Lambeck & Chappell 2001). A pesar de que el cambio en el nivel del mar puede ser comparable durante ambos máximos glaciales, la evidencia geológica y las simulaciones de los casquetes de hielo sugieren una diferente configuración, lo cual pudo haber sido ocasionado por un diferente clima durante ambos máximos glaciales (Svendsen et al. 2004, Obrochta et al. 2014, Colleoni et al. 2016).

La última glaciación se caracteriza globalmente por haber tenido dos máximas extensiones de hielo durante el EI4 y el EI2. Si bien el inicio del último ciclo glacial (subestadios 5d-5a) tuvo un gran avance, este no fue global ya que únicamente tuvo una expansión máxima en los glaciares del hemisferio norte; como son los glaciares de Asia, norte de Europa y partes del oeste de EU (Hughes et al. 2013). También en algunas áreas los glaciares se expandieron durante el interestadial

EI3, debido al incremento de la humedad. Este es el caso de Sudamérica, Tasmania y los Alpes del sur de Nueva Zelanda (Hughes et al. 2013, Palacios et al. 2020). Los glaciares de Norteamérica, incluyendo México, tuvieron su máximo avance hacia el final del UMG en el EI2, con fluctuaciones regionales debido a las diferencias de precipitación causadas por efectos de orogenia, como es el caso de las montañas del centro de México (Caballero et al. 2010, Vázquez-Selem & Heine 2011, Palacios et al. 2020). Dentro del último ciclo glacial, se han observado 26 eventos DO de enfriamiento y calentamiento (Rasmussen et al. 2014) con una duración aproximada de 500-4000 años, mientras que se tienen registrados 10 HE, enfriamientos intensos con un periodo de recurrencia de 7000 años (Lisiecki & Stern 2016) (Rashid et al., 2003, Heimming 2004, Lisiecki and Stern, 2016) (Fig. 1b).

1.5 Clima actual en México

En la zona norte del país domina el clima seco con variaciones de temperatura desde cálido hasta semifrío, en la zona sur domina el clima cálido a semicálido, húmedo a subhúmedo, mientras que en la zona centro del país domina el clima templado con variantes de semicálido hasta semifrío y por su régimen de lluvias de húmedo a subhúmedo. Los climas fríos se encuentran restringidos a áreas en el país que tienen altitudes mayores a los 4,000 msnm.

Por su posición geográfica, el trópico de Cáncer divide al país en la zona subtropical para la parte norte y la zona tropical para la parte sur. El clima del país depende de los cambios en la posición de la Zona de Convergencia Intertropical (ZCIT) así como de las celdas subtropicales de alta presión (Bermuda-Azores) y los sistemas de baja presión del oeste de latitudes medias (Fig. 2).

Cuando la ZCIT se encuentra en su posición más al norte, en verano, domina un flujo de humedad transportado por los vientos alisios (Fig. 2a). La intensificación de los vientos alisios proporciona un flujo de vapor de agua proveniente del Atlántico tropical hacia la cuenca del Caribe que provee de humedad al Golfo de México durante los meses de mayo a septiembre, conocido como la Corriente de chorro de bajo nivel del Caribe (García-Martínez y Bollasina 2020, Cook & Vizy. 2010). Este estado del tiempo se caracteriza por un periodo de sequía entre los meses de julio y agosto que causa un ciclo bimodal de la precipitación conocido como "canícula" o "midsummer drought" (Magaña et al. 1999). Mientras que en la zona noroeste de México hay un transporte de masas de aire húmedo desde el Pacífico tropical y Golfo de California hacia la Sierra Madre Occidental provocando lluvias en los meses de julio, agosto y septiembre, este sistema atmosférico es conocido como el monzón de Norteamérica (Fig. 2a) (Barlow et al. 1997, Gochis et al. 2005).

Sin embargo, cuando la ZCIT se encuentra al sur (Fig. 2b), en invierno, hay un descenso de la temperatura debido a las masas de aire polar en la zona centro y la vertiente del Golfo de

México. Además, las celdas de alta presión dominan ocasionando condiciones secas, siendo los frentes fríos que vienen del norte la principal fuente de humedad (Fig. 2b). La corriente de chorro de bajo nivel del Caribe durante los meses de octubre a abril abastece de lluvias principalmente a América central ocasionando un periodo mínimo de precipitación al sureste del país (García-Martínez y Bollasina 2020, Cook & Vizy 2010). Al noreste del país el invierno es seco ya que en el sistema monzónico la precipitación ocurre principalmente en el océano (Yim et al. 2014).

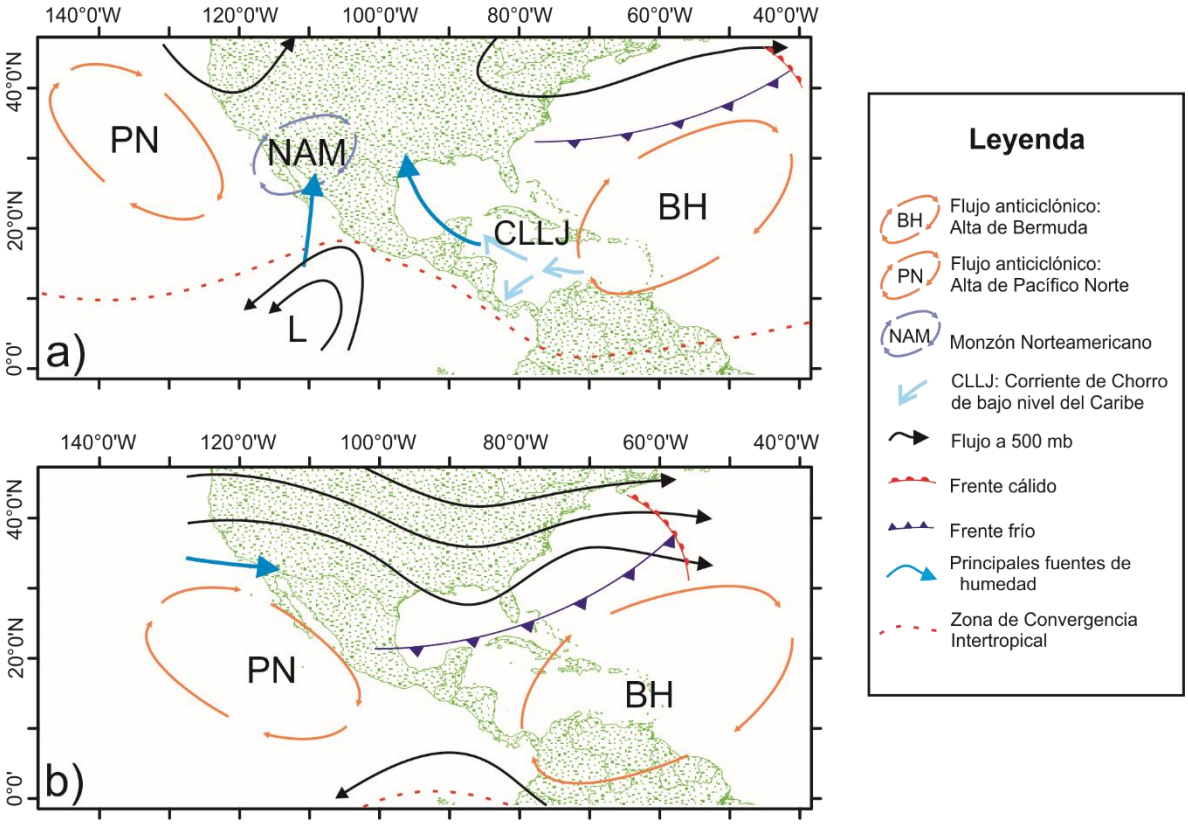

Fig. 2 Modelo climático de los principales fenómenos atmosféricos que controlan el clima actual de México. a) Durante el verano b) durante el invierno. Figura modificada a partir de Metcalfe et al. 2015, 2000 y Oster et al. 2019.

1.6 Revisión de registros paleoclimáticos durante los últimos 150 ka en México

En México se cuenta con diferentes tipos de registros naturales (Fig. 3) que permiten realizar estudios paleoambientales como registros glaciares, paleosuelos, lacustres, marinos, análisis de corales, etc., abarcando cada uno de los registros diferente temporalidad (Fig. 4). Para simplificar la revisión de los registros paleoclimáticos de México se agruparon por ventanas temporales a

partir de los estadios isotópicos. En la Tabla 1 se enlistan los trabajos paleoclimáticos realizados a partir de diferentes registros.

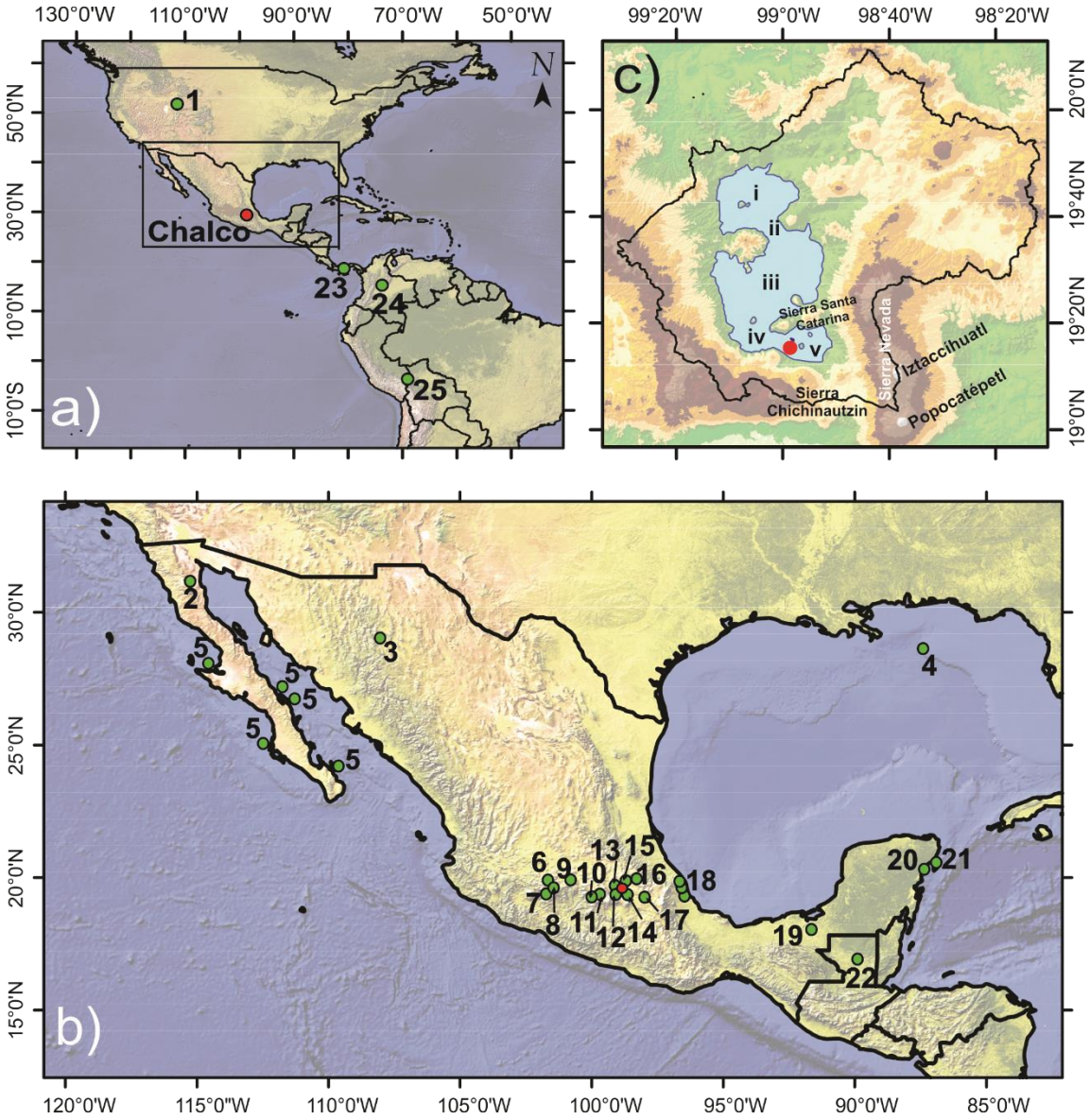

Fig. 3 Localización de los registros paleoclimáticos de México de los últimos 150 ka, así como registros de Norte y Sudamérica con los que se comparará el registro de Chalco: a) sitios del continente americano, b) sitios de México, c) ubicación del sitio de estudio (núcleo CHA08) y extensión máxima del área de los lagos del centro de México: (i) Zumpango, (ii) Xaltopan, (iii) Texcoco, (iv) Xochimilco, (v) Chalco. El círculo rojo indica el sitio de estudio. Los nombres de los sitios se encuentran en la Tabla 1 y en la figura 4.

Tabla 1. Temporalidad de los registros paleoclimáticos en México y otros registros del continente americano con los que se comparó el presente trabajo.

	Ubicación	Tipo de registro	Temporalidad	Referencia
1.	Lago Bear, EUA^{+}	Polen	EI6-EI1 (225 – 0 ka)	Jiménez-Moreno et al. (2007)
2.	Cuenca de San Felipe, Baja California Norte, parte de la provincia del desierto de Sonora	Estratigrafía, diatomeas, propiedades magnéticas	EI4-EI1 (70 – 4 ka)	Ortega-Guerrero et al. (1999) Roy et al. (2010)
3.	Lago Babícora, Chihuahua	Diatomeas	EI4-EI (65 –0 ka)	Metcalfe et al. (2002) Roy et al. (2013)
4.	Golfo de México	Geoquímica, e isótopos de oxígeno en foraminíferos	EI8-EI1 (300 – 0 ka)	Ziegler et al. (2008)
5.	Golfo de Baja California Sur	Corales	EI5e (~136 – 115 ka)	Muhs et al. (2002)
6.	Lago de Zacapu, Michoacán	Diatomeas Mineralogía magnética, susceptibilidad magnética, carbono orgánico.	EI3-EI1 (52 – 4.7 ^{14}C ka.)	(Metcalfe 1992) (Ortega-Guerrero et al. 2002)
7.	Lago de Zirahuén, Michoacán	Diatomeas, mineralogía magnética, susceptibilidad magnética, geoquímica, carbono orgánico, polen.	EI2 – 1 (17 – 0 ka)	(Ortega-Guerrero et al. 2010)
8.	Lago Pátzcuaro, Michoacán	Diatomeas	EI3-EI1 (48 –0 ka)	Bradbury (2000)
9.	Lago de Cuitzeo, Michoacán	Diatomeas y polen	EI5-EI1 (*ca.* 120? – 0 ka)	Israde-Alcántara et al. (2002, 2010)
10.	Nevado de Toluca, Estado de México	Paleosuelos	EI3-EI1 (42 – 3.5 ka)	Sedov et al. (2001)
11.	Lago Chignahuapan, Cuenca alta del Lerma, Estado de México	Diatomeas, propiedades magnéticas	EI2-EI1 (22 – 0.87 ka)	Caballero et al. (2002)
12.	Xochimilco, Cuenca de México	Diatomeas, estratigrafía, parámetros magnéticos, geoquímica	EI2 – 1 (18 – 5 ka)	(Ortega-Guerrero et al. 2022)
13.	Texcoco, Cuenca de México	Diatomeas	EI5-EI1 (~100 ka)	Bradbury (1971)
14.	Volcán Iztaccíhuatl	Registro glaciar	EI6–EI1	Vázquez-Selem & Heine (2011)
15.	Valle de Teotihuacán, Estado de México	Paleosuelos	EI3 -EI1 (24 – 2.9 ka)	Solleiro-Rebolledo et al. (2006, 2011)
16.	Lago Tecocomulco, Hidalgo, al noreste de la Cuenca de México	Estratigrafía, diatomeas, propiedades magnéticas, polen	EI3-EI1 (50–3 ka)	Caballero et al. (1999)
17.	Localidades de Tlalpan y Mamut, Tlaxcala	Paleosuelos	EI3-EI1 (38.2 – 1.3 ^{14}C ka)	Sedov et al. (2009)

18. La Mancha, Palma Sola y Punta Delgada, Veracruz	Paleosuelos y evolución del paisaje de dunas	EI5c-EI1 (91 ka – 600 a)	Solleiro-Rebolledo et al. (2022)
19. Rio de San Pedro, Tabasco	Manglares relictos	EI5 (~130 – 120 ka)	Aburto-Oropeza et al. (2021)
20. Xcaret, Península de Yucatán	Arrecife de coral fósiles	EI5 (~ 121 ka)	Blanchon et al. (2009)
21. Costa de Yucatán y la isla de Cozumel	Concreciones carbonatadas pedogénicas (calcretas)	EI6 (164 – 134 ka) EI5, estadios 5e-c (123 – 98 ka)	Valera-Fernández et al. (2020b, 2020a)
22. Petén-Itzá, Guatemala*	Polen Ostrácodos	EI7–EI1	Cruz Silva (2018), Hodell et al. (2008) (Correa-Metrio et al. 2012) Pérez et al. (2021)
23. El Valle Caldera, Panamá$^{+}$	Polen, diatomeas	EI5e (135 – 100 ka) EI5, EI2 (137 – 85 ka and 30 – 15ka)	Cárdenes-Sandí et al. (2019) Shadik et al. (2017)
24. Lago Fúquene, Colombia^{+}	Polen	EI8-EI1 (284 – 0 ka)	Groot et al. (2011)
25. Lago Titicaca, Perú/Bolivia^{+}	Diatomeas	EI9-EI1 (370 – 0 ka)	Fritz et al. (2007, 2012)

*El registro de polen del lago Petén-Itzá en Guatemala se consideró dentro de los registros para México, ya que forma parte de la provincia biogeográfica de la Península de Yucatán (Ferrusquía-Villafranca 1993), brindando información de las variaciones climáticas para el sureste de México. Los registros fuera de México se marcan con $^{+}$.

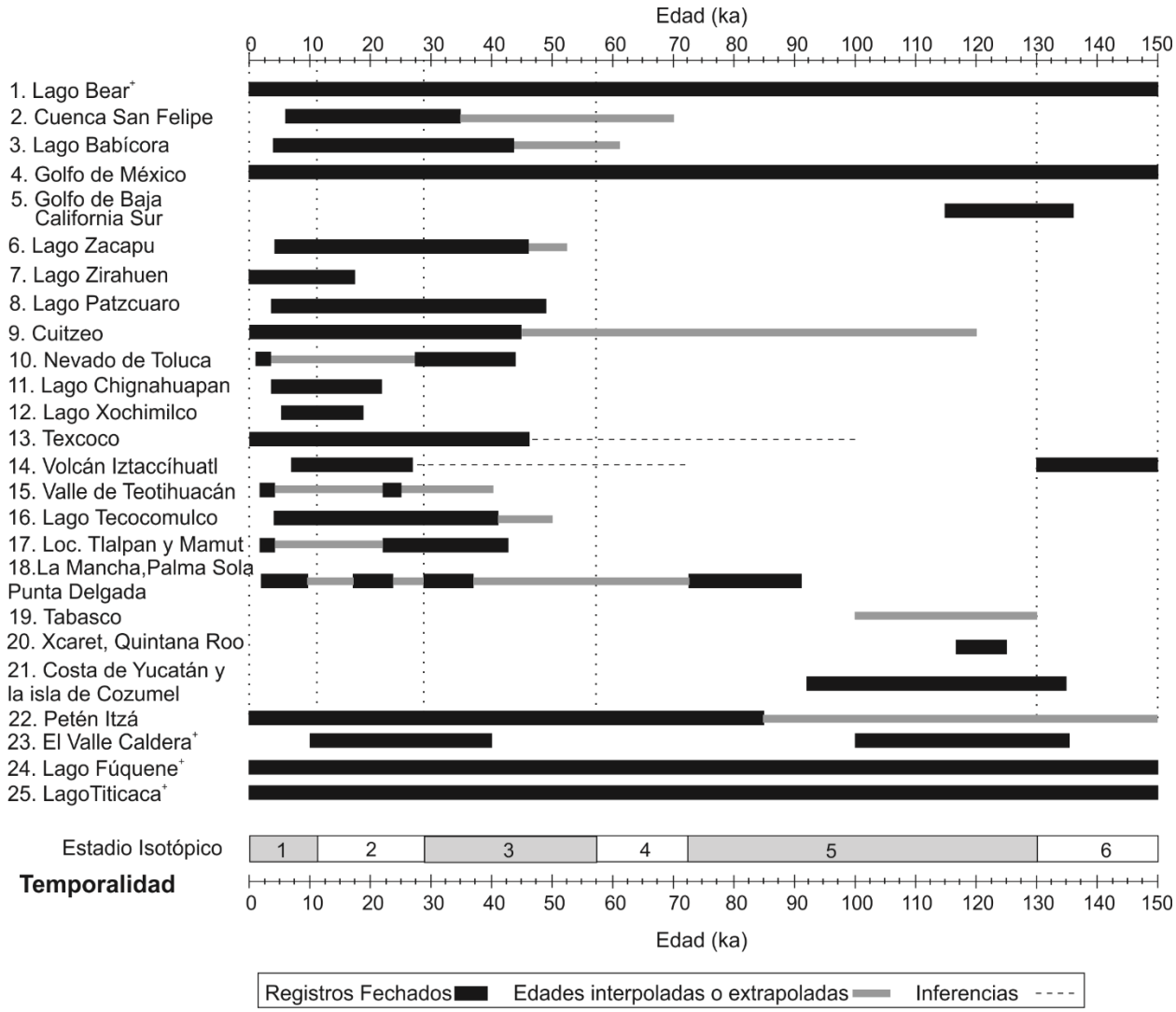

Fig. 4 Temporalidad de diferentes registros paleoclimáticos de México de los últimos 150 ka, así como registros de Norte y Sudamérica con los que se comparará el registro de Chalco. Los registros fuera de México se marcan con $^{+}$.

Estadio Isotópico 6 (EI6, 191 – 130 ka)

El registro de polen del lago Petén-Itzá sugiere una disminución de la temperatura con variaciones de humedad durante todo el EI6 (190-130 ka) en la península de Yucatán. Hacia la parte final del EI6 (160- 137 ka) la vegetación indica una disminución aun mayor de la temperatura, mientras que la ausencia de microalgas apuntan hacia una estabilización de los niveles del lago (Cruz Silva 2018). Valera-Fernández et al. (2020a, 2020b) observaron un incremento de la vegetación tipo C_4 en calcretas de la costa de Yucatán y Cozumel, lo que sugiere condiciones de aridez durante el

PMG. Los registros del sureste del país que comprenden esta ventana de tiempo señalan que hubo un descenso de la temperatura, siendo más intenso hacia la parte final del EI6. Además, se infiere que en esta región hubo condiciones áridas.

Por otro lado, para el centro de México las reconstrucciones de los avances glaciares indican que el avance Nexcoalango en el volcán Iztaccíhuatl es el más antiguo, datado en 205-175 ^{36}Cl ka. El avance Nexcoalango pudo alcanzar una altitud (~3,000 m snm) y una extensión de hielo (> 200 km^2) mucho mayor al EI2 (Vázquez-Selem & Heine 2011). Además, el registro lacustre que abarca esta ventana de tiempo, indica que los sedimentos de Chalco al final del EI6 (150 – 130 ka) presentan laminaciones que se diferencian del resto de la secuencia, infiriendo un gran cambio climático asociado a condiciones de humedad, donde el lago pudo tener un nivel profundo (Ortega-Guerrero et al. 2017, Avendaño et al. 2018) mientras que en los alrededores del lago se sugieren condiciones de vegetación abierta y bosques mesófilos (Lozano-García et al. 2022). Además, los niveles de carbón y Ti en los sedimentos señalan climas húmedos con episodios de sequias y pocos incendios en la cuenca de México durante el PMG, mientras que hacia la parte final la humedad disminuyó y los incendios se incrementaron (Martínez-Abarca et al. 2021a).

En la zona centro del país se observó un enfriamiento que ocasionó el crecimiento de grandes glaciares en las montañas más altas de la cuenca de México (Vázquez-Selem & Heine 2011). Asimismo, las condiciones debieron ser húmedas para que permitieran la acumulación de hielo en los grandes volcanes, como el Iztaccíhuatl y la presencia de un lago profundo en Chalco (Avendaño et al. 2018). La disminución de la temperatura ocasionó un desplazamiento de la ZCIT al sur, esto propició que las zonas de alta presión (Pacífico Norte y Bermuda) dominaran (Cheng et al. 2019), disminuyendo la presencia de lluvias en el sureste del país. La fuente de humedad en la zona centro del país pudo asociarse a frentes fríos, así como a los vientos del oeste. El desplazamiento de la ZCIT al sur ocasionó que los vientos del oeste también migraran, favoreciendo la entrada de humedad en la zona centro del país.

Estadio Isotópico 5 (EI5, 130 – 71 ka)

Los registros paleoclimáticos para el EI5 se enfocan principalmente en el último Interglacial (EI5e = 130-116 ka). En la zona sureste del país, los registros del Golfo de México y la península de Yucatán indican que el nivel del mar durante el EI5e fue de 4-6 m mayor al nivel actual y pudo alcanzar hasta 9 m (Blanchon et al. 2009, Aburto-Oropeza et al. 2021). El registro de polen del lago Petén-Itzá señala al último interglacial como un periodo de climas cálido-húmedos (Cruz Silva 2018) para la península de Yucatán. Además, la composición isotópica de δ^{13}C en calcretas de la costa de Yucatán sugiere climas más cálidos donde la tasa de evaporación supera la de precipitación (Valera-Fernández et al. 2020b, 2020a). En la zona sureste del país se infieren condiciones húmedas, lo cual se puede deber a los flujos de humedad provenientes del Caribe

mexicano, así como a la zona de baja presión originada por el desplazamiento de la zona de convergencia intertropical (ZCIT) más al norte que en la actualidad (Warken et al. 2019). Las asociaciones de fósiles marinos en el registro del Golfo de Baja California Sur establecen que la temperatura del océano fue más cálida que las condiciones actuales (Muhs et al. 2002). Los registros del sureste y noroeste del país sugieren que en el periodo interglacial hubo climas más cálidos a los actuales. Para el centro del país, los registros de Cuitzeo y Texcoco no presentan fechamientos en la parte basal de las secuencias, por lo que la precisión de la temporalidad es incierta (Fig. 2). Sin embargo, a partir de la extrapolación de la tasa de sedimentación se asume que ambos registros pueden abarcar el EI5, los registros de polen y diatomeas en el lago de Cuitzeo, Michoacán indican condiciones cálido-húmedas (~120 ka) (Israde-Alcántara et al. 2002, 2010). Bradbury (1971) señala que la parte basal de la secuencia de Texcoco puede alcanzar los ~ 100 ka y destaca que en esta zona los climas fueron áridos y con un nivel del lago muy somero que pudo llegar a la desecación (Bradbury 1971). El registro de Chalco sugiere un gran cambio de las condiciones climáticas comparado con el estadio isotópico anterior. La presencia de componentes calcáreos como los ostrácodos y Chara, así como las titanomagnetitas indican condiciones secas y de alta evaporación durante el EI5e (Ortega-Guerrero et al. 2017). Los cambios en la vegetación establecen el desarrollo de grandes bosques en la cuenca de México entre 127 y 125 ka AP. En el registro de polen de este lago se observan comunidades vegetales tropicales, lo que apunta a condiciones más cálidas que las presentes (Lozano-García et al. 2022).

Al comienzo de la última glaciación, en el registro de Petén-Itzá en la península de Yucatán se determina que a las comunidades vegetales fueron parecidas a las que proliferaron durante el inicio del EI6 (Cruz Silva 2018), por lo que se intuye un enfriamiento de la temperatura en la zona sureste del país. A pesar de la falta de fechamientos en la secuencia de Texcoco y Cuitzeo, las extrapolaciones de la tasa de sedimentación e inferencias de la edad en ambos registros (Bradbury 1971, Israde-Alcántara et al. 2002, 2010) se observan cambios en las diatomeas y el polen apuntando a climas fríos, la vegetación del registro de Cuitzeo señala el desarrollo de bosques mesófilos asociados con climas templado-húmedos (Israde-Alcántara et al. 2002, 2010). Lo que concuerda con el registro de polen de Chalco, donde la vegetación abierta vuelve a dominar (Lozano-García et al. 2022). Durante el inicio de la última glaciación en México se observa un ligero enfriamiento en la zona sureste del país, así como en los limitados registros del centro de México (Texcoco, Cuitzeo y Chalco), de modo que este enfriamiento general en los diferentes registros del país se propone que podría ser el subestadio 5d, a pesar de la falta de precisión de la cronología en los registros de Texcoco y Cuitzeo, lo anterior se puede confirmar por la presencia de la vegetación abierta en el registro de Chalco (Lozano-García et al. 2022).

Sin embargo, después del enfriamiento general las condiciones fueron variables en los registros paleoclimáticos del país. Las comunidades vegetales de la península de Yucatán sugieren un ligero incremento de la temperatura, aunque este cambio no determinó un remplazo completo de las comunidades, mientras que hacia el final del EI5 el espectro polínico señala condiciones frías y secas (Cruz Silva 2018). Al sureste del país las condiciones de sequía pudieron deberse al

desplazamiento al sur de la ZCIT. Al este del país, los registros de paleosuelos en Veracruz indican condiciones húmedas asociadas a suelos arcillosos con alto grado de meteorización de los minerales primarios durante los subestadios 5c-a (Solleiro-Rebolledo et al. 2022). En el centro de México el registro de Cuitzeo establece que las condiciones húmedas cambiaron a frías y secas, excepto por los conjuntos de diatomeas y microalgas que apuntan a un aumento del nivel lacustre ca. 88 ka (Israde-Alcántara et al. 2002, 2010). Mientras que en el lago de Texcoco las condiciones de humedad fueron variables con un cuerpo de agua principalmente salobre sugerido por la presencia de varias especies del género *Cyclotella* - *Stephanocyclus* (*Stephanocyclus quillensis, S. meneghinianus, Cyclotella* sp. cf. *C. stylorum* Brigthwell, *C. striata*) y por *Nitzschia frustulum* (Bradbury 1971). El registro de polen y C/N de Chalco también indican condiciones variables durante los subestadios 5c-a, con cambios entre vegetaciones tropicales (EI5c, a) y mesófilas (EI5d, b) (Lozano-García et al. 2022), así como una alta variabilidad en la productividad lacustre y terrestre durante todo el EI5. Las variaciones de temperatura superficial en el Océano Pacífico tropical, así como en el mar del Caribe y las variaciones en la Circulación meridional del Atlántico pudieron ocasionar fluctuaciones en el transporte de las masas de humedad hacia la zona sureste, este y noroeste del país (Bereither et al. 2012).

Estadio Isotópico 4 (EI4, 71-57 ka)

No se tiene registrado algún avance glaciar entre los eventos Nexcoalango (EI6) y Hueyatlaco-1 (UGM, durante el EI2) en el volcán Iztaccíhuatl, por lo que Vázquez-Selem & Heine (2011) indican que los flujos de lava del Iztaccíhuatl durante ~120 y ~140 ^{36}Cl ka, así como la gran extensión del avance glaciar Hueyatlaco-1 pudieron borrar la evidencia de glaciaciones posteriores a Nexcoalango y anteriores al UMG en este volcán. Sin embargo, en La Malinche, el Ajusco y el Nevado de Toluca pudo haber otros posibles avances entre el EI4 y/o EI3, pero estos mismos autores señalan que no se cuenta con dataciones precisas.

Durante el EI4, el registro de San Felipe, Baja California apunta a condiciones secas y la ausencia de un cuerpo de agua entre 70-45 ka (Ortega-Guerrero et al. 1999), mientras que el paleolago de Babícora, Chihuahua tuvo su máxima extensión durante el EI4 (65-57 ka). Roy et al. (2013) señala que las mayores descargas pluviales al lago se dieron durante el EI4 (antes de 58 ka), siendo las plantas terrestres la principal entrada de materia orgánica al lago durante 71-53 ka. En la zona norte del país las condiciones fueron húmedas, sin embargo, no se observan los mismos climas en la zona noroeste (San Felipe, Baja California). En esta ventana de tiempo los registros de San Felipe y Babícora presentan edades extrapoladas, por lo que podría haber sesgo al comparar ambas secuencias. No obstante, Thompson & Anderson (2000) sugieren que la gran humedad en el norte del país se debió al desplazamiento al sur de la zona de alta presión del Pacífico norte, facilitando la presencia de lluvias en la zona norte del país.

Sin embargo en el centro del país, el registro de la vegetación en Cuitzeo determina climas secos asociados a un bajo nivel del lago (Israde-Alcántara et al. 2002, 2010). En el lago de Texcoco también se observaron condiciones salobres asociadas a un cuerpo de agua somero (Bradbury 1971). Además, la vegetación del registro de Chalco sugiere una reducción de la humedad desde el EI5a (Lozano-García et al. 2022). El registro de paleosuelos en Veracruz también reporta condiciones secas asociadas al alto contenido de carbonatos pedogénicos con rizoconcreciones gruesas (Solleiro et al. 2021). Mientras que al sureste de México, el registro de polen del Lago Petén-Itzá señala que las condiciones frías y secas se mantuvieron durante el EI4 y hacia 60 ka las condiciones de frío se intensificaron (Cruz Silva 2018). En la zona centro, este y sureste del país las condiciones fueron secas, con climas fríos en el sureste del país, estas condiciones se pudieron deber al desplazamiento al sur de la ZCIT y a la reducción del flujo de humedad de la Corriente de chorro de bajo nivel del Caribe (Warken et al. 2019).

Estadio Isotópico 3 (EI3, 57-29 ka)

Durante el EI3, los registros paleoclimáticos apuntan a condiciones de humedad que permitieron la existencia de grandes lagos en Baja California y Sonora a mitad del EI3 (45 ka) (Ortega-Guerrero et al. 1999, Metcalfe et al. 2002). Para la parte noroeste las condiciones fueron húmedas favoreciendo la presencia de lagos profundos. Roy et al. (2013) sugieren la presencia de tormentas invernales relacionadas a los vientos del oeste, mientras que en verano a lluvias provenientes del sureste asociadas al monzón norteamericano. Los momentos de mayor precipitación en el verano coinciden con los eventos milenarios Dansgaard-Oescher (DO), mientras que los momentos de aridez ocurrieron por una disminución del monzón. En el centro de México los registros de Cuitzeo, Pátzcuaro y Cantabria (cerca del lago de Zacapu) indican que las condiciones fueron húmedas durante el EI3 (Bradbury 2000, Israde-Alcántara et al. 2002, 2010, Ortega et al. 2002). El lago de Pátzcuaro alcanzó su máxima profundidad al final del EI3 y principios del UMG (Bradbury 2000). El registro de Cuitzeo señala que durante el EI3 las condiciones de temperatura y humedad aumentaron ligeramente, favoreciendo un lago más profundo (Israde-Alcántara et al. 2002, 2010). El Lago de Tecocomulco también sugiere condiciones de agua dulce asociadas a un cuerpo de agua profundo y las comunidades vegetales establecen climas fríos y húmedos entre 50 – 42 ka cal AP, pero las condiciones del lago fluctúan reduciendo su nivel y la vegetación indica climas ligeramente cálidos entre 42 – 37 ka cal AP (Caballero et al. 1999). Los registros de paleosuelos de Tlaxcala, el valle de Teotihuacán y Toluca indican condiciones húmedas, en Tlaxcala se infiere que los ecosistemas de humedades estaban más extendidos que en la actualidad (Sedov et al., 2009), en el valle de Teotihuacán los suelos se formaron en paisajes boscosos estables y húmedos que hacia el final del EI3 apuntan a climas estacionales (Solleiro-Rebolledo et al. 2011) y en Toluca se observaron fluctuaciones húmedas-secas debido a las asociaciones de minerales arcillosos y la composición de isótopos estables de carbono en humus (Sedov et al. 2003). Mientras que en Texcoco el lago mantuvo un nivel somero y condiciones salobres (Bradbury

1971). De la misma forma, en los sedimentos del lago de Chalco dominaron los componentes calcáreos con coquinas de ostrácodos (Ortega-Guerrero et al. 2017), mientras que los valores de C/N indicaron una mezcla entre la vegetación terrestre y lacustre (Torres-Rodríguez et al. 2018, Martínez-Abarca et al. 2021a). La bioturbación en los sedimentos sugiere un bajo nivel del lago, que en ocasiones llegó a tener una exposición subaérea (Ortega-Guerrero et al. 2017). El análisis detallado de las diatomeas y las funciones de transferencia están disponibles para los primeros 26 m de la secuencia del Lago de Chalco (40 ka cal AP) (Caballero et al. 2019), lo que permitió la identificación de fluctuaciones a escala de tiempo orbital y milenaria (HS3-0). El registro de carbón en el lago de Chalco determinó que durante el subestadio 5a y el final del EI3 tuvieron la mayor actividad de incendios en los alrededores (Torres-Rodríguez et al. 2015, 2022, Martínez-Abarca et al. 2021a). Al este del país, el registro de Veracruz presenta paleosuelos ricos en carbonatos indicando climas secos (Solleiro-Rebolledo et al. 2022). Por otro lado al sureste del país, en el registro de Petén-Itzá se infieren rápidos cambios durante el final del EI3 (48 – 23 ka cal AP) (Hodell et al. 2008), la presencia de capas de yeso indican climas áridos asociados a los eventos milenarios Heinrich, mientras que las variaciones de humedad coinciden con la presencia de eventos milenarios DO (Hodell et al. 2008, Pérez et al. 2021). Hodell et al. (2008) asocian los periodos de sequía en el sureste del país con el desplazamiento al sur de la ZCIT, así como al debilitamiento de la circulación meridional del Atlántico, ocasionando una reducción del flujo de humedad de la Corriente de chorro de bajo nivel del Caribe.

Estadio Isotópico 2 (EI2, 29-11 ka)

Durante el EI2 en la parte norte del país, el registro de Babícora sugiere que el nivel del lago se mantuvo somero durante el UMG (Roy et al. 2013). El registro de San Felipe también apunta a condiciones de humedad entre 34 – 19 ka cal AP (Ortega-Guerrero et al. 1999). Para la zona noroeste la precipitación de verano asociada al monzón norteamericano se redujo durante el último máximo glacial e incrementó durante la deglaciación (Roy et al. 2013). En el centro de México, el registro de Cuitzeo señala que el nivel de agua tuvo muchas fluctuaciones, con dos pulsos de humedad muy marcados entre ca. 33 – 31 ka cal AP y ca. 20 – 12 ka cal AP. (Israde-Alcántara et al. 2002, 2010). Por otro lado en el lago de Pátzcuaro, la temperatura disminuyó pero las condiciones de humedad se mantuvieron durante el UMG (Bradbury 2000). En el registro de Zacapu se observaron condiciones de baja humedad que indican la ausencia de un cuerpo de agua durante el EI2 (Metcalfe 1992). En el registro de la cuenca alta del Lerma establece un cambio de un ambiente palustre a uno fluvial ~31 ka cal AP; mientras que en el lago de Chignahuapan está asociado a condiciones de agua dulce con un incremento de su nivel entre 26 – 24 ka cal AP y una disminución alrededor de 22.5 ka cal AP (Caballero et al. 2002). En el lago de Texcoco las condiciones salobres asociadas a un lago somero se mantuvieron durante todo el EI2 (Badbury 1971). En el registro de Chalco sí se observó un cambio en las asociaciones de diatomeas de un lago somero con un pH alcalino y altas concentraciones de sales durante el EI3 a un lago de agua

dulce en el EI2 (Caballero et al. 2019). El registro de Veracruz sugiere un suelo poco desarrollado con abundantes carbonatos pedogénicos, indicando climas secos (Solleiro-Rebolledo et al. 2022). Sin embargo, los registros de paleosuelos en Tlaxcala, Teotihuacán y el Nevado de Toluca apuntan a condiciones húmedas, en Tlaxcala se observó alta meteorización e iluviación arcillosa señalando un periodo de humedad estable, comparada con el EI3 (Sedov et al. 2009), los paleosuelos del valle de Teotihuacán observan condiciones ambientales principalmente secas con altos intervalos de humedad evidenciados por procesos gleyicos y actividad fluvial entre *ca.* 24 ka incluido el UMG (Solleiro-Rebolledo et al. 2011), mientras que en las zonas altas de la misma región se formaron luvisoles indicativos de ecosistemas de bosque húmedo (Solleiro-Rebolledo et al. 2006) y en el Nevado de Toluca los paleosuelos presentan signos de pedogénesis húmeda (Sedov et al. 2001). Bradbury (2000) sugiere que el desplazamiento al sur de la ZCIT propició que los vientos del oeste llevaran humedad a la zona centro-oeste de la FVTM.

Durante el UMG se registraron dos avances glaciares importantes en el volcán Iztaccíhuatl, el primer avances llamado Hueyatlaco-1 (21 – 17.5 ^{36}Cl ka) asociado a una disminución de la temperatura de 6 – 7.5º C (Lachniet & Vazquez-Selem 2005) y el segundo avance Hueyatlaco-2 (17 – 14.5 ^{36}Cl ka). Durante el UMG también se registraron avances glaciares en los volcanes del Nevado de Toluca, Ajusco, Tancítaro, Malinche, Cofre de Perote. Hacia el final del último ciclo glacial la mayor parte de los glaciares retrocedieron hacia los 14 ka cal AP, mientras que los glaciares del Cofre de Perote y Tancítaro retrocedieron hace unos 12 ka cal AP (Lachniet & Vazquez-Selem 2005, Caballero et al. 2010, Vázquez-Selem & Heine 2011). Por lo tanto, las reconstrucciones de los glaciares indican una mayor humedad al oriente y occidente del país comparado con la zona central (Caballero et al. 2010). Las reconstrucciones a partir de polen y diatomeas en el centro de México sugieren una disminución de la temperatura de 4 – 5º C durante el UMG (Correa-Metrio et al. 2013, Caballero et al. 2019). Para la parte sureste del país, en el registro de Petén-Itzá se observaron depósitos de arcillas entre 23 – 18 ka cal AP asumiendo condiciones de un lago profundo y climas relativamente húmedos, durante este periodo también se observó la presencia de comunidades vegetales no análogas a las modernas (Hodell et al. 2008, Correa-Metrio et al. 2012). La Terminación I (TI) señala un primer calentamiento de 3ºC entre ~15.5 – 13.5 ka cal AP, el cual es seguido por un retorno a condiciones frías donde la temperatura sugiere una disminución de 2º C, mientras que un segundo calentamiento se observa entre 12 – 10 ka cal AP, hasta que las condiciones modernas se establecen (Cruz Silva 2018). Mientras que en el sureste del país se observan condiciones húmedas asociadas a una menor estacionalidad e inviernos húmedos asociados a los frentes fríos del norte (Hodell et al. 2008).

Estadio Isotópico 1, únicamente del Holoceno temprano a medio (EI1, 11 – 4.2 ka)

Para el norte del país, el registro de Babícora indica condiciones áridas y un cuerpo de agua muy somero a partir de 15 ka cal AP, además hubieron fluctuaciones de humedad con intervalos donde

el lago se secó durante el Holoceno medio (Metcalfe et al. 2002). Mientras que en San Felipe, Baja California se registró un aumento del escurrimiento de aguas superficiales a partir de 12 ka cal AP. con un intervalo de aridez entre 7 – 6 ka cal AP, siendo hasta 4 ka cal AP. cuando se establecen las actuales condiciones áridas (Ortega-Guerrero et al. 1999). Por lo que, los periodos de humedad de la zona noroeste del país se asocian al monzón norteamericano (Metcalfe et al. 2015).

En el centro el país, los registros de Cuitzeo, Pátzcuaro, Tecocomulco, Texcoco y Chalco indican de forma general una reducción del nivel lacustre. En Cuitzeo el lago incrementó su salinidad hasta que alcanzó las condiciones actuales (Israde-Alcántara et al. 2002, 2010), mientras que en Pátzcuaro el lago incremento su nivel de nutrientes debido al impacto humano (Bradbury 2000).

En Tecocomulco y Texcoco desde los 16 ka cal AP se observaron ambientes muy áridos hasta el Holoceno medio, con ausencia de diatomeas entre 14.5 – 5 ka cal AP en Texcoco y entre 15 – 3.3 ka cal AP en Tecocomulco (Caballero et al. 1999). El registro del lago de Chalco indica, además de una reducción de su nivel, que la temperatura pudo aumentar entre 2.6 – 3º C en el Holoceno temprano (Caballero et al. 2019). De manera que los bajos niveles lacustres en el centro y sureste del país sugieren que los vientos alisios y la ZCIT tenían un desplazamiento al sur. Se incrementaron las condiciones de humedad al sureste del país con el restablecimiento de la Circulación meridional del Atlántico (McManus et al. 2004).

1.7 Área de estudio

Descripción geológica

La Cuenca de México (CM) ubicada en la zona centro-este de la Faja Volcánica Mexicana (FVTM), con una superficie de aproximadamente 9600 km^2, es una zona volcánica y tectónica activa delimitada al norte por las sierras de Pachuca, Tepotzotlán, Guadalupe, Patlachique y Tepozán, al este por la sierra Nevada (que incluye el Popocatepetl, Iztaccíhuatl, Tlaloc y Telapón), al oeste por la sierra de Monte Alto y las Cruces, y al sur por la Sierra de Chichinautzin (Fig. 3c). La formación de la Sierra Chichinautzin, hace 1.2 Ma (Arce *et al.*, 2013), obstruyó el antiguo drenaje de la CM dirigido al río Balsas produciendo una cuenca endorreica, lo cual permitió la acumulación de agua captada por escorrentía y del subsuelo que formaron grandes cuerpos lacustres: al norte Zumpango y Xaltocan, al este Texcoco, al sur Xochimilco y Chalco (Fig. 3c), distintos autores sugieren que estos cuerpos de agua podían llegar a formar uno solo (Díaz-Rodríguez, 2006; Rodríguez-Castillo y González-Moran, 1989).

El lago de Chalco (19º 30' N, 99º 00' O) se extendía en un área aproximada de 240 km^2 a unos 2,200 m snm (Ortega-Guerrero *et al.*, 2015). Está delimitado al este por la sierra Nevada, al norte por la sierra de Santa Catarina y al sur por la sierra Chichinautzin; antiguamente limitaba al oeste por la isla de Tláhuac, separándolo del lago de Xochimilco (Caballero, 1997). Los ríos

Amecameca y Tlalmanalco eran las principales fuentes de agua que abastecían al lago, los cuales se originaban en los volcanes Popocatépetl e Iztaccíhuatl. Recientemente el lago de Chalco se ha reducido a unas áreas pantanosas al oeste y sur del volcán de Xico que tienen una extensión de 5 km^2 en forma de C invertida (Ortiz Zamora y Ortega-Guerrero 2007); los alrededores del lago son utilizados para la agricultura (Ortega-Guerrero *et al.*, 2000), y gran parte de la planicie está urbanizada.

Clima actual en la subcuenca de Chalco

El clima en la subcuenca de Chalco es templado, sub-húmedo con lluvias en verano $C(w_0)(w_1)(w)$. La temperatura media anual es de 16.8°C con un rango de temperatura de 13.8 (enero) – 19.1(mayo) °C. La precipitación anual es de 540 mm, mientras que la evaporación anual es 1.440 mm (Fig. 6).

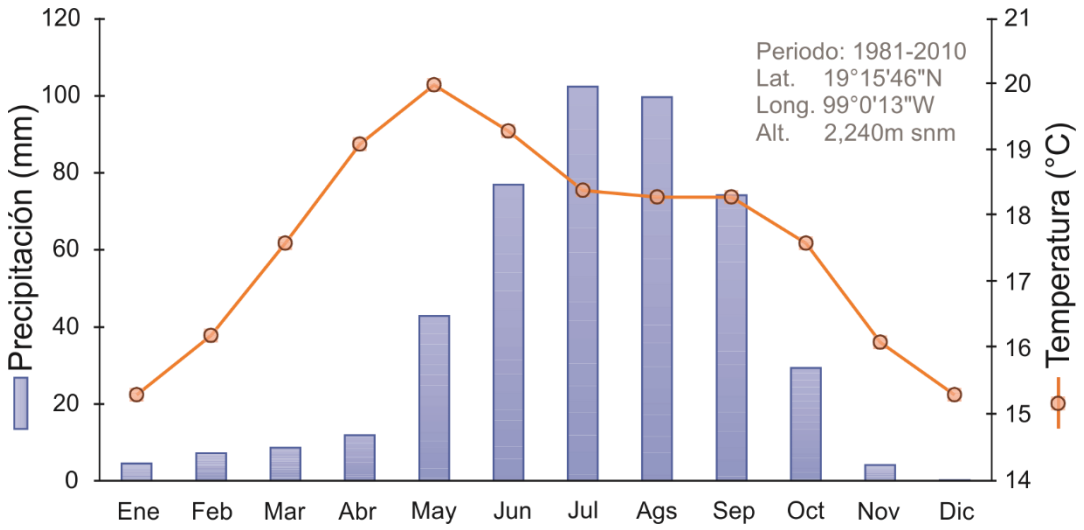

Fig. 5 Información climática de la subcuenca de Chalco. Precipitación media mensual y temperatura media mensual. Datos obtenidos de la estación meteorológica del Servicio Meteorológico Nacional, México, 2023. Estación Tláhuac – 9051.

Unidades estratigráficas del registro de Chalco

El registro del lago de Chalco cuenta con una gran resolución temporal que abarca varios ciclos glaciales consecutivos (*ca.* 400 ka) (Lozano-García et al. 2017, Brown et al. 2019, Martínez-

Abarca et al. 2021b). Para los primeros 122.4 m se tiene una secuencia maestra (núcleo CHA08) (Fig. 5) que está dividida en siete unidades litoestratigráficas principales (Ortega-Guerrero et al. 2017), donde se ha realizado el mayor parte de los estudios previos del Lago de Chalco. Para esta secuencia se desarrolló un modelo de edad formado por catorce fechamientos de ^{14}C de polen y ostrácodos, así como dos marcadores tefrocronoestratigráficos, un fechamiento a partir de 230Th/U extraído de un circón en una capa de tefra (Torres Rodríguez et al. 2015; Ortega-Guerrero et al. 2017) y un punto de anclaje a 106 m de profundidad, el cual se interpreta como la transición del EI6-EI5, con base en los cambios importantes de los conjuntos de diatomeas y sedimentos (Ortega-Guerrero et al., 2017; Avendaño et al., 2018). Las unidades litoestratigráficas de la secuencia maestra corresponden con los primeros seis estadios isotópicos marinos. A continuación, se describen brevemente cada una de las unidades litoestratigráficas (Fig. 5).

La unidad 7 (122.4 – 106 m; 146.5 – 130 ka) está compuesta por láminas finas claras/oscuras ricas en diatomeas. Las láminas claras son *ooze* de diatomeas dominados por especies del género *Stephanodiscus*, mientras que las láminas oscuras son limo con menores componentes calcáreos. Las tasas de acumulación de carbón son bajas. Hay 13 capas ricas en carbonatos a diferentes profundidades de esta unidad.

La Unidad 6 (106 – 57.5 m; 130 – 70.3 ka) muestra tres cambios sedimentarios, la parte inferior (106 – 103.2 m) consiste en limo calcáreo con frecuentes ostrácodos, diatomeas alcalófilas y halófilas y altas tasas de acumulación de carbón en su base. La sección media (103.2 – 93.3 m) presenta *Stephanodiscus* spp. sedimentos laminados claros/oscuros ricos en diatomeas. Las tasas de acumulación de carbón son altas a medias. La parte superior (93.3 – 57.5 m) está formada por sedimentos calcáreos masivos con componentes biogénicos ricos en *Chara* sp., *Phacotus*, valvas de ostrácodos, diatomeas alcalófilas y halófilas; intervalos moteados sugieren que los sedimentos tuvieron una exposición subaérea. Las tasas de acumulación de carbón vegetal son variables, pero generalmente altas.

La Unidad 5 (57.5 – 41.1 m; 70.3 – 51 ka) tiene intervalos moteados masivos que se alternan con limos laminados o estratificados con abundantes componentes biogénicos, los cuales incluyen diatomeas alcalófilas y halófilas. Las tasas de acumulación de carbón son de medias a altas.

La Unidad 4 (41.1 – 28 m, 51 – 35 ka) es muy similar a la Unidad 5 pero con proporciones más altas de componentes biogénicos y calcáreos que incluyen diatomeas alcalífilas, *Chara* sp., ostrácodos y cristales de calcita, dolomita y yeso y en la parte superior las tasas más altas de acumulación de carbón.

La Unidad 3 (CHA08 < 28 m, Cha-B 26 – 11 m) se caracteriza por limos masivos a estratificados arenosos a arcillosos orgánicos y alcalífilos ricos en diatomeas. La Tefra Tláhuac (con una edad de ~31.4 ka cal BP, Herrera Hernández 2011) está presente en esta unidad en ambas secuencias (CHA08 y Cha-B). Las tasas de acumulación de carbón son de medias a bajas.

La Unidad 2 (Cha-B 11 – 2,5 m) consiste en una alternancia masiva con limo arcilloso rico en diatomeas de agua dulce débilmente laminado con tasas de acumulación de carbón generalmente bajas, pero con algunos picos ocasionales. Esta unidad contiene evidencia de intensa actividad volcánica explosiva, que incluye la Pómez Tutti-Frutti (PTF) producida por una erupción del volcán Popocatépetl hace 17 ka cal BP (Arce et al. 2003) y la Pómez Toluca Superior (PTS) producida por el volcán Nevado de Toluca hace 12.4 ka cal BP (Sosa-Ceballos et al. 2012).

La Unidad 1 (2,5 – 0,5 m) está compuesta por granos de silicato macizos a débilmente estratificados con concreciones calcáreas, diatomeas alcalófilas y halófilas, ostrácodos y fragmentos de gasterópodos.

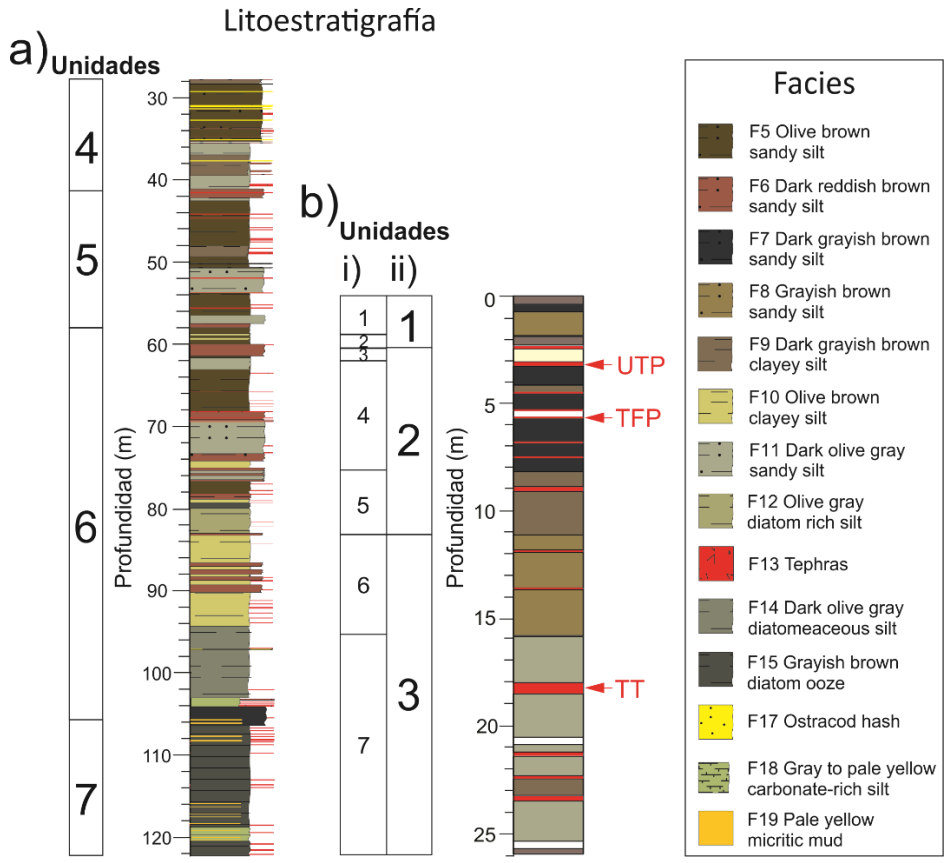

Fig. 6. Unidades estratigráficas de los núcleos del Lago de Chalco: a) estratigrafía de la secuencia maestra núcleo CHA08 (profundidad de 122.4 – 28 m, edad de 31 – 150 ka), figura tomada de Ortega-Guerrero et al. (2017). b) estratigrafía del núcleo Cha-B con las unidades originales (i) reportadas por Caballero & Ortega (1998), así como su correlación con las unidades de la secuencia maestra CHA08-CHA11 VII (ii) reportadas por Ortega-Guerrero et al. (2017). Principales tefras: PTS = Pómez Toluca Superior, PTF = Pómez Tutti-Frutti, TT = Tefra Tláhuac.

Capítulo II

2. Control climático en mineralogía magnética durante el EI6 tardío – EI3 temprano en el Lago Chalco, centro de México.

(Artículo publicado, citar como: Ortega-Guerrero B., Avendaño D., Caballero M., Lozano-García S., Brown E. T., Rodríguez A., García B., Barceinas H., Soler A. M., & Albarrán, A. (2020). Climatic control on magnetic mineralogy during the late MIS 6-Early MIS 3 in Lake Chalco, central Mexico. *Quaternary Science Reviews, 230,* 106163. https://doi.org/10.1016/j.quascirev.2020.106163)

Este artículo surge como un trabajo que integra la información de indicadores biológicos (diatomeas) y geoquímicos (minerales magnéticos y geoquímica de elementos mayores) para brindar una visión general de los cambios climáticos ocurridos durante los últimos 150 mil años. En este artículo únicamente se presentan los resultados de diatomeas de forma resumida, de acuerdo con la abundancia relativa de cuatro grupos con distribución ecológica contrastante: (1) pequeñas Fragilariaceae y (2) Stephanodiscus spp., asociadas a condiciones de agua dulce, así como la suma de las especies (3) alcalífilas y (4) halófilas. Los cuatro grupos se definieron a partir de las preferencias ecológicas de las especies de diatomeas presentes en 40 lagos del centro de México (Caballero et al., 2019).

Resumen:

Los sedimentos del lago de Chalco en el centro de México abarcan desde *ca.* 150 a 35 ka proporcionando de evidencia de la variabilidad climática en los trópicos de América del Norte asociado con el final del Estadio Isotópico 6, la transición al último Interglacial (EI5.5, *ca.* 130-115ka), y parte del último glacial (EI5.4 a principios del EI3, 115-35ka). En este artículo se aplicó un enfoque multiproxy basado en el análisis de minerales magnéticos, asociaciones de diatomeas y geoquímica de elementos mayores. La historia paleoambiental reconstruida identifica el final del EI6 más frío y húmedo que el presente, con un alto nivel lacustre y un subsecuente cambio a climas secos al comienzo del último Interglacial (*ca.* 130 ka). Se observaron grandes cambios de amplitud en la mayoría de los parámetros analizados desde *ca.* 130-74 ka que coinciden aproximadamente con MIS5 (130-71 ka). La amplitud de estos cambios disminuye durante el EI4 (71-57 ka) y la primera parte del EI3 (57-35 ka). Propusimos que las oscilaciones climáticas inferidas siguen las variaciones de insolación durante el EI6 y parte del EI5 (150-88 ka). La baja insolación de verano y primavera inhibieron la evaporación y favorecieron los altos niveles del lago. Por el contrario, la insolación máxima en primavera y verano promovieron las condiciones secas y bajos niveles del lago. Se observó una relación entre un Glacial frío-húmedo y un Interglacial cálido-seco en los registros del Lago Titicaca (Bolivia) y el Lago Chalco, lo que muestra una gran sensibilidad de los sitios tropicales de gran altitud a la variabilidad climática.

Palabras clave: Pleistoceno, Interglacial(es), Paleolimnología, Norteamérica, Propiedades magnéticas.

Quaternary Science Reviews 230 (2020) 106163

Contents lists available at ScienceDirect

Quaternary Science Reviews

journal homepage: www.elsevier.com/locate/quascirev

Climatic control on magnetic mineralogy during the late MIS 6 - Early MIS 3 in Lake Chalco, central Mexico

Beatriz Ortega-Guerrero [a, *], Diana Avendaño [b], Margarita Caballero [a], Socorro Lozano-García [c], Erik T. Brown [d], Alejandro Rodríguez [b], Bernardo García [b], Hermenegildo Barceinas [b], Ana María Soler [a], Albán Albarrán [b]

[a] Universidad Nacional Autónoma de México, Instituto de Geofísica, 04150, Ciudad de México, Mexico
[b] Universidad Nacional Autónoma de México, Posgrado en Ciencias de la Tierra, 04150, Ciudad de México, Mexico
[c] Universidad Nacional Autónoma de México, Instituto de Geología, Ciudad de México, 04150, Mexico
[d] University of Minnesota Duluth, Large Lakes Observatory and Department of Geological Sciences, Duluth, MN, 55812, USA

ARTICLE INFO

Article history:
Received 23 August 2019
Received in revised form
12 December 2019
Accepted 1 January 2020
Available online 20 January 2020

Keywords:
Pleistocene
Interglacial(s)
Paleolimnology
North America
Magnetic properties

ABSTRACT

Sediments from Lake Chalco in central Mexico spanning from ca. 150 to 35 ka ago provide evidence of paleoclimatic variability in the North American tropics associated with the end of Marine Isotopic Stage (MIS) 6, the transition to the last interglacial (MIS 5.5, ca. 130-115 ka ago), and part of the last glacial (MIS 5.4 to early MIS 3, 115 to 35 ka ago). We applied a multiproxy approach based on the analysis of mineral magnetism, diatom assemblages and major elements geochemistry. The reconstructed paleoenvironmental history identify the end of the globally cool MIS 6 as wetter than present, with high lake level, and a subsequent change to drier climates at the onset of the last interglacial (ca. 130 ka). Large amplitude changes in most of the analyzed parameters from ca. 130 to 74 ka are approximately coincident with MIS 5 (130-71 ka). The amplitude of these changes decreases in MIS 4 (71-57 ka) and the early part of MIS 3 (57-35 ka). We proposed that the inferred climatic oscillations follow insolation variations during MIS 6 and part of MIS 5 (150-88 ka). Low summer and spring insolation and lower seasonality inhibited evaporation and favored high lake levels. Conversely, maxima in spring and summer insolation promoted dry conditions and low lake levels. The major wet-cold glacial and dry-warm interglacial relationship found in Lake Titicaca (Bolivia) and Lake Chalco records shows the sensitivity of high altitude tropical sites to climatic variability.

1. Introduction

Lacustrine sedimentary records worldwide have been analyzed as archives of past climatic conditions; however, published records beyond the last glacial maximum (>20 ka) are infrequent for the tropics of North America (e.g. Caballero et al., 1999; Ortega et al., 2002; Metcalfe et al., 2007; Israde-Alcántara et al., 2010; Caballero et al., 2019). Climatic records of the past 85 ka have been published from Lake Petén Itzá (Guatemala) (Hodell et al., 2008; Mays et al., 2017), and Lake Chalco (México) (Torres Rodríguez et al., 2015, 2018). Longer records that comprise the last interglacial (ca. 130-115 ka) are practically nonexistent so far in the North American tropics. In Central America the only record is available from El Valle (Panamá) spanning the time period between 137-98 ka (Cárdenes-Sandí et al., 2019). In central Mexico the stratigraphical and sedimentological characteristics of Lake Chalco provide some inferences of paleoclimate and paleoenvironments beyond the last interglacial (Ortega-Guerrero et al., 2017; Valero-Garcés et al., 2019). From South America, long records include the sequence from Lake Titicaca (Bolivia) which covers the last ca. 370 ka (Fritz et al., 2007), and Lake Fúquene (Colombia) for the last 280 ka (Groot et al., 2011). More studies on long lacustrine sedimentary sequences will advance our understanding of climatic variations during the last interglacial/glacial cycle. Such knowledge is relevant to establish correlations with similar events recorded at sites on the opposite hemisphere and to test their synchronicity and geographical extent. These kinds of records can also be used to

* Corresponding author. Universidad Nacional Autónoma de México, Instituto de Geofísica, Ciudad Universitaria circuito exterior s/n, 04150, Ciudad de México, Mexico.
E-mail address: bortega@igeofisica.unam.mx (B. Ortega-Guerrero).

https://doi.org/10.1016/j.quascirev.2020.106163
0277-3791/

characterize the climate dynamics in the tropics, and to evaluate the response of ecosystems to similar climatic drivers, but under contrasting conditions; for example, as during interglacials without (Marine Isotopic Stage 5) and with (Marine Isotopic Stage 1) human influence.

The use of independent proxies in the interpretation of these records is recommended, in order to achieve a more comprehensible model of past environmental changes driven by climatic fluctuations. Therefore, a multiproxy approach is necessary, including a combination of techniques such as stable isotopes, elemental concentrations, biological proxies and rock magnetism analyses. Studies on environmental magnetism investigate the changes in the detrital magnetic mineral fraction and its transformation into new secondary minerals (Maher, 2007). In volcanic settings, Ti-magnetites are a common detrital fraction in lacustrine sediments (e.g. Thouveny et al., 1994). Weathering and pedogenesis processes can produce secondary minerals that can be delivered to lakes as a detrital fraction (e.g. Chen et al., 2005; Maxbauer et al., 2016a). Anoxic conditions may lead to the dissolution of Fe oxides and their transformation into sulfurs (e.g. Nowaczyk, 2011; Borruel-Abadía et al., 2015); and bacterial processes can produce secondary minerals (e.g. Lascu and Plank, 2013). The aforementioned transformations suffered by magnetic minerals depend to a great extent on climatic and environmental controls (e.g. Evans and Heller, 2003), so they are potential indicators of past climatic conditions. We present a continuous ~115 ka (150-35 ka BP) record of paleoenvironmental change inferred from rock magnetism, elemental geochemistry and synthetic results of diatom analyses from a 93 m long lacustrine sedimentary sequence collected in Lake Chalco (central México), which constitutes a unique record of most of the last interglacial/glacial cycle in the North American tropics. New insights of past climatic and environmental changes between the late MIS6 and early MIS 3 are provided through diagnostic magnetic parameters of the alteration of the primary mineralogy and the changes between freshwater and saline diatom taxa. This study differs from previous from Lake Chalco as it constitutes the longest continuous published record of past climatic and environmental conditions based on any proxy.

2. Geological setting and climate

Lake Chalco is an intervolcanic basin located at the central-eastern sector of the Trans Mexican Volcanic Belt (TMVB), a transversal continental arc that resulted from the subduction of the Cocos Plate beneath the North American Plate (Ferrari et al., 2012) (Fig. 1). The Chalco sub-basin occupies the southeastern part of the Basin of Mexico (19° 15′ N, 98° 58' W, 2230 m asl), at the southern edge of Mexico City metropolitan area. Even if in past times there was an extensive lake, it is now reduced to a shallow marsh (<3 m depth), that occupies an area of <6 km^2. The rocks in the catchment are entirely composed of volcanic deposits, mostly ranging from basalts to andesites in composition, which include scoria and ash cones, shield volcanoes and associated lava flows, fisural lava flows, domes, maars and stratovolcanoes, among them two of the highest summits in Mexico, the Popocatépetl (5452 m asl) and Iztaccíhuatl (5238 m asl), built since 1.8 Ma to present (Macías et al., 2012; Arce et al., 2013).

The climate is sub-tropical high altitude, with a mean precipitation of 540 mm/yr, concentrated during the summer months (late June to September) due to the northern migration of the Intertropical Convergence Zone (ITCZ) and the onset of hurricane season; occasional rainfall occurs during the winter caused by polar air outbreaks. Maximum temperatures (27–30 °C) occur during late spring and the lowest temperatures (4–7 °C) are observed during winter.

3. Materials and methods

3.1. Drilling, facies description and core correlation

The drilling details, core correlation, lithostratigraphy of the sequence and geochronology of the upper 122 m of the sedimentary sequence have been published previously (Ortega-Guerrero et al., 2017). Three cores were drilled in 2008 at different depths at the depocentre zone of former Lake Chalco. The cores span a composite section between 29 and 122.4 m depth: CHA08-IV (85–122 m), CHA08-V (29–72 m), CHA08-VI (70.8–85 and 106–122.4 m). The cores were drilled with a Shelby corer in 1.10 m sections with inner PVC tubes 1 m long and 10 cm in diameter; the remaining 10 cm were collected from the drilling shoe. Splitting of cores and initial description were carried out at the LacCore facility (University of Minnesota-Twin Cities). High-resolution color scans were acquired from each section using a DMT CoreScan digital linescan camera, and magnetic susceptibility was measured on split halves at 0.5 and 1 cm resolution using a Bartington MS2E sensor. The correlation of the cores was established from stratigraphic features, tephra markers and the magnetic susceptibility profiles.

Nineteen sedimentary facies had been previously established from component descriptions in smear slides and visual observations of the core faces for the entire sequence from the surficial sediments to 122.4 m depth (Ortega-Guerrero et al., 2017). However, for the section analyzed in this work, only fourteen facies are present and the rest occur only in the upper 29 m (Table 1). Based on their facies association, seven lithostratigraphic units that reflect the main stages of Lake Chalco evolution were defined for the entire sequence, of which correspond from unit 4 to unit 7 in the analyzed section in this work (Fig. 2).

The sedimentary facies defined were grouped into clastic, volcaniclastic, organic rich and chemical facies. The clastic facies are the most abundant in the sequence (F5 to F12); they vary from massive to faintly laminated silt with variable content of sand and clay and are composed of siliciclastic minerals. Organic components in these facies are commonly diatoms, ostracods, charophytes, phytolites and charcoal; other components are sponge spicules, testate amoebae, amorphous organic matter, unidentified Arthropoda fragments and occasionally *Phacotus*. The organic rich facies (F14, F15 and F17) are most commonly diatom oozes and occur less abundant as ostracod hashes. Diatom oozes form beds (<3 cm) and laminae; locally they form pairs of light/dark laminae. Ostracod hashes have a variable content of sand-size fraction clasts. The chemical facies (F18 and F19) are carbonate-rich silt beds or laminae and micritic mud. Other minor chemical components are crystals of struvite, vivianite, siderite, calcite and gypsum. Lithostratigraphic units defined from facies association were described by Ortega-Guerrero et al. (2017) and shown in Fig. 2.

3.2. Geochronology

In the upper 35 m of the master sequence, the age-depth model was constructed from fourteen ^{14}C AMS dates obtained from pollen and ostracod concentrates, and two tephrostratigraphic ages markers (Ortega-Guerrero et al., 2017, Table 1 Supplementary Material). For the deeper part of the section beyond the ^{14}C limit, chronology was established by dating zircons extracted from a tephra layer at a depth of 63.5 m using $^{230}Th/U$ (Torres Rodríguez et al., 2015), and including a tie-point at 106 m depth where a major change in sedimentary components, structure and diatom assemblage is considered to correspond to the transition from marine isotopic stage (MIS) MIS 6 to MIS 5 (Ortega-Guerrero et al., 2017; Avendaño-Villeda et al., 2018). The age obtained in by $^{230}Th/U$ dating was 76.7 ± 4.7 ka, whereas the age of the MIS6-MIS5 limit is

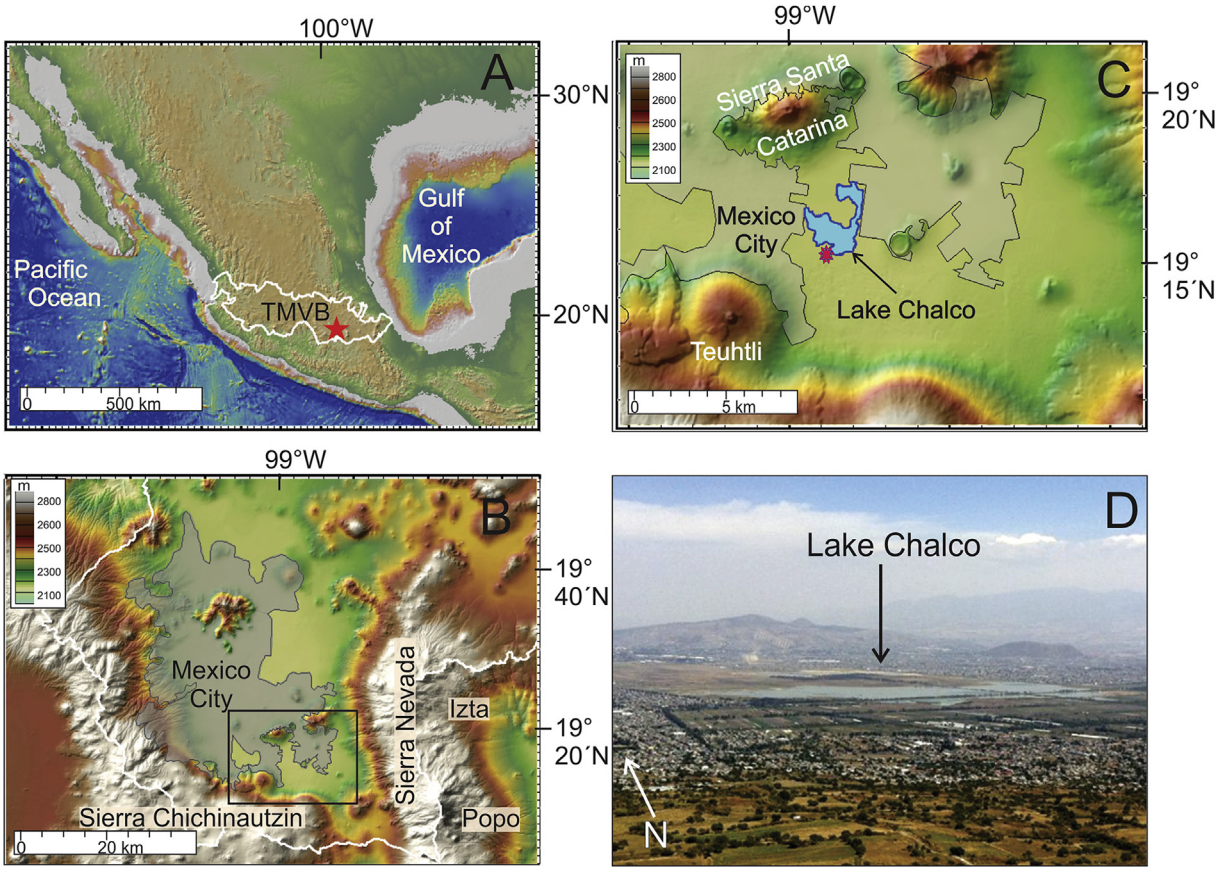

Fig. 1. Location map of Lake Chalco and drilling site. A) Extent of the Trans Mexican Volcanic Belt (TMVB) in central Mexico; red star: location of Basin of Mexico. B) Relief map showing the southern part of Basin of Mexico (white contour). Major stratovolcanoes Popocatepetl (Popo, 5605 m asl) and Iztaccihuatl (Izta, 5460 m asl) of the Sierra Nevada and location of Sierra Chichinautzin are shown. Gray shaded area correspond to the extent of Mexico City metropolitan area. The study area of figure C is outlined in black rectangle. C) Relief map of Lake Chalco and drilling sites of cores CHA08-IV, V and VI (red star). D) Lake Chalco seen from the summit of Teuhtli volcano. (For interpretation of the references to color in this figure legend, the reader is referred to the Web version of this article.)

130 ± 3 ka, according to Lisiecki and Raymo (2005) and Lisiecki and Stern (2016). The age model for the sequence, including the ^{14}C dates, the $^{230}Th/U$ age and the MIS 6-MIS 5 tie point was constructed on a P-sequence deposition model (Bronk-Ramsey, 2008) generated in the online version of OxCal 4.2 (Bronk-Ramsey, 2009) using the IntCal 13 calibration curve (Reimer et al., 2013). The age of the analyzed section of the master sedimentary sequence in this work (29–122 m) was estimated between ca. 35.6 to 150 ka (Ortega-Guerrero et al., 2017) (Fig. 3).

3.3. Geochemical and rock magnetism analyses

The elemental geochemical composition was analyzed using a COX ITRAX X-Ray Fluorescence (FRX) core scanner at 1 cm resolution using a Mo-tube X-ray source set to 30 kV and a current of 20 mA, with an exposure time of 60 s. Although the XRF scanner was capable of detecting 21 elements reliably above detection limits (Al, Si, P, S, Cl, Ar, K, Ca, Ti, V, Cr, Mn, Fe, Zn, Ga, As, Se, Rb, Sr, Zr, W), only a set of elements and their ratios were used in this work (Ca, Ti, Fe, Mn).

Cores were sampled in roughly 10 cm intervals, with minor adjustments to obtain samples from all of sedimentary facies in each core. The 840 samples acquired were placed in 8 cm^3 diamagnetic plastic cubes and stored in a cold room until all measurements were completed. Rock magnetic measurements carried out on the full set of samples consisted of mass-specific magnetic susceptibility (χ), the acquisition of anhysteretic remanent magnetization (ARM), isothermal remanent magnetization (IRM) and hysteresis parameters (saturation magnetization [Ms], saturation remanent magnetization [Mr], coercivity [Bc] and coercivity of remanence [Bcr]). Magnetic susceptibility was measured at low (976 Hz) and high (hf, 15916 Hz) frequencies in a MFK1-FA (AGICO) susceptometer. Frequency-dependent susceptibility was calculated as $\kappa fd\ \% = [(\kappa lf - \kappa hf)/\kappa lf]*100$. ARM and IRM were measured in a JR6 spinner magnetometer. ARM was imparted in a peak alternating field (AF) of 100 mT in the presence of a direct current (DC) bias field of 50 μT. The ARM susceptibility (χ_{ARM}) was obtained by normalizing the ARM by the DC biasing field. The hysteresis parameters were measured using a Princeton Measurements Corporation Micromag vibrating sample magnetometer (VSM) at room temperatures in fields up to 1 T. Saturation IRM (SIRM) was considered to be acquired in a 1 T field. IRM was measured in backfields of 100 and 300 mT after the acquisition of SIRM, and HIRM and S_{300} ratios calculated, where HIRM = 0.5 * (SIRM + $IRM_{-300\ mT}$), and S_{300} = - (IRM_{-300}/SIRM).

In 46 selected samples from the representative magnetic properties, backfield remanence curves in 100 steps were measured in the VSM in order to identify the individual components that contribute to the remanence by using the MAX UnMix program (Maxbauer et al., 2016b). The temperature-dependence of susceptibility (κ-T) was measured for selected samples in a non-controlled atmosphere from room temperature to a maximum of 700 °C using a MFK1-FA (AGICO) susceptometer.

Table 1
Main sedimentological and mineralogical features, compositional parameters for the facies defined for Lake Chalco sedimentary sequence from 29 to 122.4 m depth (Ortega-Guerrero et al., 2017).

Facies	Sedimentological features	Depositional environment
Clastic	5. **Olive brown sandy silt**. Massive to faintly laminated and bedded. Very dark grayish brown laminae (1 cm) and beds (1–2 cm). Abundant biogenic components: diatoms (occasionally partly dissolved), charophyte particles, ostracods and charcoal. Occasional clay size calcareous particles and calcite, dolomite and gypsum crystals.	Shallow lake, minor influence of lotic systems. Perimetral facies with variable phases of vegetation growth.
	6. **Very dark grayish brown to dark reddish brown sandy silt**. Presence of calcareous silt. Massive strata <15 cm thick, and beds 1–3 cm. Undulating irregular contacts. Features of vertical movement of groundwater. Scarce biogenic components: ostracod, diatoms, herbaceous fragments and charcoal.	Palustrine facies. Well drained environment, lixiviation. Subaereal exposure. Slightly to moderately pedogenic processes.
	7. **Dark grayish brown sandy silt**. Discontinuous and wavy, parallel volcaniclastic rich sandy silt beds and silt sediments. Frequent ostracods and calcareous silt. Minor amounts of diatoms.	Low lake levels. May represent distal deposits of detrital fluxes.
	8. **Grayish brown silt to sandy silt**. Decimetric (10–60 cm) massive beds, with intercalations of silt beds (2–20 cm). Sharp and irregular contacts. Sand particles disseminated in beds <15 cm thick, and in irregular bands 1–2 cm thick. Abundant biogenic components: ostracods, diatoms, spicules.	Shallow lake with minor influence of lotic systems, and occasional ash fall.
	9. **Very dark grayish brown clayey silt**. Massive to faintly laminated. Minor amounts of lithic sand. Presence of *Staurosira* spp. and *Staurosirella* spp. Sharp to gradual contacts.	Shallow freshwater lake with minor influence of lotic systems
	10. **Dark olive brown to pale yellow clayey silt**. Diffuse, wavy, parallel beds 4–10 cm. Abundant clay size calcareous (calcite, dolomite) mud. Presence of *Chara* and charcoal. Scarce to common ostracod fragments. In general minor amounts of diatoms.	Shallow alkaline lake.
	11. **Dark olive gray clayey silt**. Mottled and massive at naked eye. Centimetric to decimetric wavy bedding. Presence of clay size calcareous minerals and biogenic components: *Chara* (abundant), ostracods. Diatoms relatively less abundant partly dissolved, charcoal, phytoliths, cysts.	Shallow lake and occasional subaerial exposure.
	12. **Dark olive gray to light gray bedded and laminated diatom rich silt.** Sets of beds (2–6 cm) and laminae. Light strata are diatom ooze with scarce ostracods, detrital crystals (silicates), and calcareous mud. Dark strata are diatom rich silt. Parallel, slightly wavy strata.	Shallow alkaline-saline lake.
Volcaniclastic	13. **Black to gray ash layers**. 74 individual medium to very fine grained mafic to felsic ash layers. Massive to bedded. Frequent ostracods and variable content of diatoms. Thicknesses of 0.5–8 cm. Lower loaded contacts are common. Vivianite occurs in some tephra layers.	Pyroclastic fall deposits and volcaniclastic reworked material of unknown sources. The basaltic to dacitic deposits are more likely form the near monogenetic ranges Chichinautzin and Santa Catarina. Dacitic to rhyolithic deposits are more likely from distal stratovolcano sources.
Organic-rich	14. **Light olive brown to dark olive gray laminated diatomaceous silt and diatom ooze**. Sets of light/dark laminae. Light laminae are composed of diatom ooze dominated by *Stephanodiscus niagarae*, *S. oregonicus*, *Cyclotella quillensis, C. meneghiniana*. Presence of spicules, charcoal, and minor amounts of vivianite and gypsum. Biogenic components are covered by calcareous microcrystals. Dark laminae are composed of calcareous algae, ostracode fragments, testate amoebae, *Phacotus*, and presence of diatoms: *Surirella peisonis*, *Ephitemia* and *C. meneghiniana*.	Relatively deep (few meters), stratified, hardwater facies. Vivianite associated. Variations of saline alkaline and less saline intervals.
	15. **Grayish brown laminated diatom ooze and dark olive gray diatomaceous silt**. Sets of rhythmic light/dark laminae. Light laminae are diatom ooze dominated by *Stephanodiscus. niagarae* and *S. oregonicus*. Dark laminae are silt with minor calcareous components. Abundant diatoms: *S. niagarae*, *Fragilaria capuchina*, *Surirella peisonis*. Presence of ostracodes and scarce *Chara*. Contacts are planar, parallel.	Relatively deep (few meters), stratified, cold to temperate fresh water lake. Anoxic conditions in the hypolimnion (Avendaño-Villeda et al., 2018).
	17. **Ostracod hash**. Commonly with sand-size fraction clasts. Color variable depending on the composition of the clast fraction. Beds 1–3 cm thick. Well preserved ostracod valves. In the facies 11 *Heterocypris* spp. and *Candona* spp. are abundant. Commonly associated to facies 3, 4, 6, 7, 9 and 10.	Shallow lake, dominant endogenic sedimentation. The well preserved ostracod shells indicate low energy environment.
Chemical	18. **Dark gray to pale yellow carbonate-rich silt**. Bedded (2–15 cm thick) to laminated. Silt sized particles of autochthonous carbonate (calcite, dolomite, ankerite). Frequent intercalations of diatom ooze laminae composed of *Cyclotella meneghiniana*, *Anomoeoneis costata* and *Campilodiscus clypeus*, and cm-thick sandy layers of ostracod hash.	Shallower alkaline to saline lake, temperate.
	19. **Pale yellow micritic mud**. Banded (2–5 cm thick). Calcite is dominant, followed by siderite, dolomite, and minor amounts of clay minerals. Abundant diatoms: *S. niagarae*, *C. clypeus, S. oregonicus*, *A. costata*, and frequent ostracods.	Relatively deep (few meters), stratified, temperate, alkaline lake. Anoxic conditions in the hypolimnion (Avendaño-Villeda et al., 2018).

3.4. Diatoms

Sediment samples for diatom analyses were collected on average every 30 cm, and cleaned using HCl, H_2O_2 and HNO_3. Clean material was mounted in permanent slides using Naphrax, and diatom counts were undertaken at 1000× using an Olympus BX50 microscope. Here we present summary results on the relative abundance of small Fragilariaceae and *Stephanodiscus* spp., which are considered indicative of freshwater conditions, and the sum of alkaliphilous and halophilous taxa; these categories were defined according to the species ecological preferences defined by the analysis of diatom species distribution along 40 lakes in central Mexico (Caballero et al., 2019). Main halophilous taxa were *Anomoeoneis costata, A. sphaerophora* and *Camphylodiscus clypeus*; main alkaliphilous taxa were *Cyclotella meneghiniana, N. amphibia* and *Surirella peisonis*. *Stephanodiscus* spp includes *S. niagarae* which

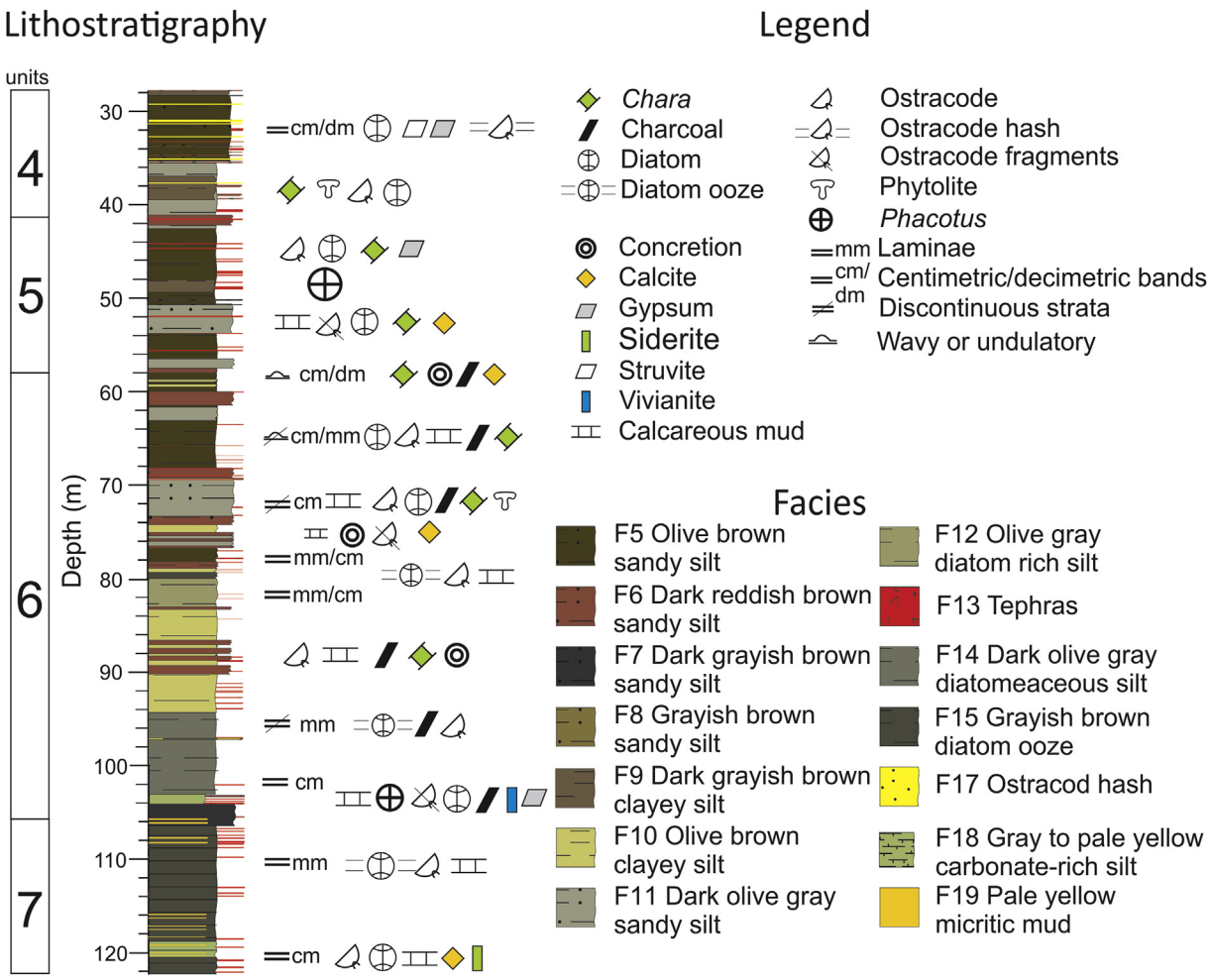

Fig. 2. Lithostratigraphy of the master sequence of cores CHA08 IV-V-VI from 29 to 122.4 m depth, showing the lithostratigraphic units 4–7 described in Ortega-Guerrero et al. (2017).

besides being indicative of freshwater conditions is also considered indicative of cooler conditions (Avendaño-Villeda et al., 2018).

4. Results

4.1. Downcore profiles

The diatoms have a distinctive distribution along the record, which mostly correlates with the lithostratigrphic units (Fig. 4). Geochemical composition and magnetic properties are strongly facies-dependent and most parameters and ratios show a good correlation with the lithostratigraphic units. Therefore, the results are described following the lithostratigraphic boundaries. The geochemical elemental ratios used are: Ca/Ti as an indicator of authigenic carbonates (e.g. Haberzettl et al., 2007); Mn/Fe as an oxidation proxy (e.g. Oliva-Urcia and Moreno, 2019); and Fe/Ti is used to identify iron diagenetic enrichment (e.g. Aufgebauer et al., 2012) (Fig. 4.).

Concentration-dependent parameters of magnetic minerals are shown in Fig. 5 and they include magnetic susceptibility (χ), χ_{ARM}, SIRM and $HIRM_{300}$. Particle-size dependent parameters include fine particle-size (SD) indicator ratio κ_{ARM}/IRM_{100} and ultrafine superparamagnetic (SP) particle-size indicator κfd %; and coercivity-dependent $HIRM_{300}$ and S_{300} ratios and parameter Bcr. They were plotted with a 5-point running average (black lines), except for the κ_{ARM}/IRM_{100} ratio. The tephra layers were excluded in the downcore magnetic profiles, in order to highlight the environmental implications of the magnetic properties results.

Unit 7 (122.4–106 m depth).

The basal unit is dominantly composed of regularly laminated sets of rhythmic light/dark fine laminae of facies 15. The diatom assemblages are dominated by freshwater taxa (*Stephanodiscus niagarae* and *S. oregonicus*), which in this unit reach their highest concentration. At the lower part of the sequence, there is a 1.5 m thick deposit of the carbonate-rich silt of facies 18. There are also 13 beds of micritic mud (F19). Peaks in Ca/Ti ratio correlate to these micritic beds and the facies 18 sediments, but in general this ratio in facies 15 sediments is rather low. This behavior is also observed in the Mn/Fe ratio. Fe/Ti relation in this unit shows the highest values in the whole sequence, and they are particularly high in the carbonate rich sediments of facies 18 and 19.

Concentration-dependent parameters χ, χ_{ARM}, SIRM and $HIRM_{300}$ show a similar pattern. Variable but high values below 118 m depth are found in the basal sediments of facies 15 and in the carbonate-rich sediments of facies 18 (χ 0.04–0.2 10^{-6} m^3/kg, χ_{ARM} 0.2–2 10^{-6} m^3/kg, SIRM 0.5–5 mAm^2/kg and $HIRM_{300}$ 0.02–0.6 mAm^2/kg). The lowest values are present where the micritic mud beds of facies 19 are more frequent, while some maxima are associated with volcaniclastic deposits. The κ_{ARM}/IRM_{100} presents its highest values below 118 m depth (~0.007 m/A), and remains

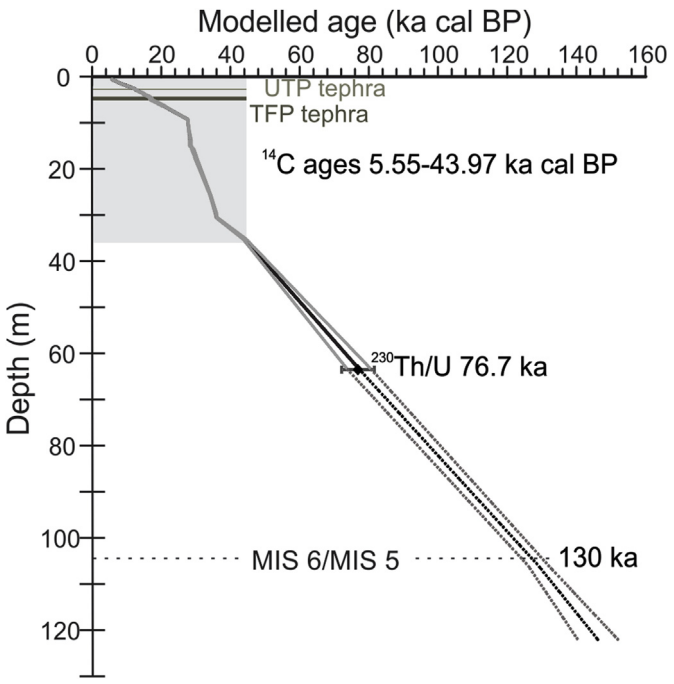

Fig. 3. Chronology of the Lake Chalco sedimentary sequence. The P-sequence model generated with calibrated ^{14}C values (shaded area) and ages of the Upper Toluca Pumice (UTP), Tutti Frutti Pumice (TFP), the $^{230}Th/U$ age and the age boundary of MIS 6/MIS 5 (Table 1 Supplementary Material).

mostly constant upwards the record. The κfd% is very variable (as in all the record), with average values 3–6%. The upper section of this unit (above 118 m depth), presents some of the lowest concentration-dependent parameters values in all the record; χ is mostly lower than 0.08 10^{-6} m^3/kg, χ_{ARM} ranges from 0.05 to 1.9 10^{-6} m^3/kg, SIRM varies from 0.3 to 4.7 mAm^2/kg and $HIRM_{300}$ from 0.01 to 0.5 mAm^2/kg. This unit presents some of the lowest coercivity values of the entire record. $HIRM_{300}$, S_{300} and Bcr present similar variations, the higher coercivity is found in the sediments of facies 18 ($HIRM_{300}$ ~ 0.5 mAm^2/kg, S_{300} ~ 0.75, Bcr ~ 120 mT), the lowest in the sections with higher abundance of facies 19 sediments ($HIRM_{300}$ 0.001–0.08, S_{300} 0.8–0.9, Bcr 52–80), while the facies 15 sediments present intermediate values. The κfd% shows large variations (1–10%); it peaks where concentration is high (ca. 114 m depth), and in general is lower between 113 and 106 m depth (average 1–6%).

Unit 6 (106–57.5 m depth).

A sharp change is recorded in most parameters at 106 m depth, with the onset of sediments of facies 7. Calcareous biogenic components (*Chara* sp., ostracods, calcareous particles and some *Phacotus* loricas) are common in the entire unit. Higher Ca/Ti ratio is also a common characteristic of this unit. Diatoms decrease their concentration in relation to the previous unit, and are dominated by alkaliphilous and halophilous species such as *Cyclotella meneghiniana* or *Campylodiscus clypeus*, and large struvite crystals are found, as well as occasional calcite and gypsum. This pattern is interrupted at around 100 m depth, where the laminated sediments of facies 14 are dominated by freshwater *Stephanodiscus* spp. diatom taxa and diatom concentration slightly increases. This variation is also observed in the decrease of Ca/Ti ratio. Upwards, there are several changes in facies association and calcareous clayey silt massive sediments of facies 10 (up to 83.3 m depth), and facies 11 and 5 become dominant towards the top of the unit. Along the unit, the sandy facies 6 are frequent. Sediments of facies 6, 7, 10, 11

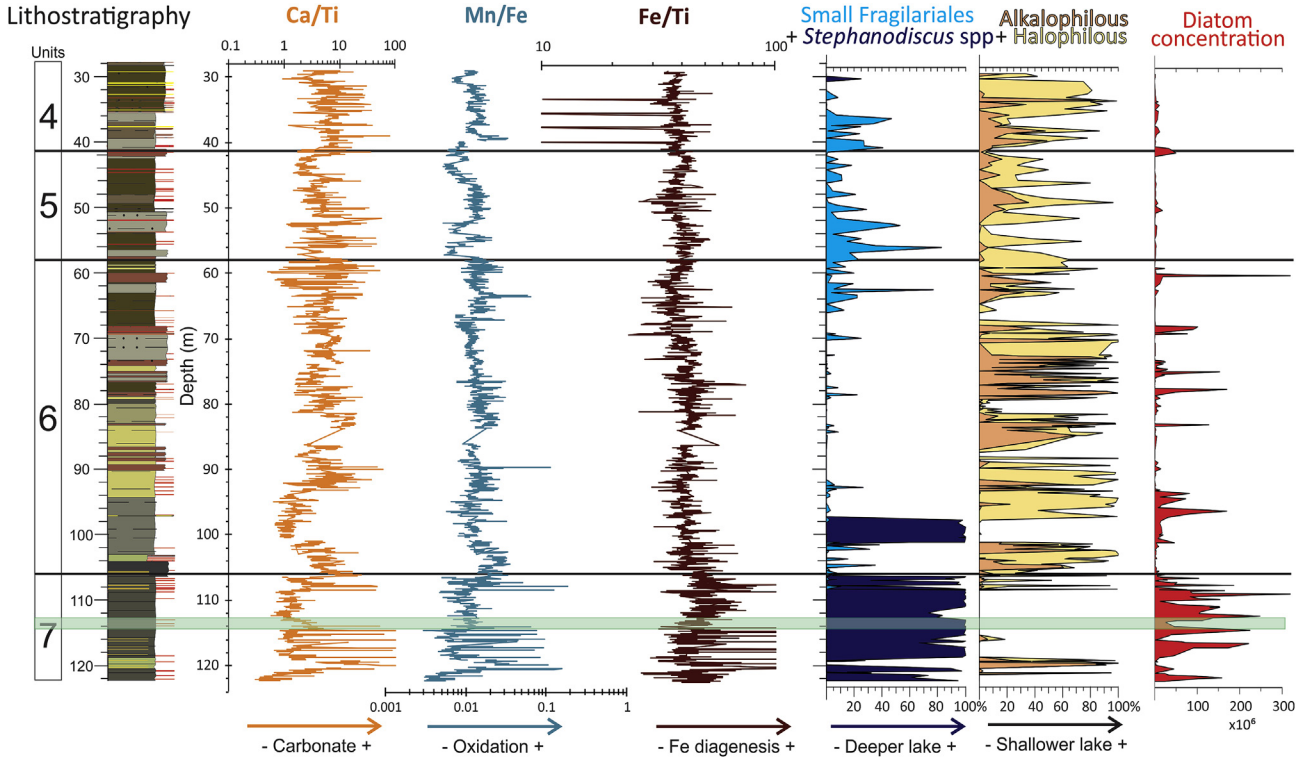

Fig. 4. Lithostratigraphy of master sequence of CHA08 cores and geochemical data. Ca/Ti is an indicator of authigenic carbonate in the lake. Mn/Fe ratio is an oxidation indicator. Fe/Ti is a proxy of diagenetic Fe enrichment. Freshwater diatom taxa (small Fragilariales and *Stephanodiscus* spp.), and alkaliphilous and halophilous taxa show nearly an opposite distribution. Diatom concentration is expressed in 10^6 valves/gram of dry sediment.

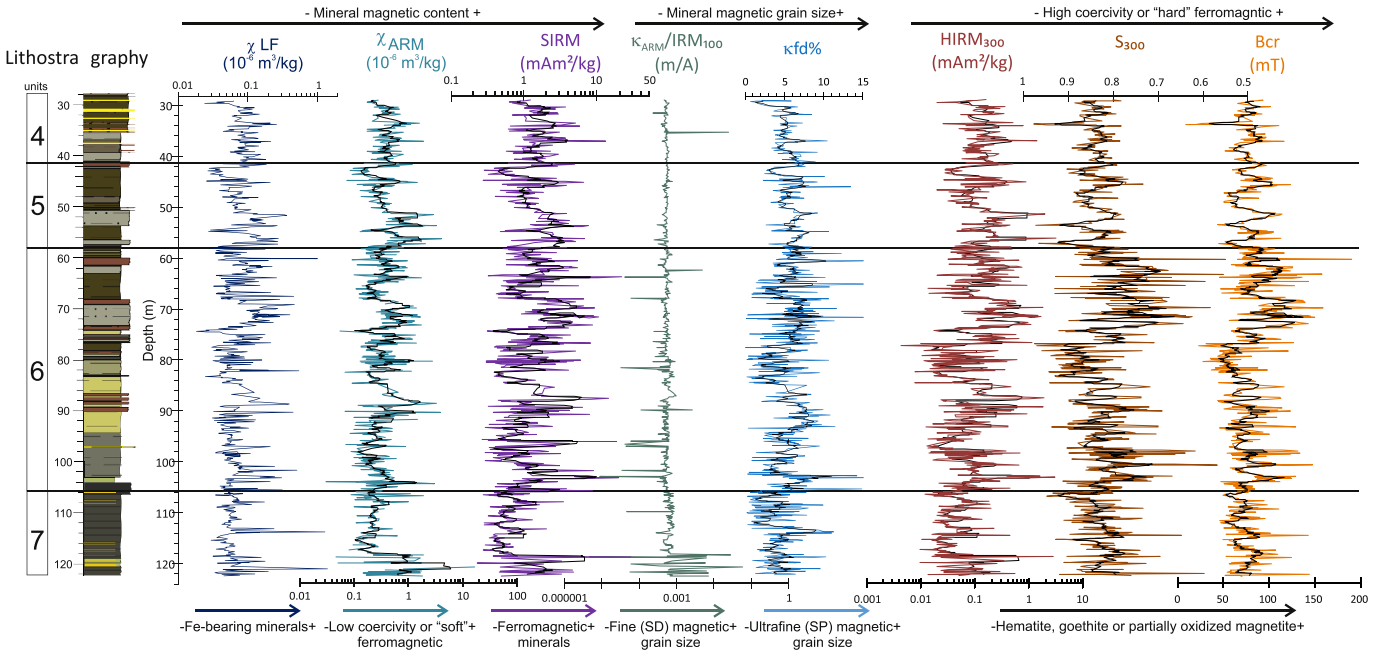

Fig. 5. Down-core profiles of magnetic parameters of CHA08 Lake Chalco cores. Concentration-dependent parameters χ, χ_{ARM}, SIRM and $HIRM_{300}$, grain size-dependent ratio κ_{ARM}/IRM_{100} and κfd%, and magnetic mineralogy indicators $HIRM_{300}$, S_{300} and Bcr. The black lines are 5-point running average.

and 18 present relatively high Ca/Ti. Mn/Fe ratios are relatively high in the lower part of this unit, in facies 7 and 18. Fe/Ti remains relatively constant along this unit.

Most of the magnetic parameters show their highest amplitude fluctuations along this unit. χ, χ_{ARM}, SIRM, κfd%, $HIRM_{300}$ and S_{300} have their highest values in the lower part of the unit, in facies 18 and 14, and in the sandy sediments of facies 6 and 11 (χ 0.06–4.5, χ_{ARM} 0.2–1.5, SIRM 1–20, κfd% 3–15%, $HIRM_{300}$ 0.1–1.8); and the lowest in the facies 10, 12 and 5. The coercivity parameters also show a strong correlation among them and with the sedimentary facies. As in the case of the concentration parameters, the highest coercivities are found in sediments of facies 18, and in the sandy sediments of facies 11, 7 and 6 (S_{300} 0.55–0.7, Bcr 70–160); while the lowest coercivities are present in the facies 10, 12 and 5.

Unit 5 (57.5–41.1 m depth).

This unit is comprised mainly by the sediments of facies 5 and 11, and occasionally by the facies 9 and 6. Below 50.6 m depth the sediments are mostly massive with mottled intervals, and above this depth are bedded at centimetric to decimetric scale. Calcareous organic and inorganic components are common. Diatoms are a minor constituent, small Fragilariales, which have their highest abundances in this unit, alternate with alkaliphilous and halophilous diatoms. Where facies 11 and 6 sediments are present, Ca/Ti (~10–50) and Mn/Fe (~0.01–0.02) are relatively higher. Fe/Ti shows minor fluctuations between 30 and 50.

Magnetic mineral concentration proxies show their highest values in the unit at its bottom, where the sandy sediments of facies 11 are more abundant (χ 0.1–0.35, χ_{ARM} 0.4–4, SIRM 1–8, $HIRM_{300}$ 0.06–3). Concentration parameters values decrease upward, above 50 m depth, in facies 5 sediments (χ ~ 0.04, χ_{ARM} 0.08, SIRM ~ 0.3, $HIRM_{300}$ ~ 0.03). Several higher values are associated to clastic-rich sediments of facies 5 around 45 m depth. Coercivity variations are similar to those found in the concentration parameters. Coercivity is higher in facies 11 sediments ($HIRM_{300}$ ~ 3, S_{300} ~ 0.78, Bcr ~ 120), and diminishes in the upper part of the unit, except around 45 m depth where concentration values increase. κfd% varies in average 4–8%.

Unit 4 (41.1–29 m depth).

This unit is composed mainly by facies 5 and 11 and in lower proportion by facies 6, 9 and 17. Sediments of facies 5 have higher sand-size clastic content than in lower beds of the same facies. Sediments are mostly massive, centimetric and decimetric beds are visible at some intervals. In the lower section (41.1–35.5 m depth) the same alternation between the small Fragilariales and the alkaliphilous and halophilous diatoms is observed. In the upper part of this unit, the higher frequency of ostracod hash beds of facies 17 is characteristic. *Chara* sp. is also a main biogenic carbonate producer present in this part. Diatoms are occasionally partly dissolved and dominated by alkaliphilous and halophilous species as *Cyclotella meneghiniana*, *Nitzschia frustulum*, *Navicula elkab* and *Chaetoceros* spp. Ca/Ti ratio shows high values, mostly 3–10, with peaks (30) in facies 6 and 17. Mn/Fe and Fe/Ti present rather uniform values, similar to those of the lower part of unit 5.

Magnetic mineral concentration and coercivity are relatively high along the unit (χ ~ 0.06–0.25, χ_{ARM} 0.2–2, and SIRM 0.7–6; $HIRM_{300}$ 0.06–0.5, S_{300} 0.78–0.88, Bcr 60–120). Slightly lower concentration values are found in facies 9 sediments around 38 m depth, in facies 5 sediments at ca. 33 m depth, and in the topmost sediments of this unit. Coercivity fluctuations are also analogous to the observed in concentration, it is lower in facies 9 and 5, and relatively higher in the rest of the sediments. κfd% has no clear relationship with the sedimentary facies, it varies between 4 and 7% in average in most of this unit, and decreases at the top of the sequence.

4.2. Magnetic properties of sedimentary facies

4.2.1. Temperature-dependence of susceptibility (κ-T)

The thermomagnetic analyses show in all cases an increase in magnetic susceptibility after heating. The cooling curves (Fig. 6, blue lines), reflect the formation of new magnetic minerals during the heating (Fig. 6, red lines). The first derivative of the heating and cooling curves helps to identify the range of temperatures at which the main inflection of these curves occurred. The subtle inflection

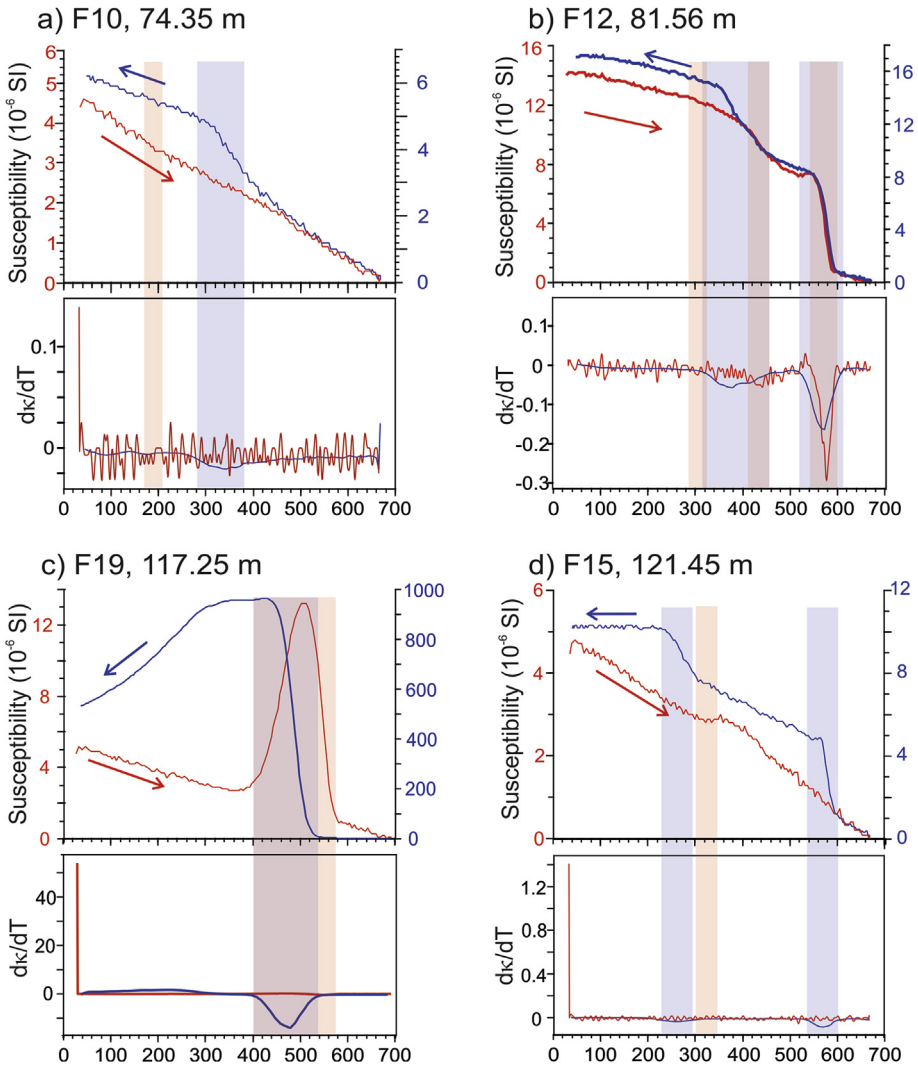

Fig. 6. Thermomagnetic curves (κ vs. temperature, or κ-T) for selected samples of different facies (Fx) and depths (m) from Lake Chalco. First derivative curve (dκ/dT), show the main inflections of the heating (red rectangles) and cooling (blue rectangles) curves. Note the different scales of magnetic susceptibility (κ) for the heating curves (red) and the cooling curves (blue). (For interpretation of the references to color in this figure legend, the reader is referred to the Web version of this article.)

found near 200 °C in several samples corresponds to the Curie temperature (TC) of Ti-rich titanomagnetite (Fig. 6a). The TC range from 400 to 500 °C correspond to Ti-poor titanomagnetite, and the TC near 580 °C correspond to almost pure magnetite (Fig. 6b). The samples containing Ti-magnetite/magnetite content show the most reversible curves of all samples (Fig. 6a and b). In these samples, the cooling curves indicate the persistence of these more thermally stable mineral phases after heating.

Some samples exhibit an inflection around 300 °C in the heating curves and a large increase in κ in the cooling curves, which may be due to the inversion of Ti-maghemite (Fig. 6b and d) (Özdemir and O'Reilly, 1982; Liu et al., 2005). Carbonate rich sediments have a singular upward peak between 400 and 580 °C during warming (Fig. 6c), a behavior typical of the transformation of siderite into magnetite (Housen et al., 1996; Isambert et al., 2003; Vázquez-Castro et al., 2008). In this sample (Fig. 6c), the 100-fold increase in κ after heating is remarkable.

All samples measured show a decrease in κ during heating in temperatures higher than 600 °C, which indicate the presence of Ti-hematite or hematite. These mineral phases may correspond to detrital minerals, or to the transformation of titanomaghemite into (Ti)-hematite, which in turn is transformed into magnetite during the cooling process.

4.2.2. *Hysteresis properties*

The Day diagram (Day et al., 1977; Dunlop, 2002a, 2002b), represents the distribution of coercivity and magnetization parameters. However, as the diagram has been shown to be ambiguous for the definition of domain states (Roberts et al., 2018), caution should be taken when using it as a guide to particle sizes. However, the distribution in the diagram can provide information about environmental processes (e.g. Rodelli et al., 2019). Samples fall on the PSD region, some of them close to the SD + SP mixture curve (Fig. 7a), but overall most of them plot away from the MD region. Selected samples from representative sedimentary facies in the Day diagram show the variability of hysteresis parameters within certain facies (Fig. 7b); for instance, sediments of facies F5 and F6 plot along the main extremes of all sample population. In general terms, the sediments with a higher content of sand-size grains plot in the PSD region towards the MD area, whereas those samples with finer-size particles plot close to the SD + SP mixing lines. Samples from tephra layers are displayed to emphasize the

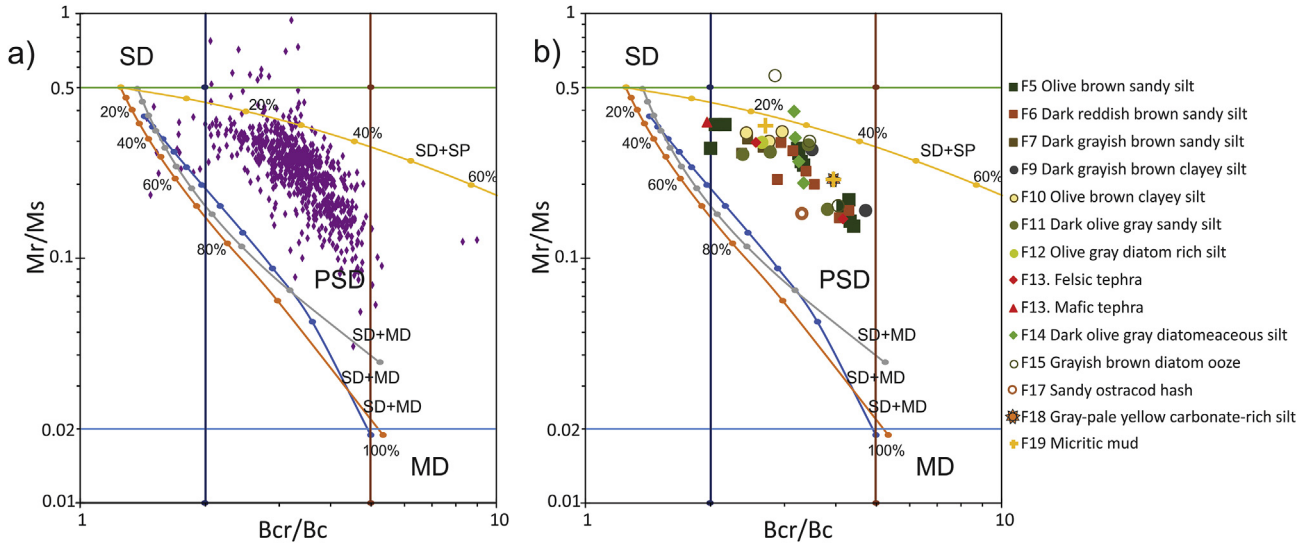

Fig. 7. Day plot (Mr/Ms versus Bcr/Bc) (Day et al., 1977). For the full data set (a), and selected samples with their sedimentary facies indicated (b). Theoretical mixing curves for magnetite mixtures are from Dunlop (2002a, 2002b).

range of coercivity and magnetization that relatively pristine grains may present.

4.2.3. Decomposition of IRM demagnetization curves

IRM demagnetization measurements were conducted on a collection of samples representative of the different sedimentary facies. The decomposition of the IRM curves allows to quantify the changes of the different fractions of magnetic mineralogy that contribute to the magnetic remanence, and therefore estimate the origin of the individual contributions and their variability over time. After unmixing of the IRM (Maxbauer et al., 2016b), most samples present 3 components, and a few are composed of 2 or 4 components (Fig. 1 Supplementary material, Table 2 Supplementary material). A very low coercivity component of a mean coercivity (Bh) < 20 mT, with a dispersion parameter (DP) from 0.11 to 0.70, and an observed contribution (OC) from 3 to 30% of the total signal, is present in most samples. This is attributable to pedogenic or detrital soft magnetite (Egli, 2004; Lascu and Plank, 2013). Components of intermediate coercivity have [1] Bh 20–30 mT (DP 0.26–0.67; OC 6–23%), [2] 30–60 mT (DP 0.17–0.53; OC 7–97%), and [3] 60–100 mT (DP 0.20–0.45; OC 6–87%), respectively. The intermediate coercivity component [1] is typical of coarse detrital magnetite (Egli, 2003). The average DP observed for the intermediate coercivity [2] and [3] components are in general higher than values reported for low and high coercivity magnetofossils, 0.19 and 0.15, respectively (Egli, 2004), which indicates that the higher DP components correspond to non-biogenic or altered magnetite crystals. Components of relatively higher coercivity have a Bh 100–125 mT (DP 0.35–0.48; OC 54–91%), 125–200 mT (DP 0.20–0.41; OC 46–78%), and >200 mT (DP 0.12–0.42; OC 1–7%). These higher Bh components can be interpreted as the contribution of oxidized magnetites/maghemites (van Velzen and Dekkers, 1999; Chen et al., 2005) or ultrafine hematite (Maxbauer et al., 2016c). Fig. 8 emphasizes the broad distribution of coercivities (Bh) and the large dispersion (DP) of modelled components in all the sedimentary facies of Lake Chalco. Only a constrained population of the mineral components have coercivities and narrow DP distribution to be considered as low coercivity magnetofossils, samples from facies 15 (118.19 and 121.47 m) and from facies 5 (54.84 and 66.5 m depth) (Table 2 Supplementary material). The relative percent contributions are summarized and shown according to the stratigraphic position in Fig. 5.

5. Discussion

5.1. Origin of magnetic minerals in cores CHA08 sediments

The results of our rock magnetic study show that the remanence is controlled mostly by low coercivity (Bh < 125 mT) ferromagnetic minerals, held by detrital partially oxidized Ti-magnetite/maghemite according to the κ-T measurements. The detrital components have large DP, which implies a large grain size range. The range of coercivities found in the low coercivity (Bh < 125 mT) fraction may be due to different degrees of partial oxidation of Ti-magnetites. As (Ti)-magnetites are the most common detrital magnetic mineral in the volcanic rocks that outcrop in the basin, it is feasible that different degrees of partial oxidation of Ti-magnetites (via maghemitization) increased the range of coercivities of original minerals (e.g. van Velzen and Dekkers, 1999), and consequently increased the Bh and DP. The oxidation occurs at the borders of the grains inwards, while Fe^{2+} is oxidized and removed from the crystal (Maxbauer et al., 2016c). As the diffusion of Fe^{2+} progress, an oxidized (maghemitized) shell is formed around an unoxidized (magnetite) core (Ge et al., 2014). The low-temperature oxidation of (Ti) magnetite to (Ti) maghemite can occur under oxic conditions in soils of the catchment area during weathering or diagenetic processes (e.g. van Velzen and Dekkers, 1999; Chen et al., 2005). The effect of the oxidation may be large in Ti-magnetites, increasing Mr/Ms and hardening the coercivity (Roberts et al., 2018), and this could cause the shift in the position for the most oxidized samples towards the top in the Day plot (Fig. 7).

In addition to Ti-magnetites/maghemites, the component of higher coercivity identified (Bh > 125 mT), suggests also the presence of hematite or goethite. The κ-T measurements also suggest the presence of hematite. In soils, goethite is favored in cool and moist conditions that only rarely experience prolonged intervals of aridity (e.g. Maxbauer et al., 2016c). By contrast, hematite is more abundant in subtropical or tropical soils with frequent episodes of prolonged dryness (e.g. Cornell and Schwertmann, 2003). The alteration of magnetite/maghemite or clay minerals, and the

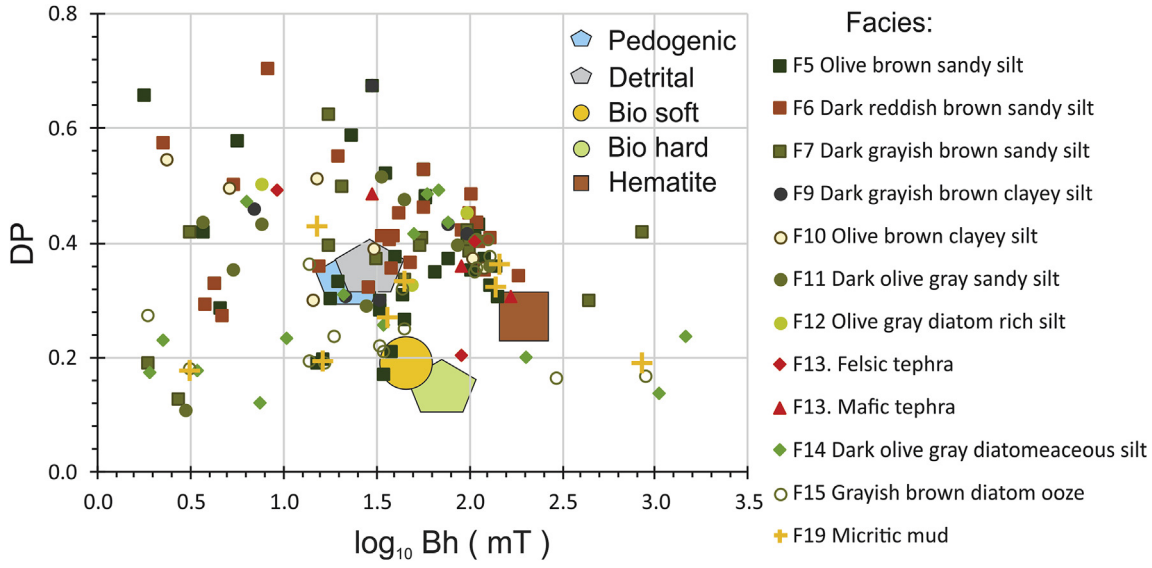

Fig. 8. Plot of the median coercivity (Bh) versus dispersion parameter (DP) for the magnetic components of sedimentary facies from Lake Chalco. The magnetic components were obtained from the unmixing of IRM demagnetization curves (Maxbauer et al., 2016b). Large symbols represent the end-members defined by Egli (2003, 2004) for pedogenic magnetite, detrital, low-coercivity magnetofossils (bio soft), high coercivity magnetofossils (bio hard) and hematite components.

dehydratation of goethite to hematite, can result in the formation of hematite (Maxbauer et al., 2016c). Hematite tends to have broad coercivity spectra that extends from low to high values, depending on the grain size; fine-grained hematite (16–100 nm) have coercivity values of ~10–200 mT, while large hematite crystals (0.1–2 mm) have even lower coercivity values of ~10–30 mT (Özdemir and Dunlop, 2014). Given the Bh values of the higher coercivity components in Lake Chalco sediments (>125 mT), they could reflect fine-grained hematite.

The relative abundance of the softest magnetic component (Bh < 20 mT), which can be attributable to pedogenic or detrital magnetite, was found in most of the analyzed samples. This soft component has no apparent clear relationship with the sedimentary facies or stratigraphic position, which make us think it can be both of origins. The presence of ultrafine SP minerals is suggested by κfd% > 6% in all units, in particular in unit 6 sediments (Fig. 5; Table 2 Supplementary Material), but they may have several possible origins and mineralogy. They can be either authigenic, detrital pedogenic, or magmatic minerals included in the detrital silicates, both magnetite or hematite. The formation of new minerals concerning redox processes is an aspect that is discussed later. The interplay between the magnetic minerals and past climatic fluctuations is discussed below.

5.2. Paleoenvironmental implications

The deposition of Unit 7 sediments occurred between ca. 146 to 130 ka (122.4–106 m depth), during the late part of Marine Isotopic Stage 6 (MIS 6, 191-130 ka BP), in cooler than present conditions as inferred from the presence of *Stephanodiscus* spp., a genus that today has a very restricted distribution in Mexico, but that was abundant in sedimentary sequences dating to the last glacial maximum in several records from the region (Bradbury, 2000; Metcalfe et al., 1991; Caballero et al., 2002; Valadez et al., 2005) (Fig. 9). The diatoms indicate also a fresh and relatively deep lake and thus relatively humid conditions (Avendaño-Villeda et al., 2018), a deep lake with anoxic bottom conditions was also favorable for the preservation of bands and laminae in the sediments. Diatom productivity is at its highest during this period. In the sediments below 118 m depth (ca. 146-141.5 ka, facies 15 and 18), the locally high χ_{ARM}, κ_{ARM}/IRM and κfd% values suggest the presence of SD and SP particles in some horizons, although it has been documented that interacting SP or PSD particles behave as SD (Muxworthy et al., 2003). In this section, the coercivity analysis shows that ~60% of the coercivity has a mean Bh of ~107 mT (Fig. 5), which is attributable to partially oxidized Ti-magnetite. However, there is also a magnetically soft component that contributes ~20% to the remanence, which may correspond to soft magnetosomes (Bh ~ 33 mT, DP ~ 0.2) (Egli, 2004; Lascu and Plank, 2013). The high values of χ and SIRM indicate higher ferrimagnetic (e.g. magnetite) mineral content, and higher Fe/Ti ratios point to an iron diagenetic enrichment, or lack of dissolution, which we suggest represents the magnetosomes. In agreement with the preserved laminae, this implies the existence of an oxic-anoxic interface, where the magnetotactic bacteria exist (Moskowitz et al., 2008). Therefore, the magnetic properties indicate that, in the lowest section of the record, higher sedimentary input by runoff under wetter environments coexisted with lower oxygen concentrations at the water/sediment interface, conditions that temporally favored the formation and preservation of magnetotactic bacteria. Together, these processes resulted in the accumulation of detrital Ti-magnetite and fine-grained non-interacting SD equidimensional magnetite in the sediment (Egli, 2004; Lascu and Plank, 2013). At around 120 m depth (ca. 144 ka) the lake records a temporary change in environmental conditions. The facies 18 carbonate-rich sediments, the lower diatom concentration dominated by alkaliphilous and halophilous species and the higher values of Ca/Ti and Mn/Fe, indicate higher salinity, oxic bottom water conditions and thus suggest a lowering in lake level. The magnetic mineral parameters are highly variable in this section, but a moderate increase in coercivity is observed. Later on, a return to the previous higher lake level and anoxic bottom-water conditions is recorded.

In the upper part between 118 and 106 m depth (ca. 141.5-130 ka), where the laminae are best preserved, magnetic mineral concentration parameters decrease, large MD grains (low κ_{ARM}/IRM) were found, and coercivity analysis point to the lack of magnetosomes. This suggests a change in environmental conditions with respect to the previous stage. Siderite was observed in the

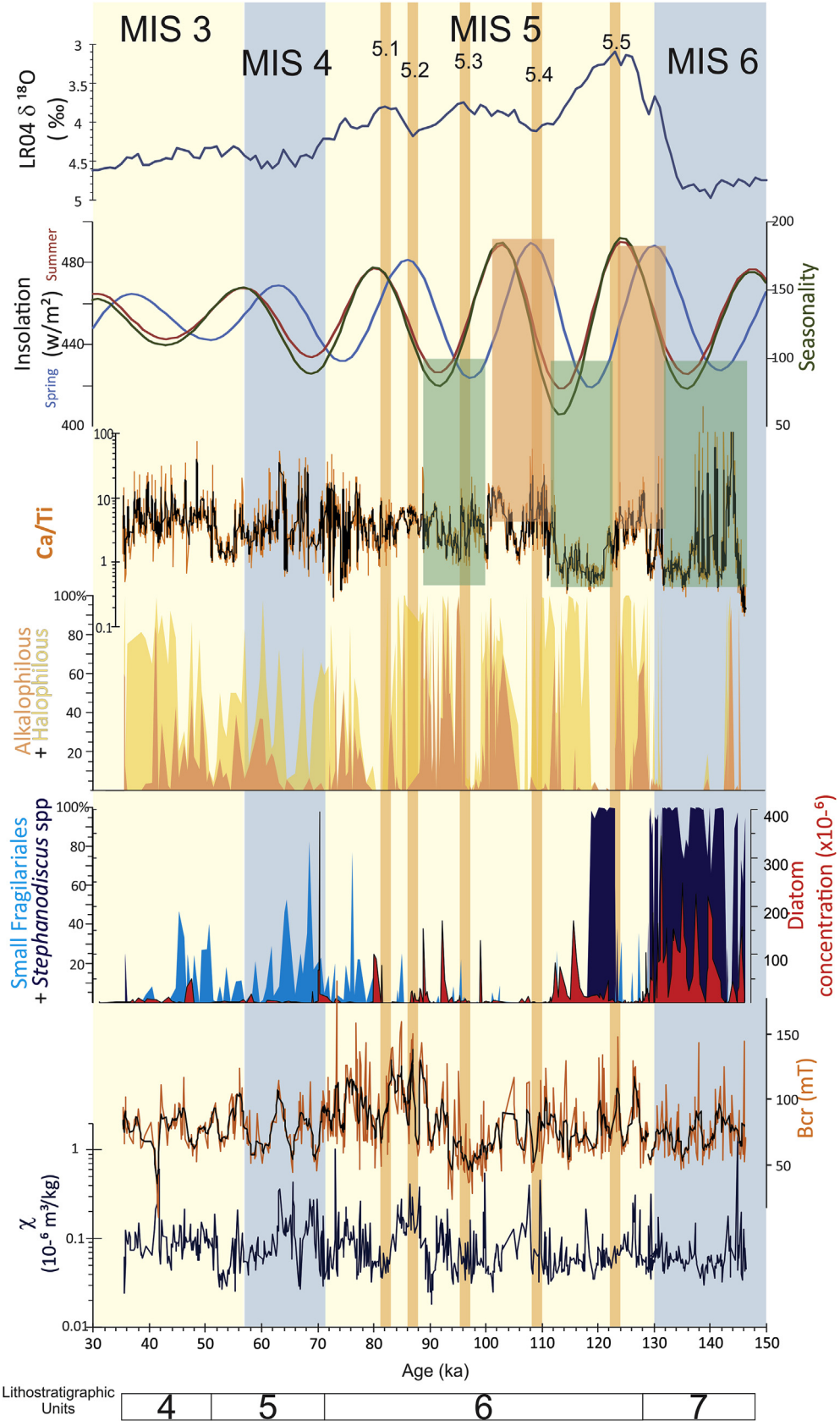

Fig. 9. Selected concentration (χ) and coercivity (Bcr) rock magnetic parameters, diatoms and carbonate content (Ca/Ti, 7-point-running average in black), plotted in time scale (ka) along the lithostratigraphic units, spring and summer insolation curves for 20°N obtained in the AnalySeries software (Paillard et al., 1996) according to the Laskar et al. (2004) solution, seasonality (summer-winter insoltation), and the benthic $\delta^{18}O$ LR04 stack (Lisiecki and Raymo, 2005). Diatom record of deeper lake levels (Fragilariales and *Stephanodiscus* spp.) is plotted along diatom concentration. Blue shades indicate the cooler marine isotopic stages (MIS) 6 and 4, and pale yellow shades indicate the warmer MIS 5 and 3, and peaks of substages 5.5–5.1 (according to the Lisiecki and Raymo, 2005 nomenclature). Orange (green) shades point the occurrence of drier (less dry) conditions that correlate with maxima (minima) of spring and summer insolation. (For interpretation of the references to color in this figure legend, the reader is referred to the Web version of this article.)

carbonate rich sediments of this section, where Fe/Ti has some of the highest values in the record and Ca/Ti shows extreme peaks. κ-T measurements also pointed to the presence of siderite in the warming curve, which showed a characteristic peak above 400 °C as converted to magnetite (Housen et al., 1996; Vázquez-Castro et al., 2008). Under anoxic-non-sulfidic conditions, magnetite is unstable and may transform to siderite ($FeCO_3$) (Berner, 1981). The decrease in κ_{ARM}/IRM ratio and the lower κfd% indicate a coarsening of magnetic minerals. These characteristics suggest the preferential dissolution of the finest Fe-oxide magnetic minerals under reducing-non-sulfidic conditions and the re-precipitation of the paramagnetic siderite. A deeper lake with periods of anoxic reducing conditions in the bottom may have prevented the preservation of magnetosome crystals, if they were formed at all. As the diatom assemblages in the micritic mud are mostly of freshwater habitats (Avendaño-Villeda et al., 2018), higher biological productivity must trigger an increase of pH and reduced the solubility of carbonates (Kelts and Hsü, 1978), promoting the precipitation of calcite and occasionally siderite in an anoxic bottom.

In this section, between 118 and 106 m depth, the most abundant magnetic component (~46–70%) is consistently harder (Bh 126–144 mT, DP 0.3–0.4) than in the lower part. This relatively hard phase may correspond to highly oxidized detrital Ti-magnetite/maghemite, hematite or goethite. We cannot make a definitive conclusion about the presence of goethite as our saturating fields (1 T) were too low to magnetize this mineral (Rochette et al., 2005). Hematite is less reactive in reducing environments than Ti-magnetites (Franke et al., 2007; Garming et al., 2007), whereas goethite is likely to have formed in the soils during the, in general, moist and cool climates inferred from diatoms. Regardless the composition of the Fe-oxides present, this implies that, in spite the existence of recurring anoxic conditions inferred for this section, the dissolution did not affect the totality of the Fe oxides and coarser particles were preserved (Jelinowska et al., 1997). The end of the MIS 6 (ca. 132-130 ka, 108.5–106 m depth) is characterized by oscillations in the diatom concentration and species, showing fluctuations between freshwater Fragilariales and halophilous and alkaliphilous species, which suggest relatively short-term alternations between drier and moister climate.

A change in environmental conditions is clearly observed in sedimentological, geochemical and magnetic characteristics and the diatom record after ca. 130 ka (106 m depth), at the beginning of the last interglacial (Fig. 9). Variations in magnetic parameters (mainly concentration and coercivity) are coeval with the change in facies deposition. The increase of the calcareous sedimentary components is reflected in increased Ca/Ti and in the alkaliphilous and halophilous diatoms. More oxic environment (>Mn/Fe) allowed the preservation of Fe oxides, and the diatom concentration records the lowest values (Fig. 5). The low concentration of diatoms may be a result to dilution by higher clastic components input (silt and clay), and lower diatom productivity during drier periods with higher lake salinity.

In units 6, 5 and 4, κ-T measurements and unmixed demagnetization of IRM curves indicate that the magnetic mineralogy is essentially the same, partially oxidized detrital Ti-magnetites are the main magnetic carriers and a smaller fraction (<21%) that may correspond to pedogenic magnetite (Bh < 20), and only the proportion among the fractions of different coercivity varies. Higher $HIRM_{300}$ also point to higher production of magnetically harder minerals (e.g maghemite, partially oxidized magnetite, hematite or goethite), especially in Unit 6 sediments (Fig. 5). The frequency dependence (κfd%, 2–5%, mean 5%) found in units 6, 5 and 4 indicates the existence of ultrafine SP minerals, which may be associated with the pedogenic component. Hematite may also be present, but its origin is probably secondary as a result of low-temperature oxidation of primary Ti-magnetite.

The changes in the concentration and in the coercivity spectra are related to the variability in the magnetic mineralogy. The carbonate-rich sediments tend to have higher coercivities and also higher abundance of alkaliphilous and halophilous diatoms (Fig. 9). The carbonate precipitation, the diatom species and the abundance of calcareous components as ostracods and *Chara*, indicates a saturated water column, a shallower lake, and in consequence environments with negative evaporation/precipitation balance. This suggests that higher oxidation of Ti-magnetites occurred during dry periods. The amplitude of fluctuations of rock magnetism parameters is higher in Unit 6, which is roughly coincident with MIS 5 (130-71 ka), but decrease in units 5 and 4, whose sediments were accumulated approximately during MIS 4 (71-57 ka) and the early part of MIS 3 (57-35 ka), respectively.

During the global warmer temperatures of MIS 5 occur the highest amplitude variability of the analyzed proxies. The maximum in coercivity parameters (e.g. Bcr) and alkaliphilous and halophilous diatoms, along with calcareous sedimentary components and higher carbonate content (>Ca/Ti), indicate that higher evaporation and prolonged dry periods during warmer conditions alternated with less dry and probably temperate environments (Fig. 9). At the early MIS 5 (ca. 130-123 ka, 106-101 m depth), the increases in sedimentary input (>χ), in coercivity (Bcr), in the geochemical ratios Ca/Ti and Mn/Fe, and the dominance of alkaliphilous and halophilous diatoms, mark the onset of dry conditions. This interval was followed by a return of a phase (ca. 123 to 118 ka, 101-97 m depth), after the peak of the last interglacial period (5.5, 123 ka), of conditions similar than those present during MIS 6, as indicated by the diatom freshwater species and the lowering of Ca/Ti. Later, during the MIS 5 (ca. 118 to 80 ka, 97-66 m depth), *Stephanodiscus* spp. disappears, diatom concentration decreases and alkaliphilous and halophilous diatom species become dominant, with only the sporadic presence of small Fragilariales. During this period, higher carbonate content (>Ca/Ti) and higher coercivity is found, whose maximum are at around ca. 102 and 86 ka (84 and 71 m, respectively). Decreases in the carbonate content (<Ca/Ti) occur when halophilous diatoms are dominant (as at ca. 116, 106, 93 and 84 ka). Together, all these characteristics indicate that dry conditions prevailed during most of the MIS 5. Under this environment the higher oxidation of Fe-bearing minerals occurred, and Chalco was a shallow lake of alkaline-saline waters as result of high evaporation, whose conditions were unfavorable for the flowering and preservation of diatoms. The end of MIS 5 (80–71 ka, 66-61 m depth) is characterized by swings between small Fragilariales freshwater diatoms and alkaliphilous - halophilous diatom species. The peaks of Fragilariales are coeval with lower Ca/Ti and coercivity, which indicate a change towards less dry climatic conditions.

Through the globally colder MIS 4 (71–57 ka, 58.2–46.3 m depth), freshwater and saline-alkaline diatoms oscillate as during the end of MIS 5, although the Fragilariales show higher abundance than during the previous stage; however, diatom concentration remains low. Minimum [maximum] in carbonate content (Ca/Ti) correlate to peaks of Fragilariales [alkaliphilous + halophilous] ca. 69, 65 and 59 ka [ca. 63 and 67.5 ka], which are nearly coincident with decreases [increases] in Bcr. The characteristics of MIS 4 suggest that periods of higher evaporation, dry conditions and a saline-alkaline environment in the lake alternated with reduced evaporation, less dry conditions and freshwater lake periods, the later probably associated to colder climate. Even though Fragilariales diatoms point to a moderate amelioration of dry conditions, the climate was mostly dry. This period (69–59 ka) has been associated with high fire activity and drought frequency in the Chalco basin (Torres Rodríguez et al., 2015, 2018).

Similar characteristics to those that occurred during MIS 4 are

recorded during the analyzed period of MIS 3 (57–35 ka, 46.3–29 m depth). At the early MIS 3 (ca. 55 to 51 ka, 44.5–41 m depth) lower carbonate content (<Ca/Ti) coincide with higher content of halophilous diatoms and low concentrations of Fragilariales. After ca. 51 ka, variations between freshwater and alkaline-saline lake alternate until ca. 39 ka, thereafter halophilous diatoms become dominant. Peaks in drier conditions occur around ca. 55 and 38 ka. These drier conditions are also documented in the pollen record of Lake Chalco (Torres-Rodríguez et al., 2018). Our data suggest that even if dry conditions persisted in the globally cooler MIS 4 and in the less cool early MIS 3, they were of lesser intensity than in MIS 5.

In contrast to MIS 6, in which high values of magnetic susceptibility (χ) and magnetic concentration-dependent parameters are associated with higher runoff under wetter conditions and the preservation of magnetotactic bacteria, high χ is coeval with several of the inferred drier conditions during MIS 5-3 (except around ca. 102, 90, 74 and 68 ka). In several paleoclimatic records, χ is interpreted as a proxy of increased rainfall (e.g. Hodell et al., 2008). However, the Lake Chalco data show that mineral magnetic concentration is also associated to sedimentary input by surficial runoff under drier conditions, probably associated with an unprotected catchment surface or littoral by the lack of vegetation cover and, hence, higher sediment availability.

Modern precipitation in central Mexico occurs substantially during the summer, when tropical convective activity as in the northward migration of Intertropical Convergence Zone, the easterly waves or tropical cyclones, constitutes the elements that result in precipitation (Magaña et al., 2003). The highest temperatures are reached in spring, just before the summer rainy season starts. A relative minimum in precipitation in the middle of the rainy season is observed over southern Mexico, related to fluctuations in sea surface temperature over tropical eastern Pacific, in turn modulated by the effects of incoming insolation (Magaña et al., 2003). Previous studies have shown that Lake Chalco display a pattern of orbital scale climatic variability that follows evaporation-insolation and seasonality (highest summer and lowest winter insolation) over the last ca. 40 ka (Lozano García et al., 2015; Caballero et al., 2019). In those studies, the highest carbonate content and salinity are associated to maxima in summer insolation and seasonality. In contrast, lower salinities and lowest temperatures during the last glacial maximum (LGM) correspond with minima in spring and summer insolation. In the longer record of Lake Chalco presented in this work, these relationships are recognized for some intervals. The cold and humid conditions recorded at the end of MIS 6 (except during a short period around ca. 144 ka), correlate with low spring insolation (Fig. 9). As discussed before, the freshwater diatom species found in the micritic mud suggest that carbonate content is related to a reduced the solubility of carbonates rather than a carbonate precipitation controlled by evaporative concentration. Minima of spring and summer insolation and lower evaporation (<Ca/Ti) are also observed at ca. 122-112 ka, and less clearly at ca. 100-88 ka. At the onset of MIS 5, maxima in spring and summer insolation and seasonality correlate with higher Ca/Ti, and this relationship is also observed between ca. 112-100 ka. For younger times, as seasonality decreases, the relation between carbonate content and insolation is not evident, which highlights that other climatic forcing than orbital scale precession induced insolation exerts higher control over climatic variability.

5.3. Regional patterns of climatic variability

In the pollen record of El Valle at the Central Panamanian lowlands, warmer than present conditions have been inferred between 126-118 ka, peaking around MIS 5.5 (123 ka), which are coeval to a decrease in precipitation with a propensity toward drought (Cárdenes-Sandí et al., 2019). The authors also found that during the following 118-97 ka period precipitation was similar or slightly wetter than modern. The Lake Chalco record shown here also suggests very dry conditions at ca. 127 ka, which prevail during most of the last interglacial, which is not consistent with the relatively humid conditions in Panamanian lowlands. Further south in the austral hemisphere, the Lake Titicaca records positive water balance and high lake levels coincide with glacial extent in adjacent Andes cordillera; conversely, a negative water balance and extremely low lake levels correspond to global warm periods, with the most saline (driest) periods occur during the last interglacial (D'Agostino et al., 2002; Fritz et al., 2007). The cold and wet conditions found in the Lake Titicaca record during global glacial stages are similar to those found in Lake Chalco during late MIS 6. On Iztaccíhuatl volcano (at the southeastern part of the basin of Mexico), the most extensive recorded glacial advance (Nexcolango) occurred during MIS 6 at around 190 ka and reached ca. 3000 m a.s.l. (Vázquez-Selem and Heine, 2011). This altitude is nearly coincident with the upper limit of the Sierra Nevada piedmont. This suggests that the MIS 6 is recorded in central Mexico as a particular cold and humid glacial period, more intense than MIS 2. In the Lake Petén Itzá sedimentary sequence in lowland Guatemala, moist conditions are recorded from ca. 85 to 48 ka (Hodell et al., 2008), which are contemporary to the drier/wetter oscillations found in Lake Chalco during the late MIS 5, the MIS 4 and the early MIS 3. In the Lake Peten Itzá record, a shift towards drier conditions and the onset of dry-wet alternations were found in sediments after ca. 48 ka, which, in Lake Chalco, coincide with the return to dry conditions.

The major wet-cold/dry-warm changes found along the Titicaca and Chalco lacustrine records imply a strong influence of the eccentricity. This cold/wet relationship is not found during the Last Glacial Maximum (ca. 26.5–19 ka BP) in the Lake Chalco diatom record, where the coldest phases are coincident with low precipitation (Caballero et al., 2019), suggesting that the MIS 6 and the LGM are not perfect analogues. Our data highlights the influence on local and regional climate of shorter scale climatic variability (orbital and millennial).

Within the uncertainties and limits of our time-scale model, the 150-32 ka Lake Chalco record, precession-induced insolation apparently influenced the precipitation along the last glacial.

6. Conclusions

The multiproxy investigation in the sediments of Lake Chalco presented here provides one of the longest records of the paleoclimatic conditions in the North American tropics.

Our results indicate that coeval variations of magnetic properties with geochemical data and diatom assemblages reflect the major climatic changes that occurred between ca. 35 and 150 ka BP, since the transition from the glacial MIS 6 to the last interglacial MIS 5.5, and through the last glacial (MIS 5.4 to the initial part of MIS 3).

The mineral magnetic assemblage of lacustrine sediments is controlled by relatively low coercivity (Bh < 125 mT) ferromagnetic minerals, likely held by detrital partially oxidized Ti-magnetite/maghemite. Weathering or diagenetic processes have altered in different degrees the detrital low coercivity mineral population by partial oxidation of Ti-magnetites (via maghemitization). The nearly opposite distribution of freshwater diatom taxa (small Fragilariales and *Stephanodiscus* spp.), and alkaliphilous and halophilous taxa enabled us to infer changes from deep to shallow lake levels, the later also recognized by higher carbonate content.

Humid and cooler than present conditions occurred during the

MIS 6 record, with deeper lake levels after ca. 141.5 ka. The main environmental change is observed in all analyzed parameters after ca. 130 ka, at the beginning of the last interglacial when lake level dropped and climate became drier. A return to moister and cooler conditions is recorded after the peak of the last interglacial period (5.5, 123 ka). Large amplitude changes between 130-74 ka are roughly coincident with the MIS 5. The higher magnetic concentration and higher coercivity, along with larger carbonate content and the predominance of alkaliphilous and halophilous diatoms suggest that higher oxidation of Ti-magnetites occurred during dry periods. The amplitude of these changes decreases in MIS 4 (71-57 ka) and the early part of MIS 3 (57-35 ka).

Within the limitations of our age model, we observe that the variations in the analyzed parameters follow orbital-scale climatic oscillations at the early part of our Lake Chalco record. Low summer and spring insolation and lower seasonality inhibited evaporation and favored high lake levels during the MIS 6. During the global warmer MIS 5 correlation between maxima in spring and summer insolation and drier conditions is found around ca. 130-122 and 112-100 ka.

The Lake Chalco data shown in this work also suggest very dry conditions by ca. 127 ka, and their persistence during most of the last glacial, which contrast with the relatively humid conditions in Panamanian lowlands. The cold and wet conditions found in the Lake Titicaca record during global glacial stages are similar to those found in Lake Chalco during the glacial MIS 6.

This cold/wet relationship is not found during the Last Glacial Maximum (ca. 26.5–19 ka BP) in the Lake Chalco diatom record, where the coldest phases are coincident with drier conditions (Caballero et al., 2019), suggesting that the MIS 6 and the LGM are not perfect analogues.

These major wet-cold/dry-warm changes are related to the global glacial/interglacial transition from MIS 6 to the last interglacial MIS 5.5, which implies a strong influence of eccentricity. However, in the last glacial between 144-88 ka, precession-induced insolation changes controlled precipitation.

Declaration of competing interest

The authors declare that they have no conflicts of interests to this work.

CRediT authorship contribution statement

Beatriz Ortega-Guerrero: Data curation, Investigation, Writing - original draft. **Diana Avendaño:** Formal analysis, Writing - original draft. **Margarita Caballero:** Data curation, Investigation, Writing - original draft. **Socorro Lozano-García:** Writing - original draft. **Erik T. Brown:** Formal analysis. **Alejandro Rodríguez:** Formal analysis. **Bernardo García:** Formal analysis. **Hermenegildo Barceinas:** Formal analysis. **Ana María Soler:** Formal analysis. **Albán Albarrán:** Formal analysis.

Acknowledgements

This project was possible by the financial funding of projects UNAM-PAPIIT (Universidad Nacional Autónoma de México) IV100215, IN105918, IN103819and CONACyT 130963; and the support of the Ejido Tulyehualco authorities that facilitated the access to the drilling site. We thank the staff of National Lacustrine Facility (LacCore, University of Minnesota), D. Schnurrenberger, A. Myrbo, A. Noren and K. Brady for assistance with initial core description. XRF core scanning were performed at the Large Lakes Observatory, University of Minnesota-Duluth. Hysteresis parameters were measured at the Institute for Rock Magnetism, University of Minnesota. The IRM is made possible through the Instrumentation and Facilities program of the National Science Foundation, Earth Science Division and by funding from the University of Minnesota. We thank M. Jackson and all the IRM staff for their invaluable assistance. We also thank Dr. Susana Sosa for technical support during field and laboratory work. C.L. Romero and S. García collaborated in the elaboration of the figures. The authors thank to two anonymous reviewers whose comments and suggestions improved the manuscript.

Appendix A. Supplementary data

Supplementary data to this article can be found online at https://doi.org/10.1016/j.quascirev.2020.106163.

References

Arce, J.L., Layer, P.W., Lassiter, J.C., Benowitz, J.A., Macías, J.L., Ramírez-Espinosa, J., 2013. 40Ar/39Ar dating, geochemistry, and isotopic analyses of the quaternary Chichinautzin volcanic field, south of Mexico City: implications for timing, eruption rate, and distribution of volcanism. Bull. Volcanol. 75 (12), 774.

Aufgebauer, A., Panagiatopoulos, K., Wagner, B., Schaebitz, F., Viehberg, F.A., Vogel, H., Zanchetta, G., Sulpizio, R., Leng, M.J., Damaschke, M., 2012. Climate and environmental change over the last 17 ka recorded in sediments from Lake Prespa (Albania/F.Y.R. of Macedonia/Greece). Quat. Int. 274, 122–135. https://doi.org/10.1016/jquaint.2012.02.015.

Avendaño-Villeda, D.A., Caballero, M., Ortega-Guerrero, B., Lozano-García, S., Brown, E., 2018. Condiciones ambientales a finales del Estadio Isotópico 6 (EI 6: > 130000 años) en el centro de México: caracterización de una sección de sedimentos laminados proveniente del Lago de Chalco. Rev. Mex. Ciencias Geol. 3582, 168–178.

Bradbury, J.P., 2000. Limnologic history of Lago de Pátzcuaro, Michoacán, México for the past 48,000 years: impacts of climate and man. Palaeogeogr. Palaeoclimatol. Palaeoecol. 163, 69–95.

Berner, R.A., 1981. A new geochemical classification of sedimentary environments. J. Sediment. Petrol. 51, 359–365.

Borruel-Abadía, V., Gómez-Paccard, M., Larrasoaña, J.C., Rico, M., Valero-Garcés, B., Moreno, A., Jambrina-Enríquez, M., Soto, R., 2015. Late Pleistocene to Holocene palaeoenvironmental variability in the north-west Spanish mountains: insights from a source-to-sink environmental magnetic study of Lake Sanabria. J. Quat. Sci. 30 (3), 222–234. https://doi.org/10.1002/jqs.2773.

Bronk-Ramsey, C., 2008. Deposition models for chronological records. Quat. Sci. Rev. 27, 42–60.

Bronk-Ramsey, C., 2009. Bayesian analysis of radiocarbon dates. Radiocarbon 51 (1), 337–360.

Caballero, M., Lozano, S., Ortega, B., Urrutia, J., Macias, J.L., 1999. Environmental characteristics of lake Tecocomulco, northern basin of Mexico, for the last 50,000 years. J. Paleolimnol. 22 (4), 399–411.

Caballero, M., Ortega, B., Valadez, F., Metcalfe, S., Macias, J.L., Sugiera, Y., 2002. Sta. Cruz Atizapan: a 22-ka lake level record and climatic implications for the late Holocene human occupation in the Upper Lerma Basin, central Mexico. Palaeogeogr. Palaeoclimatol. Palaeoecol. 186, 217–235.

Caballero, M., Lozano-García, S., Ortega-Guerrero, B., Correa-Metrio, A., 2019. Quantitative estimates of orbital and millenial scale climatic variabiliy in central Mexico during the las 40,000 years. Journal of Quaternayr Science Reviews 205, 62–75, 0.1016/j.quascirev.2018.12.002 (SCI=4.334).

Cárdenes-Sandí, G.M., Shadik, C.R., Correa-Metrio, A., Gosling, W.D., Cheddadi, R., Bush, M.B., 2019. Central American climate and microrefugia: a view from the last interglacial. Quat. Sci. Rev. 205, 224–233.

Chen, T., Xu, H., Xie, Q., Chen, J., Ji, J., Lu, H., 2005. Characteristics and genesis of maghemite in Chinese loess and paleosols: mechanism for magnetic susceptibility enhancement in paleosols. Earth Planet. Sci. Lett. 240, 790–802.

Cornell, R., Schwertmann, U., 2003. The Iron Oxides. Structure, Properties, Reactions, Occurrences and Uses. In: 2nd, Completely Revised and Extended Edition. Wiley-VCH, p. 664.

D'Agostino, K., Seltzer, G.O., Baker, P.A., Fritz, S.C., Dunbar, R.B., 2002. Late-Quaternary lowstands of Lake Titicaca: evidence from high-resolution seismic data. Palaeogeogr. Palaeoclimatol. Palaeoecol. 179, 97–111.

Day, R., Fuller, M., Schmidt, V., 1977. Hysteresis properties of titanomagnetites: grain-size and compositional dependence. Phys. Earth Planet. Inter. 13, 260–266.

Dunlop, D., 2002a. Theory and application of the Day plot (Mrs/Ms versus Hcr/Hc) 1. Theoretical curves and tests using titanomagnetite data. J. Geophys. Res. 107 https://doi.org/10.1029/2001JB000486.

Dunlop, D., 2002b. Theory and application of the Day plot (Mrs/Ms versus Hcr/Hc) 2. Application to data for rocks, sediments, and soils. J. Geophys. Res. 107 https://doi.org/10.1029/2001JB000487.

Egli, R., 2003. Analysis of the field dependence of remanent magnetization curves. J. Geophys. Res., Solid Earth 108 (B2), 2081. https://doi.org/10.1029/2002JB002023.

Egli, R., 2004. Characterization of individual rock magnetic components by analysis of remanence curves. 3. Bacterial magnetite and natural processes in lakes. Phys. Chem. Earth 29, 869–884.
Evans, M.E., Heller, F., 2003. Environmental Magnetism. Principles and Applications of Environmagnetics. Academic Press, San Diego.
Ferrari, L., Orozco-Esquivel, T., Manea, V., Manea, M., 2012. The dynamic history of the Trans-Mexican Volcanic Belt and the Mexico subduction zone. Tectonophysics 522, 122–149.
Franke, C., Pennock, G.M., Drury, M.R., Engelmann, R., Lattard, D., Garming, J.F.L., von Dobeneck, T., Dekkers, M.J., 2007. Identification of magnetic Fe-Ti oxides in marine sediments by electron backscatter diffraction in scanning electron microscopy. Geophys. J. Int. 170, 545–555.
Fritz, S., Baker, P.A., Seltzer, G.O., Ballantyne, A., Tapia, P., Cheng, H., Edwards, L.R., 2007. Quaternary glaciation and hydrologic variation in the South American tropics as reconstructed from the Lake Titicaca drilling project. Quat. Res. 68, 410–420.
Garming, J.F.L., von Dobeneck, T., Franke, C., Bleil, U., 2007. Low-temperature partial magnetic self-reversal in marine sediments by magnetostatic interaction of titanomagnetite and titanohematite intergrowths. Geophys. J. Int. 170, 1067–1075.
Ge, K., Williams, W., Liu, Q., Yu, Y., 2014. Effects of the core-shell structure on the magnetic properties of partially oxidized magnetite grains: experimental and micromagnetic investigations. Geochem. Geophys. Geosyst. 15, 2021–2038. https://doi.org/10.1002/2014.C005265.
Groot, M.H.M., Bogotá, R.G., Lourens, L.J., Hooghiemstra, H., Vriend, M., Berrio, J.C., Tuenter, E., Van der Plicht, J., Van Geel, B., Ziegler, M., others, 2011. Ultra-high resolution pollen record from the northern Andes reveals rapid shifts in montane climates within the last two glacial cycle. Clim. Past 7, 299–316.
Haberzettl, T., Corbella, H., Fey, M., Janssen, S., Lucke, A., Mayr, C., Ohlendorf, C., Schabitz, F., Schleser, G., Wille, M., Wulf, S., Zolitschka, B., 2007. Lateglacial and Holocene wet–dry cycles in southern patagonia: chronology, sedimentology and geochemistry of a lacustrine record from Laguna Potrok Aike, Argentina. Holocene 17, 297–310. https://doi.org/10.1177/0959683607076437.
Hodell, D.A., Anselmetti, F.S., Ariztegui, D., Brenner, M., Curtis, J.H., Gilli, A., Grzesik, D.A., Guilderson, T.J., Müller, A.D., Bush, M., Correa-Metrio, A., Escobar, J., Kutterolf, S., 2008. An 85-ka record of climate change in lowland Central America. Quat. Sci. Rev. 27 (11–12), 1152–1165.
Housen, B.A., Banerjee, S.K., Moskowitz, B.M., 1996. Low-temperature magnetic properties of siderite in marine sediments. Geophys. Res. Lett. 23, 2843–2846.
Isambert, A., Valet, J.P., Gloter, A., Guyot, F., 2003. Stable Mn-magnetite derived from Mn-siderite by heating in air. J. Geophys. Res.: Solid Earth 108 (B6).
Israde-Alcántara, I., Velázquez-Durán, R., Lozano-García, M.S., Domínguez-Vázquez, G., Garduño-Monroy, V.H., 2010. Evolución Paleolimnológica del Lago Cuitzeo, Michoacán durante el Pleistoceno-Holoceno. Bol. Soc. Geol. Mex. 62 (3), 345–357.
Jelinowska, A., Tucholka, P., Wieckowski, K., 1997. Magnetic properties of sediments in a Polish lake: evidence of a relation between the rock magnetic record and environmental changes in Late Pleistocene and Holocene sediments. Geophys. J. Int. 129, 727–736.
Kelts, K., Hsü, K.J., 1978. Freshwater carbonate sedimentation. In: Lakes. Springer, New York, pp. 295–323.
Lascu, I., Plank, C., 2013. A new dimension to sediment magnetism: charting the spatial variability of magnetic properties across lake basins. Glob. Planet. Chang. 110, 340–349.
Laskar, J., Robutel, P., Joutel, F., Gastineau, M., Correia, A.C.M., 2004. A long-term numerical solution for the insolation quantities of the Earth. Astron. Astrophys. 428, 261–285.
Lisiecki, L.E., Raymo, M.E., 2005. A Pliocene-Pleistocene stack of 57 globally distributed benthic δ18O records. Paleoceanography 20, PA1003.
Lisiecki, L.E., Stern, J.V., 2016. Regional and global benthic d18O stacks for the last glacial cycle. Paleoceanography 31, 1368–1394.
Liu, Q., Deng, C., Yu, Y., Torrent, J., Jackson, M.J., Banerjee, S.K., Zhu, R., 2005. Temperature dependence of magnetic susceptibility in an argon environment: implications for pedogenesis of Chinese loess/palaeosols. Geophys. J. Int. 161, 102–112.
Lozano García, M.S., Ortega, B., Roy, P.D., Beramendi-Orosco, L., Caballero, M., 2015. Climatic variability in the northern sector of the American tropics since the latest MIS 3. Quat. Res. 84, 262–271. https://doi.org/10.1016/j.yqres.2015.07.002.
Macías, J.L., Arce, J.L., García-Tenorio, F., Layer, P.W., Rueda, H., Reyes-Agustín, G., López-Pizaña, F., Avellán, D., 2012. Geology and geochronology of tlaloc, telapon, Iztaccíhuatl and Popocatépetl volcanoes, sierra Nevada, central Mexico. In: Aranda-Gómez, J.J., Tolson, G., Molina-Garza, R.S. (Eds.), The Southern Cordillera and beyond, vol. 25. Geological Society of America, pp. 163–193 (Field Guide).
Magaña, V.O., Vázquez, J.L., Pérez, J.L., Pérez, J.B., 2003. Impact of El Niño precipitation in Mexico. Geofis. Int. 42 (3), 313–330.
Maher, B.A., 2007. Environmental magnetism and climate change. Contemp. Phys. 48 (5), 247–274.
Maxbauer, D.P., Feinberg, J.M., Fox, D.L., Clyde, W.C., 2016a. Magnetic minerals as recorders of weathering, diagenesis, and paleoclimate: a core–outcrop comparison of Paleocene–Eocene paleosols in the Bighorn Basin, WY, USA. Earth Planet. Sci. Lett. 452, 15–26.
Maxbauer, D.P., Feinberg, J.M., Fox, D.L., 2016b. MAX UnMix: a web application for unmixing magnetic coercivity distributions. Comput. Geosci.-Uk 95, 140–145.
Maxbauer, D.P., Feinberg, J.M., Fox, D.L., 2016c. Magnetic mineral assemblages in soils and paleosols as the basis for paleoprecipitation proxies: a review of magnetic methods and challenges. Earth Sci. Rev. 155, 28–48.
Mays, J.L., Brenner, M., Curtis, J.H., Curtis, K.V., Hodell, D.A., Correa-Metrio, A., Escobar, J., Dutton, A.L., Zimmerman, A.R., Guilderson, T.P., 2017. Stable carbon isotopes (d13C) of total organic carbon and long-chain n-alkanes as proxies for climate and environmental change in a sediment core from Lake Petén-Itzá, Guatemala. J. Paleolimnol. 57, 307–319. https://doi.org/10.1007/s10933-017-9949-z.
Metcalfe, S.E., Street-Perrott, F.A., Perrott, R.A., Harkness, D.D., 1991. Palaeolimnology of the Upper Lerma Basin, Central Mexico: a record of climatic change and anthropogenic disturbance since 11,600 yr BP. J. Paleolimnol. 5, 197–218.
Metcalfe, S.E., Davies, S.J., Braisby, J.D., Leng, M.J., Newton, A.J., Terrett, N.L., ÓHara, S.L., 2007. Long and short-term change in the Pátzcuaro Basin, central Mexico. Palaeogeogr. Palaeoclimatol. Palaeoecol. 247, 272–295.
Moskowitz, B.M., Bazylinski, D.A., Egli, R., Frankel, R.B., Edwards, K.J., 2008. Magnetic properties of marine magnetotactic bacteria in a seasonally stratified coastal pond (Salt Pond, MA, USA). Geophys. J. Int. 174, 75–92.
Muxworthy, A., Williams, W., Virdee, D., 2003. Effect of magnetostatic interactions on the hysteresis parameters of single-domain and pseudo-single-domain grains. J. Geophys. Res. 108 (B11), 2517. https://doi.org/10.1029/2003JB002588.
Nowaczyk, N.R., 2011. Dissolution of titanomagnetite and sulphidization in sediments from Lake Kinneret, Israel. Geophys. J. Int. 187, 34–44.
Oliva-Urcia, B., Moreno, A., 2019. Discerning the major environmental processes that influence the magnetic properties in three northern Iberia mountain lakes. Catena 182, 104130. https://doi.org/10.1016/j.catena.2019.104130.
Ortega, B., Caballero, C., Lozano, S., Israde, I., Vilaclara, G., 2002. 52 000 years of environmental history in Zacapu basin, Michoacan, Mexico: the magnetic record. Earth Planet. Sci. Lett. 202, 663–675.
Ortega-Guerrero, B., Lozano-García, M.S., Herrera-Hernández, D., Caballero, M., Beramendi Orosco, L.E., Bernal, J.P., Torres-Rodríguez, E., Avendaño-Villeda, D., 2017. Lithostratigraphy and physical properties of lacustrine sediments of the last ca. 150 kyr from Chalco basin, central México. J. South Am. Earth Sci. 79, 507–524.
Özdemir, Ö., Dunlop, D.J., 2014. Hysteresis and coercivity of hematite. J. Geophys. Res., Solid Earth 119, 2582–2594. https://doi.org/10.1002/2013JB010739.
Özdemir, Ö., O'Reilly, W., 1982. An experimental study of the intensity and stability of thermoremanent magnetization acquired by synthetic monodomain titanomagnetite substituted by aluminium. Geophys. J. Int. 70 (1), 141–154.
Paillard, D., Labeyrie, L., Yiou, P., 1996. Macintosh program performs time-series analysis. Eos Trans. AGU 77, 379.
Reimer, P.J., Bard, E., Bayliss, A., Beck, J.W., Blackwell, P.G., Ramsey, C.B., Grootes, P.M., 2013. IntCal13 and Marine13 radiocarbon age calibration curves 0-50,000 years cal BP. Radiocarbon 55 (4), 1869–1887.
Roberts, A.P., Tauxe, L., Heslop, D., Zhao, X., Jiang, Z., 2018. A critical appraisal of the "Day" diagram. J. Geophys. Res.: Solid Earth 123 (4), 2618–2644.
Rochette, P., Mathé, P.-E., Esteban, L., Rakoto, H., Bouchez, J.-L., Liu, Q., Torrent, J., 2005. Non-saturation of the defect moment of goethite and fine-grained hematite up to 57 Teslas. Geophys. Res. Lett. 32, L22309 https://doi.org/10.1029/2005GL024196.
Rodelli, D., Jovane, L., Giorgioni, M., Rego, E.S., Cornaggia, F., Benites, M., et al., 2019. Diagenetic fate of biogenicsoft and hard magnetite in chemically stratified sedimentary environments of Mamanguá Ría, Brazil. J. Geophys. Res.: Solid Earth 124, 2313–2330, 10.1029/.
Thouveny, N., Debeaulieu, J.L., Bonifay, E., Creer, K.M., Guiot, J., Icole, M., Johnsen, S., Jouzel, J., Reille, M., Williams, T., Williamson, D., 1994. Climate variations in Europe over the past 140 kyr deduced from rock magnetism. Nature 371, 503–506.
Torres Rodríguez, E., Lozano-García, S., Priyadarsi, R., Ortega, B., Beramendi, L., Correa Metrio, A., Caballero, M., 2015. Last Glacial droughts and fire regimes in the central Mexican highlands. J. Quat. Sci. 30 (1), 88–99.
Torres-Rodríguez, E., Lozano-García, S., Caballero-Miranda, M., Ortega-Guerrero, B., Sosa-Nájera, S., Roy, P.D., 2018. Pollen and non-pollen palynomorphs of Lake Chalco as indicators of paleolimnological changes in high-elevation tropical central Mexico since MIS 5. J. Quat. Sci. 33 (8), 945–957.
Valadez, F., Oliva, G., Vilaclara, G., Caballero, M., Rodriguez, D.C., 2005. On the presence of *Stephanodiscus niagarae* Ehrenberg in central Mexico. J. Paleolimnol. 34, 147–157. https://doi.org/10.1007/s10933-005-0810-4.
Valero-Garcés, B., Stockhecke, M., Lozano-García, S., Ortega-Guerrero, B., Caballero, M., Fawcett, P., Werne, J.P., Brown, E., Sosa-Nájera, S., 2019. Stratigraphy and Sedimentology of the Upper Pleistocene – Holocene Lake Chalco, México Basin. Limnogeology: Progress, Challenges and Opportunities: A Tribute to Beth Gierlowski-Kordesch. Editors: Michael R Rosen, Lisa Park-Boush, David B. Finkelstein, Sila Pla Pueyo. Springer (in press) (In revision).
van Velzen, A.J., Dekkers, M.J., 1999. Low-temperature oxidation of magnetite in loess–paleosol sequences: a correction of rock magnetic parameters. Stud. Geophys. Geod. 43, 357–375.
Vázquez-Castro, G., Ortega-Guerrero, B., Rodríguez, A., Caballero, M. y, Lozano-García, S., 2008. Mineralogía magnética como indicador de sequía en los sedimentos lacustres de los últimos ca. 2,600 años de Santa María del Oro, occidente de México. Rev. Mex. Ciencias Geol. 25 (1), 21–38.
Vázquez-Selem, L., Heine, K., 2011. Late quaternary glaciation in Mexico. In: Quaternary Glaciations - Extent and Chronology, Part III: South America, Asia, Africa, Australia, Antarctica 233-242. Elsevier, Amsterdam.

Capítulo III

3. Distribución ecológica de *Stephanodiscus niagarae* Ehrenberg en el centro de México y su modelo de nicho durante el último máximo glacial en la zona Neártica.

(Artículo publicado, citar como: Avendaño D., Caballero M., & Vázquez, G. (2021). Ecological distribution of *Stephanodiscus niagarae* Ehrenberg in central Mexico and niche modeling for its last glacial maximum habitat suitability in the Nearctic realm. *Journal of Paleolimnology*, *66*, 1-14. https://doi.org/10.1007/s10933-021-00178-w)

Este artículo tiene como objetivo conocer la distribución ecológica en el centro de México de una especie en particular, ***Stephanodiscus niagarae****, la cual es una especie que domina en diferentes secciones del registro de Chalco y después desaparece. Sin embargo, es una especie que actualmente es abundante en otras zonas de Norteamérica. Al conocer su ecología y distribución en Norteamérica surgió la idea de que esta especie migró al sur durante los periodos fríos (glaciales) por lo que puede utilizarse como un indicador de condiciones glaciales en el centro de México. Esta es la idea que se plantea y discute a continuación.*

Resumen:

Stephanodiscus niagarae Ehrenberg actualmente está restringida a regiones específicas del centro de México, sin embargo, durante el Pleistoceno tardío tuvo una distribución más amplia en el país. Este cambio en la distribución es similar a los observados por varios organismos que migran hacia el sur durante el frío clima glacial, lo que respalda la hipótesis que el centro de México actuó como refugio glacial para estas especies. Este estudio tiene como objetivo apoyar esta hipótesis para *S. niagarae* así como analizar su distribución ecológica en ambientes modernos del centro de México. Para ello, se estudiaron 18 muestras de 16 lagos localizados alrededor de la ciudad de México, seleccionados entre 46 lagos a lo largo de la Faja Volcánica Transmexicana. Los conjuntos de diatomeas en sedimentos superficiales, así como los parámetros climáticos, hidroquímicos y nutrientes de cada lago se analizaron mediante un análisis de correspondencia canónica. Además, se creó un modelo de nicho ecológico (MNE) con datos de ocurrencia moderna (n = 47) y variables ambientales (WorldClim) para producir mapas de distribución potencial de *S. niagarae* durante el presente y el último máximo glacial (UMG) en la zona Neártica. *Stephanodiscus niagarae* se observó únicamente en 4 sitios (abundancia < 10 %) del centro de México, está asociada a condiciones templadas subhúmedas en lagos de agua dulce con una dominancia iónica: [Mg^{2+}] - [Ca^{2+}] - [HCO^{3-}] y una alta turbidez: mesotrófico-hipertófico (basados en valores de Clorofila α), pero con tendencia a la limitación de fósforo. En nuestros sitios de estudio, *S. niagarae* mostró bajas abundancias en conjuntos de diatomeas dominados por *Aulacoseira* spp. La temperatura (media anual, media de los trimestres más fríos y cálidos) fue identificada por el MNE como la principal variable ambiental que controla su distribución, siendo su distribución moderna al norte de Estados Unidos, sur de Canadá y restringida a las tierras altas del oeste y centro de México. Mientras que, el escenario del UMG (con un enfriamiento de -5.5º C) identificó las tierras altas occidentales y centrales en México y sur de los Estados Unidos como áreas que respaldan el enfoque de que la Sierra Madre Occidental podría haber actuado como un corredor migratorio que ofrece hábitats adecuados para una migración hacia el sur en el centro de México durante los periodos fríos (glaciales). En conclusión, la distribución de *S. niagarae* en las montañas centrales y occidentales de México está controlada por los cambios de temperatura y su presencia puede estar asociada con periodos más fríos (glaciales).

Palabras clave: Diatomeas, biogeografía, periodos glaciales, *Stephanodiscus niagarae*

J Paleolimnol
https://doi.org/10.1007/s10933-021-00178-w

ORIGINAL PAPER

Ecological distribution of *Stephanodiscus niagarae* Ehrenberg in central Mexico and niche modeling for its last glacial maximum habitat suitability in the Nearctic realm

Diana Avendaño · Margarita Caballero · Gabriela Vázquez

Received: 26 May 2020 / Accepted: 27 January 2021

Abstract *Stephanodiscus niagarae* Ehrenberg is currently restricted to specific regions of central Mexico, however, during the late Pleistocene, it had a wider distribution in the country. This change in distribution is similar to those observed for several organisms that migrated southwards during cold, glacial climates, supporting the hypothesis that central Mexico acted as glacial refugia for these species. This study aims to support this hypothesis for *S. niagarae* as well as to analyze its ecological distribution in modern environments in central Mexico. For this purpose we studied 18 samples from 16 lakes located around Mexico City, selected among 46 lakes along the Trans-Mexican Volcanic Belt. Diatom assemblages in superficial sediments, and climatic, hydrochemistry, and nutrient parameters of each lake were analyzed by means of canonical correspondence analyses. Additionally, we created an ecological niche model (ENM) with modern occurrence data (n = 47) and environmental variables (WorldClim) to produce potential distribution maps of *S. niagarae* during the present time and under the LGM conditions in the Nearctic realm. *S. niagarae* was recorded only in 4 sites in central Mexico (abundances < 10%) associated with temperate, subhumid conditions in freshwater lakes with $[Mg^{2+}] - [Ca^{2+}] - [HCO_3^-]$ ionic dominance and high turbidity, mesotrophic to hypertrophic systems (based on chlorophyll *a* values), but with a tendency to P-limitation. In our study sites *S. niagarae* showed low abundances in diatom assemblages dominated by *Aulacoseira* spp. Temperature (annual mean, coldest and warmest quarters means) was identified by ENM as the main environmental variable controlling its distribution, with its highest modern support in the USA, southern Canada, and a restricted distribution in the highlands of western and central Mexico. Whereas, the LGM scenario (− 5.5 °C) identified the western and central highlands in Mexico and southern USA as the highest probability distribution areas supporting the approach that the Sierra Madre Occidental could have acted as a migration corridor offering suitable habitats for a southward migration into central Mexico during colder (glacial)

Supplementary Information The online version contains supplementary material available at (https://doi.org/10.1007/s10933-021-00178-w).

D. Avendaño (✉)
Posgrado de Ciencias de la Tierra, Instituto de Geofísica, Universidad Nacional Autónoma de México, Ciudad Universitaria, 04510 Ciudad de México, Mexico
e-mail: da.avendano.v@ciencias.unam.mx

M. Caballero
Laboratorio de Paleolimnología, Instituto de Geofísica, Universidad Nacional Autónoma de México, Ciudad Universitaria, 04510 Ciudad de México, Mexico
e-mail: maga@igeofisica.unam.mx

G. Vázquez
Instituto de Ecología, A.C., Carretera antigua a Coatepec 351, El Haya, 91073 Xalapa, Veracruz, Mexico
e-mail: gabriela.vazquez@inecol.mx

Published online: 12 March 2021

periods. In conclusion, *S. niagarae* distribution in the central and western mountains of Mexico is controlled by temperature changes and its presence may be associated with colder (glacial) periods.

Keywords Diatoms · Biogeography · Glacial periods · *Stephanodiscus niagarae*

Introduction

Stephanodiscus niagarae Ehrenberg (1845) is a diatom species that has been widely studied in North America, in both modern environments and fossil records (Theriot and Stoermer 1984a; Stoermer et al. 1989). In modern environments it is common in all the Great Lakes and surrounding areas of Canada and the USA (Theriot and Stoermer 1984b; Håkansson and Kling 1989; Julius et al. 1998; Pla et al. 2005; Lashaway and Carrick 2010; Reavie et al. 2014a) and it has also been reported from sites in north-western USA (Oregon, Washington, Montana and Wyoming) (Edmondson et al. 2003; Bradbury et al. 2004; Theriot et al. 2006). It is recognized as a good ecological indicator by several authors that consider it a planktonic diatom in freshwater bodies with circumneutral pH (Theriot and Stoermer 1984a; Fritz et al. 1993; Bradbury 2000). The presence of *S. niagarae* is also associated with temperate to cold conditions in modern (Stoermer and Ladewski 1976; Brugam 1983; Bradbury et al. 2004; Colman et al. 2004; Reavie et al. 2014b) and paleolimnological studies (Bradbury 1971, 2000). Reavie et al. (2014a, b) observed that in the Great Lakes, particularly in lake Erie, *S. niagarae* was most abundant during spring associated with cool, high-nutrient, and turbid environments. This diatom has been found in a wide range of trophic conditions, even though it seems to have a preference for eutrophic lakes (Rawson 1956; Theriot and Stoermer 1984a), however, its abundance decreases in areas with heavy industrial pollution and habitat disturbance (Stoermer and Jang 1970; Julius et al. 1998).

In contrast to its relatively wide modern distribution in northern USA and Canada, living populations of this species in Mexico have only been reported from two sites in the central highlands of the Trans-Mexican Volcanic Belt (TMVB) (Oliva-Martínez et al. 2005; Valadez et al. 2005). Nevertheless, this diatom was a much more abundant taxon in the region during the late Pleistocene (Davies et al. 2002) and its abundance reduced greatly during the early Holocene (Valadez et al. 2005). We have documented 9 sites (Fig. 1a, ESM1) where *S. niagarae* was abundant in late Pleistocene to early Holocene sediments. In six of them it was present in sediments dating to the last glacial ($\sim$ 70–12 ka BP): Babícora (Metcalfe et al. 2002), Pátzcuaro (Bradbury 2000), Zacapu (Metcalfe 1995), Cuitzeo (Israde-Alcántara et al. 2002, 2010b, 2018), Tecocomulco (Caballero et al. 1999) and Chalco (Caballero and Ortega Guerrero 1998; Caballero et al. 2019). And in three it was also abundant in sediments dating to the previous glaciation (> 120 ka BP): Cuitzeo (Israde-Alcántara et al. 2002), Texcoco (Bradbury 1971), and Chalco (Avendaño et al. 2018).

This change in the geographic distribution of *S. niagarae* between the late Pleistocene and present seems to be related to the extensive changes in climate and landscape conditions in North America during late Pleistocene compared to the Holocene (present). Certainly, there is wide evidence that some plants, insects and vertebrate species migrated southwards during cold glacial climates, when the continental ice sheets extended over North America (Graham et al. 1996; Hewitt 2000; Jackson et al. 2000; Waltari et al. 2007; Pardi and Graham 2019). For example, evidence of fossil Pleistocene mammals in Mexico suggest a southern displacement from the USA along corridors of suitable climates, with central Mexico acting as a glacial refugia for mammals as well as for other organisms (Ceballos et al. 2010; Pardi and Graham 2019). Even though such studies have seldom been undertaken with small, aquatic organism such as diatoms, here we propose that central Mexico was also a refugia for *S. niagarae* during past glacial periods. This is not the first time that the concept of glacial refugia has been applied for diatoms, as for example Spaulding et al. (1999, 2010) proposed that the presence of endemic lineages of diatoms in Antarctica responded to the continuous presence of ice-free habitats that acted as refugia during the repeated glacial cycles of the Cenozoic.

To support the refugia hypothesis, in this research we used ecological niche models (ENMs) to generate suitable habitat maps for *S. niagarae* under modern climatic conditions and also during the cooler, last

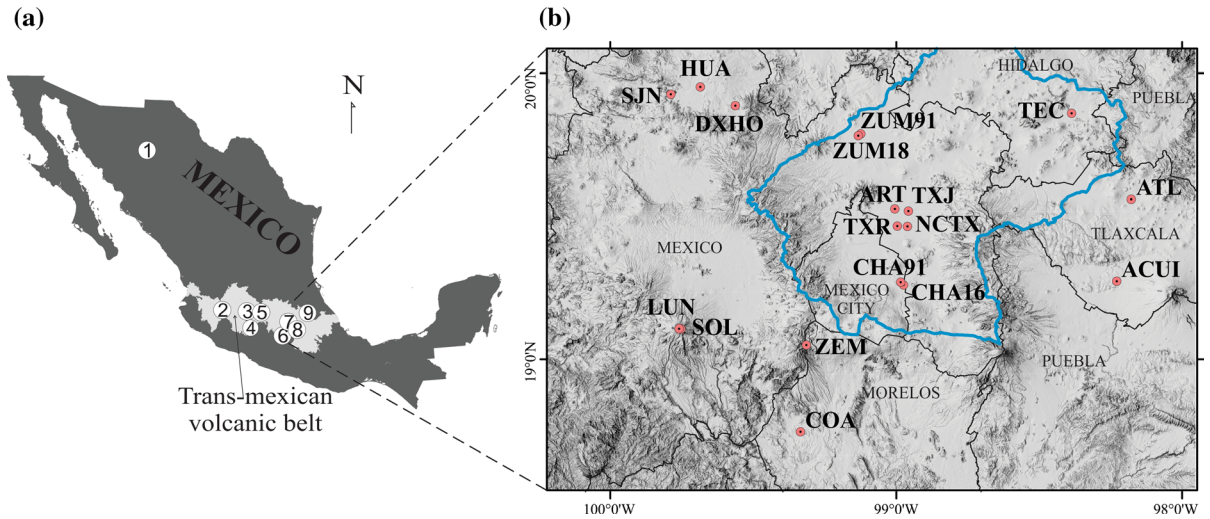

Fig. 1 Location maps. **a** Map of Mexico with the Trans-Mexican Volcanic Belt (light gray shaded area) and the location of the 9 fossil records of *Stephanodiscus niagarae*: 1. Babícora, 2. Chapala, 3. Zacapu, 4. Pátzcuaro, 5. Cuitzeo, 6. Chignahuapan, 7. Texcoco, 8. Chalco, 9. Tecocomulco. **b** Research area with the location of study sites around Mexico City (black lines show state borders and blue line delimits the Basin of Mexico): San Juanico (SJN), La Huaracha (HUA), Danxhó (DXHO), Zumpango (ZUM91 and ZUM18), La Luna (LUN), El Sol (SOL), Zempoala (ZEM), Coatetelco (COA), Texcoco Artemia (ART), Texcoco Jalapango (JTX), Texcoco Recreativo (TXR), Texcoco Nabor Carrillo (NCTX), Chalco (CHA91 and CHA16), Acuitlapilco (ACUI), Atlangatepec (ATL), and Tecocomulco (TEC)

glacial maximum (LGM, 26–19 ka cal BP). We also aimed to analyze the present distribution of *S. niagarae* in central Mexico and its relationship with environmental variables such as temperature, salinity, ionic dominance and nutrient levels in lakes located along the TMVB. This research could contribute to future paleolimnologic and paleoclimatic reconstructions of Pleistocene glacial intervals in Mexico, when this species was most abundant.

Study sites

Based on the high abundances (30%) reported for *S. niagarae* in modern samples from the Santa Elena canal (Oliva-Martínez et al. 2005; Valadez et al. 2005), we decided to resample this site to record the environmental variables where this species lives today in central Mexico. However, when we visited the site, the canal was dry and could not be sampled, but we realized that it drained a nearby dam (Danxhó) from where we took water and surface sediment samples. These samples confirmed the presence of *S. niagarae* in the water column and sediments from Danxhó, and we now believe that the *S. niagarae* population previously reported for the Santa Elena canal might ultimately have come from the nearby dam. This site (Santa Elena-Danxhó), located to the NW of Mexico City, was the only one among 40 lakes in the TMVB where relatively high abundances (> 10%) of *S. niagarae* were identified (Davies et al. 2002; Caballero et al. 2019), therefore for this study we decided to analyze in further detail the distribution of this species in other lakes around Mexico City, in an area defined by the following geographical coordinates: 18° 36′–20° 12′ N and 97° 53′–100° 18′ W (Fig. 1b). Within the defined study region, 10 of the 40 lakes from the Caballero et al. (2019) central Mexico modern diatoms database were included, and we add in this work data from 6 new sites and 2 sites that were resampled (Zumpango and Chalco) between 2016 and 2018, giving a total of 18 samples from 16 sites around Mexico City where the presence and distribution of *S. niagarae* was explored.

The study region is located in the central area of the TMVB, where topography defines closed lacustrine basins of tectonic and volcanic origin (Fig. 1a). Altitude ranges from 980 to 4280 m asl, and it is associated to a climatic gradient from warmer conditions in the lowlands, with annual average temperatures of ∼ 24 °C, to high-altitude cold climates with annual averages of ∼ 4 °C. Precipitation ranges from ∼ 560 to ∼ 1200 mm and it is concentrated

during a summer rainy season, even though occasional rainfall also occurs during the winter (SMN 2019).

Materials and methods

Sampling and analytical methods for all sites followed those described in Sigala et al. (2017). In brief, geographical location (latitude, longitude, altitude) was determined using a handheld navigator (GARMIN GPSMAP 62 stc) and confirmed in Google Earth. Mean annual temperature (MAT, °C), precipitation (MAP, mm $year^{-1}$) and evaporation (MAE, mm $year^{-1}$) for all sites were taken from the closest meteorological stations (SMN 2019). Water depth (m) was measured in the field with a portable depth sounder (Speedtech instruments). Field measurements included Secchi disk depth (m) and depth profiles for temperature (°C), oxygen concentration (mg L^{-1}), pH, and electric conductivity (EC, µS cm^{-1}) determined using a multiparametric probe (Hydrolab Quanta G).

For water chemistry we took one sample at 0.5 m depth at a centrical location site of each lake. Cation samples were acidified in the field using concentrated (55%) HNO_3 and all the samples were kept in refrigeration until they were analyzed. Standardized methods were used for the analysis of major ions (APHA 1995, 1998; APHA et al. 2005; Armienta et al. 2008). Total alkalinity and ions concentration units were meq L^{-1} and to determine ionic dominance concentrations were transformed to percentages. Salinity was expressed as total dissolved solids (TDS, mg L^{-1}).

Nutrients determinations (APHA 1998) included ammonium, nitrites, and nitrates, which were added to express as dissolved inorganic nitrogen (DIN, µM), as well as total phosphorus (TP, µM), soluble reactive phosphorus (SRP, µM) and silica (SiO_2, µM). In the field the ammonium and nitrates samples were acidified using concentrated H_2SO_4 (98%). The following nutrient ratios were calculated: DIN:TP, DIN:SRP, SiO_2:DIN, and SiO_2:SRP. For chlorophyll *a* (mg m^{-3}) samples were extracted using (90%) methanol and measured using a spectrophotometer. Calculations were done based on Holden equations (Meeks 1974). Chlorophyll *a* and nutrients determinations were not performed for 7 of the 18 samples (Acuitlapilco, Chalco91, Coatetelco, Texcoco Artemia, Texcoco Jalapango, Texcoco Recreativo, and Zumpango91) which defined a reduced nutrient subset of 11 lakes. The information for each of the 16 studied lakes was summarized in a format similar to that presented in Sigala et al. (2017) and are presented as Electronic Supplementary Material (ESM2).

Diatom analysis

For diatom analysis superficial sediment from each site was collected with a Ekman dredge. 0.5 g of dry sediment was treated with (10%) HCl to eliminate carbonates and (30%) H_2O_2 to digest organic matter. If necessary, 5 ml of HNO_3 was added to accelerate the elimination of organic matter. Permanent slides were prepared with 200 µl aliquots of final solution using Naphrax (refraction index of 1.66) as mounting medium. Each sample was analyzed using a light microscope (Olympus BX50) at 1000 ×. A minimum of 100 to 400 valves was counted for each sample and relative abundances were calculated as species percentages. Diatoms were identified based on Håkansson and Locker (1981); Theriot and Stoermer (1981); Krammer and Lange-Bertalot (1986, 1988, 1991); Gasse 1986; Krammer et al. (1991); Håkansson (2002); Yu (2011). To confirm the taxonomy of some species, including *S. niagarae,* valves were observed using a scanning electron microscope (SEM JEOL JCM-6000PLUS). A detailed description and illustrations of *S. niagarae* in the lakes from central Mexico is included in Electronic Supplementary Material (ESM3).

Statistical analyses

Canonical correspondence analyses (CCAs) were performed with each of the two data subsets, identified as hydrochemistry (n = 18) and nutrients (n = 11). The environmental variables used were selected to avoid high correlation between them, correlation between variables was tested by means of an exploratory principal component analysis (not shown). The hydrochemistry CCA was done using temperature (MAT), precipitation (MAP), TDS, percentage of major ion concentrations ($[CO_3^{2-} + HCO_3^+]$, $[Cl^-]$, $[Ca^{2+}]$, $[Mg^{2+}]$ and $[Na^+ + K^+]$), and pH. Caballero et al. (2019) found that the two high altitude sites El Sol and La Luna represented outliers along the temperature gradient in the central Mexico data set, therefore we excluded

these lakes from this analysis. The nutrient CCA was performed using DIN, SRP and Secchi disk depth. All variables (except pH) and diatom abundances were transformed ($\log_{10} + 1$) to stabilize their variance. All of the analyses were carried out using the R software (R Development Core Team 2009), especially the "vegan" package (Oksanen et al. 2019).

Ecological niche modeling

Modern occurrences in the USA and Canada for *S. niagarae* were documented through a bibliographic review using online scientific literature databases. One occurrence point for each lake was taken, except for larger lakes with several sampling sites, when different points were considered if they were at least 20 km apart. Our final list of modern occurrences for *S. niagarae* consisted of 47 sites, 43 for the USA and Canada (ESM1) and four of our locations in central Mexico (Acuitlapilco, Danxhó, La Huaracha and San Juanico, ESM2). The nine late Pleistocene occurrences of *S. niagarae* in Mexico were also identified through a bibliographic review (ESM1).

To characterize the ecological niche of *S. niagarae* we used bioclimatic variables (2.5 arc minute spatial resolution, $\sim$ 5 km) from the WorldClim database (version 1.4 data for 1960–1990, Hijmans et al. 2005). These variables were used as environmental predictors, and clipped to adjust to the Nearctic realm, which extends from Canada to central Mexico. We calculated Pearsons's correlation coefficients for all pairs of bioclimatic variables to avoid collinearity between them and 11 out of the 19 bioclimatic variables were chosen (ESM1) by their low correlation ($|r| < 0.25$) using the 'NicheToolbox' package (Osorio-Olvera et al. 2020). The potential distributional area during the LGM of *S. niagarae* was modeled using analogous data layers from the Community Climate System Model (CCSM4, Gent et al. 2011). These layers were also clipped for the Nearctic realm.

The ENM was built using Maxent (Phillips et al. 2006) via the 'kuenm' package (Cobos et al. 2019). For model calibration, we created candidate models by combining the 11 selected bioclimatic variables into 9 sets of environmental predictors (ESM1) all sets including annual mean temperature (BIO1). Model calibrations were performed with 17 combinations of regularization multipliers (0.1–1.0 at intervals of 0.1, 2–6 at intervals of 1, 8 and 10) and all possible combinations of linear, quadratic and product feature classes. We selected the best model according to the 'kuenm' criteria of statistical significance based on low partial receiver operating characteristic (ROC) values, predictive power calculated by low omission rate at 5% and model complexity using Akaike information criterion (AICc), delta AICc ≤ 2 and high AICc weights, in that order of priority (Cobos et al. 2019). The final model was created with the best selected parameter set using 10 replicate bootstrap resamplings and final model transfers to the LGM scenario using an extrapolation with clamping (extrapolation which considers a constant response in areas with different environments from those in the calibration area) (Cobos et al. 2019) onto past-climate CCSM4 for the Nearctic zone. The projected LGM scenario was also validated using the distribution of *S. niagarae* late Pleistocene sites in Mexico.

Results

Salinity and ionic dominance

The 18 samples included in this study ranged from freshwater to mesosaline, and they had a wide range of ionic dominances (Fig. 2). In the anion field (Fig. 2a) most of the freshwater lakes (TDS < 500 mg L^{-1}) had a $[HCO_3^-] + [CO_3^{2-}]$ dominance, the subsaline lakes (500–3000 mg L^{-1}) had a higher proportion of sulfates and chlorides and those with the highest salinities (TDS > 3000 mg L^{-1}, hyposaline to mesosaline) showed $[Cl^-]$ dominance. On the cation diagram (Fig. 2b) there is also a clear gradient from the freshwater lakes dominated by $[Ca^{2+}] - [Mg^{2+}]$ to the higher salinity lakes (hyposaline to mesosaline) dominated by $[Na^+] + [K^+]$.

Nutrients and trophic level

Trophic status of the lakes in this study was determined based on their chlorophyll *a* values (OECD 1982), and they ranged from ultra-oligotrophic (La Luna) to hypertrophic (Chalco16, La Huaracha, Texcoco Nabor Carillo, Zumpango18). Possible nutrient limitation in these lakes was identified according to their DIN and SRP concentrations compared to the nutrient starvation limits of 0.1 μM for SRP and 7 μM for DIN (Reynolds 1999), as well as whether their

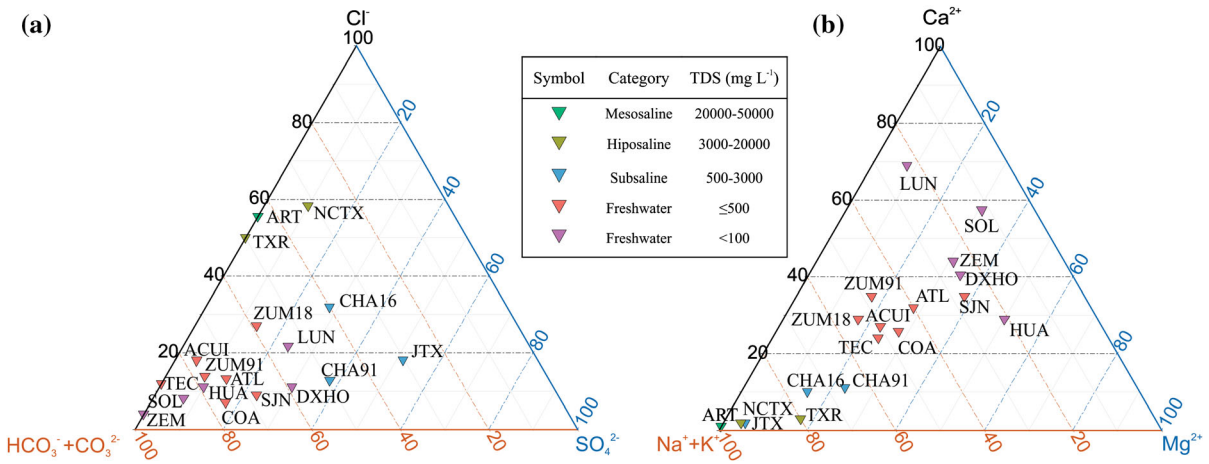

Fig. 2 Ternary diagram comparing major **a** anion and **b** cation percentages of 18 sampling sites in central Mexico. Abbreviations are the same as in Fig. 1. Salinity categories are based on Kolbe (1927) and Fritz (2007)

DIN:SRP ratios were above or below the 16N:1P Redfield ratio (Redfield 1958) or the 16Si:1P and 1Si:1N ratios (Xu et al. 2008) (Fig. 3a). According to these criteria, five sites have N:P ratios above the 16N:1P Redfield ratio (P limitation) but only four (Danxhó, La Huaracha, La Luna, and Zempoala) had SRP concentrations below the starvation limits and could therefore be considered to be limited by this element. On the other hand, one lake (El Sol) showed concentrations below the starvation values for both DIN and SRP and therefore was co-limited by both nutrients. Regarding SiO_2, only Texcoco Nabor Carrillo had Si:SRP ratios below the 16Si:1P ratio suggesting silica limitation (Fig. 3b).

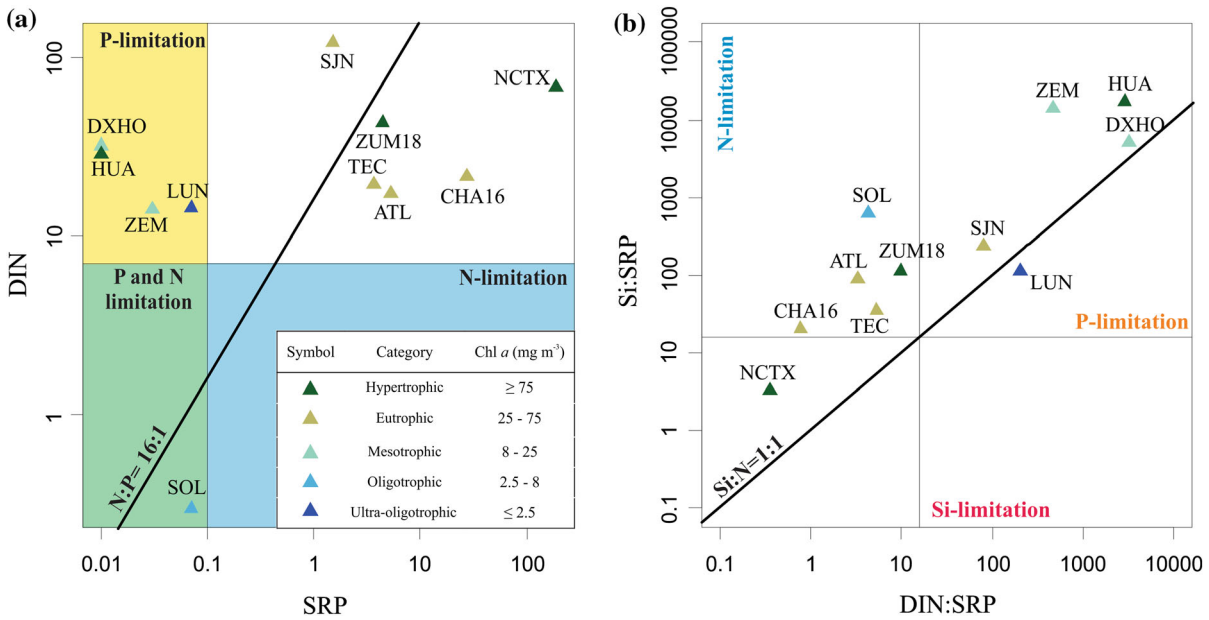

Fig. 3 Nutrient concentrations comparisons of 11 lakes in central Mexico. **a** Variation of DIN:SRP stoichiometric ratios, diagonal line represents the Redfield (1958) N:P = 16:1 ratio, shaded areas represent nutrient limiting values according to Reynolds (1999) SRP < 0.1 µM y DIN < 7 µM. **b** Variation of Si:SRP and DIN:SRP stoichiometric ratio, diagonal line represents Si:N = 1:1 ratio according to Redfield (1958). Abbreviations correspond to Fig. 1. Trophic categories are based on annual maximum chlorophyll values according to OECD (1982)

Distribution of *Stephanodiscus niagarae* in central Mexico

Frustules of *Stephanodiscus niagarae* were identified only in four of the 18 analyzed samples: La Huaracha, San Juanico, Danxhó, and Acuitlapilco, even though relative abundances were low (< 10%). In fact these were the only lakes in which this species was present in percentages above 1% in the full set of 46 lakes in central Mexico (Caballero et al. 2019) for which we have data (Fig. 4). Scarce valves of *S. niagarae* were counted in two lakes (Burro and Teremendo), but they only reached relative abundances of ∼ 0.5%. In other two lakes (Pátzcuaro and Atotonilco) some fragments of *S. niagarae* were also observed, but they were considered to represent reworked material as older lacustrine sediments outcrop within their basins (Davies et al. 2002; Israde-Alcántara et al. 2010a). The highest relative abundance was observed in La Huaracha with 6.0% followed by Danxhó 5.3%, San Juanico 4.1%; and the lowest was in Acuitlapilco with 1.1%. Total diatom abundance in these lakes ranged from 2.0 to 70.6 $\times$ 10^6 valves g^{-1} of dry sediment and therefore the lake with the highest concentrations of *S. niagarae* expressed as valves per gram of dry sediment was Danxhó (3.8 $\times$ 10^6), followed by La Huaracha (0.9 $\times$ 10^6), with low values in San Juanico (0.08 $\times$ 10^6), and Acuitlapilco (0.05 $\times$ 10^6).

The diatom assemblages in these four lakes were dominated by *Aulacoseira* spp., either *A. ambigua*

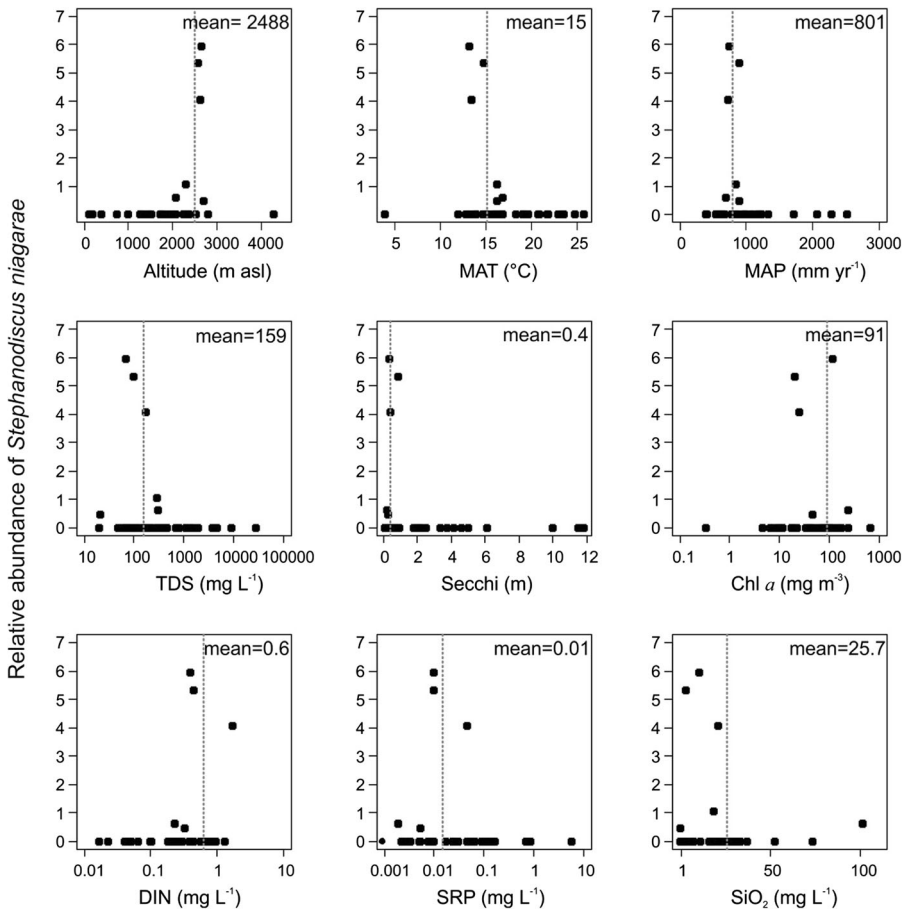

Fig. 4 Relative abundances of *Stephanodiscus niagarae* in 46 lakes studied along the Trans-Mexican Volcanic Belt, central Mexico (including new sites from this study and those from Caballero et al. 2019) in relation with altitude, mean annual temperature (MAT) and precipitation (MAP), total dissolved solids (TDS), Secchi disk depth, Chlorophyll *a* (Chl *a*), dissolved inorganic nitrogen (DIN), soluble reactive phosphorus (SRP), and SiO_2. Dashed lines show average values of the variables for the lakes where *Stephanodiscus niagarae* was present

(Grunow) Simonsen (1979) in Huaracha and Danxhó or *A. granulata* (Ehrenberg) Simonsen (1979) and its variety *A. granulata* var. *angustissima* (O.Müller) Simonsen (1979) in San Juanico and Acuitlapilco. Other diatom species that were abundant in these sites were *Cyclostephanos dubius* (Hustedt) Round in Theriot et al. (1988) in Huaracha, *Aulacoseira alpigena* (Grunow) Krammer (1991) in San Juanico, *Asterionella formosa* Hassall (1850) and *Fragilaria crotonensis* Kitton (1869) in Danxhó, and *Cyclotella meneghiniana* Kützing (1844) in Acuitlapilco.

The four lakes where *S. niagarae* was present were preferentially located at altitudes around 2500 m asl (Fig. 4), associated to cool and humid conditions (MAT $\sim$ 15 °C, MAP $\sim$ 800 mm year^{-1}). They were freshwater lakes (with TDS $\leq$ 500 mg L^{-1}), with turbid waters (Secchi disk depth $<$ 1 m) and mesotrophic to hypertrophic conditions according to their chlorophyll *a* concentrations (Fig. 4). They ranged from 0.40 to 1.69 mg L^{-1} in DIN, 0.01 to 0.05 mg L^{-1} in SRP, and SiO_2 from 3.1 to 21.3 mg L^{-1} (Fig. 4).

The variance inflation factors (VIF) of all variables in the CCA performed with the hydrochemistry data set (Fig. 5a, b) were $<$ 10 indicating low correlation between predictors. The CCA1 (λ = 0.78, p = 0.008 and proportion explained of 10%) correlated positively with TDS, [$Na^+ + K^+$] %, MAT, [Cl^-] % and pH and negatively with precipitation, [Ca^{2+}] % and [Mg^{2+}] %. Whereas CCA2 (λ = 0.57, p = 0.5 and proportion explained of 10%) correlated positively with carbonates. The sites in the hydrochemistry CCA (Fig. 5a) follow a salinity gradient and its associated change in dominant ions from [$CO_3^{2-} + HCO_3^+$]- $-$ [Ca^{2+}] $-$ [Mg^{2+}] % to [Cl^-] $-$ [$Na^+ + K^+$] % dominated. The three lakes in which *S. niagarae* was most abundant are located to the left-bottom sector of the graph, at the low end of the [$Na^+ + K^+$] %, TDS, [Cl^-] % and MAT gradients. In the species biplot (Fig. 5b) *S. niagarae* is also located to the left-bottom sector of the graph and it clusters with other species that were also present in the diatom assemblages of these lakes, mainly *Aulacoseira ambigua, A. alpigena*, and *Cyclostephanos dubius*, and more distantly *Asterionella formosa*, *Aulacoseira granulata, A. granulata* var. *angustissima,* and *Fragilaria crotonensis.*

The VIF of all variables in the CCA performed with the nutrients subset (Fig. 6a, b) were $<$ 3 indicating low correlation between predictors. CCA1 (λ = 0.87, p = 0.001 and proportion explained of 16%) correlated positively with DIN and negatively with Secchi disk depth. CCA2 (λ = 0.81, p = 0.007 and proportion explained of 15%) corresponded negatively with SRP. This nutrient CCA shows that the sites are distributed along a trophic gradient (Fig. 6a) with the lower trophic level and clearer water (higher Secchi disk

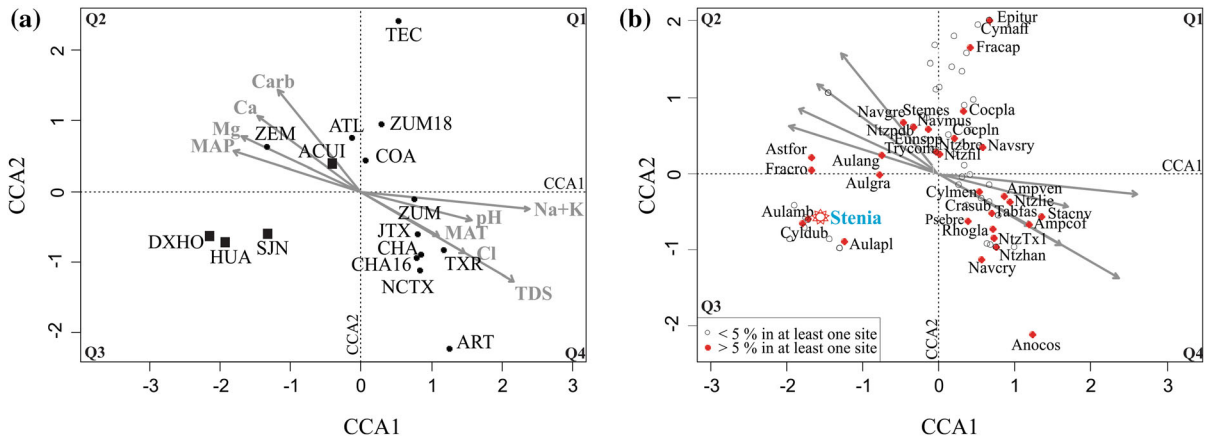

Fig. 5 Hydrochemistry canonical correspondence analysis (CCA1 vs. CCA2) of studied samples in central Mexico. **a** Hydrochemistry CCA (n = 16) including mean annual temperature (MAT), mean annual precipitation (MAP), mean annual evaporation (MAE), total dissolved solids (TDS), percentage of major ion concentrations ([$CO_3^{2-} + HCO_3^+$], [Cl^-], [Ca^{2+}], [Mg^{2+}] and [$Na^+ + K^+$]), and pH. **b** Diatom species distribution in the hydrochemistry CCA. Abbreviations correspond to Fig. 1. Squares represent sites where *S. niagarae* is present. Location of *S. niagarae* is the red star and blue words. The full names of the species and their codes are listed in Electronic Supplementary Material 1 (ESM1). (Color figure online)

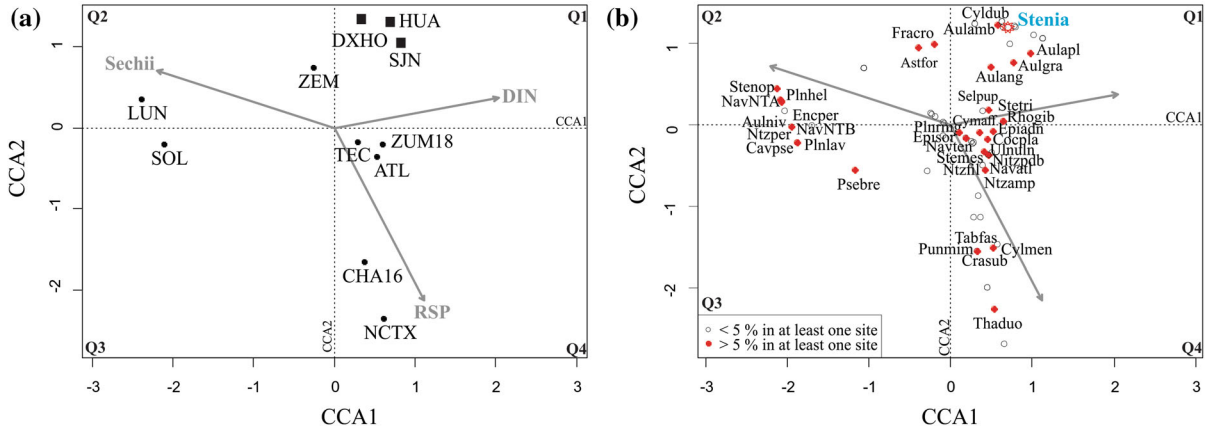

Fig. 6 Nutrient canonical correspondence analysis (CCA1 vs. CCA2) of studied samples in central Mexico. **a** Nutrient CCA (n = 11) including Secchi disk, dissolved inorganic nitrogen (DIN), soluble reactive phosphorus (SRP); **b** diatom species distribution in the nutrient CCA. Abbreviations correspond to

Fig. 1. Squares represent sites where *S. niagarae* is present. Location of *S. niagarae* is the red star and blue words. The full name of the species and their codes are listed in Electronic Supplementary Material 1 (ESM1). (Color figure online)

depth) sites located to the left of the diagram. In the species biplot (Fig. 6b) the diatom species clearly split in three groups, to the left those most abundant in clear (high Secchi disk depth) waters with low SRP and DIN, to the bottom-right, those present in turbid waters (low Secchi disk depth) with higher SRP and to the top-right, those preferring turbid waters with higher DIN values. *S. niagarae* is located in this last group of diatoms and it clusters with the same species as in the hydrochemistry CCA, mainly *A. ambigua* and, *C. dubius*, more distantly *Asterionella formosa*, *Aulacoseira alpigena*, *A. granulata, A. granulata* var. *angustissima,* and *Fragilaria crotonensis.*

Ecological niche modeling

We created 1071 candidate models by combining the 9 sets of environmental predictors. The results of the model evaluation showed the best model had in general a good performance with a partial ROC of 0.00, an omission rate at 5% of 0.04, delta AICc of 0.94 and weight AICc of 0.55. The best candidate model corresponded to environmental variables set 8 (ESM1), that included as environmental predictors mean annual temperature (BIO1) and the mean temperatures of the warmest and the coldest quarters (BIO10 and BIO11 respectively), and linear-product as feature class.

The modern potential distribution map of *S. niagarae* (Fig. 7a), showed a high probability of distribution in southern Canada and northern USA, with a more restricted probability of distribution along the western mountains of Mexico (Sierra Madre Occidental) and on the TMVB in central Mexico. Whereas ENM transfer to the LGM scenario (Fig. 7b) shows an expanded potential distribution in the southern part of the USA and along the highlands of western and central Mexico. For the LMG scenario, the late Pleistocene fossil observations (Fig. 7b) were located in the higher probability distribution areas, indicating a good performance of the model.

Discussion

Ecological distribution of *Stephanodiscus niagarae* in central Mexico

In this paper we examined the modern distribution of *Stephanodiscus niagarae* in central Mexico and its relationship with environmental variables. From a set of 46 lakes in the TMVB (new sites in this work and those in Caballero et al. 2019) it was only present with abundances higher than 1% in 4 of them (La Huaracha, San Juanico, Danxhó and Acuitlapilco). These lakes were located in surrounding areas of Mexico City, at altitudes of around 2500 m asl, with cool, humid conditions (MAT ~ 15 °C, MAP ~ 800 mm $year^{-1}$). We studied in more detail the distribution of *S. niagarae* in 18 samples collected within a region

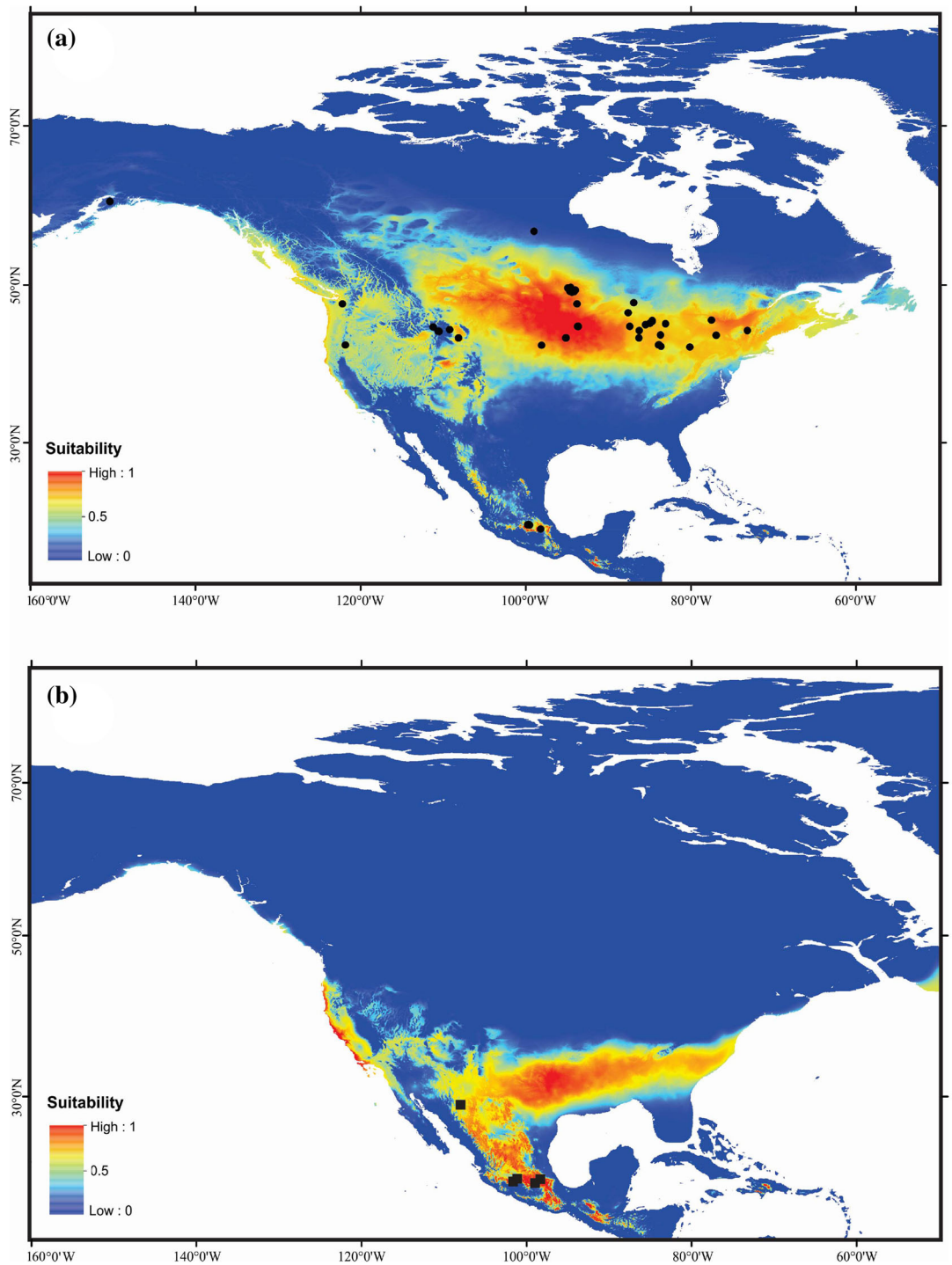

Fig. 7 Ecological niche models (ENMs) of *Stephanodiscus niagarae*. **a** Potential distribution map of *S. niagarae* during present time. Points correspond to sites with reported living populations of *S. niagarae* (Electronic Supplementary Material 1, ESM1) used for the calibration and evaluation of the model. **b** Projected distribution under last glacial maximum (LGM) conditions. Squares show fossil locations during last glacial maximum (ESM1)

around Mexico City, exploring its relationship with hydrological variables and trophic conditions.

The hydrochemistry CCA ordination (Fig. 5a, b) separates the three lakes where *S. niagarae* had its highest abundances (La Huaracha, San Juanico and Danxhó) because of their relatively low MAT, low TDS, low [Na] + [K] % and [Cl^-] %, but relatively high MAP as well as a [Mg^{2+}] − [Ca^{2+}] % dominance. These results agree with Fritz et al. (1993, 2001), who reports that *S. niagarae* is rare or absent in lakes with salinity above 3000 mg L^{-1}. In this CCA *S. niagarae* clusters with *Aulacoseira ambigua, A. alpigena*, and *Cyclostephanos dubius,* and more distantly with *Asterionella formosa*, *Aulacoseira granulata*, *A. granulata* var. *angustissima,* and *Fragilaria crotonensis,* all of which were abundant diatom taxa in these three lakes.

The nutrient CCA ordination (Fig. 6) separates the three lakes where *S. niagarae* had its highest abundances (La Huaracha, San Juanico and Danxhó) by their high turbidy (low Secchi disk depth), high DIN but relatively low SRP values. Even though according to their chlorophyll *a* concentrations these lakes ranged from mesotrophic (Danxhó) to hypertrophic (La Huaracha), all of them had high N:P ratios and two of them (La Huaracha and Danxhó) were identified as P-limited by their low SRP concentrations. These results are in agreement with Kilham et al. (1996), who reports moderate to high N:P ratios (OECD 1982) in Yellowstone lakes where *S. niagarae* is present. All this suggests that *S. niagarae* has a preference for high turbidity and relatively high productivity systems (high chlorophyll *a* values), but with high N:P ratios and a tendency to P limitation. Our results are also consistent with Rawson (1956) and Stoermer and Jang (1970), who consider *S. niagarae* as a eutrophic species. The preference of *S. niagarae* for relatively turbid waters can explain why this species was not present in other relatively cool, high-altitude lakes like Zempoala or El Sol, as these lakes had clear waters (high Secchi disk depths) and therefore plotted to the left of the nutrients CCA diagram. This conclusion agrees with Reavie et al. (2014b) who associated it to cold, high-nutrient and turbid environments in Lake Erie.

Current and past potential distribution of *Stephanodiscus niagarae*

The ENM developed identified that temperature (annual mean, coldest and warmest quarters means) was the most important environmental variable to define habitat suitability for *S. niagarae* in areas like northern USA and southern Canada (Fig. 7a), which are effectively the areas where *S. niagarae* is presently an abundant planktonic diatom (Theriot and Stoermer 1984a; Edlund et al. 2004). This ENM model showed restricted habitat suitability for this species in specific mountain regions of western (Sierra Madre Occidental) and central Mexico (TMVB) primarily because of its temperate climate due to altitude, as indicated by the preferential presence of *S. niagarae* in lakes located at around 2500 m asl in central Mexico.

The projected LGM scenario for *S. niagarae* was modeled with the CCSM4 projection which includes a mean temperature decrease of − 5.5 °C (Brady et al. 2013). This decrease in temperature is in agreement with pollen-based and diatom-based transfer functions from Lake Chalco, which estimated a temperature reduction during the LGM in central Mexico between − 4 and − 5 °C (Correa-Metrio et al. 2013; Caballero et al. 2019). The LGM scenario of *S. niagarae* identifies areas with highest potential in southern EUA as well as the western and central highlands in Mexico (Fig. 7b). This high probability distribution in the highlands of Mexico is confirmed by the distribution of lacustrine fossil records in northwestern and central Mexico with a high abundance of *S. niagarae* (Fig. 7b).

Comparing the projected distributions under current and LGM conditions for *S. niagarae,* there are important latitudinal differences which imply an expansion of habitat suitability for this species in central Mexico during the LGM. The LGM scenario suggest that the highlands along the Sierra Madre Occidental could have acted as a migration corridor offering suitable habitats for this species to disperse into central Mexico, which is one of the migration corridors suggested by Ceballos et al. (2010).

Stewart et al. (2009) reported that temperate taxa could remain with a limited northern distribution (northern refugia), but based on the latitudinal displacements of *S. niagarae* during cold events, we speculate that its fundamental niche expands southwards, whereas during warm periods (e.g. present day)

its maximum extension is in USA and Canada, while in Mexico is present with a scattered distribution at low densities. This southern refugia pattern is consistent with the responses of temperate taxa during glacial periods, as for example the boreal and cool-temperate conifers in eastern North America that had a southern displacement during the LGM (Jackson et al. 2000).

Our findings highlight the importance of *Stephanodiscus niagarae* as indicator of cold periods in the central and western mountains of Mexico. Potentially, *S. niagarae* could contribute in paleolimnologic and paleoclimatic reconstructions as a stratigraphic marker for previous glacial periods.

Acknowledgements This research was funded by DGAPA-IV-100215 "Cambio Climático y Medio Ambiente en la historia del lago de Chalco" and DGAPA-PAPIIT-IN103819 "Variabilidad climática y paleoambientes durante la terminación II (130 ka): el paso del penúltimo glacial (MIS 6) al penúltimo interglaciar (MIS 5)". Diana Avendaño thanks the Posgrado de Ciencias de la Tierra, UNAM and CONACyT (CVU 854736) for finnancial support. We also thank: Dr. Ma. Aurora Armienta and the staff in the Laboratorio de Quimica Análitica, Instituto de Geofisica, UNAM for major anions and SiO_2 analysis; Ariadna Martinez and Daniela Cela from the "Red de Ecología Funcional" laboratory at the Instituto de Ecología, A.C. (INECOL), Xalapa, Mexico, for the nutrients analysis; Laura Gómez Lizárraga for excellent technical assistance with the different stages of sample preparation with the scanning electron microscope and Alejandra Ubaldo Guerra provided assistance during the field work. We also thank Dr. Whitmore, Dr. Reavie and two anonymous reviewers for their valuable comments that greatly improved our manuscript.

References

American Public Health Association (APHA) (1995) Standard methods for the examination of water and wastewater. American Public Health Association, Washington

American Public Health Association (APHA) (1998) Standard methods for the examination of water and wastewater. American Public Health Association, Washington

American Public Health Association (APHA), American Water Works Association (AWWA), Water Pollution Control Federation (WPCF) (2005) Standard methods for the examination of water and wastewater. American Public Health Association, Washington

Armienta MA, Vilaclara G, De la Cruz-Reyna S et al (2008) Water chemistry of lakes related to active and inactive Mexican volcanoes. J Volcanol Geotherm Res 178:249–258. https://doi.org/10.1016/j.jvolgeores.2008.06.019

Avendaño D, Caballero M, Ortega-Guerrero B et al (2018) Environmental conditions at the end of the Isotopic Stage 6 (IS 6: > 130000 years) in the center of Mexico: Characterization of a section of laminated sediments from Lake Chalco. Rev Mex Ciencias Geol 35:168–178. https://doi.org/10.22201/cgeo.20072902e.2018.2.649

Bradbury JP (1971) Paleolimnology of Lake Texcoco, Mexico. Evidence from diatoms. Limnol Oceanogr 16:180–200. https://doi.org/10.4319/lo.1971.16.2.0180

Bradbury JP (2000) Limnologic history of Lago de Patzcuaro, Michoacan, Mexico for the past 48,000 years: impacts of climate and man. Palaeogeogr Palaeoclimatol Palaeoecol 163:69–95. https://doi.org/10.1016/S0031-0182(00)00146-2

Bradbury JP, Colman SM, Dean WE (2004) Limnological and climatic environments at Upper Klamath Lake, Oregon during the past 45 000 years. J Paleolimnol 31:167–188. https://doi.org/10.1023/B:JOPL.0000019232.74649.02

Brady EC, Otto-bliesner BL, Kay JE, Rosenbloom N (2013) Sensitivity to glacial forcing in the CCSM4. J Clim 26:1901–1925. https://doi.org/10.1175/JCLI-D-11-00416.1

Brugam RB (1983) The relationship between fossil diatom assemblages and limnological conditions. Hydrobiologia 98:223–235. https://doi.org/10.1007/BF00021023

Caballero M, Ortega Guerrero B (1998) Lake levels since about 40,000 years ago at Lake Chalco, near Mexico City. Quat Res 50:69–79. https://doi.org/10.1006/qres.1998.1969

Caballero M, Lozano S, Ortega B et al (1999) Environmental characteristics of Lake Tecocomulco, northern basin of Mexico, for the last 50,000 years. J Paleolimnol 22:399–411. https://doi.org/10.1023/A:1008012813412

Caballero M, Lozano-García S, Ortega-Guerrero B, Correa-Metrio A (2019) Quantitative estimates of orbital and millennial scale climatic variability in central Mexico during the last ~40,000 years. Quat Sci Rev 205:62–75. https://doi.org/10.1016/j.quascirev.2018.12.002

Ceballos G, Arroyo-Cabrales J, Ponce E (2010) Effects of Pleistocene environmental changes on the distribution and community structure of the mammalian fauna of Mexico. Quat Res 73:464–473. https://doi.org/10.1016/j.yqres.2010.02.006

Cobos ME, Townsend Peterson A, Barve N, Osorio-Olvera L (2019) Kuenm: An R package for detailed development of ecological niche models using Maxent. PeerJ 7:e6281. https://doi.org/10.7717/peerj.6281

Colman SM, Bradbury JP, Rosenbaum JG (2004) Paleolimnology and paleoclimate studies in Upper Klamath Lake, Oregon. J Paleolimnol 31:129–138. https://doi.org/10.1023/B:JOPL.0000019235.72107.92

Correa-Metrio A, Bush M, Lozano-García S, Sosa-Nájera S (2013) Millennial-scale temperature change velocity in the continental northern neotropics. PLoS ONE 8:e81958. https://doi.org/10.1371/journal.pone.0081958

Davies SJ, Metcalfe SE, Caballero ME, Juggins S (2002) Developing diatom-based transfer functions for Central Mexican lakes. Hydrobiologia 467:199–213. https://doi.org/10.1023/A:1014971016298

Edlund M, Kingston J, Heiskary S (2004) Expanding a sediment diatom reconstruction model to eutrophic Southern Minnesota Lakes. Environmental Outcomes Division Minnesotta Pollution Control Agency. CFMS Contract No. A45276, Minnesota

Edmondson WT, Abella SEB, Lehman JT (2003) Phytoplankton in Lake Washington: long-term changes 1950–1999. Arch Hydrobiol Suppl 139:275–326

Fritz S (2007) Salinity and climate reconstruction from diatoms in continental lake deposits. In: Elias SA (ed) Encyclopedia of quaternary science. Elsevier, Amsterdam, pp 514–522

Fritz SC, Juggins S, Battarbee RW (1993) Diatom assemblages and ionic characterization of lakes of the Northern Great Plains, North America: a tool for reconstructing past salinity and climate fluctuations. Can J Fish Aquat Sci 50:1844–1856. https://doi.org/10.1139/f93-207

Fritz SC, Cumming BF, Gasse F, Laird KR (2001) Diatoms as indicators of hydrologic and climatic change in saline lakes. In: Stoermer EF, Smol JP (eds) The diatoms: applications for the environmental and earth sciences. Cambridge University Press, Cambridge, pp 41–72

Gasse F (1986) East African diatoms: Taxonomy, Ecological Distribution. Bibliotheca Diatomologica, Stuttgart

Gent PR, Danabasoglu G, Donner LJ, Holland MM, Hunke EC, Jayne SR, Lawrence DM, Neale RB, Rasch PJ, Vertenstein M, Worley P, Yang ZL, Zhang M (2011) The community climate system model version 4. J Clim 24:4973–4991. https://doi.org/10.1175/2011JCLI4083.1

Graham RW, Lundelius EL Jr, Graham MA, Schroeder EK, Toomey RS III, Anderson E, Barnosky AD, Burns JA, Churcher CS, Grayson DK, Guthrie DR, Harington CR, Jefferson GT, Martin LD, McDonald GH, Morlan RE, Semken HA Jr, Webb DS, Werdelin L, Wilson MC (1996) Spatial response of mammals to late quaternary environmental fluctuations FAUNMAP working group. Science 272:1601–1606. https://doi.org/10.1126/science.272.5268.1601

Håkansson H (2002) A compilation and evaluation of species in the general *Stephanodiscus*, *Cyclostephanos* and *Cyclotella* with a new genus in the family Stephanodiscaceae. Diatom Res 17:1–139. https://doi.org/10.1080/0269249X.2002.9705534

Håkansson H, Locker S (1981) *Stephanodiscus* Ehrenberg 1846, a Revision of the species described by Ehrenberg. Nova Hedwigia 35:117–150

Håkansson H, Kling H (1989) A light and electron microscope study of previously described and new *Stephanodiscus* species (Bacillariophyceae) from Central and Northern Canadian lakes, with ecological notes on the species. Diatom Res 4:269–288. https://doi.org/10.1080/0269249X.1989.9705076

Hewitt G (2000) The genetic legacy of the Quaternary ice ages. Nature 405:907–913. https://doi.org/10.1038/35016000

Hijmans RJ, Cameron SE, Parra JL et al (2005) Very high resolution interpolated climate surfaces for global land areas. Int J Climatol 25:1965–1978. https://doi.org/10.1002/joc.1276

Israde-Alcántara I, Garduño-Monroy VH, Ortega Murillo R (2002) Paleoambiente lacustre del cuaternario tardío en el centro del lago de Cuitzeo. Hidrobiologica 12:61–78

Israde-Alcántara I, Miller WE, Garduño-Monroy VH et al (2010a) Palaeoenvironmental significance of diatom and vertebrate fossils from Late Cenozoic tectonic basins in west-central México: a review. Quat Int 219:79–94. https://doi.org/10.1016/j.quaint.2010.01.012

Israde-Alcántara I, Velázquez-Durán R, Socorro Lozano García M et al (2010b) Evolución Paleolimnológica del Lago Cuitzeo, Michoacán durante el Pleistoceno-Holoceno. Bol Soc Geol Mex 62:345–357

Israde-Alcántara I, Domínguez-Vázquez G, Gonzalez S et al (2018) Five Younger Dryas black mats in Mexico and their stratigraphic and paleoenvironmental context. J Paleolimnol 59:59–79. https://doi.org/10.1007/s10933-017-9982-y

Jackson ST, Webb RS, Anderson KH et al (2000) Vegetation and environment in Eastern North America during the last glacial maximum. Quat Sci Rev 19:489–508

Julius M, Stoermer EF, Taylor CM, Schelske CL (1998) Local extirpation of *Stephanodiscus niagarae* (Bacillariophyceae) in the recent limnological record of Lake Ontario. J Phycol 34:766–771. https://doi.org/10.1046/j.1529-8817.1998.340766.x

Kilham SS, Theriot EC, Fritz SC (1996) Linking planktonic diatoms and climate change in the large lakes of the Yellowstone ecosystem using resource theory. Limnol Oceanogr 41:1052–1062. https://doi.org/10.4319/lo.1996.41.5.1052

Kolbe RW (1927) Zur ökologie, morphologie und systematik der brackwasser-diatomeen: Die kieselalgen des Sperenberger salzgebiets. G. Fischer Jena, Berlin-Dahlem

Krammer K, Lange-Bertalot H (1986) 2/1. Bacillariophyceae. 1. Teil: Naviculaceae. In: Ettl H, Gerloff J, Heynig H, Mollenhauer D (eds) Sübwasserflora von Mitteleuropa. G. Fischer Verlag, Stuttgart

Krammer K, Lange-Bertalot H (1988) 2/2. Bacillariophyceae. 2. Teil: Bacillariaceae, Epithemiaceae, Surirellaceae. In: Ettl H, Gerloff J, Heynig H, Mollenhauer D (eds) Sübwasserflora von Mitteleuropa. G. Fischer Verlag, Stuttgart

Krammer K, Lange-Bertalot H (1991) 2/4. Bacillariophyceae. 4. Teil: Achnanthaceae. Kritische Ergänzungen zu Navicula (Lineolatae) und Gomphonema. In: Ettl H, Gerloff J, Heynig H, Mollenhauer D (eds) Sübwasserflora von Mitteleuropa. G. Fischer Verlag, Stuttgart

Krammer K, Lange-Bertalot H, Håkansson H, Nörpel M (1991) 2/3 Bacillariophyceae. 3. Teil: Centrales, Fragilariaceae, Eunotiaceae. In: Ettl H, Gerloff J, Heynig H, Mollenhauer D (eds) Sübwasserflora von Mitteleuropa. G. Fischer Verlag, Stuttgart

Lashaway AR, Carrick HJ (2010) Effects of light, temperature and habitat quality on meroplanktonic diatom rejuvenation in Lake Erie: Implications for seasonal hypoxia. J Plankton Res 32:479–490. https://doi.org/10.1093/plankt/fbp147

Meeks CJ (1974) Chlorophylls. In: Stewart PDW (ed) Algal physiology and biochemistry. Blackwell Scientific Publications, Oxford, pp 161–175

Metcalfe S (1995) Holocene environmental change in the Zacapu Basin, Mexico: a diatom-based record. The Holocene 5:196–208. https://doi.org/10.1177/095968369500500207

Metcalfe S, Say A, Black S et al (2002) Wet conditions during the last glaciation in the Chihuahuan Desert, Alta Babicora Basin, Mexico. Quat Res 57:91–101. https://doi.org/10.1006/qres.2001.2292

Oksanen J, Blanchet FG, Friendly M, Kindt R, Legendre P, McGlinn D, Minchin PR, O'Hara RB, Simpson GL, Solymos P, Stevens MHH, Szoecs E, Wagner H (2019) Vegan: community ecology package. The R Project for Statistical Computing. http://CRAN.R

Oliva-Martínez MG, Ramírez-Martínez JG, Garduño-Solórzano G, Cañetas Ortega J, Ortega MM (2005) Diatoms of three

bodies of water from wetlands Jilotepec-Ixtlahuaca, Estado de Mexico. Hidrobiologica 15:1–26

Organization for Economic Cooperation and Development (OECD) (1982) Eutrophication of waters. Organization for Economic Cooperation and Development, Paris

Osorio-Olvera L, Lira-Noriega A, Soberón J, Townsend PA, Falconi M, Contreras-Díaz RG, Martínez-Meyer E, Barve V, Barve N (2020) ntbox: an R package with graphical user interface for modeling and evaluating multidimensional ecological niches. Methods Ecol Evol 11:1199–1206. https://doi.org/10.1111/2041-210X.13452

Pardi MI, Graham RW (2019) Changes in small mammal communities throughout the late Quaternary across eastern environmental gradients of the United States. Quat Int 530–531:80–87. https://doi.org/10.1016/j.quaint.2018.05.041

Phillips SJ, Anderson RP, Schapire RE (2006) Maximum entropy modeling of species geographic distributions. Ecol Modell 190:231–259. https://doi.org/10.1016/j.ecolmodel.2005.03.026

Pla S, Paterson AM, Smol JP et al (2005) Spatial Variability in Water Quality and Surface Sediment Diatom Assemblages in a Complex Lake Basin: Lake of the Woods, Ontario, Canada. Int J Gt Lake Res 31:253–266. https://doi.org/10.1016/S0380-1330(05)70257-4

R Development Core Team (2009) R: a language and environment for statistical computing, 3.1. http://www.R-project.org

Rawson DS (1956) Algal indicators of trophic lake types. Limnol Oceanogr 1:18–25

Reavie ED, Barbiero RP, Allinger LE, Warren GJ (2014a) Phytoplankton trends in the Great Lakes 2001–2011. J Gt Lake Res 40:618–639. https://doi.org/10.1016/j.jglr.2014.04.013

Reavie ED, Heathcote AJ, Chraïbi S (2014b) Laurentian Great Lakes phytoplankton and their water quality characteristics, including a diatom-based model for paleoreconstruction of phosphorus. PLoS ONE 9:e104705. https://doi.org/10.1371/journal.pone.0104705

Redfield AC (1958) The biological control of chemical factors in the environment. Am Sci 64:205–221

Reynolds CS (1999) Non-determinism to probability, or N: P in the community ecology of phytoplankton nutrient ratios: Arch. Fur Hydrobiol 146:23–35

Servicio Meteorológico Nacional (SMN) (2019) Información Estadística Climatológica. https://smn.conagua.gob.mx/es/climatologia/informacion-climatologica/informacion-estadistica-climatologica. Accessed 1 May 2019

Sigala I, Caballero M, Correa-Metrio A et al (2017) Basic limnology of 30 continental waterbodies of the Transmexican Volcanic Belt across climatic and environmental gradients. Bol Soc Geol Mex 69:313–370. https://doi.org/10.18268/bsgm2017v69n2a3

Spaulding SA, Kociolek JP, Wong D, Kociolek IP (1999) A taxonomic and systematic revision of the genus Muelleria (Bacillariophyta). Phycologia 38:314–341. https://doi.org/10.2216/i0031-8884-38-4-314.1

Spaulding SA, Van de Vijver B, Hodgson DA, McKnigth DM, Verleyen E, Stanish L (2010) Diatoms as indicators of environmental change in antarctic and subantarctic freshwaters. In: Smol J, Stoermer EF (eds) The diatoms: applications for the environmental and earth sciences. Cambridge University Press, New York, pp 267–284

Stewart JR, Lister AM, Barnes I, Dalén L (2009) Refugia revisited: Individualistic responses of species in space and time. Proc R Soc B Biol Sci 277:661–671. https://doi.org/10.1098/rspb.2009.1272

Stoermer EF, Jang JJ (1970) Distribution and relative abundance of dominant plankton diatoms in Lake Michigan. Gt Lakes Res Div, Michigan

Stoermer EF, Ladewski TB (1976) Apparent optimal temperatures for the occurrence of some common phytoplankton species in southern Lake Michigan. Gt Lakes Res Div, Michigan

Stoermer EF, Emmert G, Schelske CL (1989) Morphological variation of *Stephanodiscus niagarae* Ehrenb. (Bacillariophyta) in a Lake Ontario sediment core. J Paleolimnol 2:227–236. https://doi.org/10.1007/BF00202048

Theriot EC, Stoermer EF (1981) Some aspects of morphological variation in *S. niagarae* (Bacillariophyceae). J Phycol 17:64–72. https://doi.org/10.1111/j.1529-8817.1981.tb00820.x

Theriot EC, Stoermer EF (1984a) Principal component analysis of character variation in *Stephanodiscus niagarae* Ehrenb.: Morphological variation related to Lake Trophic status. In: Mann DG (ed) 7th international diatom symposium. Otto Koeltz Science Publishers, Koenigstein, pp 97–111

Theriot EC, Stoermer EF (1984b) Principal component analysis of variation in *Stephanodiscus rotula* and *S. niagarae* (Bacillariophyceae). Syst Bot 9:53–59. https://doi.org/10.2307/2418407

Theriot EC, Fritz SC, Whitlock C, Conley DJ (2006) Late Quaternary rapid morphological evolution of an endemic diatom in Yellowstone Lake, Wyoming. Paleobiology 32:38–54. https://doi.org/10.1666/02075.1

Valadez F, Oliva G, Vilaclara G et al (2005) On the presence of *Stephanodiscus niagarae* Ehrenberg in central Mexico. J Paleolimnol 34:147–157. https://doi.org/10.1007/s10933-005-0810-4

Waltari E, Hijmans RJ, Peterson AT et al (2007) Locating pleistocene refugia: comparing phylogeographic and ecological niche model predictions. PLoS ONE 2:e563. https://doi.org/10.1371/journal.pone.0000563

Xu J, Ho AYT, Yin K et al (2008) Temporal and spatial variations in nutrient stoichiometry and regulation of phytoplankton biomass in Hong Kong waters: Influence of the Pearl River outflow and sewage inputs. Mar Pollut Bull 57:335–348. https://doi.org/10.1016/j.marpolbul.2008.01.020

Yu A (2011) *Stephanodiscus niagarae*. In: Diatoms North Am. https://diatoms.org/species/stephanodiscus_niagarae. Accessed 6 Sep 2019

Capítulo IV

4. Especies de *Cyclotella* (Bacillariophyceae) presentes en sedimentos que datan del Estadio isotópico 5 del Lago Chalco, centro de México, con especial referencia a dos nuevas especies: *Cyclotella poyeka* and *Cyclotella tlalocii*.

(Artículo publicado, citar como: Avendaño, D., & Caballero, M. (2021). *Cyclotella* (Bacillariophyceae) species present in sediments dating to Marine Isotope Stage 5 from Lake Chalco, central Mexico, with special reference to two new species: *Cyclotella poyeka* and *Cyclotella tlalocii*. *Diatom Research*, *36*(4), 323-344. https://doi.org/10.1080/0269249X.2021.2010808)

Meses después de la publicación del presente artículo se realizó un cambio taxonómico de tres especies de ***Cyclotella*** *(Kützing) Brébisson al género* ***Stephanocyclus*** *Skabitschevsky, incluyendo a* ***Cyclotella meneghiniana****, que actualmente está aceptada taxonómicamente como* ***Stephanocyclus meneghinianus*** *(Kützing) Kulikovskiy, Genkal & Kociolek, por lo que en esta publicación aparece con su basiónimo, sin embargo, en el resto del texto se maneja el nombre aceptado. Además, en el artículo Avendaño et al. (2023) (Capítulo VI) se hace la transferencia de* ***Cyclotella quillensis*** *al género* ***Stephanocyclus.***

En el registro de Chalco hay dos especies del género ***Cyclotella*** *y dos especies del género* ***Stephanocyclus*** *que dominan en diferentes intervalos de la secuencia. Este artículo surgió como un estudio taxonómico de dos diatomeas que estaban identificadas inicialmente como* ***"Cyclotella sp. cf. C. stylorum Brightwell****". A continuación, se realizó una revisión bibliográfica de la taxonomía de* ***S. meneghinianus*** *y* ***S. quillensis****, así como la identificación de dos nuevas especies:* ***C. poyeka*** *y* ***C. tlalocii****. Además, se discute la afinidad ecológica de cada especie a partir de su distribución moderna y/o de la distribución moderna de las especies con las que están asociadas en el registro fósil.*

Resumen:

El lago de Chalco es uno de los pocos lagos en México que tiene una secuencia sedimentaria larga y continua que cubre el Pleistoceno superior (> 150 mil años). El contenido de diatomeas de sus sedimentos lacustres incluye una variedad de especies céntricas. En particular, los sedimentos que datan del Estadio isotópico 5 (EI5) estaban alternativamente dominados por cuatro *Cyclotella* spp. y *Stephanocyclus* spp.: *S. meneghinianus, S. quillensis*, y dos nuevas especies que se describen aquí: *C. poyeka* y *C. tlalocii*. Estas dos nuevas especies de *Cyclotella* se parecen a *C. stylorum* Brightwell, debido a la presencia de cámaras marginales. Sin embargo, las nuevas especies del Lago Chalco se diferencian por la disposición de las cámaras marginales y los fultoportulae marginales con tres poros satelitales. *Cyclotella poyeka* y *C. tlalocii* difieren entre sí por la proporción relativa del área central al diámetro de la cara valvar, la distribución de las fultoportulae centrales y el patrón de estrías. Se discuten las afinidades ecológicas de las cuatro especies de *Cyclotella* en los sedimentos del EI5 del Lago Chalco con base en su distribución moderna (para *C. meneghinianus* y *S. quillensis*) y sus conjuntos fósiles (para *S. quillensis*, *C. tlalocii* y *C. poyeka*), lo que llevó a la conclusión de que *C. tlalocii* era una especie de agua dulce mientras que *S. meneghinianus, S. quillensis* y *C. poyeka* prosperaron en condiciones salinas.

Palabras clave: diatomeas céntricas, alveolos complejos, cámaras marginales, taxonomía de diatomeas, Stephanodiscaceae, Pleistoceno, ecología de diatomeas.

Diatom Research, 2022
https://doi.org/10.1080/0269249X.2021.2010808

Cyclotella (Bacillariophyceae) species present in sediments dating to Marine Isotope Stage 5 from Lake Chalco, central Mexico, with special reference to two new species: *Cyclotella poyeka* and *Cyclotella tlalocii*

DIANA AVENDAÑO[1]* & MARGARITA CABALLERO[2]

[1]*Posgrado de Ciencias de la Tierra, Instituto de Geofísica, Universidad Nacional Autónoma de México, Ciudad de México, México;*
[2]*Laboratorio de Paleolimnología, Instituto de Geofísica, Universidad Nacional Autónoma de México, Ciudad de México, México*

Lake Chalco is one of the few lakes in Mexico that has a long, continuous sedimentary sequence covering the Upper Pleistocene (> 150 000 yrs). The diatom content of its lacustrine sediments includes a variety of centric species. In particular, the sediments dating to Marine Isotope Stage 5 (MIS5) were alternately dominated by four *Cyclotella* spp: *C. meneghiniana* Kützing, *C. quillensis* Bailey, and two new species which are described here: *C. poyeka* and *C. tlalocii*. These two new *Cyclotella* spp. resemble *C. stylorum* Brightwell, because of the presence of marginal chambers. Nevertheless, the new species from Lake Chalco have a different structure of the marginal chambers and marginal fultoportulae with three satellite pores. *Cyclotella poyeka* and *C. tlalocii* differ from each other by the relative proportion of the central area to valve face diameter, the central fultoportula arrangement, and the striation pattern. Ecological affinities of the four *Cyclotella* species in the MIS5 sediments from Lake Chalco are discussed based on their modern distribution (for *C. meneghiniana* and *C. quillensis*) and their fossil assemblages (for *C. quillensis*, *C. tlalocii* and *C. poyeka*), leading to the conclusion that *C. tlalocii* was a freshwater species while *C. meneghiniana, C. quillensis,* and *C. poyeka* thrived in saline conditions.

Keywords: *centric diatoms, complex alveoli, marginal chambers, diatom taxonomy, Stephanodiscaceae, Pleistocene, diatom ecology*

Introduction

Cyclotella (Kützing) Brébisson is a polyphyletic genus (Alverson et al. 2007), traditionally defined *(Cyclotella sensu lato)* as being a drum-shaped centric diatom with different patterns of ornamentation in the central and marginal areas (Lowe 1975, McFarland & Collins 1978, Serieyssol 1981, Servant-Vildary 1986, Loginova 1990). This relatively simple definition allowed for many unrelated taxa to be grouped together, however with time its concept has gradually narrowed, as species have been transferred to other cyclotelloid genera such as *Lindavia* (F. Schütt) De Toni, & Forti, *Tertiarius* Håkansson, & Khursevich, *Discostella* Houk, & Klee, *Fascinorbis* Stone, Edlund, & A.J.Alverson, *Pantocsekiella* Kiss, & Ács, *Cyclostephanos* Round or *Pliocaenicus* Round & Håkansson.

The current morphological criteria for *Cyclotella (sensu stricto)* (Håkansson 2002, Alverson et al. 2011, Khursevich & Kociolek 2012, Nakov et al. 2015) include a drum-shaped centric diatom with: (i) a flat or tangentially undulated central area, (ii) a striated marginal area, (iii) a ring of marginal fultoportulae located on costae or recessed costae, and (iv) one or several rimoportulae that interrupt the ring of marginal fultoportulae. Externally the central area can be either smooth, colliculate, or with apparently radial striation, but the only perforations are the central fultoportulae, which can range from none to several. The marginal radiating striae vary from uni- to multiseriate fascicles separated by interstriae. Internally, the central and marginal fultoportulae are surrounded by two or three satellite pores and marginal areolae are closed by cribra. The marginal area is composed of alveoli, divided internally by costae that can be equal, defining simple alveoli, or thicker (raised) and thinner (recessed or secondary) costae defining complex alveoli, which may be expanded into chambers. The marginal chamber is a space on the inside of the valve encompassing more than one alveolus. Alveoli can be partially occluded internally by siliceous sheets (membranes) extending from the central area (central lamina or centripetal roofing) or the margin (marginal lamina or centrifugal roofing). Under light microscopy (LM) these silica sheets appear as one or two shadow rings crossing the alveoli. Some species can have a ring of spines at the valve face / mantle junction.

Cyclotella (*s.s.*) taxa are present in the geological record from the middle Miocene, with important radiations during the Late Miocene and Pliocene (Krebs et al.

*Correspondence author. E-mail: da.avendano.v@ciencias.unam.mx
Associate Editor: Jeffery Stone

(Received 14 January 2021; accepted 16 August 2021)

Published online 02 Feb 2022

1987, Temniskova-Topalova et al. 1994, Khursevich & Kociolek 2012). Currently, this genus has over 120 modern and fossil species (Khursevich & Kociolek 2012, Guiry et al. 2020), which are common in freshwater, brackish, or coastal marine environments (Prasad et al. 1990, Rühland et al. 2015). It is a predominantly freshwater genus known to have a wide tolerance for saline environments, with some species living in coastal marine waters (Håkansson 2002, Prasad & Nienow 2006). In paleoenvironmental reconstructions *Cyclotella* spp. have frequently been used to infer past changes in salinity related to climatic variability (Tapia et al. 2003, Caballero et al. 2019). Interestingly, *Cyclotella* taxa have been identified as dominant in many lacustrine deposits dating from warmer interglacial periods (Bradbury 1971, Rioual et al. 2001, Paillès et al. 2018). This situation seems to be the case in the record from Lake Chalco, central Mexico (Fig. 1), where *Cyclotella* taxa (*s.s.*) are abundant in sediments dating to the warmer Marine Isotopic Stages (MIS) 5, 4 and 3, while they are nearly absent in the sediments dating to MIS6 and MIS2 glacial periods (Avendaño-Villeda et al. 2018, Caballero et al. 2019, Ortega-Guerrero et al. 2020).

In this paper, we report four *Cyclotella* species that are present in the sediments from Lake Chalco dating to MIS5 (130–71 kyr cal BP). These include *Cyclotella meneghiniana* Kützing and *C. quillensis* Bailey which have been previously reported in modern environments and fossil records from central Mexico (Bradbury 1971, Cantoral-Uriza 1997, Caballero et al. 2019) as well as two new species that are described herein.

Methods

Study area

Lake Chalco is located at the southeastern end of the Basin of Mexico (Fig. 1b), in a region characterized by a temperate, subhumid climate, with a mean temperature of 16.8°C and average annual precipitation of 537 mm, concentrated in the summer months. The remnant waterbody that persists today has alkaline, subsaline, hypertrophic waters (pH = 9.2 and, TDS = 1890 mg L^{-1}, Chl a ~ 160 mg m^{-3}, Avendaño et al. 2021). Its modern diatom flora is dominated by *C. meneghiniana* and *Thalassiosira* aff. *duostra* Pienaar (Buendía-Flores et al. 2019).

Lake Chalco has a long lacustrine sedimentary sequence and, for this study, diatom analyses were performed on sediments from a composite master sequence (CHA08, 122.4 m composite depth, 19.26°N, 98.97°W, Fig. 1b) that spans the late MIS6 to the early MIS3 (*ca.* 150–35 kyr cal BP). Drilling details, lithostratigraphy, and geochronology of this sequence have been published previously (Ortega-Guerrero et al. 2017, 2020) and diatom assemblages from these sediments have been reported in Avendaño-Villeda et al. (2018), Torres-Rodriguez et al. (2018), and Ortega-Guerrero et al. (2020).

Diatom analysis

Sediments for diatom analysis were prepared by acid digestion (HCl 10%) followed by gentle boiling (80°C) in a mixture of concentrated (30%) H_2O_2 and 10% $Na_4P_2O_7$. When organic matter concentration was high, 5–10 mL of H_2SO_4 were also added. Permanent microscope slides were prepared with 200 µL aliquots of the final solution using NaphraxTM (Brunel Microscopes Ltd) as a mounting medium. Identification was carried out under LM (Olympus BX50) at 1000 ×. Selected samples were also examined with scanning electron microscopy (SEM). Cleaned diatom samples were deposited on aluminium stubs, air-dried and gold-coated in a Jeol JFC-1100 Fine Coat Ion Sputter with an ionization-time of 5 min (1.5 kV, 6–7 mA). Stubs were examined with a JEOL JCM-6000PLUS SEM operating at an accelerating voltage of 15 kV under high vacuum or with a JEOL JSM6360LV SEM at an accelerating voltage of 15–20 kV under high vacuum. Diatom identification and descriptive terminology followed specialized literature (Ross & Sims 1972, Anonymous 1975, Ross et al. 1979, Krammer et al. 1991, Theriot & Serieyssol 1994, Håkansson 2002).

The archive halves of the CHA08 master sequence are stored in the LacCore facility, University of Minnesota, in Minneapolis, USA; the working halves and treated diatom samples are stored in the Laboratory of Paleolimnology, Institute of Geophysics, National University of Mexico (UNAM), Mexico City, Mexico. The holotypes for *C. poyeka* (slide MEXU AL5565 and sediment MEXU AL5566) and *C. tlalocii* (slide MEXU AL5567 and sediment MEXU AL5568) were deposited in the National Herbarium of Mexico (MEXU), Institute of Biology, UNAM, Mexico City, Mexico. Isotypes for both *C. poyeka* (ENCB 26215) and *C. tlalocii* (ENCB 26216) were deposited in the Herbarium of the National School of Biological Sciences (ENCB), National Polytechnic Institute, Mexico City, Mexico. Additional isotype slides were deposited in the Herbarium of the Institute of Ecology, A.C. Mexico (XAL).

Results

Summary results of the main diatom assemblages in the CHA08 sequence were published in Ortega-Guerrero et al. (2020). In that work, diatoms were grouped into four ecological assemblages, small Fragilariales, *Stephanodiscus* Ehrenberg spp., alkaliphilous and halophilous taxa (Fig. 2). These groups were based on species ecological preferences according to their distribution along 40 lakes in central Mexico (Caballero et al. 2019). *Stephanodiscus* spp. indicate cooler, freshwater conditions (Caballero et al. 2019, Avendaño et al. 2021) that were dominant during MIS6

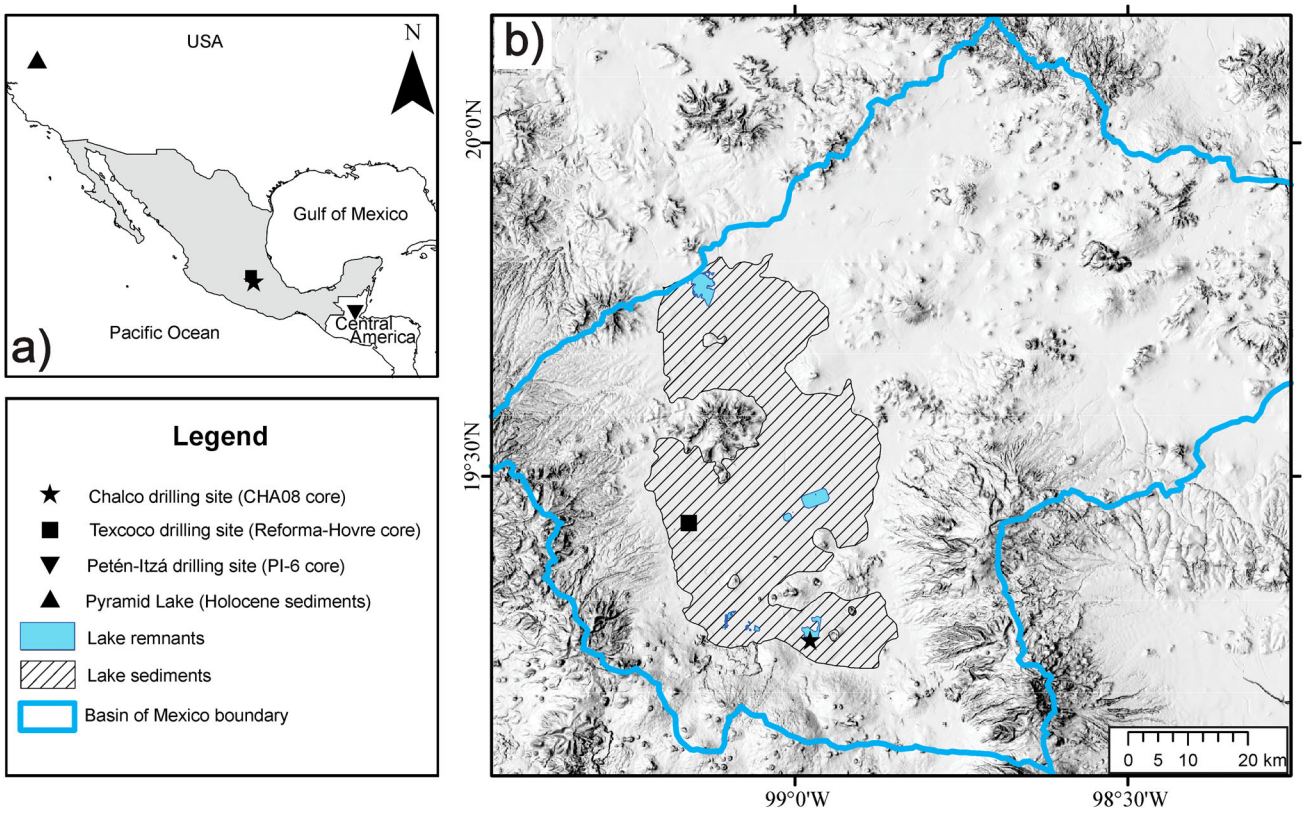

Fig. 1. Location maps. (a) Location map of Lake Chalco in central Mexico and of other sites mentioned in the text. (b) Location of the CHA08 drilling site in Lake Chalco, and of the Reforma core in Lake Texcoco, both in the Basin of Mexico.

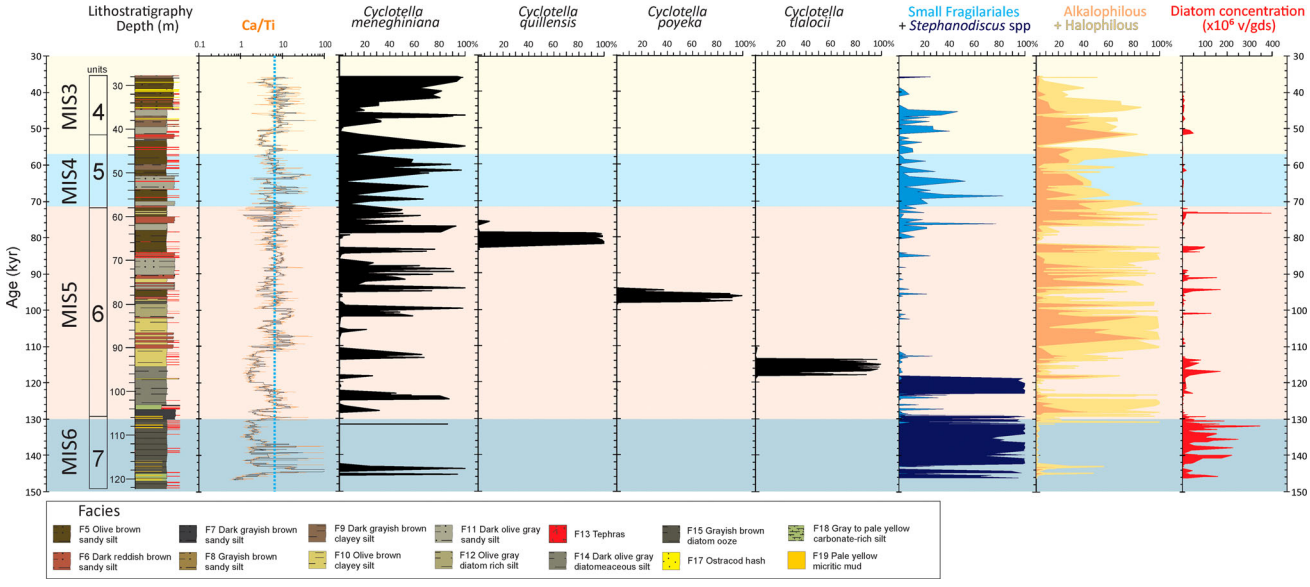

Fig. 2. Chronology, Marine Isotopic Stages (MIS), stratigraphic units and lithostratigraphy of the CHA08 master sequence from Lake Chalco, Basin of Mexico. The graph shows the Ca/Ti geochemical data (blue line represents the mean value), diatom abundance of the four *Cyclotella* taxa in the sequence, of the four ecological diatom groupings (small *Fragilariales*, *Stephanodiscus* spp, alkaliphilous and halophilous taxa) and diatom valve concentration in valves per gram of dry sediment (v/gds).

(Fig. 2), on the other hand, alkaliphilous and halophilous taxa indicate alkaline-saline environments that were dominant during MIS5 to MIS3 warmer conditions (Fig. 2). In the sediments from MIS5 the diatom assemblages are alternately dominated by four *Cyclotella* species (Fig. 2): *C. meneghiniana*, *C. quillensis* and two taxa that were

initially identified as close to *C. stylorum* Brightwell, but after detailed LM and SEM observations are here described as new species: *C. poyeka* and *C. tlalocii*.

Taxonomic descriptions

Cyclotella meneghiniana Kützing (Figs 3–10)

The size range and all other morphological characteristics of our specimens (Table 1) are within the published ranges (Håkansson & Chepurnov 1999, Meyer et al. 2001, Håkansson 2002). The central area is flat to tangentially undulate, sometimes with radial grooves (Figs. 6–7). Internally, the central fultoportulae (1–4) have a short tubulus surrounded by three satellite pores (Figs. 8–9). Depressed interstriae alternate with raised striae composed of 6–8 rows of areolae that continue onto the mantle (Fig. 7). A ring of spines is irregularly present at the valve face / mantle junction (Fig. 7). Internally the marginal fultoportulae are situated on every first to third costa (Figs. 8–10) delimiting simple marginal alveoli, sometimes with a central lamina (Figs. 3, 6). One rimoportula is present on a costa (Fig. 9–10).

Stratigraphic range in Chalco: Upper Pleistocene to Holocene. This species is part of the modern diatom flora at Chalco (Buendía-Flores et al. 2019) and is also very abundant in sediments dating to MIS3, MIS4, MIS5, and parts of MIS6 in the CHA08 sequence (Fig. 2). The main stratigraphic distribution of this species is from 131–35 kyr cal BP (130–30 m cd), with a short-lived increase during MIS6 from 146–143 kyr cal BP (122–119 m cd) and a reappearance in the Chalco record during the mid-Holocene.

Cyclotella quillensis L.W. Bailey (Figs 11–23)

The size of our specimens (45–72 µm diameter) (Table 1) is within the widest published range for the species (11–70 µm) (Håkansson 2002). The central area has a slight tangential undulation (Figs 11–17) and can be smooth or with radial groves (Edlund & Burge 2016) (Figs 12–14, 17). Numerous central fultoportulae (15–41) are present in a loosely circular arrangement (Figs 18–19). Internally central fultoportulae are surrounded by three satellite pores (Fig. 20). Striae are uni- to bi-seriate, occasionally having up to four rows of areolae towards the margin (Fig. 21); striae lie in the depressions of the circumferential undulations, alternating with raised interstriae. Håkansson & Kling (1994) report that *C. quillensis* has spines on the interstriae, whereas Battarbee et al. (1984) and Håkansson (2002) indicate that spines are on the striae, so this might be a variable characteristic. Our specimens have a ring of spines on the striae at the valve face / mantle junction (Fig. 21), just above the external openings of the marginal fultoportulae. Marginal fultoportulae have three satellite pores. In the literature, it is reported that every costa has a fultoportula, except for the one with the rimoportula (Håkansson 2002), however, while several of our

Table 1. Comparison of morphological features of *Cyclotella meneghiniana, C. quillensis* and *C. alchichicana.*

Features	*Cyclotella meneghiniana*[1]	*Cyclotella quillensis*[1]	*Cyclotella meneghiniana*[3,5,6]	*Cyclotella quillensis*[2,3,7]	*Cyclotella alchichicana*[4]
Valve diameter (µm)	10–40	45–72	5–45	11–70	35–63
Valve undulation	Flat to tangential	Slightly tangential	Flat to slightly tangential	Strongly tangential	Slightly tangential
Character of the central area	Humps and radial grooves	Radial grooves	Humps, hollows, ridges, radial grooves	Smooth with radial grooves	Smooth with radial grooves and granules
Central area to diameter ratio	1/2–2/3	4/5	1/2–2/3	4/5	2/3
CFP number, arrangement, structure	1–4, nd, 3 pores	15–41, irregular ring, 3 pores	1–4, nd, 3 pores	1 to > 60, irregular ring, 3 pores	7–19, irregular ring, 3 pores
Costae in 10 µm	8–10	8	6–10	6–10	8–10
Spines	p	p	p	p	p, spinules, granules
MFP:costa, position, structure	1:1, on costa, 3 pores	1:1, on costa, 3 pores	1:1, on costa, 3 pores	1:1, on costa, 3 pores	1:(0)1–2, on costa, 3 pores
RP number, position, slit orientation	1 stalked, on costa, radial	1 stalked, on costa, radial to oblique	1 stalked, on costa, radial	1 stalked, on costa, radial	1 stalked, on costa, oblique

Notes: p: present, np: not present, nd: no data, CFP: central fultoportulae, MFP: marginal fultoportulae, RP: rimoportula.
[1]This study, [2]Battarbee et al. (1984), [3]Håkansson (2002), [4]Oliva et al. (2006), [5]Houk et al. (2010), [6]Lowe & Kheiri (2015), [7]Edlund & Burge (2016).

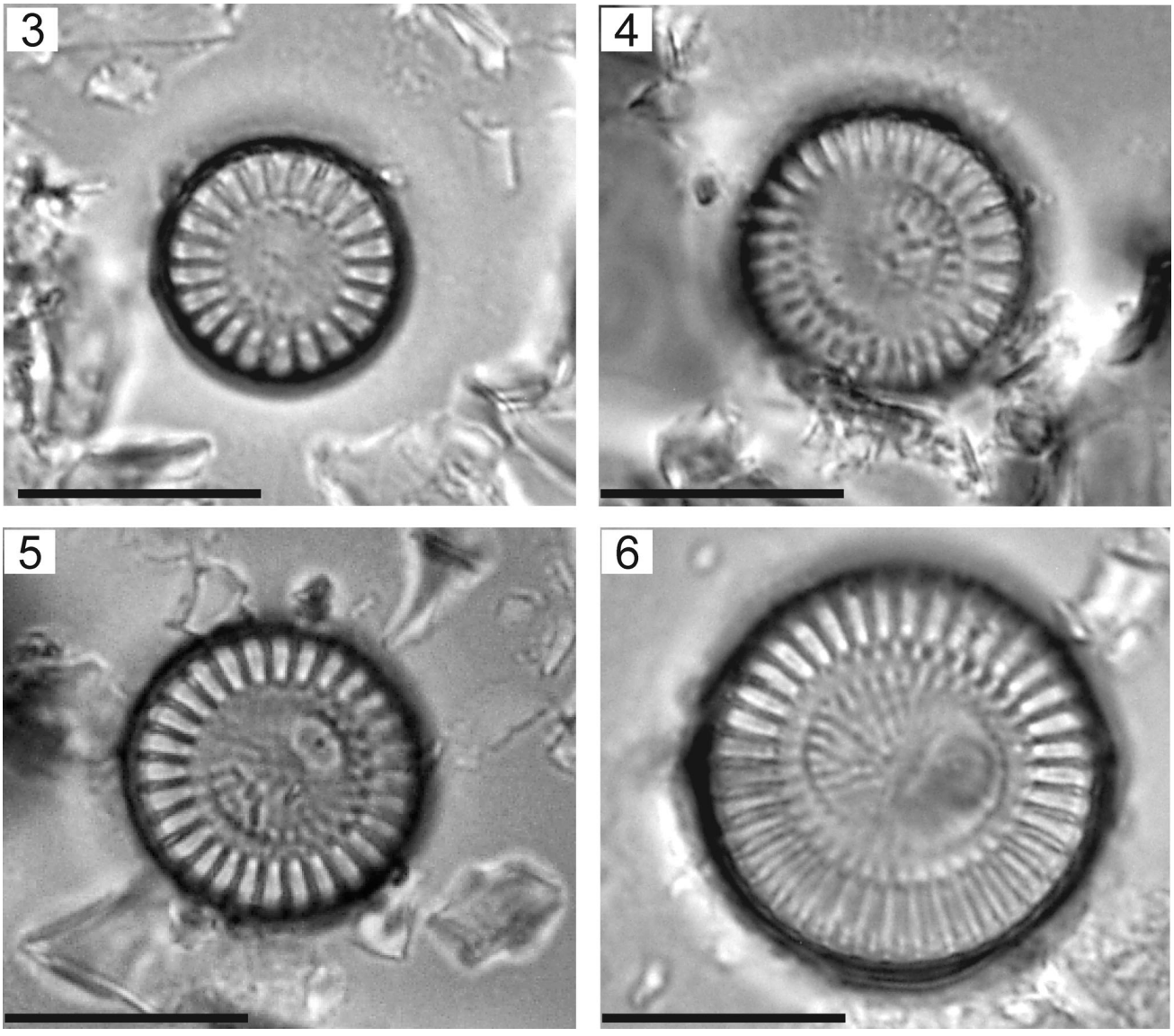

Figs. 3–6. LM micrographs of *Cyclotella meneghiniana* showing the different sizes of the valves. Scale bars = 10 µm.

specimens have this arrangement (Fig. 22), others have costae without marginal fultoportulae (Fig. 23). Marginal alveoli are simple and partially occluded by a central lamina that can be seen as a concentric marginal shadow line under LM (Figs. 22–23). Internally, a single rimoportula is situated on a costa, and consists of a stalked labium with a slit opening that is parallel to slightly oblique to the costa (Fig. 23).

Stratigraphic range in Chalco: Upper Pleistocene. This species is very abundant in the CHA08 sediments during part of MIS5 only, from 84–75 kyr cal BP (68–61 m cd). It is totally absent in the rest of the sequence.

Cyclotella poyeka Avendaño & Caballero sp. nov. (Figs 24–48)

Valves circular, 13–50 µm in diameter (Table 2). Central area with strong tangential undulation, and a smooth valve face (Figs 24–35). Several central fultoportulae (2–16) are predominantly positioned in an arc on the uplift of the undulation, although other central fultoportulae are loosely distributed over the rest of the valve (Figs 36–39). Externally the fultoportulae have slightly thickened openings and internally a short tubulus is surrounded by three satellite pores (Fig. 39). The marginal area consists of raised striae alternating with depressed interstriae. The striae have four rows of areolae, up to 5–8 towards the margin (Figs 40–44). No spines or spinulae are present at the valve face / mantle junction, but siliceous granules can be found on the mantle. Internally, the valve has complex alveoli or marginal chambers (3.5–4 in 10 µm) defined by raised costae and containing one (occasionally two) recessed costa. Therefore each chamber has two (occasionally three) alveolus openings (Figs 36–38, 39, 45–47) even though two adjacent raised costae

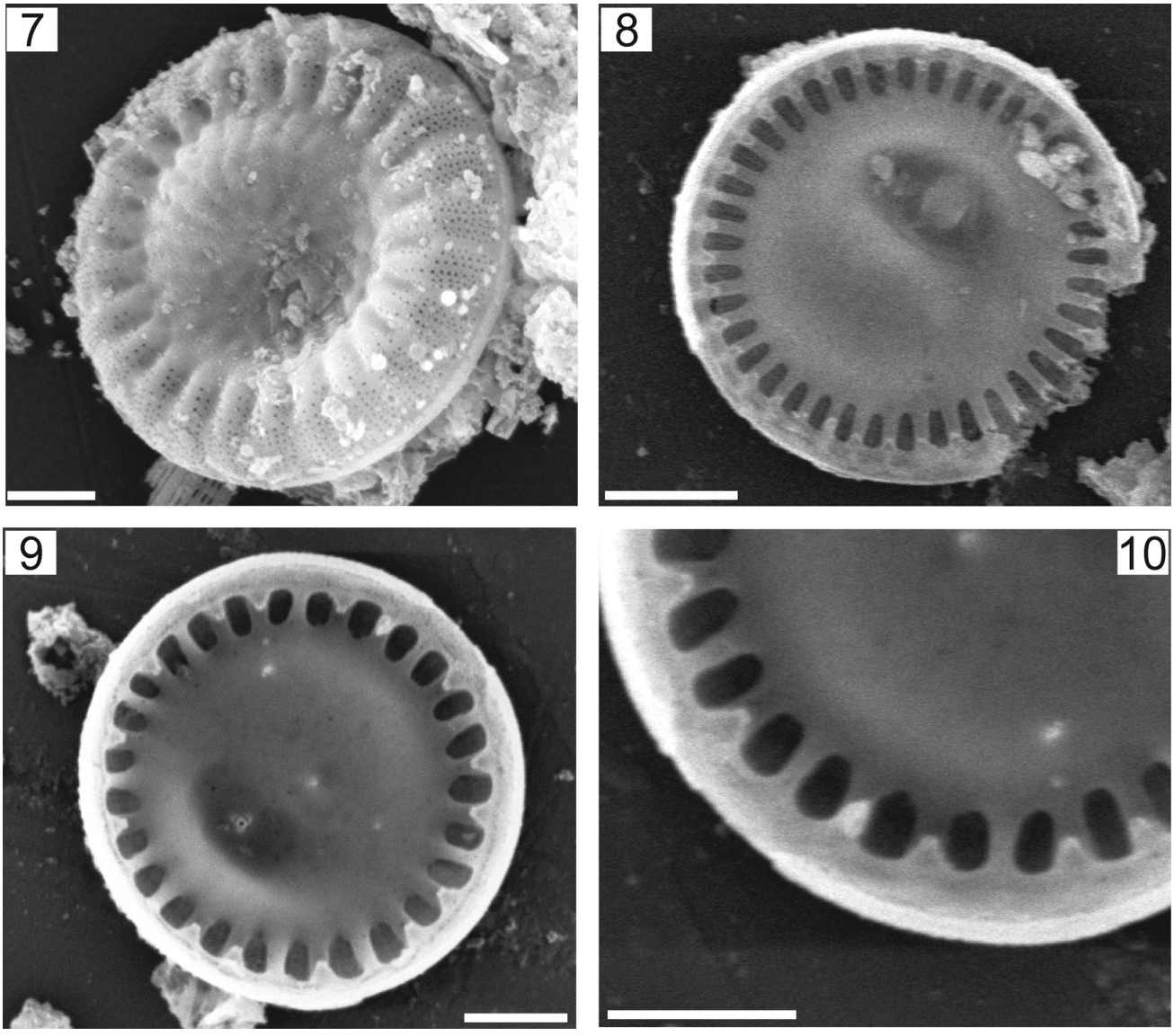

Figs. 7–10. SEM micrographs of *Cyclotella meneghiniana.* Fig 7. External valve view with tangential undulation and radial grooves. Figs 8–9. Internal valve views with central and marginal fultoportulae. Fig 10. Detail of the internal view of the marginal area with the marginal fultoportulae and the rimoportula. Scale bars = 5 µm (Fig. 8); 2 µm (Figs 7, 9–10).

can occasionally be present (Figs 36–37, 48). The alveoli are partially occluded by a central lamina that can be seen as a concentric marginal shadow line under the LM (Figs 26–28, 30). The marginal fultoportulae have slightly thickened external openings (arrows in Figs 42–44), three satellite pores and are present on every recessed costa (Figs 45–48). A single rimoportula is present, with a stalked and often bent labium, obliquely orientated slit opening (Figs 36–38, 47–48). The rimoportula interrupts the ring of marginal fultoportulae and lies between a recessed and raised costa, or rarely between two fultoportulae on recessed costae (Figs 47–48). The external rimoportula opening is circular to elliptical (asterisks in Figs 42–43).

Holotype: MEXU slide AL5565 (holotype = Figs. 24–27) and material AL5566 deposited in the National Herbarium of Mexico (MEXU), Institute of Biology, National Autonomous University of Mexico, Mexico City, Mexico. Holotype from sample CHA08-VI-9-40, 78.78 m cd (estimated age of 95.7 kyr cal BP).

Isotype: ENCB slide 26215 (isotype = Figs. 28–30) deposited in the Herbarium of the National School of Biological Sciences (ENCB), National Polytechnic Institute, Mexico City, Mexico. Additional isotype slides deposited in the Herbarium of the Institute of Ecology, A.C. Mexico (XAL) from sample CHA08-VI-9-95, 79.33 m cd (estimated age of 96.4 kyr cal BP).

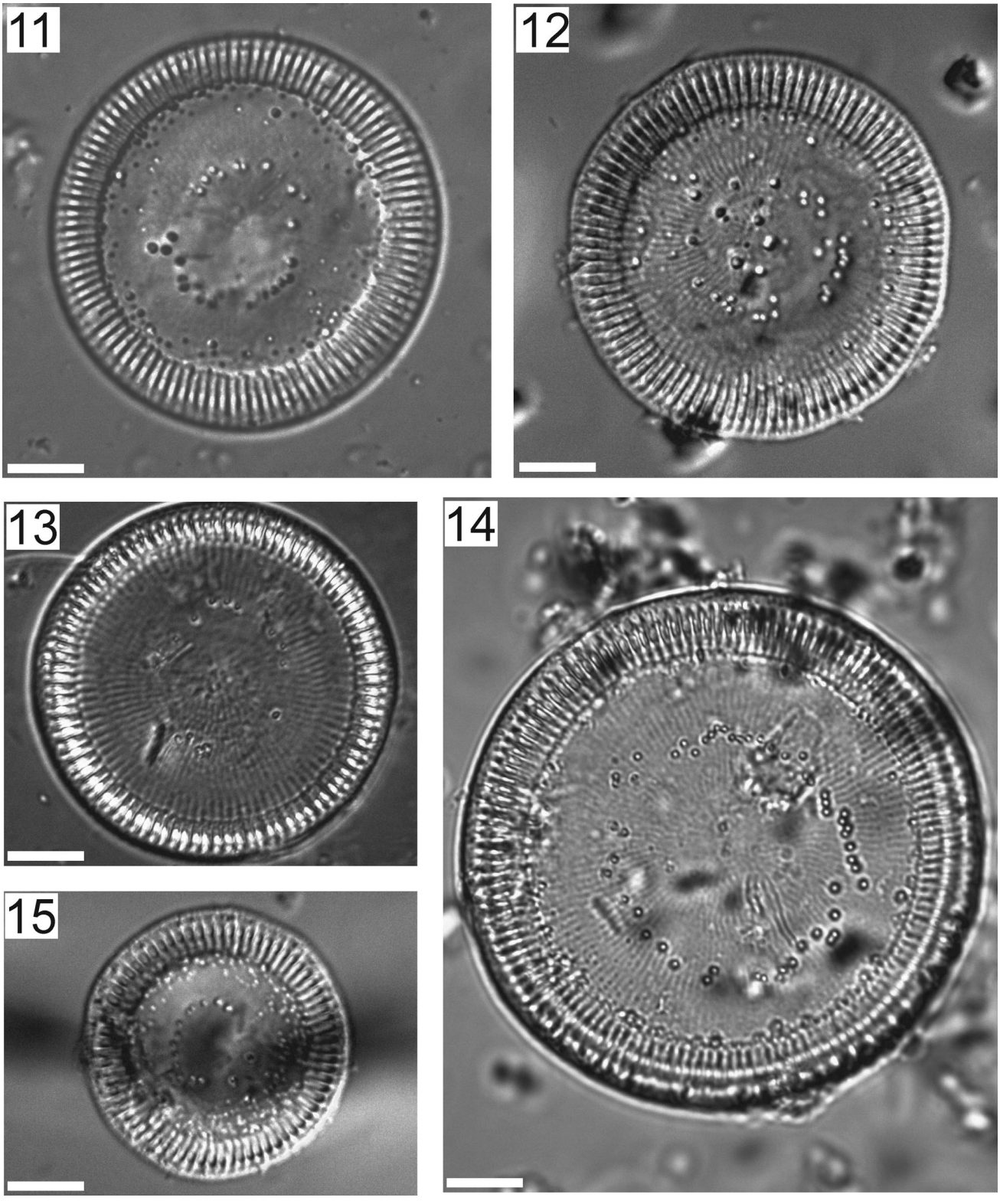

Figs. 11–15. LM micrographs of *Cyclotella quillensis* showing central lamina, simple alveoli and radial grooves in the central area. Scale bars = 10 µm.

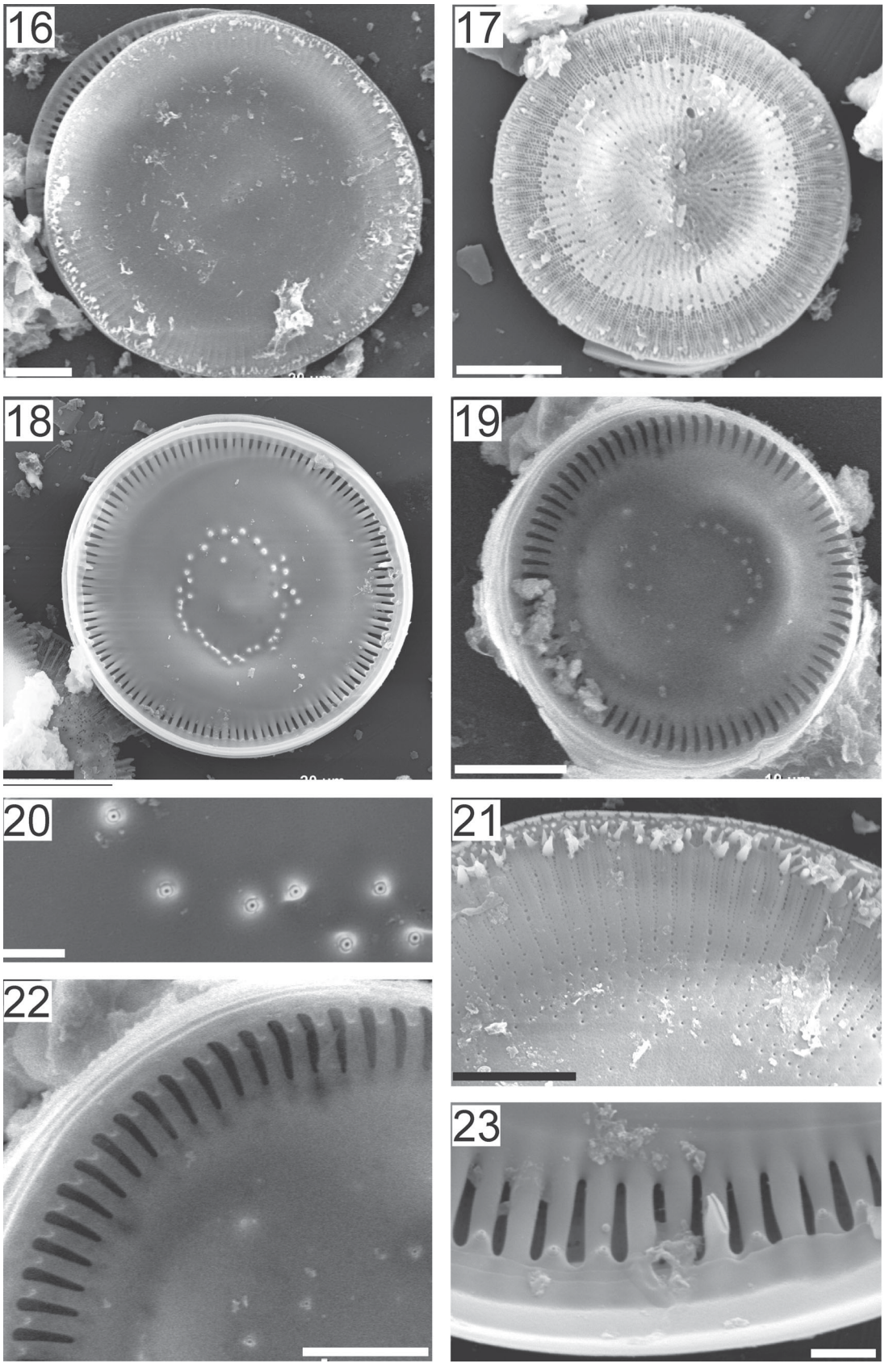

Figs. 16–23. SEM micrographs of *Cyclotella quillensis*. Figs 16–17. External valve views, Fig. 17 is a corroded specimen. Figs 18–19. Internal valve views with valve face fultoportulae in a circular arrangement. Fig. 20. Detail of internal valve view of the central fultoportulae with three satellite pores. Fig. 21. Detail of external valve view of the marginal striation, with one to two areola rows and spinulae at the valve face/mantle junction. Fig. 22. Detail of internal valve view of marginal fultoportulae. Fig. 23. Detail of internal valve view of the rimoportula labium. Scale bars = 10 μm (Figs 16–19); 5 μm (Figs 21–22); 2 μm (Figs 20, 23).

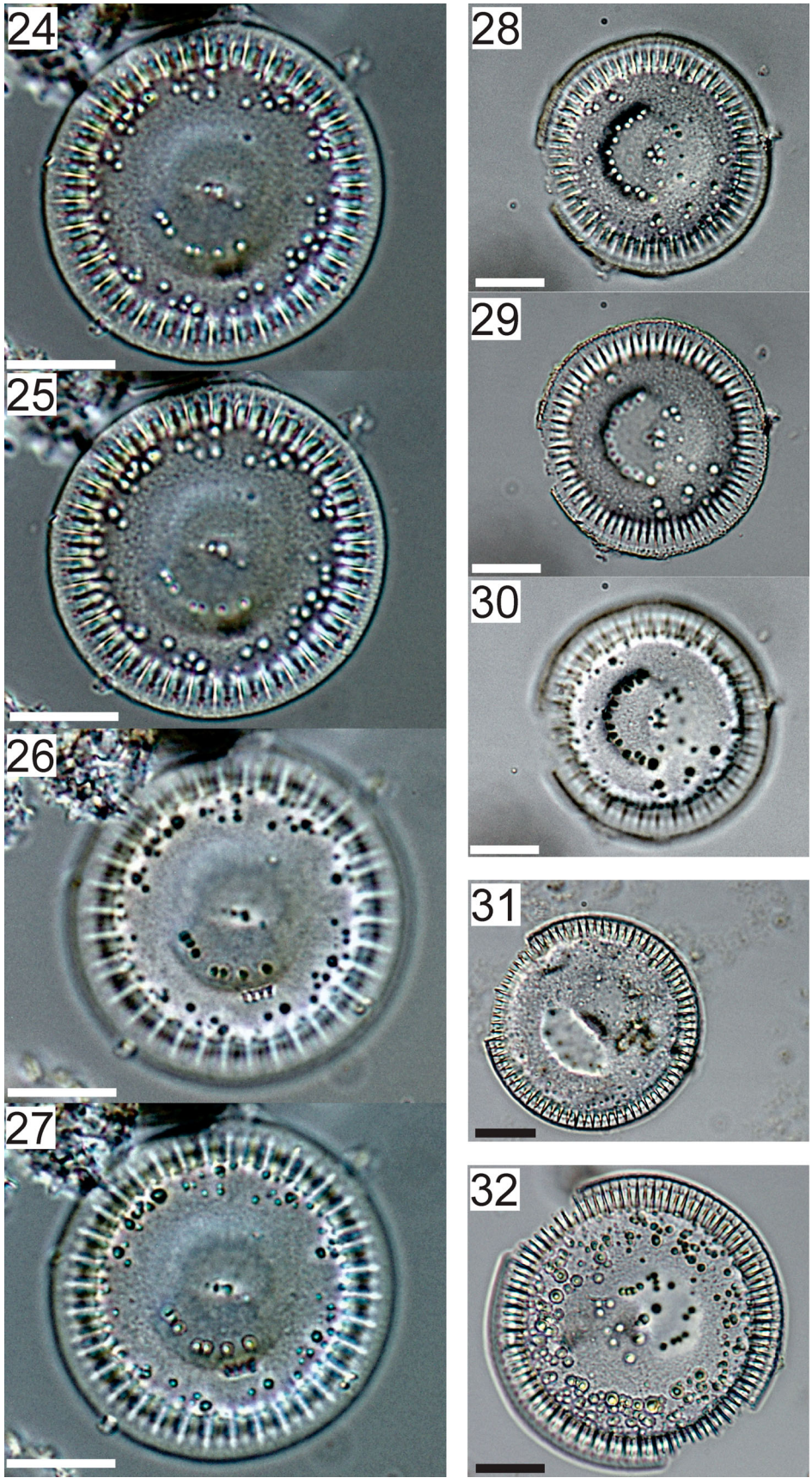

Figs. 24–32. LM micrographs of *Cyclotella poyeka* showing size variation. Figs 24–27. Holotype (slide MEXU AL5565), focus through various valvar planes. Figs 28–30. Isotype (slide ENCB 26215). Focus through various valvar planes. Fig. 31. Isotype (slide XAL). Focus on marginal area. Scale bars = 10 µm.

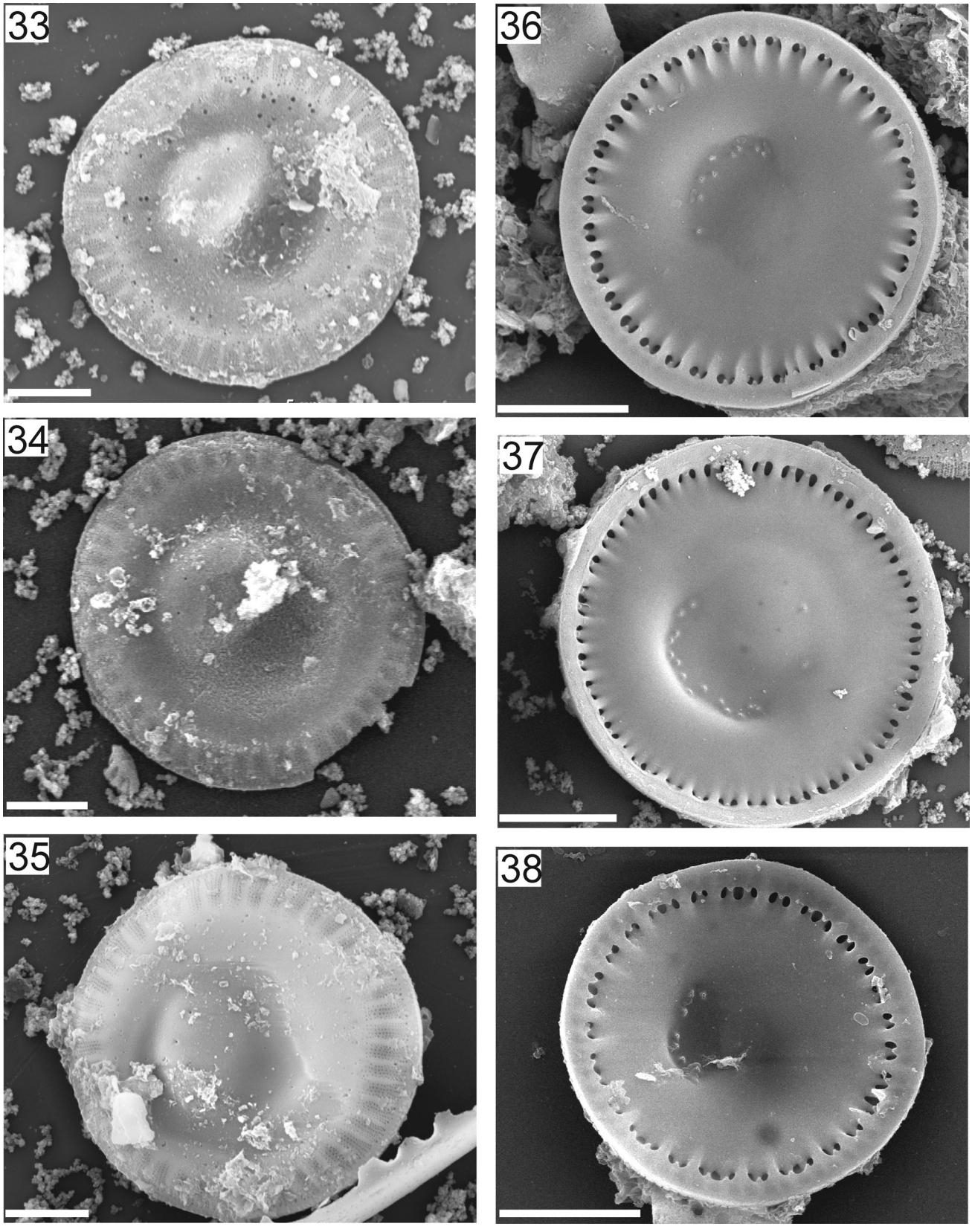

Figs. 33–38. SEM micrographs of *Cyclotella poyeka,* external and internal views of valves. Figs 33–35. External valve views with different tangential undulation. Figs 36–38. Internal valve view showing central fultoportulae forming an arc on the uplift of the undulation. Scale bars = 10 μm (Figs 36–38); 5 μm (Figs 33–35).

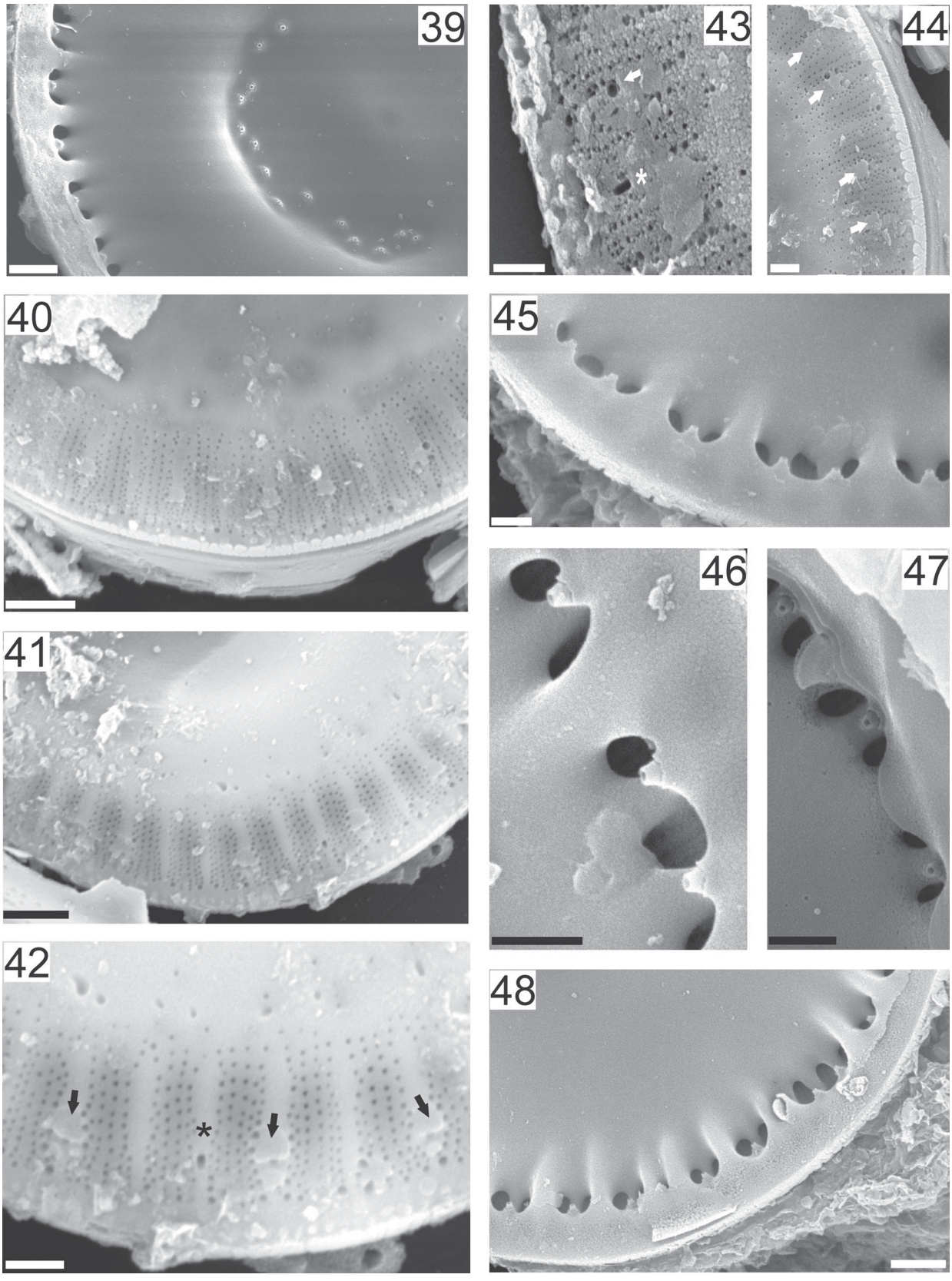

Figs. 39–48. SEM micrographs of *Cyclotella poyeka,* details of structure in external and internal views. Fig. 39. Detail of internal valve view showing central fultoportulae with three satellite pores. Figs 40–41. Detail of external valve view showing striation. Figs 42–44. Detail of external valve view showing fultoportulae opening (arrow) and elliptical opening of the rimoportula (asterisk). Figs 45–46. Detail of internal valve view showing marginal chambers with one or two recessed costae with fultoportulae. Fultoportulae have three satellite pores. Figs 47–48. Detail of internal valve view showing rimoportula and marginal fultoportulae on the recessed costae. Scale bars = 2 µm (Figs 39–41, 48); 1 µm (Figs 42–47).

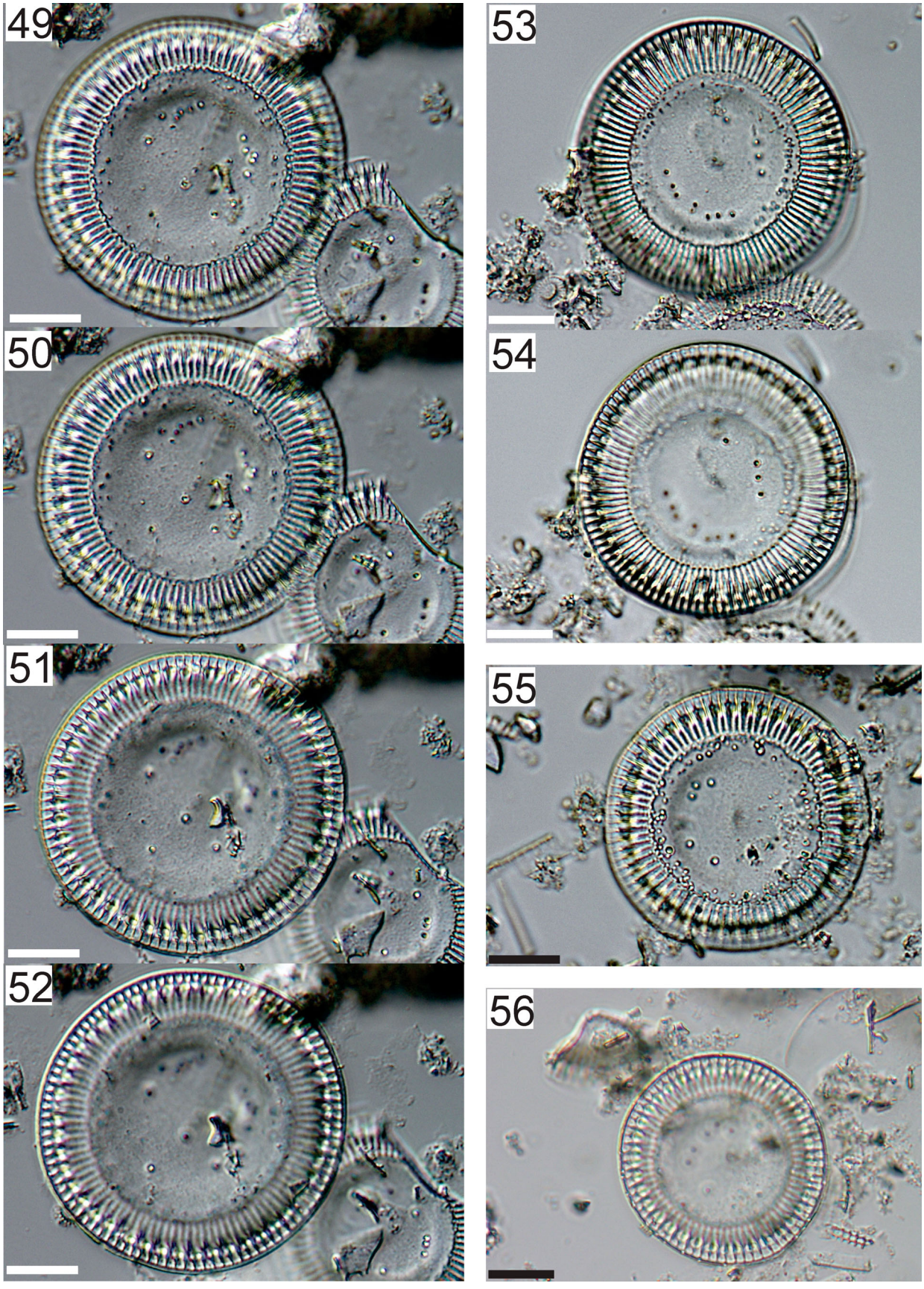

Figs. 49–56. LM micrographs of *Cyclotella tlalocii* showing size variation. Micrographs at different focus showing central lamina and marginal chambers. Figs 49–52. Holotype (slide MEXU AL5567), focus through various valvar planes. Figs 53–54. Isotype (slide ENCB 26216), focus through various valvar planes. Fig. 55. Isotype (slide XAL). Focus on marginal area. Scale bars = 10 µm.

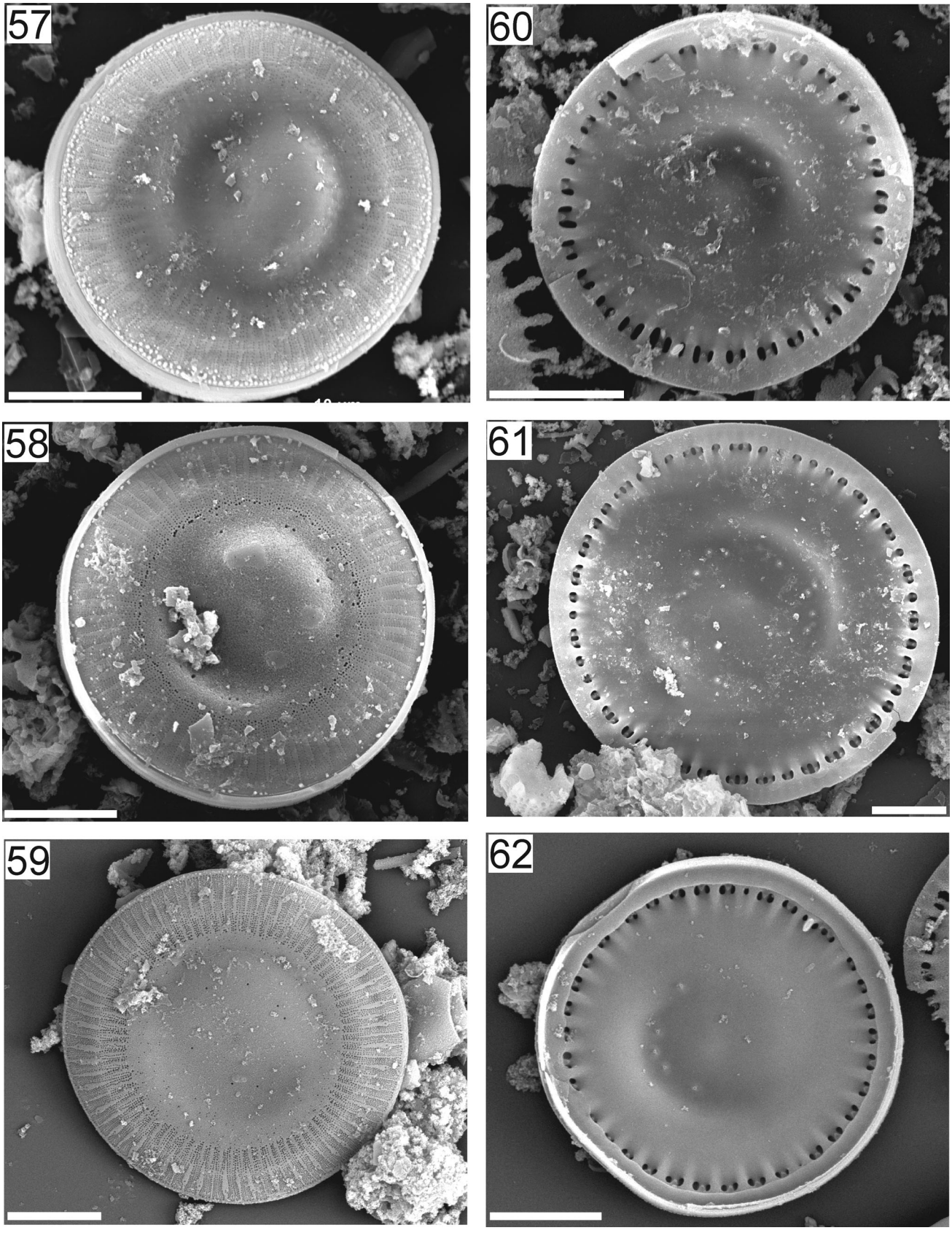

Figs. 57–62. SEM micrographs of *Cyclotella tlalocii,* external and internal view of valves. Figs 57–59. External valve view with tangential undulation. Figs 60–62. Internal valve view showing central fultoportulae in a circular arrangement and marginal chambers with one or two recessed costae. Scale bars = 10 µm.

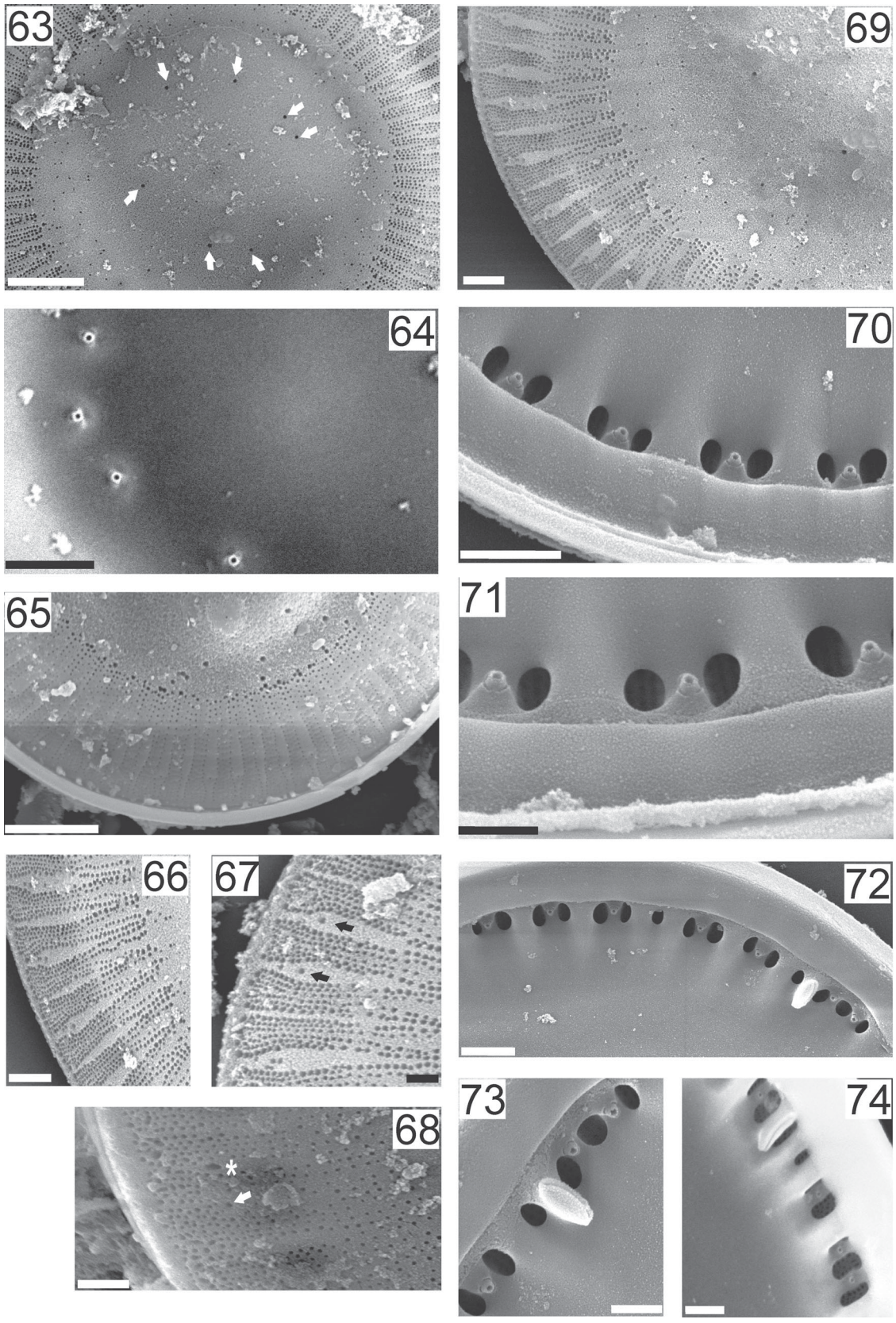

Figs. 63–74. SEM micrographs of *Cyclotella tlalocii,* details of structure in external and internal view. Fig. 63. Detail of external valve view showing central area and fultoportula openings (arrows). Fig. 64. Detail of internal valve view showing central fultoportulae with three satellite pores. Figs 65–69. Detail of external valve view showing marginal striation. Figs 67–68. Details of fultoportulae (arrows) and rimoportula openings (asterisk). Figs 70–71. Internal valve view showing marginal chambers with fultoportulae on recessed costae. Fultoportulae have three satellite pores. Figs 72–74. Detail of internal valve view showing fultoportula and rimoportulae on the recessed costae. Rimoportulae have a radially orientated slits. Scale bars = 5 µm (Figs 63–64); 2 µm (Figs 65–66, 69–70, 72, 74); 1 µm (Figs 67–68, 71, 73).

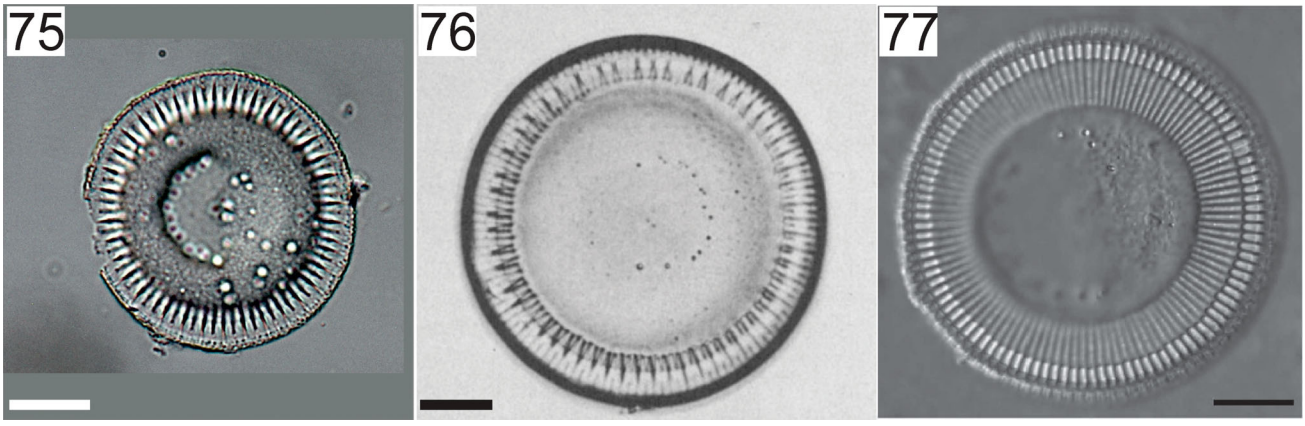

Figs. 75–77. *Cyclotella poyeka, C.* cf. *stylorum* reported by Krebs et al. (1987) and *C. petenensis*. Fig. 75. LM micrograph of *Cyclotella poyeka* (isotype) in sediments from Lake Chalco, Mexico (slide ENCB 26216). Fig. 76. LM micrograph of *Cyclotella* cf. *stylorum* in Holocene sediments from Pyramid Lake, Nevada, USA, reproduced from fig. 4L in Krebs et al. (1987), Fig. 77. LM micrograph of *C. petenensis* in Lake Petén-Itzá, reproduced from fig. 1 of Paillès et al. (2018) with permission from Magnolia Press. Scale bars = 10 µm.

Type Locality: Lacustrine plain between the towns of Tlahuac and Tulyehualco (19.26 °N, 98.97 °W, 2240 m asl), municipality of Tlahuac, Mexico City, Mexico.

Etymology: The specific epithet *poyeka* derives from the word *poyek* in the local Nahuatl language, meaning saline.

Stratigraphic range in Chalco: Upper Pleistocene. This species is very abundant in the CHA08 sediments during part of MIS5, from 98 to 94 kyr cal BP (80–76 m cd) but is absent from the rest of the sequence.

Ecology and distribution: Saline conditions. Fossil, known only from the type locality but potentially also present in: (i) sediments dating to MIS5 in Lake Texcoco, Mexico, identified as *Cyclotella* cf. *stylorum* (Bradbury 1971), and in (ii) Holocene sediments from Pyramid Lake, USA, identified as *Cyclotella* cf. *stylorum* (Krebs et al. 1987).

Cyclotella tlalocii Avendaño & Caballero sp. nov. (Figs 49–74)

Valves are circular, 25–70 µm in diameter. The central area is slightly tangentially undulated (Figs 49–59) with several central fultoportulae (4–13) arranged in a loosely circular distribution around the central area (see arrows in Figs 60–63). These fultoportulae have a slightly thickened external opening and internally a short tubulus surrounded by three satellite pores (Fig. 64). Internally the valve face is smooth and the only perforations are evident in well-preserved valves are of the central fultoportulae. Externally the valve face is smooth, but may have several pores increasing in density towards the transition with the marginal area (Figs 57–59, 63, 65). The marginal area is formed of a series of larger pores with no clear interstriae, transitioning to smaller pores with wider interstriae wider towards the margin of the valve. Interstriae reach their maximum width at the valve face / mantle junction. At this point striae contain four rows of areolae, 5–6 on the mantle, as interstriae gradually narrow (Figs 65–69). The valve margin is relatively flat, with slightly depressed interstriae. No spines or spinulae are present at the valve face / mantle junction, but granulae are sometimes present on the mantle (Figs 57 , 59). Internally the valve has complex marginal alveoli or chambers (3.5–4 in 10 µm) defined by raised costae, and containing one (occasionally two) recessed costae (Figs 70–74). Alveoli are partially occluded by a central lamina (Figs 60–62) that is evident as a shadow or concentric marginal line under light microscopy (Figs 51–56). The marginal fultoportulae have slightly thickened external openings (arrows in Figs 67–68) and internally have three satellite pores surrounding a central tube, positioned on every recessed costa (Figs 70–73). A single rimoportula is present interrupting the ring of marginal fultoportulae. Internally the rimoportula has a stalked labium and the slit is radial to the costa. The rimoportula is situated on a slightly recessed costa, between a raised costa and a fultoportula on a recessed costa (Figs 60, 74), or more rarely between two fultoportulae on recessed costae (Figs 72–73). The external rimoportula opening is elliptical (asterisk in Fig. 68).

Holotype: MEXU slide AL5567 (holotype = Figs. 49–52) and material AL5568 deposited in the National Herbarium of Mexico (MEXU), Institute of Biology, National Autonomous University of Mexico, Mexico City, Mexico. Holotype from sample CHA08-IV-10-70, 96.66 m cd (estimated age 117.4 kyr cal BP).

Isotype: ENCB slide 26216 (isotype = Figs. 53–54) deposited in the Herbarium of the National School of Biological Sciences (ENCB), National Polytechnic Institute, Mexico City, Mexico. Additional isotype slides deposited in the Herbarium of the Institute of Ecology, A.C. Mexico (XAL) from sample CHA08-IV-10-30, 96.26 m cd (estimated age 116.9 kyr cal BP).

Type Locality: Lacustrine plain between the towns of Tlahuac and Tulyehualco (19.26 °N, 98.97 °W, 2240 m asl), municipality of Tlahuac, Mexico City, Mexico.

Etymology: The specific epithet *tlalocii* derives from the name of the Aztec god of rain (Tlaloc).

Stratigraphic range in Chalco: Upper Pleistocene. This species is very abundant in the CHA08 sediments during part of MIS5, from 118 to 112 kyr cal BP (97–92 m cd), absent from the rest of the sequence.

Ecology and distribution: Freshwater conditions. Fossil known only from the type locality.

Discussion

Taxonomic comparisons

The Chalco specimens of *C. quillensis* corresponded to the morphological criteria for the species. However, as mentioned above, some specimens did not have a marginal fultoportula on every costa. In central Mexico there is another species of *Cyclotella* that is very close to *C. quillensis*; *Cyclotella alchichicana* Oliva, Lugo, Alcocer & Cantoral. This is an endemic species of the nearby hyposaline, Lake Alchichica (Oliva et al. 2006). The main morphological difference between this species and *C. quillensis* is the arrangement of marginal fultoportulae, which are present on every third costa (instead of on every costa as in *C. quillensis*) (Table 1). In this way, some of the MIS5 specimens from Chalco show morphological variability that seems to be intermediate between *C. quillensis* and *C. alchichicana*.

The two new species from Chalco, *C. poyeka* and *C. tlalocii,* can be easily differentiated from *C. meneghiniana* and *C. quillensis* by the presence of complex marginal alveoli or chambers, visible under LM. These new *Cyclotella* species have a very similar marginal chamber structure, but they can be differentiated by three main characteristics (Table 2): (i) the higher relative proportion of the central area of the valve face in *C. poyeka* (3/4–4/5) compared to *C. tlalocii* (1/2–2/3); (ii) the central fultoportula arrangement, predominantly positioned in an arc on the uplift of the undulation in *C. poyeka*, but distributed in a circular pattern in *C. tlalocii*; (iii) the unique pattern of striation in *C. tlalocii*, with interstriae that reach their a maximum width at the valve face / mantle junction.

These new *Cyclotella* species from Chalco can also be differentiated from other modern *Cyclotella* species with marginal chambers, such as *C. cubiculata* Sar, Sunesen & Lavigne, *C. desikacharyi* Prasad, *C. striata* (Kützing) Grunow, and *C. stylorum* Brightwell, (Table 2). The central area of *C. cubiculata* is colliculate and occupies almost half the valve face, compared with *C. poyeka* and *C. tlalocii* that have a smooth valve surface and a larger central area (3/4–4/5 and 1/2–2/3 valve face, respectively) (Table 2). The alveolus density is also different, *C. cubiculata* has 4–6 chambers in 10 µm (Sar et al. 2010), while both *Cyclotella*

Table 2. Comparison of morphological features between *C. poyeka,* and *C. tlalocii* and other *Cyclotella* species with marginal chambers.

Features	*Cyclotella poyeka*[1]	*Cyclotella tlalocii*[1]	*Cyclotella cubiculata*[7]	*Cyclotella desikacharyi*[5]	*Cyclotella striata*[2,3,4,6]	*Cyclotella stylorum*[2,6]
Valve diameter (µm)	13–50	25–70	23–63	12–30	20–67	25–67
Valve undulation, character of the central area	Slight to strongly tangential, smooth	Slightly tangential, smooth	Strongly tangential, colliculate	Strongly tangential, slightly colliculate	Slight to strongly tangential, colliculate	Strongly tangential, colliculate
Central area to diameter ratio	3/4–4/5	1/2–2/3	~ 1/2	~ 1/2	2/3–3/4	~ 1/2
CFP number, pattern, structure	2–16, arc, 3 pores	4–13, iregular ring, 3 pores	5–15, arc, 3 pores	2–16, arc, (2) 3 pores	np or 1–3, nd, 3 pores	6-12, arc, 3 pores
Costae in 10 µm	7–8	9–10	11–13	15–19	8–10	8–10
Spines	np, granules p	np, granules p	np, granules p	np, granules p	p, granules	np
MFP: costa, position, structure	1:2(3), on recessed costa, 3 pores	1:2(3), on recessed costa, 3 pores	1:2(3), on recessed costa, 2 pores	1:2(3), on recessed costa, 3 pores	1:2–4(5), on recessed costa, 3 pores	1:1, on recessed costa, 2 pores
MC in 10 µm, AO in each chamber, RC:MC	3.5–4, 2–3,1–2	3.5–4, 2–3,1–2	4–6, 2–3,1–2	nd, 2–3,1–2	3–4, 2–3,1–3	2–3, 3–4,1–1
RP number, position, slit orientation	1 stalked, on recessed costa, oblique	1 stalked, on recessed costa, radial	1 stalked, on recessed costa, oblique	1 stalked, on raised costa, tangential	1 stalked, on costa, tangential	1 stalked, on recessed costa, radial

Notes: p: present, np: not present, nd: no data, AO: alveolus opening, MC: marginal chamber, CFP: central fultoportulae, MFP: marginal fultoportulae, RC: raised costae, RP: rimoportula.
[1]This study, [2]Lange & Syvertsen (1989), [3]Håkansson (1996), [4]Håkansson (2002), [5]Prasad & Nienow (2006), [6]Houk et al. (2010), [7]Sar et al. (2010).

species from Chalco have 3.5–4 in 10 µm. Furthermore, the marginal fultoportulae of *C. cubiculata* have two satellite pores, those in *C. poyeka* and *C. tlalocii* have three. In *C. desikacharyi*, the whole valve surface is covered with rows of siliceous granules (Prasad & Nienow 2006), which are absent in both of the new Chalco species (*C. poyeka* and *C. tlalocii*). The striation of *C. desikacharyi* is also finer (15–19 / 10 µm) compared with the thicker striae for *C. poyeka* and *C. tlalocii* (7–8 and 9–10 in 10 µm, respectively). *Cyclotella striata* has a colliculate central area with few (1–3) central fultoportulae, which contrasts with the numerous fultoportulae in both *C. poyeka* and *C. tlalocii* (Table 2). In addition, *C. striata* has a ring of marginal spinulae and marginal fultoportulae on every third or fourth costae, whereas both new *Cyclotella* taxa from Chalco lacked spinulae and the marginal fultoportulae openings were on every recessed costae. Finally, the specimens from Chalco show some similarities with *C. stylorum* although there are also notable differences. Chamber density in *C. poyeka* and *C. tlalocii* is higher (3.5–4 in 10 µm) than in *C. stylorum* (2–3 in 10 µm), and chamber structure is different with 3–4 alveolus openings (2–3 recessed costae) in *C. stylorum* (Lange & Syvertsen 1989) compared to 2–3 alveolus openings (1–2 recessed costae) in *C. poyeka* and *C. tlalocii*. Additionally, both *Cyclotella* taxa from Chalco had marginal fultoportulae with three satellite pores, whereas in *C. stylorum* they only have two.

With respect to the fossil record, *Cyclotella* species with marginal chambers were reported from Lake Baikal (Khursevich et al. 2001), however, these taxa were also characterized by marginal fultoportulae with two satellite pores (Khursevich et al. 2001), unlike those from Chalco with three satellite pores. Additionally, fossil *Cyclotella* species with marginal chambers have been reported from the western United States (McLaughlin 1992, Kociolek & Khursevich 2013). Three of these species (*C. oregonica* Kociolek & Khursevich, *C. jonesii* McLaughlin, and *C. idahica* Kociolek & Khursevich) had rhomboidal to elliptical valve outlines, whereas *C. poyeka* and *C. tlalocii* have circular valves. Another species, *C. stoermeri* Kociolek & Khursevich, has a central area with loculate areolae and internally domed cribra, while in both new *Cyclotella* species from Chalco the only perforations in the central area of the valve were the fultoportulae.

Ecological affinities

Cyclotella meneghiniana is a cosmopolitan diatom recognized for its salinity tolerance, ranging from fresh to brackish water (Tuchman et al. 1984, Fritz et al. 1993, Håkansson & Chepurnov 1999, Håkansson 2002). This is a planktonic or periphytic taxon that can live at a wide range of water depths (Lowe 1974, Gaiser et al. 2011, Montoya-Moreno et al. 2012, Altuner 2017). For example, Phoondee et al. (2019) reports its occurrence from 0–12 m depth in Thailand, whereas, Sigala et al. (2017) observed it from 0.5–65 m depth in Mexican lakes. In the lakes along the Trans-Mexican volcanic belt in central Mexico, this species has its higher abundances in subsaline to hyposaline, alkaline (pH > 7.5) waters (Davies et al. 2002, Sigala et al. 2017, Caballero et al. 2019, Avendaño et al. 2021). It is the dominant taxon in the modern environments of Lake Chalco, currently characterized by subsaline waters with $[HCO_3^-] > [SO_4^{2-}] > [Cl^-]$–$[Na^+ + K^+] > [Ca^{2+}] > [Mg^{2+}]$ ionic dominance, and hypertrophic conditions (Buendía-Flores et al. 2019, Avendaño et al. 2021). In the Lake Chalco fossil record, *C. meneghiniana* is one of the most abundant taxa in the MIS3, MIS4, and MIS5 sediments (Fig. 2), together with other halophilous and alkaliphilous taxa that suggest the presence of subsaline to hyposaline conditions. On the other hand, it is almost absent from sediments dating to the glacial conditions during MIS6 and MIS2 (Avendaño-Villeda et al. 2018, Caballero et al. 2019) during which *Stephanodiscus* spp. are abundant and indicate the presence of cool, freshwater conditions in Chalco. These changes in the abundance of *C. meneghiniana* are probably associated with this species having maximum growth rates under warmer conditions (23–26°C) (Shafik et al. 1997, Mitrovic et al. 2010), but also to its better growth in subsaline to hyposaline waters, environments favoured by higher evaporation rates during warmer intervals (Caballero et al. 2019).

Cyclotella quillensis was described from the saline Quill Lakes from Saskatchewan, Canada (Bailey 1922). It has also been found in other saline lakes in Canada (e.g., Medicine Lake, Battarbee et al. 1984) and the USA (e.g., Alkaline, Pyramid, Devils Lake, Hanna & Grant 1931, Kilham et al. 1996, Salm et al. 2009a, 2009b). For example, Battarbee et al. (1984) reported it from mesosaline to hypersaline, alkaline lakes in North Dakota (TDS > 7000 mg L^{-1}, pH > 8.2) with $[SO_4^{2-}] > [Cl^-] > [HCO_3^-]$ and $[Na^+ + K^+] > [Mg^{2+}] > [Ca^{2+}]$ ionic dominance. Fritz et al. (1991) associated *C. quillensis* with dry climate periods, with an increased salinity in the sedimentary record from Devils Lake. According to Fritz et al. (1993), the salinity optimum estimations for *C. quillensis* were higher (20.56 ‰) than for *C. meneghiniana* (3.38 ‰).

It is not clear if *Cyclotella quillensis* is present in modern environments from central Mexico. Even though it has been reported from hyposaline Lake Alchichica (Metcalfe 1988, Oliva et al. 2001), these reports correspond to specimens belonging to *Cyclotella alchichicana* (Oliva et al. 2006). Cantoral-Uriza (1997) and Montejano et al. 2000 reported *C. quillensis* from calcareous springs in La Huasteca, and Montejano et al. (2004) from the lower Pánuco River, but the presence of this taxon in lotic ecosystems seems unusual, given that it thrives better in saline

environments. In the fossil record, *C. quillensis* was previously reported in sediments from Lake Texcoco, also in the Basin of Mexico (Fig. 1b). As in Lake Chalco, Bradbury (1971) observed this species peaking over a short interval in sediments (> 50 kyr cal BP) from western Lake Texcoco (Reforma core), where the author used it as an indicator for brackish conditions. We also consider that the presence of *C. quillensis* in sediments dating to around 80 kyr cal BP is an indication of increased lake salinity and probably also a change in dominant ions, from [HCO_3^-] to [Cl^-]–[SO_4^{2-}], that allowed this species to displace *C. meneghiniana*. During the brief interval when *C. quillensis* was dominant (80% of counts) the only other species present were *Anomoeoneis costata* (Kützing) Hustedt and *A. sphaerophora* Pfitzer, which are known to thrive in high salinity environments (Bradbury 1971, Saros & Fritz 2002). Even though the modern distribution of *C. quillensis* is preferentially in saline lakes from USA and Canada, our data show that in the past (~ 80 kyr cal BP) it had a wider distribution in central Mexico. Considering that some of the Chalco specimens show a morphological transition to *C. alchichicana* (absence of marginal fultoportulae on some costae) we suggest that *C. quillensis* from Chalco is the possible ancestor of the endemic species, *C. alchichicana*.

Cyclotella tlalocii and *C. poyeka* were also dominant in the Lake Chalco sediment record for short intervals during MIS5 (~ 115 and ~ 96 kyr cal BP respectively). However, each species was part of a different diatom assemblage, showing distinct ecological preferences. *Cyclotella tlalocii* is dominant in a stratigraphic interval dominated by *Stephanodiscus niagarae* Ehrenberg (Fig. 2), displacing the latter from the record. It is present in association with other freshwater species that are tolerant of high nutrient levels, such as *Aulacoseira granulata* (Ehrenberg) Simonsen, *Pseudostaurosira brevistriata* (Grunow) Williams & Round, *Discostella stelligera* (Cleve & Grunow) Houk & Klee and *Cyclostephanos dubius* (Hustedt) Round (Wang et al. 2009, Saros et al. 2014, Bicudo et al. 2016). We therefore conclude that *C. tlalocii* thrived in freshwater, eutrophic environments. This is also supported by the low Ca/Ti values (Fig. 2) that suggest low autogenic carbonate deposition during the time that this species was abundant. We propose that *C. tlalocii* is an endemic of Lake Chalco that evolved during a time of rapid temperature change, from a period of cooler conditions during which *Stephanodiscus* spp. were dominant, to warmer conditions when *Cyclotella* spp. could take over as the dominant taxa. However when lake salinity increased this species was replaced by *C. meneghiniana* and eventually became extinct.

On the other hand, *C. poyeka* was dominant over a stratigraphic interval otherwise dominated by *C. meneghiniana* in association with halophilous species such as *A. costata, A. sphaerophora*, *Campylodiscus clypeus* (Ehrenberg) Ehrenberg ex Kützing, and *Rhopalodia gibberula* (Ehrenberg) O.Müller. All these species thrive in saline environments, which supports the interpretation that *C. poyeka* preferred these conditions. Also, a saline condition agrees with high Ca/Ti (Fig. 2) values, a proxy for autogenic calcium carbonate precipitation. *Cyclotella poyeka* very likely corresponds with what Bradbury (1971) identified as *C.* cf. *stylorum* in sediments from western Lake Texcoco (Reforma core) that could also date to MIS5 (even though the chronological control of this sequence is very poor). There are no illustrations of the diatoms identified by Bradbury (1971) in the sediments from Texcoco to confirm this, but *C. poyeka* (Fig. 75) closely resembles the specimen illustrated under the same name (*C.* cf. *stylorum*, Fig. 76) from Pyramid Lake by the same author (Krebs et al. 1987). Paillès et al. (2018) suggested that *C.* cf. *stylorum* from Texcoco (Bradbury 1971) could be conspecific with *C. petenensis* Sylvestre, Paillès & Escobar, a fossil taxon abundant in the Lake Petén-Itzá sediments dating from MIS3 to MIS2 (Paillès et al. 2018) (Fig. 1a). However, we consider this very unlikely, given that *C. petenensis* does not have complex alveoli (Fig. 77), and would therefore be difficult to mistake as a taxon close to *C. stylorum*. We suggest that it is more probable that this unidentified species from the western part of Lake Texcoco corresponds, or at least is close to *C. poyeka,* due to the geographic proximity between both lakes (Chalco and Texcoco) (Fig. 1b) and their similar high salinity conditions. If it is confirmed that *C. poyeka* and *C.* cf. *stylorum* from Lake Texcoco and Pyramid Lake are the same species, then the distribution of *C. poyeka* would extend to North America, and under this scenario it is likely that the specimens from the Basin of Mexico were the source of those present in Pyramid Lake. We propose that *C. poyeka* evolved in Lake Chalco during MIS5 as a response to unstable climatic conditions that favoured rapid changes in the salinity and ionic dominance of the lake. Thus both new *Cyclotella* species from Chalco seem to have evolved in response to changing physical conditions (temperature for *C. tlalocii*, salinity for *C. poyeka*) during successive climatic oscillations. A similar evolutionary scenario has been proposed for the non-modern analogue diatom communities in Lake Baikal spanning the last 5 Ma (Khursevich et al. 2001).

Some interpretations of the evolution of the genus *Cyclotella* assume that salt tolerance originated independently in two main lineages within the genus, defined by the number of satellite pores on the marginal fultoportulae (Håkansson 2002). The first group comprises species with two satellite pores (i.e., *C. atomus* Hustedt, *C. choctawhatcheeana* Prasad, *C.baltica* (Grunow) Håkansson, C. *litoralis* Lange & Syvertsen, *C. stylorum).* The second group comprises species with three satellite pores, including *C. meneghiniana, C. striata, C. desikacharyi, C. quillensis, C. alchichicana* as well as the two new species from Chalco, *C. poyeka* and *C. tlalocii.* However phylogenetic studies suggest that *C. meneghiniana, C. quillensis,*

C. cryptica Reimann, Lewin & Guillard and *C. gamma* Sovereign form a closely related group (Alverson et al. 2007, 2011, Ács et al. 2016), while *C. striata* and *C. stylorum*; form another closely related group, even though *C. striata* has marginal fultoportulae with three satellite pores and *C. stylorum* has only two.

It has also been suggested that the presence of a central lamina and/or of marginal chambers are adaptations within *Cyclotella* distinguishing salt-tolerant species (Prasad et al. 1990, Prasad & Nienow 2006). Three groups within the genus have been proposed. Group 1 includes species with no central lamina or marginal chambers, such as *C. atomus* and *C. meneghiniana* group. These are the least salt-tolerant species. Group 2 includes species with central laminae but lacking marginal chambers, such as *C. baltica, C. choctawhatcheeana, C. litoralis, C. scaldensis* Muylaert & Sabbe, *C. quillensis* and *C. alchichicana*. These species have a higher preference for saline-brackish waters. Group 3 includes species with central laminae and marginal chambers such as *C. desikacharyi, C. striata, and C. stylorum,* and includes brackish to truly marine forms. According to this classification, *C. poyeka* and *C. tlalocii* would belong to the last group. While the inferred ecology of *C. poyeka* would agree with this interpretation, it conflicts with the inferred ecology of *C. tlalocii*, as this was probably a freshwater species, despite having central laminae and marginal chambers. This suggests that the presence of these features is not necessarily associated with a tolerance for saline environments.

Acknowledgements

Laura Gómez Lizárraga gave technical assistance for sample preparation and observation with the scanning electron microscopy. Dr. Nienow provided advice on the taxonomy of *Cyclotella stylorum*. Dr. Socorro Lozano and Dr. Beatriz Ortega have been lead collaborators in the Chalco drilling projects and their support has been fundamental for the recovery, description and dating of the sediment sequence. We also thank two anonymous reviewers, Dr. Eileen J. Cox and Dr. Jeffery Stone for their valuable comments that greatly improved our manuscript.

Disclosure statement

No potential conflict of interest was reported by the author(s).

Funding

This research was funded by the National University of Mexico (UNAM), projects PAPIIT IN100820 'Registros Interglaciares del Centro de México' and DGAPA-PAPIIT-IN103819 'Variabilidad climática y paleoambientes durante la terminación II (130 ka): El paso del penúltimo glacial (MIS 6) al penúltimo interglaciar (MIS 5)'. Diana Avendaño thanks the Posgrado de Ciencias de la Tierra, UNAM and CONACyT (Consejo Nacional de Ciencia y Tecnología) [CVU 854736] for financial support.

References

Ács É., Ari E., Duleba M., Dressler M., Genkal S. I., Jakó É., Rimet F., Ector L. & Kiss K. T. 2016. *Pantocsekiella*, a new centric diatom genus based on morphological and genetic studies. *Fottea, Olomouc* 16: 56–78.

Altuner Z. 2017. An investigation on the benthic diatoms of Murat River (Muş) and comparison with Ehrenberg's study. *Journal of New Results in Science* 6: 17–23.

Alverson A. J., Beszteri B., Julius M. L. & Theriot E. C. 2011. The model marine diatom *Thalassiosira pseudonana* likely descended from a freshwater ancestor in the genus *Cyclotella*. *BMC Evolutionary Biology* 11: 1–8.

Alverson A. J., Jansen R. K. & Theriot E. C. 2007. Bridging the Rubicon: phylogenetic analysis reveals repeated colonizations of marine and fresh waters by thalassiosiroid diatoms. *Molecular Phylogenetics and Evolution* 45: 193–210.

Anonymous 1975. Proposals for a standardization of diatom terminology and diagnosis. *Nova Hedwigia* 53: 323–334.

Avendaño-Villeda D. A., Caballero M., Ortega-Guerrero B., Lozano-García S. & Brown E. 2018. Condiciones ambientales a finales del Estadio Isotópico 6 (EI 6: > 130000 años) en el centro de México: caracterización de una sección de sedimentos laminados proveniente del Lago de Chalco. *Revista Mexicana de Ciencias Geológicas* 35: 168–178.

Avendaño D., Caballero M. & Vázquez G. 2021. Ecological distribution of *Stephanodiscus niagarae* Ehrenberg in central Mexico and niche modeling for its last glacial maximum habitat suitability in the Nearctic realm. *Journal of Paleolimnology* 66: 1–14. doi:10.1007/s10933-021-00178-w.

Bailey L. W. 1922. Diatoms from the Quill Lakes, Saskatchewan, and from Airdrie, Alberta. *Contributions to Canadian Biology* 11: 157–165.

Battarbee R. W., Keister C. M. & Bradbury J. P. 1984. The frustule morphology and taxonomic relationship of *Cyclotella quillensis* Bailey. In: *Proceedings of the 7th International Diatom Symposium* (Ed. by D. Mann), pp. 173–184. Philadelphia.

Bicudo D. C., Tremarin P. I., Almeida P. D., Zorzal-Almeida S., Wengrat S., Faustino S. B., Costa L. F., Bartozek E. C. R., Rocha A. C. R., Bicudo C. E. M. & Morales E. A. 2016. Ecology and distribution of *Aulacoseira* species (Bacillariophyta) in tropical reservoirs from Brazil. *Diatom Research* 31: 199–215.

Bradbury J. P. 1971. Paleolimnology of Lake Texcoco, Mexico. Evidence from diatoms. *Limnology and Oceanography* 16: 180–200.

Buendía-Flores M., Tavera R., Novelo E. & Espinosa-Matias S. 2019. Composición florística y diversidad de diatomeas bentónicas del lago Chalco, México. *Revista Mexicana de Biodiversidad* 90: 1–18.

Caballero M., Lozano-García S., Ortega-Guerrero B. & Correa-Metrio A. 2019. Quantitative estimates of orbital and millennial scale climatic variability in central Mexico during the last ~40,000 years. *Quaternary Science Reviews* 205: 62–75.

Cantoral-Uriza E. 1997. *Diatomeas (Bacillariophyceae) de ambientes Loticos en la cuenca baja de la Huasteca*

Potosina. Ph.D. Thesis, Universidad Nacional Autónoma de México, Mexico.

Davies S. J., Metcalfe S. E., Caballero M. E. & Juggins S. 2002. Developing diatom-based transfer functions for Central Mexican lakes. *Hydrobiologia* 467: 199–213.

Edlund M. & Burge D. 2016. *Cyclotella quillensis* [online]. Diatoms of North America. Available from: https://diatoms.org/species/cyclotella_quillensis [Accessed 8 October 2020].

Fritz S. C., Juggins S. & Battarbee R. W. 1993. Diatom assemblages and ionic characterization of lakes of the Northern Great Plains, North America: a tool for reconstructing past salinity and climate fluctuations. *Canadian Journal of Fisheries and Aquatic Sciences* 50: 1844–1856.

Fritz S. C., Juggins S., Battarbee R. W. & Engstrom D. R. 1991. Reconstruction of past changes in salinity and climate using a diatom-based transfer function. *Nature* 352: 706–708.

Gaiser E. E., McCormick P. V., Hagerthey S. E. & Gottlieb A. D. 2011. Landscape patterns of periphyton in the Florida Everglades. *Critical Reviews in Environmental Science and Technology* 41: 92–120.

Guiry M. D., Guiry M. D. & Guiry G. M. 2020. *Cyclotella* (Kützing) Brébisson, 1838, nom. et typ. cons [online]. AlgaeBase. National University of *Irland*, Galway. Available from: https://www.algaebase.org/search/genus/detail/?genus_id=43757&-session=abv4:AC1F0F3E05604081CBhS51B9B500 [Accessed 23 September 2020].

Håkansson H. 1996. *Cyclotella striata* complex: typification and new combinations. *Diatom Research* 11: 241–260.

Håkansson H. 2002. A compilation and evaluation of species in the general *Stephanodiscus, Cyclostephanos* and *Cyclotella* with a new genus in the family Stephanodiscaceae. *Diatom Research* 17: 1–139.

Håkansson H. & Chepurnov V. 1999. A study of variation in valve morphology of the diatom *Cyclotella meneghiniana* in monoclonal cultures: effect of auxospore formation and different salinity conditions. *Diatom Research* 14: 251–272.

Håkansson H. & Kling H. 1994. *Cyclotella agassizensis* nov. sp. and its relationship to *C. quillensis* Bailey and other prairie *Cyclotella* species. *Diatom Research* 9: 289–301.

Hanna G. D. & Grant W. M. 1931. Diatoms of Pyramid Lake, Nevada. *Transactions of the American Microscopical Society* 50: 281–297.

Houk V., Klee R. & Tanaka H. 2010. Atlas of freshwater centric diatoms with a brief key and descriptions. Part III. Stephanodiscaceae A. *Cyclotella, Tertiarius, Discostella. Fottea* 10 (supplement): 1–498.

Khursevich G. K., Karabanov E. B., Prokopenko A. A., Williams D. F., Kuzmin M. I. & Fedenya S. A. 2001. Biostratigraphic significance of new fossil species of the diatom genera *Stephanodiscus* and *Cyclotella* from Upper Cenozoic deposits of Lake Baikal. *Micropaleontology* 47: 47–71.

Khursevich G. & Kociolek J. P. 2012. A preliminary, worldwide inventory of the extinct, freshwater fossil diatoms from the orders Thalassiosirales, Stephanodiscales, Paraliales, Aulacoseirales, Melosirales, Coscinodiscales, and Biddulphiales. *Nova Hedwigia* 141: 315–364.

Kilham S. S., Theriot E. C. & Fritz S. C. 1996. Linking planktonic diatoms and climate change in the large lakes of the Yellowstone ecosystem using resource theory. *Limnology and Oceanography* 41: 1052–1062.

Kociolek J. P. & Khursevich G. K. 2013. Morphology of some fossil lacustrine centric species from the western United States assigned to the genus *Cyclotella* (Bacillariophyta), including four described as new. *Phytotaxa* 127: 81–99.

Krammer K., Lange-Bertalot H., Håkansson H. & Nörpel M. 1991. 2/3 Bacillariophyceae. 3. Teil: Centrales, Fragilariaceae, Eunotiaceae. In: *Sübwasserflora von Mitteleuropa* (Ed. by H. Ettl, J. Gerloff, H. Heynig & D. Mollenhauer), p. 576. G. Fischer Verlag, Stuttgart-Jena.

Krebs W. N., Bradbury J. P. & Theriot E. 1987. Neogene and quaternary lacustrine diatom biochronology, western USA. *PALAIOS* 2: 505–513.

Lange C. B. & Syvertsen E. E. 1989. *Cyclotella litoralis* sp. nov. (Bacillariophyceae), and its relationships to *C. striata* and *C. stylorum*. *Nova Hedwigia* 48: 341–356.

Loginova L. P. 1990. Classification of the diatom genus *Cyclotella*. In: *Proceedings of the 10th International Diatom Symposium* (Ed. by H. Simola), pp. 37–53. Koeltz Scientific Books, Koenigstein.

Lowe R. & Kheiri S. 2015. *Cyclotella meneghiniana* [online]. Diatoms of North America. Available from: https://diatoms.org/species/cyclotella_meneghiniana [Accessed 4 September 2020].

Lowe R. L. 1974. *Environmental requirements and pollution tolerance of freshwater diatoms*. U.S. Environmental Protection Agency, Cincinnati.

Lowe R. L. 1975. Comparative ultrastructure of the valves of some *Cyclotella* species (Bacillariophyceae). *Journal of Phycology* 11: 415–424.

McFarland B. H. & Collins G. B. 1978. A key to the species of the diatom genus *Cyclotella* (Kütz.) Bréb., based on new morphological data. Abstract, In: *26th annual meeting of North American Benthological Society* pp. 35. Winnipeg, Mannitoba.

McLaughlin R. B. 1992. *Cyclotella jonesii*, a new diatom species from Pliocene deposits at Chiloquin, Oregon, U.S.A.. *Diatom Research* 7: 95–101.

Metcalfe S. E. 1988. Modern diatom assemblages in Central Mexico: the role of water chemistry and other environmental factors as indicated by TWINSPAN and DECORANA. *Freshwater Biology* 19: 217–233.

Meyer B., Wulf M. & Håkansson H. 2001. Phenotypic variation of life-cycle stages in clones of three similar *Cyclotella* species after induced auxospore production. *Diatom Research* 16: 343–361.

Mitrovic S. M., Hitchcock J. N., Davie A. W. & Ryan D. A. 2010. Growth responses of *Cyclotella meneghiniana* (Bacillariophyceae) to various temperatures. *Journal of Plankton Research* 32: 1217–1221.

Montejano G., Cantoral-Uriza E. A. & Carmona-Jiménez J. 2004. Algas de ambientes lóticos en la cuenca baja del río Pánuco. In: *Biodiversidad de la Sierra Madre Oriental* (Ed. by I. Luna, J. J. Morrone & D.

Espinosa), pp. 111–126. Las prensas de Ciencias, Universidad Nacional Autónoma de México, México.

Montejano G., Carmona-Jimenez J. & Cantoral-Uriza E. A. 2000. Algal communities from calcareous springs in La Huasteca, central México: a synthesis. In: *Aquatic ecosystems of Mexico* (Ed. by M. Munawar, S. G. Lawrence, I. F. Munawar & D. F. Malley), pp. 135–149. Backhuys, Leiden.

Montoya-Moreno Y., Sala S. E., Vouilloud A. A. & Aguirre N. 2012. Diatomeas (Bacillariophyta) perifíticas del Complejo Cenagoso de Ayapel, Colombia. I / Periphytic diatoms (Bacillariophyta) of Ayapel flood plain, Colombia. *I.* Caldasia 34: 457–474.

Nakov T., Guillory W. X., Julius M. L., Theriot E. C. & Alverson A. J. 2015. Towards a phylogenetic classification of species belonging to the diatom genus *Cyclotella* (Bacillariophyceae): transfer of species formerly placed in *Puncticulata, Handmannia, Pliocaenicus* and *Cyclotella* to the genus *Lindavia. Phytotaxa* 217: 249–264.

Oliva M. G., Lugo A., Alcocer J. & Cantoral-Uriza E. A. 2006. *Cyclotella alchichicana* sp. nov. from a saline mexican lake. *Diatom Research* 21: 81–89.

Oliva M. G., Lugo A., Alcocer J., Peralta L. & Del Rosario Sánchez M. 2001. Phytoplankton dynamics in a deep, tropical, hyposaline lake. *Hydrobiologia* 466: 299–306.

Ortega-Guerrero B., Avendaño D., Caballero M., Lozano-García S., Brown E. T., Rodríguez A., García B., Barceinas H., Soler A. M. & Albarrán A. 2020. Climatic control on magnetic mineralogy during the late MIS 6 – early MIS 3 in Lake Chalco, central Mexico. *Quaternary Science Reviews* 230: 106–163.

Ortega-Guerrero B., Lozano-García S., Herrera-Hernández D., Caballero M., Beramendi-Orosco L., Bernal J. P., Torres-Rodríguez E. & Avendaño-Villeda D. 2017. Lithostratigraphy and physical properties of lacustrine sediments of the last ca. 150 kyr from Chalco basin, central México. *Journal of South American Earth Sciences* 79: 507–524.

Paillès C., Sylvestre F., Escobar J., Tonetto A., Rustig S. & Mazur J. C. 2018. *Cyclotella petenensis* and *Cyclotella cassandrae*, two new fossil diatoms from Pleistocene sediments of Lake Petén-Itzá, Guatemala, Central America. *Phytotaxa* 351: 247–263.

Phoondee Y., Pumas C. & Peerapornpisal Y. 2019. Biomonitoring by phytoplankton diversity and biovolume depth profile of the Pasak Jolasid Reservoir, Lopburi Province, Thailand. *Journal of Biotech Research* 10: 170–182.

Prasad A. K. S. K. & Nienow J. A. 2006. The centric diatom genus *Cyclotella*, (Stephanodiscaceae: Bacillariophyta) from Florida Bay, USA, with special reference to *Cyclotella choctawhatcheeana* and *Cyclotella desikacharyi*, a new marine species related to the *Cyclotella striata* complex. *Phycologia* 45: 127–140.

Prasad A. K. S. K., Nienow J. A. & Livingston R. J. 1990. The genus *Cyclotella* (Bacillariophyta) in Choctawhatchee Bay, Florida, with special reference to *C. striata* and *C. choctawhatcheeana* sp. nov. *Phycologia* 29: 418–436.

Rioual P., Andrieu-Ponel V., Rietti-Shati M., Battarbee R. W., de Beaulieu J.-L., Cheddadi R., Reille M., Svobodova H. & Shemesh A. 2001. High-resolution record of climate stability in France during the last interglacial period. *Nature* 413: 293–296.

Ross R., Cox E. J., Karayeva N. I., Mann D. G., Paddock T. B. B., Simonsen R. & Sims P. A. 1979. An amended terminology for the siliceous components of the diatom cell. *Nova Hedwigia* 64: 513–533.

Ross R. & Sims P. A. 1972. The fine structure of the frustule in centric diatoms: a suggested terminology. *British Phycological Journal* 7: 139–163.

Rühland K. M., Paterson A. M. & Smol J. P. 2015. Lake diatom responses to warming: reviewing the evidence. *Journal of Paleolimnology* 54: 1–35.

Salm C. R., Saros J. E., Fritz S. C., Osburn C. L. & Reineke D. M. 2009a. Phytoplankton productivity across prairie saline lakes of the Great Plains (USA): a step toward deciphering patterns through lake classification models. *Canadian Journal of Fisheries and Aquatic Sciences* 66: 1435–1448.

Salm C. R., Saros J. E., Martin C. S. & Erickson J. M. 2009b. Patterns of seasonal phytoplankton distribution in prairie saline lakes of the northern Great Plains (U.S.A.). Aquattic *Biosystems* 5: 1746–1448.

Sar E., Sunesen I. & Lavigne A. 2010. *Cymatotheca*, *Trybliоptychus*, *Skeletonema* and *Cyclotella* (Thalassiosirales) from Argentinian coastalwaters. Description of *Cyclotella cubiculata* sp. nov. *Vie et Milieu* 60: 133–154.

Saros J. E., Strock K. E., Mccue J., Hogan E. & Anderson N. J. 2014. Response of *Cyclotella* species to nutrients and incubation depth in Arctic lakes. *Journal of Plankton Research* 36: 450–460.

Saros J. & Fritz S. 2002. Resource competition among saline-lake diatoms under varying N/P ratio, salinity and anion composition. *Freshwater Biology* 47: 87–95.

Serieyssol K. K. 1981. *Cyclotella* species of late Miocene age from St. Bauzite, France. In: *Proceedings of the 6th International Diatom Symposium* (Ed. by R. Ross), pp. 27–42. Otto Koeltz, Koenigstein.

Servant-Vildary S. 1986. Fossil *Cyclotella* species from Miocene deposit of Spain. In: *Proceedings of the 8th International Diatom Symposium* (Ed. by M. Ricard), pp. 495–511. Otto Koeltz, Koenigstein.

Shafik H. M., Herodek S., Vörös L., Présing M. & Kiss K. T. 1997. Growth of *Cyclotella meneghiniana* Kutz. I. Effects of temperature, light and low rate of nutrient supply. *Annales de Limnologie-International Journal of Limnology* 33(3): 139–147.

Sigala I., Caballero M., Correa-Metrio A., Lozano-García S., Vázquez G., Pérez L. & Zawisza E. 2017. Basic limnology of 30 continental waterbodies of the Transmexican Volcanic Belt across climatic and environmental gradients. *Boletín de la Sociedad Geológica Mexicana* 69: 313–370.

Tapia P. M., Fritz S. C., Baker P. A., Seltzer G. O. & Dunbar R. B. 2003. A late quaternary diatom record of tropical climatic history from Lake Titicaca (Peru and Bolivia). *Palaeogeography, Palaeoclimatology, Palaeoecology* 194: 139–164.

TEMNISKOVA-TOPALOVA D., VALEVA M. & OGNJANOVA-RUMENOVA N. 1994. Nonmarine biostratigraphy of some genera of subclass Centrophycidae from South Bulgaria. In: *Proceedings of the 11th International Diatom Symposium* (Ed. by J. P. KOCIOLEK), pp. 301–310. California Academy of Sciences, San Francisco.

THERIOT E. & SERIEYSSOL K. 1994. Phylogenetic systematics as a guide to understanding features and potential morphological characters of the centric diatom family Thalassiosiraceae. *Diatom Research* 9: 429–450.

TORRES-RODRÍGUEZ E., LOZANO-GARCÍA S., CABALLERO-MIRANDA M., ORTEGA-GUERRERO B., SOSA-NÁJERA S. & DEBAJYOTI-ROY P. 2018. Pollen and non-pollen palynomorphs of Lake Chalco as indicators of paleolimnological changes in high-elevation tropical central Mexico since MIS 5. *Journal of Quaternary Science* 33: 945–957.

TUCHMAN M. L., THERIOT E. & STOERMER E. F. 1984. Effects of low level salinity concentrations on the growth of *Cyclotella meneghiniana* Kütz. (Bacillariophyta). *Archiv fur Protistenkunde* 128: 319–326.

WANG C., LI X., LAI Z., TAN X., PANG S. & YANG W. 2009. Seasonal variations of *Aulacoseira granulata* population abundance in the Pearl River Estuary. *Estuarine, Coastal and Shelf Science* 85: 585–592.

Capítulo V

5. Diversidad y distribución de diatomeas lacustres a lo largo de la Faja Volcánica Transmexicana.

(Artículo publicado, citar como: Avendaño, D., Caballero, M. & Vázquez G. (2023). Diversity and distribution of lacustrine diatoms along the Trans-Mexican Volcanic Belt. *Freshwater Biology*, 68, 391– 405. https://doi.org/10.1111/fwb.14033)

Este artículo inicio como punto de partida para comprender la ecología de las diatomeas de 49 muestras en 46 lagos que se localizan a lo largo de la Faja Volcánica Transmexicana, confirmando su potencial en las reconstrucciones paleoambientales. En este artículo se resalta la estrecha afinidad que existe entre las especies de diatomeas en relación las condiciones de salinidad y temperatura de los lagos y se explora la diversidad a nivel regional.

Resumen:

La Faja volcánica Transmexicana es reconocida como una zona altamente biodiversa para la cual presentamos un estudio de la diversidad de diatomeas y distribución de especies en los lagos. Nuestro objetivo fue identificar los taxones de diatomeas con la ocupación regional más alta, explorar la diversidad a nivel regional, identificar las principales variables asociadas con la distribución de las especies y presentar valores óptimos de promedios ponderados para las variables que podrían proporcionar una referencia valiosa para futuras investigaciones paleoambientales. Se utilizaron abundancias relativas de diatomeas en sedimentos superficiales de lagos para estimar diferentes métricas de diversidad, así como diversidades alfa, gamma y beta. Se identificaron grupos de lagos con conjuntos de diatomeas similares mediante análisis de conglomerados, mientras que se utilizó el análisis de correspondencia canónica (ACC) para evaluar la asociación entre la composición de diatomeas y las variables climáticas, morfométricas, hidroquímicas y tróficas. Se estimaron valores óptimos de promedio ponderados para salinidad y temperatura. De un total de 184 taxones de diatomeas, tres eran endémicas de uno o dos lagos y ocho tenían la mayor ocupación regional, dos de ellos asociados a ambientes de alta salinidad (*Stephanocyclus meneghinianus, Nitzschia frustulum*) y el resto a condiciones de agua dulce (*Aulacoseira ambigua, A. granulata, A. granulata* var. *angustissima, Discostella stelligera, Fragilaria crotonensis, Achnanthidium minutissimum*). Sorprendentemente, los taxones endémicos, así como los taxones de alta ocupación regional, eran en su mayoría formas plantónicas o epipélicas móviles con alto potencial de dispersión. Nuestros resultados muestran 13 grupos de lagos con conjuntos de diatomeas similares, en estrecha concordancia con la diversidad beta que predijo la presencia de 12 comunidades. Hubo un alto recambio de especies (βSIM = 0.97) y el ACC mostró que la principal variable ambiental que define estos grupos fue la salinidad, pero que la temperatura, precipitación, profundidad y el fósforo reactivo soluble también fueron significativos. Además, no hubo evidencia de un patrón de diversidad altitudinal. Este es el primer estudio de la flora de diatomeas de los lagos en el centro de México que analiza la diversidad y distribución de especies a lo largo de gradientes ambientales que incluyan variables climáticas, morfométricas, hidroquímicas y relacionadas con el estado trófico.

Palabras clave: Bacillariophyta, diversidad verdadera, riqueza de especies, lagos tropicales, ecología de diatomeas.

Received: 24 January 2022 | Revised: 16 November 2022 | Accepted: 21 November 2022

DOI: 10.1111/fwb.14033

ORIGINAL ARTICLE

Freshwater Biology WILEY

Diversity and distribution of lacustrine diatoms along the Trans-Mexican Volcanic Belt

Avendaño Diana[1] | Caballero Margarita[2] | Vázquez Gabriela[3]

[1]Posgrado de Ciencias de la Tierra, Instituto de Geofísica, Universidad Nacional Autónoma de México, Ciudad Universitaria, México City, Mexico

[2]Laboratorio de Paleolimnología, Instituto de Geofísica, Universidad Nacional Autónoma de México, Ciudad Universitaria, México City, Mexico

[3]Instituto de Ecología A.C., Veracruz, Mexico

Correspondence
Caballero Margarita, Laboratorio de Paleolimnología, Instituto de Geofísica, Universidad Nacional Autónoma de México, Ciudad Universitaria, México City 04510, México.
Email: maga@igeofisica.unam.mx

Funding information
Universidad Nacional Autónoma de México, proyecto PAPIIT 100820 "Registros Interglaciares del Centro de México".

Abstract

1. The Trans-Mexican Volcanic Belt is recognised as a highly biodiverse zone and we present a study of diatom diversity and species distributions in its lakes. We aimed to identify diatom taxa with the highest regional occupancy, explore diversity at a regional level, identify the main variables associated with species distributions, and present weighted average optima for variables that could provide a valuable reference for future palaeoenvironmental research.
2. We used the relative abundances of diatoms in surficial lake sediments to estimate different diversity metrics and alpha, beta and gamma diversities. Groups of lakes with similar diatom assemblages were identified by means of cluster analysis whereas canonical correspondence analysis (CCA) was used to evaluate the association between diatom composition and climatic, morphometric, hydrochemical and trophic status related variables. Weighted average optima were estimated for salinity and temperature.
3. From a total of 184 diatom taxa, three were endemic to one or two lakes and eight had the largest regional occupancy, two of which were associated with high salinity environments (*Stephanocyclus meneghinianus*, *Nitzschia frustulum*) and the rest with freshwater conditions (*Aulacoseira ambigua*, *A. granulata*, *A. granulata* var. *angustissima*, *Discostella stelligera*, *Fragilaria crotonensis*, *Achnanthidium minutissimum*). Surprisingly, endemic taxa as well as those with high regional occupancy were mostly planktic or epipelic motile forms, with high dispersal potential. Our results showed 13 clusters of lakes with similar diatom assemblages, in close agreement with beta diversity which predicted the presence of 12 communities. There was high species turnover ($\beta_{SIM} = 0.97$) and CCA showed not only that the main environmental variable defining these groups was salinity, but also that temperature, precipitation, depth, and soluble reactive phosphorus were meaningful variables. There was no evidence of an altitude–diversity pattern.
4. This study emphasises the strong influence that climatic variables have on species distribution when relatively broad geographical areas, with large climatic gradients are analysed.

KEYWORDS
Bacillariophyta, diatom ecology, species richness, tropical lakes, true diversity

1 | INTRODUCTION

Diatoms are unicellular, photosynthetic organisms, present in the phytoplankton and phytobenthos of most aquatic ecosystems (Battarbee et al., 2002; Julius & Theriot, 2010). Their ecological distribution along environmental gradients such as pH, salinity or trophic gradients has been studied in different regions of the world, frequently to use them as a tool for water quality evaluation (De La Rey et al., 2008; Lobo et al., 2016; Stenger-Kovács et al., 2007) or for the reconstruction of past environments (Fritz et al., 1993; Gasse et al., 1995; Wilson et al., 1996). Furthermore, in recent decades macroecological studies, which traditionally were undertaken with larger organisms, have extended to include microorganisms such as diatoms (Soininen & Teittinen, 2019).

Central Mexico represents an interesting area for the study of diatom species diversity and distribution given that it represents a highly biodiverse region in a transition zone between the Nearctic and the Neotropical realms (Figure 1a) (Morrone, 2020). Furthermore, the Trans-Mexican Volcanic Belt (TMVB) in central Mexico extends over a series of six globally or continentally outstanding biodiverse aquatic ecoregions (Abell et al., 2008) (Figure 1b). In lakes along the TMVB, Caballero et al. (2019), Davies et al. (2002) and Metcalfe (1988) studied the diatom assemblages preserved in surface sediment samples and demonstrated that ionic concentration (measured either as electric conductivity, salinity or alkalinity) was highly correlated with species distribution. Furthermore, Caballero et al. (2019) showed that other variables such as temperature and precipitation also were associated with diatom species distributions, and successfully developed transfer functions for salinity, temperature and precipitation, reconstructing these variables for the last 40,000 years in Lake Chalco, central Mexico. The role of trophic status and nutrient gradients has been less explored in this region, but it also is likely to be an important influence for diatom distribution (Hill, 2006). The relatively large calibration dataset used for the development of the transfer functions in Caballero et al. (2019) offers the opportunity to not only document diatom distribution along ecological gradients, but also to explore their biodiversity, an aspect that has not been studied before in the region. This kind of analysis can help to address questions that have been posed in previous ecological studies of diatoms in other regions of the world (Soininen & Teittinen, 2019), which include: What is the role of climate factors such as temperature in diatom species distribution? Is there niche conservation in diatoms? Do diatoms exhibit an altitudinal diversity pattern? Is spatial diversity dominated by turnover or nestedness? Is regional occupancy by diatoms controlled by their dispersal potential? Is endemism common amongst diatoms? Are endemic taxa mostly attached, low-profile species of weak dispersal potential?

In this paper we present diatom abundance and diversity data from a set of 49 surface sediment samples collected from 46 lakes along the TMVB from which we aim to: (a) assess the diatom species richness, diversity and dominance, as well as their alpha, beta and gamma diversities, (b) evaluate whether there is a linear correlation between species richness and altitude, (c) identify endemic taxa and also the species with the highest regional occupancy (highest abundance and frequency) in the area, (d) identify the main variables that are associated with species distributions in the region, including climatic, morphometric, hydrochemical and trophic status related variables, and (e) develop salinity and temperature distribution optima for the most abundant taxa, as these values will provide a reference for future palaeoenvironmental research in the area.

2 | METHODS

2.1 | Study area

The study sites are located along the six aquatic ecoregions that converge in the TMBV (Figure 1b). Most of the lakes are in the higher altitude, endorheic Lerma ecoregion, but they also spread over the adjacent subtropical coastal basins, three of which drain to the Pacific (Santiago, Ameca, and Balsas) and two to the Gulf of Mexico (Pánuco and Papaloapan). The climate of the region is closely associated with the intricate topography of the TMVB, its steep altitudinal gradients define climates that range from warm to cold and from dry to humid, all sharing a summer rainy season related to the northerly migration of the Intertropical Convergence Zone, the easterly trade wind flow, and the onset of the Mexican Monsoon.

2.2 | Description of the dataset

The dataset analysed in this paper included climatic, morphometric, hydrochemical and trophic status related variables from lakes distributed along the TMVB in central Mexico, which were studied as part of previous surveys (Avendaño et al., 2021; Caballero et al., 2019; Sigala et al., 2017; Vázquez & Caballero, 2013). The information for the 46 lakes in the dataset was determined following uniform methodologies for fieldwork and laboratory analyses which are detailed in Sigala et al. (2017). Climatic data for all of the lakes were obtained from the closest meteorological stations (full list in Table S1) and included average annual temperature (AAT), precipitation (AAP) and evaporation (AAE). Morphometric data for all of the lakes included area, depth and relative depth (maximum depth expressed as a percentage of diameter). Hydrochemical data for all the lakes corresponded to single measurements at the time of

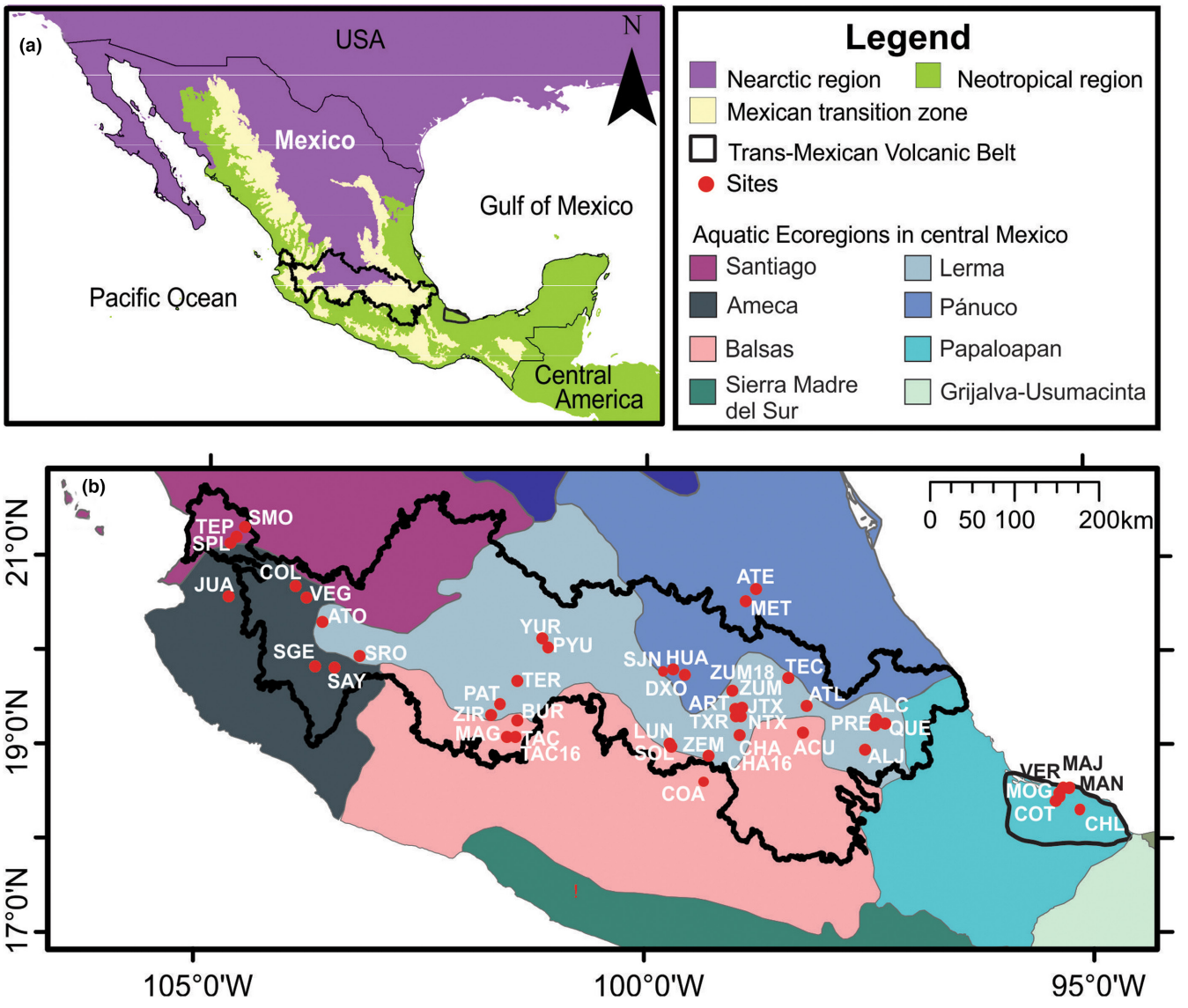

FIGURE 1 Location maps. (a) the Trans-Mexican Volcanic Belt (TMVB) in central Mexico as part of the transition zone between the Nearctic and the Neotropical realms. (b) Location of the study sites along the six basins that converge in the TMVB, abbreviations and full names as listed in Table S1.

sampling and included pH, electric conductivity, salinity expressed as total dissolved solids (TDS), alkalinity, ionic dominance expressed as ion relative abundances ([% Ca^{2+}], [% Mg^{2+}], [% Na^{+} + % K^{+}]; [% HCO_3^{-} + % CO_3^{2-}], [% Cl^{-}], [% SO_4^{2-}]) and Secchi disk depth (Sigala et al., 2017). Trophic status-related variables were determined only for a subset of 42 lakes; these data included total phosphorus (TP), soluble reactive phosphorus (SRP), dissolved inorganic nitrogen (DIN: ammonium + nitrites + nitrates) and chlorophyll-*a* concentrations (Chl*a*).

The data set also included diatom taxa relative abundances (%) based on diatom counts of a minimum of 100–300 valves from 49 surface sediment samples collected from the 46 study lakes (three lakes were sampled twice in different years). Surface sediment samples were collected using an Ekman dredge from a central area in each lake, retrieving only the top ~1 cm of sediment (Sigala et al., 2017). For diatom analyses, 0.5 g dry sediment was treated with (10%) hydrochloric acid (HCl) to eliminate carbonates and (30%) hydrogen peroxide (H_2O_2) to eliminate organic matter (if necessary, concentrated nitric acid [HNO_3] was used to accelerate organic matter elimination). Permanent slides were prepared with 200–µl aliquots of final solution using Naphrax (Brunel Microscopes Ltd). The species with the largest regional occupancy in the dataset were identified using a frequency of occurrence versus mean relative abundance graph. Frequency of occurrence was determined as the percentage of the sites where each species was present and the mean abundance as the average of their relative abundances at the sites where they were present (sites with zero abundance were not considered). The Continental Algae Data Base (bdLACET; Novelo & Tavera, 2021) was used to verify if diatom species had been reported previously for Mexico.

2.3 | Diatom diversity measurements

The sampling efficiency of the species diversity studied in each lake was evaluated using rarefaction-extrapolation curves and sample coverage tests with 50 bootstrap replicates to estimate 95% confidence intervals. These estimates were generated using the "iNEXT" package (v.2.0.20; Hsieh et al., 2016) in R (here and elsewhere in the paper: v.3.6.0; R Development Core Team, 2009). Three diversity metrics were used – species richness, Shannon diversity and Simpson dominance – which are part of the true diversities ${}^{q}D$ (Chao et al., 2014; Hill, 1973; Jost, 2007). Species richness is the number of taxa present in each sample (S) and is equivalent to Hill's effective number of species of order $q = 0$ (${}^{0}D = S$). Shannon diversity was estimated by Hill's effective number of species of order $q = 1$ (${}^{1}D$) which is based on Shannon index (${}^{1}D = \exp H'$) and represents the number of evenly distributed species in a sample. Simpson dominance was estimated by Hill's effective number of species of order $q = 2$ which is the reciprocal of the Simpson index (${}^{2}D = 1/D$) and represents the number of dominant species in a sample which can fluctuate between 1 (highest dominance) and ${}^{0}D$. In addition, alpha, gamma and beta diversities were estimated (Jost, 2007); alpha diversity is the average species richness in the samples ($\alpha = {}^{0}D_{avg}$), whereas gamma diversity is the species richness in the full dataset ($\gamma = {}^{0}D_{tot}$). Beta diversity ($\beta_w = \gamma/\alpha$) (Whittaker, 1960) shows how many times larger is the total diversity compared to the average diversity per site and represents the number of different communities in the studied area. Beta diversity reflects the biological complexity of the region, it is lowest when one community dominates the landscape, so minimal species turnover between sampling units is expected, and it increases as the communities share a lower number of species in the landscape (Jost, 2007), whether this is related to species turnover (replacement) or nestedness (reduction in the number of species). The turnover (β_{SIM}) and nestedness (β_{SNE}) components of the beta diversity were estimated based on an absence/presence matrix and Sørensen dissimilarities, using the "betapart" package (Baselga & Orme, 2012) in R (version 3.6.0, R Development Core Team, 2009). Besides, to evaluate if species richness reduced with altitude, a Pearson's linear correlation coefficient was estimated between species richness (${}^{0}D$) and altitude using the program PAST v.2.17 (Hammer et al., 2001).

2.4 | Diatom species distribution analyses

Groups of lakes with similar diatom compositions were identified through a cluster analysis with the unweighted pair group method with arithmetic mean (UPGMA) using the Pearson's correlation coefficient as distance measurement. A bubble plot was generated for the lake groups and the 89 most abundant diatom taxa (>5% in at least one sample). The cluster analysis was performed using "factoextra" (v.1.0.7; Kassambara & Mundt, 2020) and "vegan" (v.2.5.5; Oksanen et al., 2019) packages and the bubble plot was generated using the "rioja" package (v.0.9.21; Juggins, 2019) in R (version 3.6.0, R Development Core Team, 2009).

In order to explore the relation between diatom species distribution and environmental gradients a canonical correspondence analysis (CCA) was performed (ter Braak, 1986) for the subset of samples for which all the variables are available. The variables (except for pH) and relative diatom abundances were transformed ($\log_{10}+1$) to improve the linearity and homogeneity of variances, and the "downweight" function was used to reduce the influence of rare species. A series of partial CCAs were run to explore the importance of each variable at explaining diatom distribution. A Pearson's linear correlation matrix (Table S2) was generated to identify groups of highly related variables amongst which one was selected to reduce redundancy, and in this way the following variables were chosen: lake area, sample depth, AAT, AAP, AAE, TDS, pH, [% HCO_3^- + % CO_3^{2-}], [% Mg^{2+}], SRP, DIN, Chl*a* and Secchi disk depth. In previous analyses (Caballero et al., 2019; Sigala et al., 2017), two high-altitude sites (El Sol and La Luna, 4,283 m above sea level [asl]), located in the crater of the Nevado de Toluca volcano, were identified as outliers in the temperature gradient and for this reason they were excluded from the CCA. Besides, two lakes (Atotonilco and Sayula) showed very low diatom counts (<100 valves), and also were excluded; therefore, the CCA analysis was run using a subset of 38 samples. A Monte Carlo permutation test (999) was used to determine the statistical significance of the CCA. These analyses were performed using the "vegan" package (v.2.5.5; Oksanen et al., 2019) in R (version 3.6.0, R Development Core Team, 2009). Besides, to provide a reference for future palaeoenvironmental reconstructions, the optima and distribution ranges for salinity (TDS) and temperature (AAT) were calculated for the 89 most abundant taxa by means of weighted averaging regression and calibration (Birks et al., 1990) using the "optimos.prime" package (v.0.1.2; Sathicq et al., 2020) in R (version 3.6.0, R Development Core Team, 2009).

Finally, a graphical representation of the ecological environment of the TMVB was generated by using the temperature (Bio1) and precipitation (Bio12) variables from the Worldclim project (www.worldclim.com; Hijmans et al., 2005) extracting 100,000 random points for the whole of Mexico of which 4,500 correspond to the TMVB (including the "Los Tuxtlas" region in the Papaloapan basin) using the "raster" package (v.3.4.5, Hijmans et al., 2020) in R (version 3.6.0, R Development Core Team, 2009). The studied sites were overlaid on this graph to show their representativeness of the ecological envelope that characterises the TMVB.

3 | RESULTS

3.1 | Characteristics and environmental gradients in the studied lakes

Most of the lakes (22) belonged to the Lerma ecoregion, six to the Papaloapan, five to each of the Pánuco, Ameca and Balsas basins, and three to the Santiago basin (Figure 1b). The lakes had areas that

ranged from 1.3 to 17,000 ha and depths from less than 0.5 to 65 m (Figure 2a). Most of them, particularly the larger ones (>1,000 ha), were shallow (<10 m). Only 15 were deeper than 10 m and these were mostly volcanic craters (Alberca de Tacámbaro, Manantiales, Quechulac, Chalchoapan, La Preciosa, Aljojuca, Majahual, Alchichica and Santa María del Oro). The studied lakes covered a wide range of altitudes and climatic conditions (Figure 2b), altitude and AAT ranged from 4,283 m asl and 3.9°C in the lakes El Sol and La Luna, in the crater of the Nevado de Toluca volcano, to ~120 m asl and 25.7°C in the sites from "Los Tuxtlas" in the Papaloapan basin (Colorada, Chalchoapan, Manantiales, Majahual, Mogo and Verde). Annual average precipitation also had a wide range of variability from <400 mm yr^{-1} in Alchichica, La Preciosa and Quechulac, to ~2,500 mm yr^{-1} in the "Los Tuxtlas" lakes. The hydrochemistry of the lakes was very diverse (Figure 2c; Table S1). For example pH ranged from 6.3 to 9.6, salinity (TDS) from 20 to 28,427 mg L^{-1} whereas ionic composition ranged from [% HCO_3^-] – [% Ca^{2+}] ~ [% Mg^{2+}] ~ [% Na^+] in the freshwater lakes (TDS < 500 mg L^{-1}; categories defined in Figure 2c) to [% Cl^-] ≥ [% CO_3^{2-}] – [% Na^+] dominance in the higher salinity sites (TDS > 3,000 mg L^{-1}), following an evaporative concentration and carbonate precipitation pattern (Sigala et al., 2017). Only the lakes from the "Los Tuxtlas" (Colorada, Verde, Majahual, Mogo, Manantiales and Chalchoapan), had low salinities but high [% Cl^-]; this can be explained by their geographical proximity to the Gulf of Mexico.

The lakes also covered a wide range of nutrient concentrations, with SRP ranging from <0.01 to 366 µM and DIN from <0.1 to 305 µM (Figure 2d; Table S1). In terms of their trophic status, based on their Chl*a* concentrations (categories defined in Figure 2d), they ranged from ultra-oligotrophic (Chl*a* = 0.3 mg m^{-3}) Lake La Luna to hypertrophic sites such as Texcoco-Nabor Carrillo (Chl*a* = 670 mg m^{-3}), Chalco (265 mg m^{-3}), Zumpango (247 mg m^{-3}) or Alberca de Teremendo (245 mg m^{-3}). Most of the lakes were either hypertrophic or eutrophic (55%) and only five lakes (12%) were oligotrophic (El Sol, La Preciosa, Quechulac, Zirahuén) or ultra-oligotrophic (La Luna). According to the limiting thresholds established for SRP and DIN by Reynolds (1999) (Figure 2d), at the moment of sampling eight lakes showed P-limitation (La Preciosa, Alberca de Tacámbaro-2016, Danxhó, La Huaracha, Zempoala, Alberca de Teremendo, Atezca, and La Luna), seven had N-limitation (Alchichica, Manantiales, Majahual, Alberca de Tacámbaro, Juanacatlán, Piscina de Yuriria, and Santa María del Oro), and two had P- and N-co-limitation (El Sol and Zirahuén).

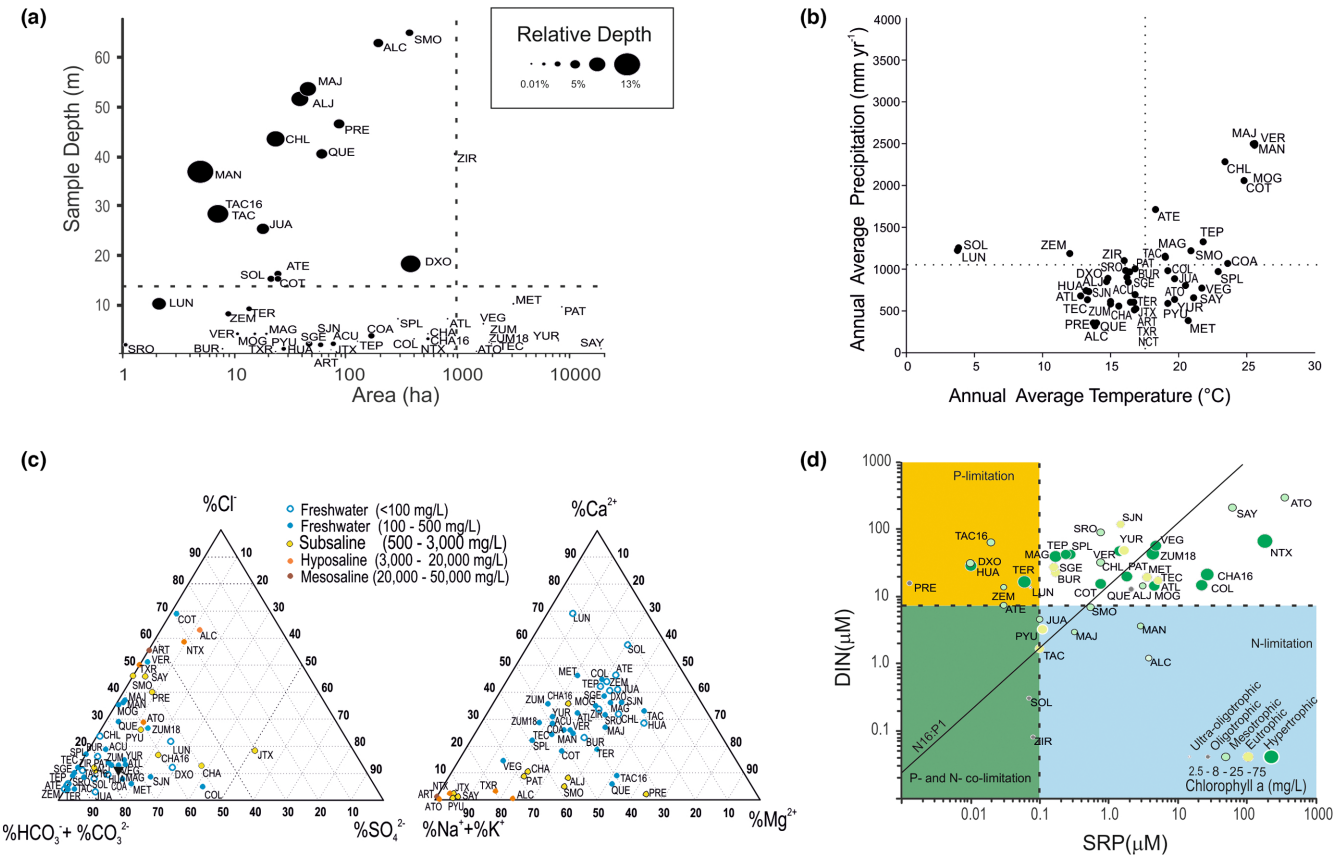

FIGURE 2 Characteristics of the study lakes: (a) morphometric parameters (area, depth and relative depth), dotted lines represent average values; (b) climatic parameters (average annual temperature vs. total annual precipitation), dotted lines represent average values; (c) ionic dominance and salinity, salinity categories adapted from Fritz (2007); (d) soluble reactive phosphorus (SRP), dissolved inorganic nitrogen (DIN) and chlorophyll-*a* concentrations in surface waters. Dotted lines denote nutrient starvation limits according to Reynolds (1999) (SRP <0.1 µM, DIN <7 µM), diagonal line denotes the Redfield N16:P1 relationship and trophic categories are according to OECD (1982).

3.2 | Diatom species composition and distribution

A total of 184 diatom taxa were recorded (the full taxonomic and alphabetical lists including abbreviations are in Tables S3 and S4), of which 18 (10%) represent first reports for Mexico (Novelo & Tavera, 2021). From the total, only 21 taxa (11.4%) were present in >10 lakes (>20% of sites) and only eight (4% of total) also had high mean relative abundances (>10%) (Figures 3 and 4). These eight high occupancy taxa were distributed in the Coscinodiscophyceae: *Aulacoseira ambigua*, *Aulacoseira granulata*, *A. granulata* var. *angustissima*; Mediophyceae: *Stephanocyclus meneghinianus* (formerly *Cyclotella meneghiniana*), *Discostella stelligera*; and Bacillariophyceae, subclasses Fragillariophycidae: *Fragilaria crotonensis*, and Bacillariophycidae: *Achnanthidium minutissimum* and *Nitzschia frustulum*. Besides, 17 taxa (9%) also had high mean relative abundances (>10%), even though they were present in fewer sites (<20%), whereas 146 taxa (79%) were considered as rare, as they were present in lower abundances and in fewer sites (Figure 3).

Three of the taxa (1.6%) were identified as endemic: *Cyclotella alchichicana* is endemic to Lake Alchichica (Oliva et al., 2006), and the two species from the Nevado de Toluca high-altitude lakes identified as *Navicula* NTA and *Sellaphora* (*Navicula*) NTB in Caballero (1996), are endemic to these lakes (El Sol and La Luna), as they have not been reported from any other sites. In addition to these, 14 taxa (7.6%; listed in Tables S3 and S4) could not be assigned to any described species, and they might represent new and probably also endemic taxa for the region. The 14 unidentified taxa were rare, except for two *Cyclostephanos* spp. from Lake Metztitlán.

3.3 | Diatom diversity

The rarefaction curves and the sample coverage tests showed that the diatom counts performed gave a good representation of the species inventory for the studied sites, with a minimum coverage of 0.94 of the expected species richness (Figure S5). Diatom valves were present in the sediments from all of the studied sites; however, in two (Atotonilco and Sayula), valve counts were <100, and in another two lakes (Pátzcuaro and Texcoco-*Artemia*) counts were <200, low valve counts were a consequence of a low diatom valve concentration in the sediments, most likely related to high erosion rates around these lakes. In the rest of the lakes counts were >200 valves.

The gamma diversity (γ) of the dataset is defined by the total species richness (184 taxa), whereas the species richness per site (^0D) ranged from 3 to 28 taxa, with an average (α diversity) of nearly 16 species (α _ 15.6); the lakes with the highest species richness ($^0D > 25$) were Chalco, Atlangatepec, Zempoala and Tecocomulco, whereas those with the lowest ($^0D < 10$) were Texcoco-*Artemia*, La Luna, Texcoco-Nabor Carrillo and Danxhó (Figure 5). The average Shannon diversity (^1D) was of nearly six effective species per site ($^1D_{avg} = 5.7$, range 1.4–12.3), whereas the average Simpson diversity (^2D) was of four dominant species per site ($^2D_{avg} = 3.9$, range 1.1–9.4) (Figure 5). The sites with the highest Shannon and Simpson diversities were Burro, Chalchoapan, Alchichica, Tecocomulco and Atlangatepec, whereas those with the lowest were Juanacatlán, Texcoco-*Artemia*, Alberca de Tacámbaro, Santa Rosa and Colorada Ver. The beta diversity was of nearly 12 effective assemblages in the area ($\beta_w = 11.8$), with a high turnover component ($\beta_{SIM} = 0.97$, $\beta_{SNE} = 0.01$). The species richness (^0D) showed no significative correlation with altitude ($r = 0.05$ $p = 0.7$).

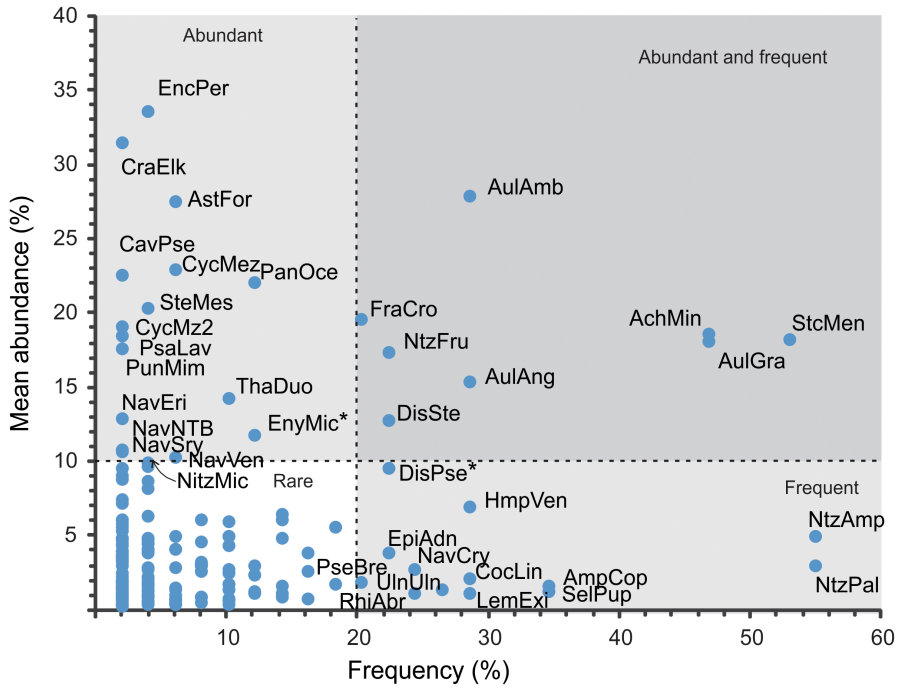

FIGURE 3 Regional occupancy diagram of species in the central Mexico dataset. Frequent species were present in >20% of the sites, abundant species had mean abundances >10%. Species full names, authorities and abbreviations are presented in Tables S3 and S4.

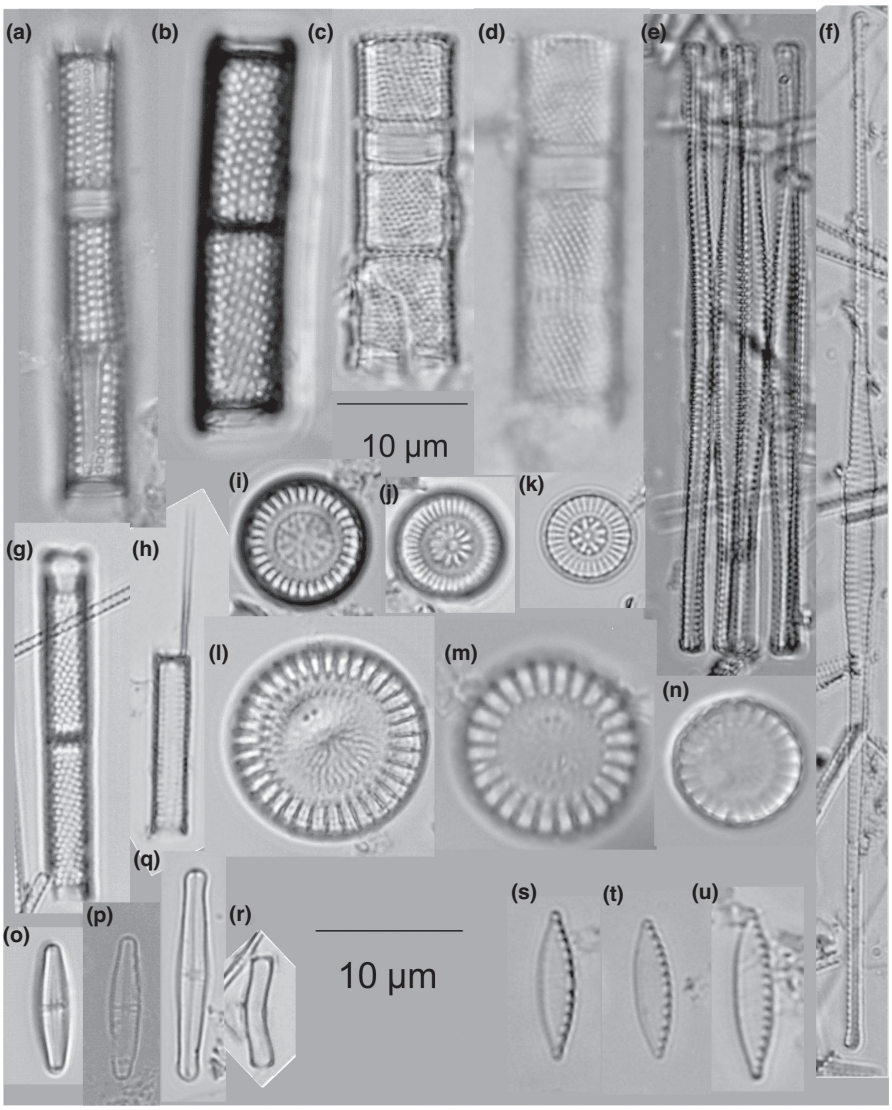

FIGURE 4 Plate showing the eight high regional occupancy diatom taxa in the lakes from central Mexico: (a, b) *Aulacoseira granulata*; (c, d) *A. ambigua*; (e, f) *Fragilaria crotonensis*; (g, h) *A. granulata* var. *angustissima*; (i–k) *Discostella stelligera*; (l–n) *S. meneghinianus*; (o–r) *Achnanthidium minutissimum*; and (s–u) *N. frustulum*

3.4 | Diatom species distribution

The cluster analysis divided the study sites into nine groups (branching distance = 0.90) and a total of 13 subgroups (branching distance = 0.85) that had characteristic diatom assemblages (Figure 6). Group 1 included the two high-altitude sites El Sol and La Luna where diatoms such as *Encyonema perpusillum*, *Cavinula pseudoscutiformis*, *Psammothidium levanderi* and *Navicula* (*Sellaphora*) NTB were abundant. Four individual lakes formed groups 2 to 5: Alchichica, Tecocomulco, Mogo and Piscina de Yuriria. These lakes separated from the rest of the sites because of their unusual diatom assemblages; in two of these lakes some of their diatom species were absent from other sites, for example *Cyclotella choctawhatcheeana* and *Cyclotella alchichicana* were present only in lake Alchichica (Group 2), whereas *Craticula elkab* was present only in Piscina de Yuriria (Group 5). The other two lakes had unusually high abundances of some species like *Cocconeis placentula* in Lake Tecocomulco (Group 3) or *Discostella pseudostelligera* in Lake Mogo (Group 4).

Group 6a included the only two samples (Zirahuén and Alberca de Tacámbaro in 2016) where *Pantocsekiella ocellata* was abundant and Group 6b included the low-altitude, high-temperature sites at "Los Tuxlas" and Alberca de Tacámbaro, where *A. minutissimum* was abundant. Group 7 included lakes with low salinities (<200 mg L^{-1}) where *Discostella stelligera* (7a) and *A. ambigua* (7b) were abundant, whereas Group 8 included the higher salinity sites (mostly ≥500 mg L^{-1}) in the dataset where the most common taxa were *N. frustulum* (8a), *S. meneghinianus* and *Nitzschia amphibia* (8b). Group 9 included lakes with intermediate salinities (~200 to ~500 mg L^{-1}) where *A. granulata*, *A. granulata* var. *angustissima* (9a), *F. crotonensis* or *Asterionella formosa* (9b) were abundant. These 13 lake groups and their characteristic diatoms species were in general in good agreement with those identified in the previous survey by Davies et al. (2002).

In the CCA (Figure 7) the first two axes explained 14.0% of the total variance and Monte Carlo permutation tests indicated that they were highly significant ($p < 0.001$). The variance inflation factors (VIF) of all variables were low (<6) indicating a low correlation

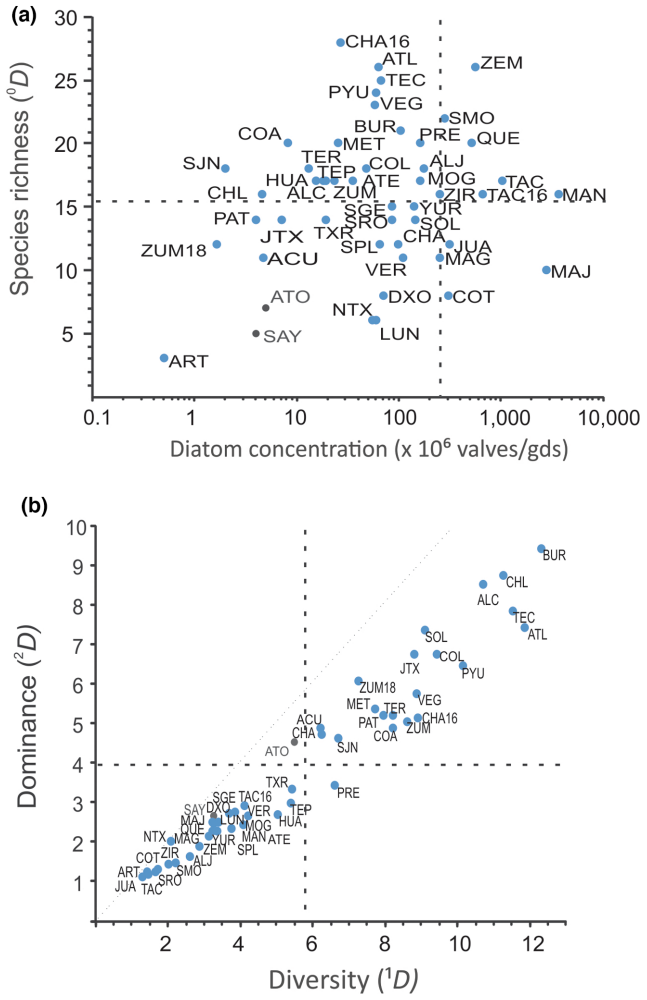

FIGURE 5 Diatom true diversities (^1D) and (^2D) from 49 surface sediment samples from central Mexico. Dotted lines represent average values. Green dots correspond to sites with the lowest species richness ($^0D < 10$) and orange dots to sites with the highest species richness ($^0D > 25$)

between them and the most important environmental variable (longest arrow) was TDS (Figure 7a). The partial CCAs showed that the variables that had a higher significance in explaining diatom distribution in the dataset ($p < 0.001$) were TDS, AAT, AAP, sampling depth and SRP. Axis 1 ($\lambda = 0.58$, $p < 0.001$, proportion explained = 7.9%) correlated negatively with TDS and pH and positively with AAP and [% HCO_3^- + % CO_3^{2-}], whereas axis 2 ($\lambda = 0.45$, $p < 0.001$, proportion explained = 6.1%) correlated positively with sampling depth and AAT and negatively with SRP, DIN, Chla and lake area. In the axis 1 versus axis 2 plot, the groups of sites formed in the cluster analysis were easily identified (except for Group 1 as the lakes from the Nevado de Toluca were excluded). The sites and species from Group 8 correlated with high salinity and high SRP as they plotted to the bottom left of the diagram, whereas those from groups 2 and 5 correlated to high salinities but lower SRP levels and were located to the top left of the diagram. Sites and species in groups 3, 9 and 7 were associated to lower, intermediate salinities, and they were towards the centre (groups 3 and 9) and right (Group 7) of axis 1. Species and lakes in these groups were distributed along axis 2 according to increasing DIN concentrations. Finally, the sites and species in groups 4 and 6, associated to low salinity, but also to high temperature and high precipitation, plotted to the top right of the diagram.

The WA optima of the 89 most abundant taxa were estimated for two of the most important environmental gradients identified in the CCA (longest arrows), salinity (TDS) and temperature (AAT) (Table S6); these variables were selected because they also were of relevance for palaeoenvironmental reconstructions. These estimates will be a useful reference for future diatom based palaeoclimatic and palaeolimnological studies, mostly when transfer functions are not possible as a result of the high abundance of extinct taxa. The values for the 38 most abundant and frequent taxa are presented in Figure 8. Amongst these, the species that had the highest optima in the TDS gradient were from groups 2, 5 and 8. Those with the lowest TDS optima were mostly from Group 1, but also from groups 6a, 7 and 9b. Along the temperature gradient, on the one hand the species with the highest (warmer) optima were mostly from groups 4 and 6b, and on the other, the species with the lowest (cooler) optima were mostly from groups 1 and 9b.

The lakes that were selected for this study cover most of the environmental variability within the ecological envelope of the TMVB (Figure 9). Lakes in groups 6, 7 and 9 are representative of temperate climates (12–23°C AAT), with a precipitation range from ~600 to 1,200 mm $year^{-1}$, which can be considered typical of the TMVB conditions. By contrast, the saline lakes in groups 2, 5 and 8 concentrated towards the lower precipitation extreme, whereas the lakes from "Los Tuxtlas" (Group 6), on the wetter (AAP ≥2000 mm y^{-1}) and warmer (AAT ~25°C) conditions along this ecological space. The high-altitude lakes in the Nevado de Toluca, El Sol and La Luna (Group 1), clearly represent marginal conditions in this ecological space, corresponding with the coldest climates (AAT < 10°C).

4 | DISCUSSION

In this work diatom diversity was explored from surface sediment samples collected from lakes along the TMVB. These kinds of samples have several advantages and disadvantages for this kind of analyses. On the one hand, they are not only low-cost and technically easy to collect, but also integrate diatoms across time and space offering a good representation of planktic, periphytic and benthic habits, allowing inclusion of taxa that might have a restricted temporal distribution (Battarbee et al., 2002). On the other hand, taphonomic factors could cause frustule fragmentation and dissolution (Battarbee et al., 2005) and variable sedimentation rates between the studied sites could bias species richness estimates as the time window represented by each sample will be different (Smol, 1981). However, the rarefaction curves suggest that our data were adequate and recorded at least 94% of species richness. Our results showed a diatom flora with a species richness of 184 taxa (γ diversity), which certainly represents a minimum for the region. This number constitutes about 16% of the overall diatom species richness in

Mexico according to a survey by Novelo and Tavera (2011), in which a total diatom species richness of 1,160 taxa was estimated for the country. This might seem a low representation, but it has to be taken into account that the present study only included lentic systems from a restricted region in Mexico (the TMVB), whereas the work from Novelo and Tavera (2011) included all continental habitats across

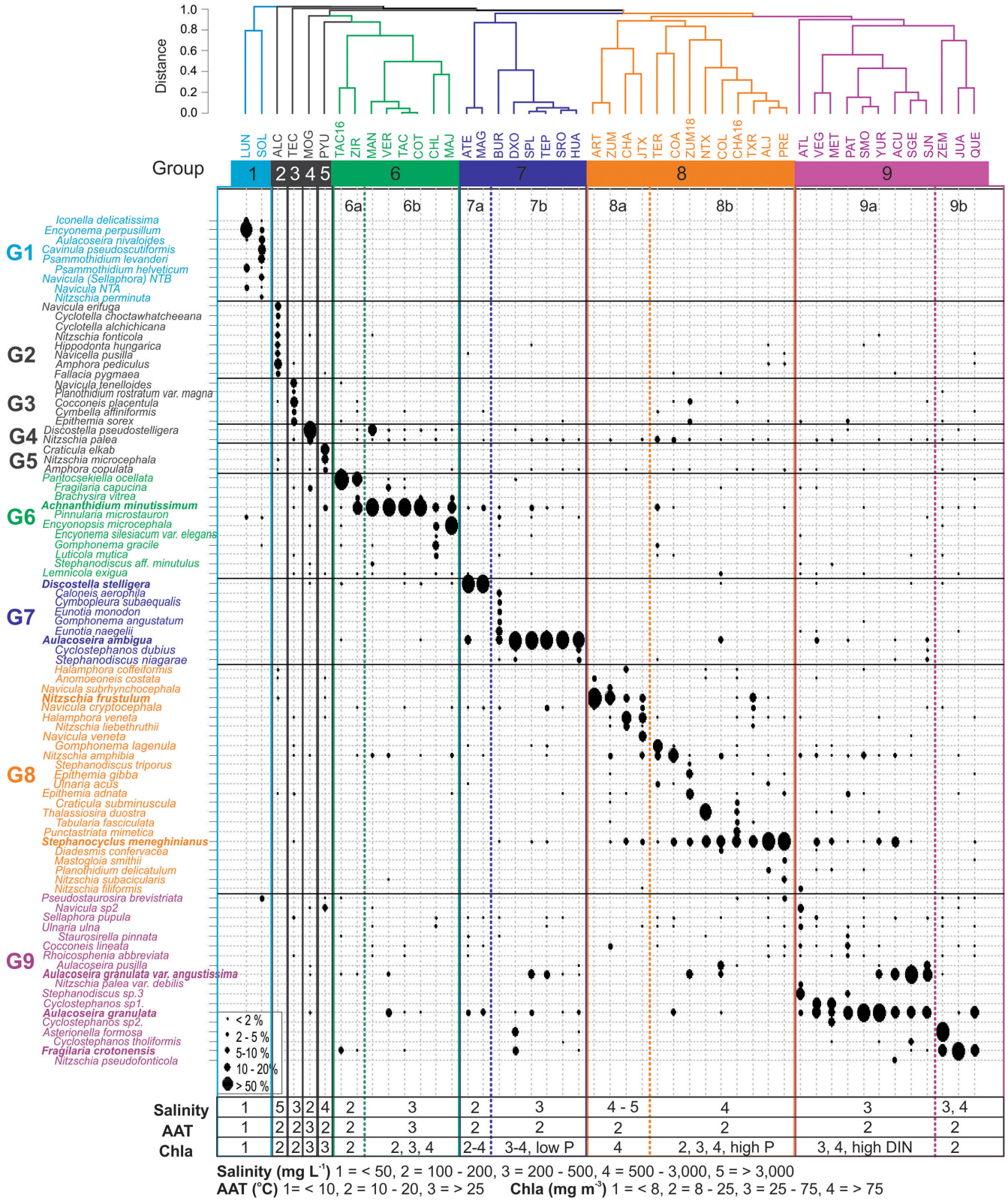

FIGURE 6 Cluster analysis and diatom species (>5%) distribution in 47 surface sediment samples from lakes in Central Mexico. In bold are the eight most abundant and frequent taxa in the dataset and indented taxa represent rare species. Site full names and abbreviations are listed in Table S1.

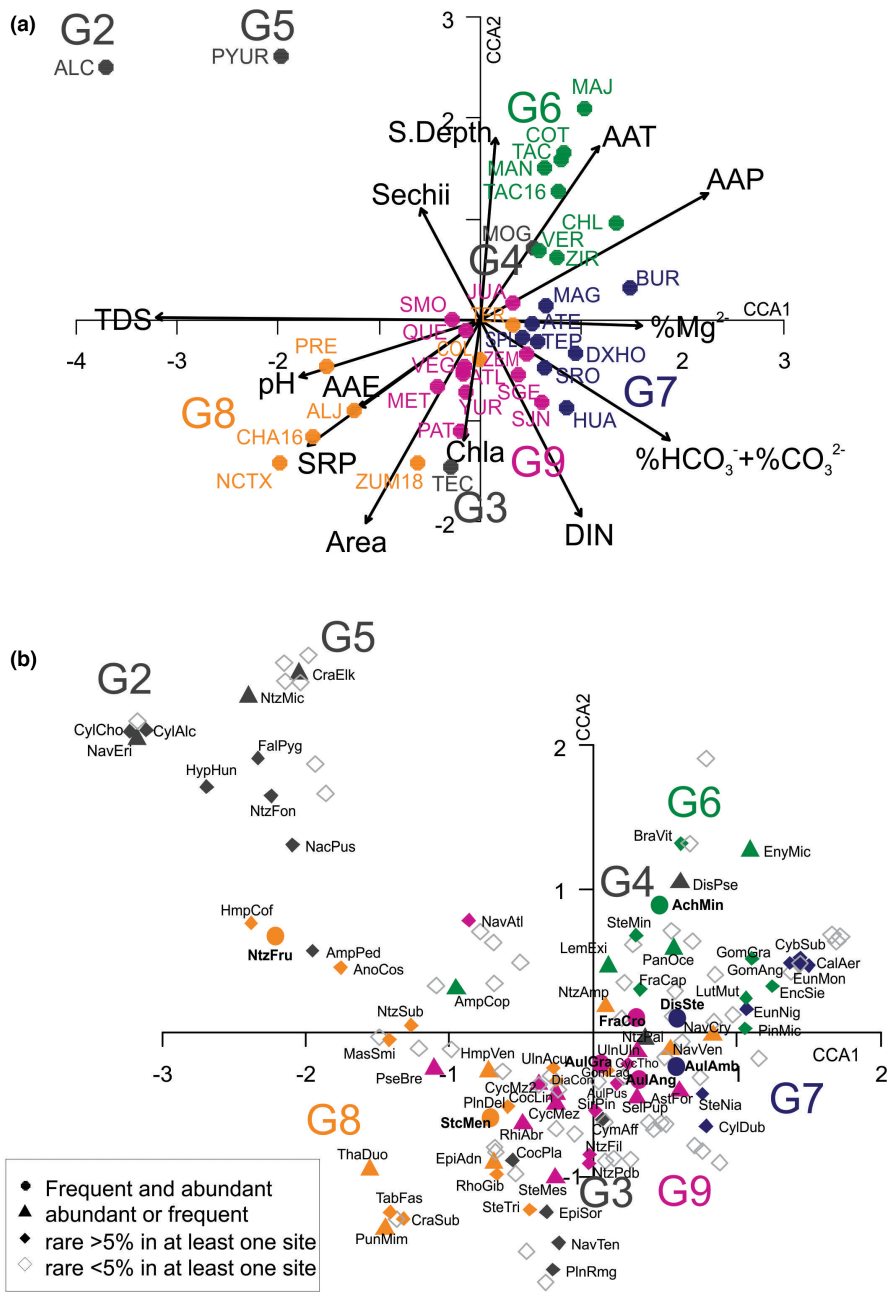

FIGURE 7 Canonical correspondence analysis (CCA, axis 1 vs. axis 2) for morphometric, hydrochemical, environmental and trophic state related variables and diatom species relative abundances from 38 samples in the Trans-Mexican Volcanic Belt: (a) sites plot; (b) species plot. G = groups as identified in the cluster analysis in Figure 6. AAE, annual average evaporation; AAP, annual average precipitation; AAT, annual average temperature; area, lake area; S. depth, sampling depth; SRP, soluble reactive phosphorus;TDS, total dissolved solids. Species full names and codes are in Tables S3 and S4.

the country (e.g., rivers, sub-aereal environments, lagoons, lakes.). If we compare our data to similar surveys based on surface sediment samples from lakes in the region, the γ diversity found in the present work is similar. For example, Davies et al. (2002) reported 186 taxa in a survey that included 53 surface sediment samples from 31 lakes in central Mexico; Pérez et al. (2013) reported 282 diatom taxa for a set of 63 lakes in Yucatán, Belize, and Guatemala, and Haberyan et al. (1997) reported 140 taxa from 25 sites in Costa Rica.

Amongst the diatom taxa present in the region, our analyses identified only three (1.6%) that were endemic, restricted to lakes that clearly represented extremes in the climatic envelope of the TMVB: the hyposaline lake Alchichica and the high-altitude, low pH, and low-salinity lakes in the Nevado de Toluca. Contrary to what was expected, these endemic taxa included one planktic form (*C. alchichicana*), and two epipelic, motile forms (*Navicula* NTA and *Sellaphora* NTB), which are life forms considered to have a high dispersal potential (Benito, Fritz, Steinitz-Kannan, Tapia, et al., 2018), allowing us to speculate that these endemic taxa were constrained mostly by environmental filtering rather than by dispersal limitation. Our analysis also identified eight taxa with a high regional occupancy that can be considered representative of the lacustrine ecosystems of the TMVB. Six had a planktonic habit, whereas one (*N. frustulum*) was an epipelic, motile taxon, again life forms considered to have a high dispersal potential, but in this case this agrees with their cosmopolitan distributions. The habit of *A. minutissimum* is somewhat unclear; it is mostly considered a low-profile, benthic form, even though our previous work suggests that it has some capacity to incorporate into the planktic community as it was abundant in phytoplankton net

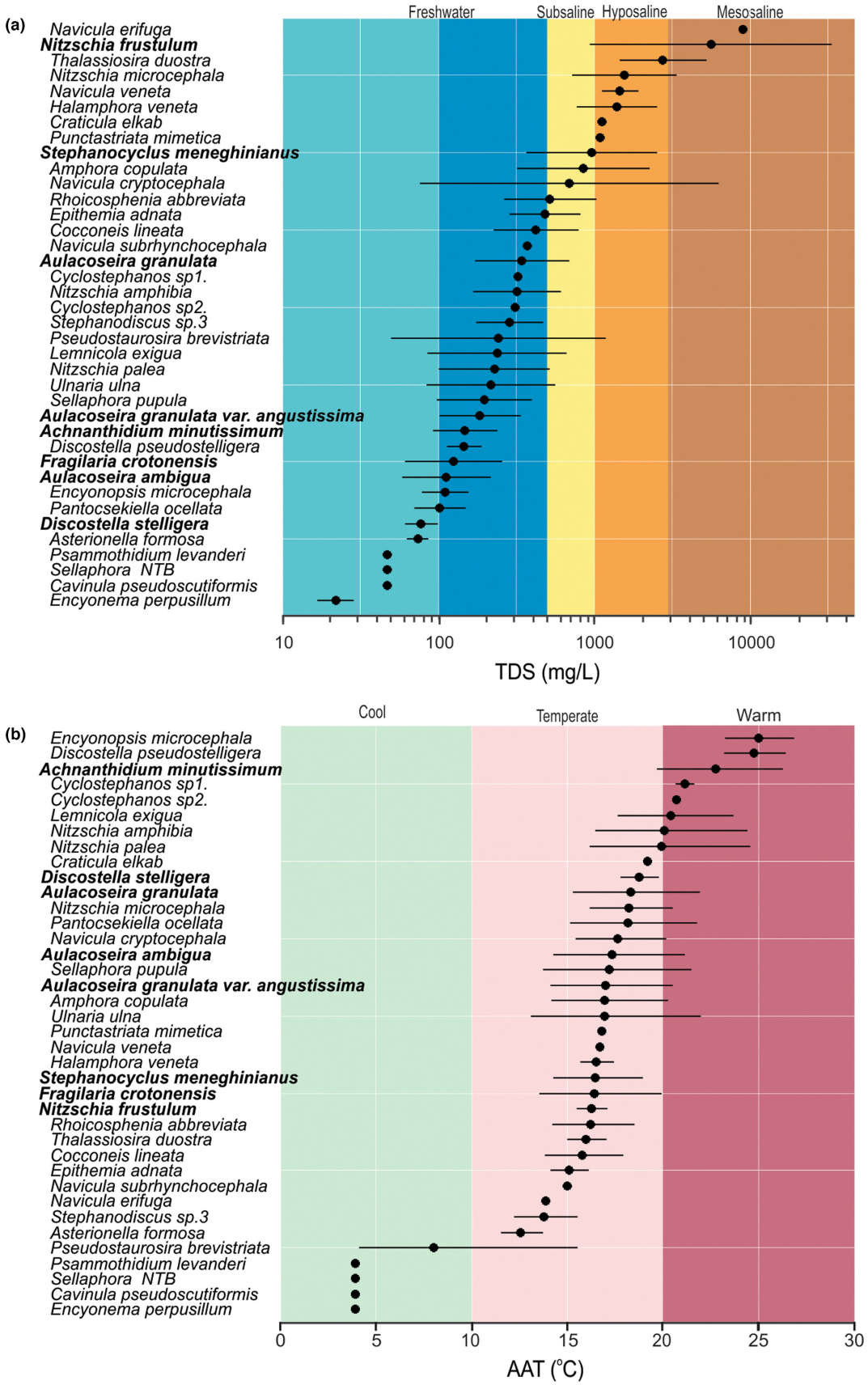

FIGURE 8 Optima and tolerance for (a) salinity (TDS) and (b) temperature (AAT) for the 38 most frequent and abundant taxa in the studied lakes from the Trans-Mexican Volcanic Belt. AAT, average annual temperature; TDS, total dissolved solids. In bold are the eight taxa with the largest regional occupancy.

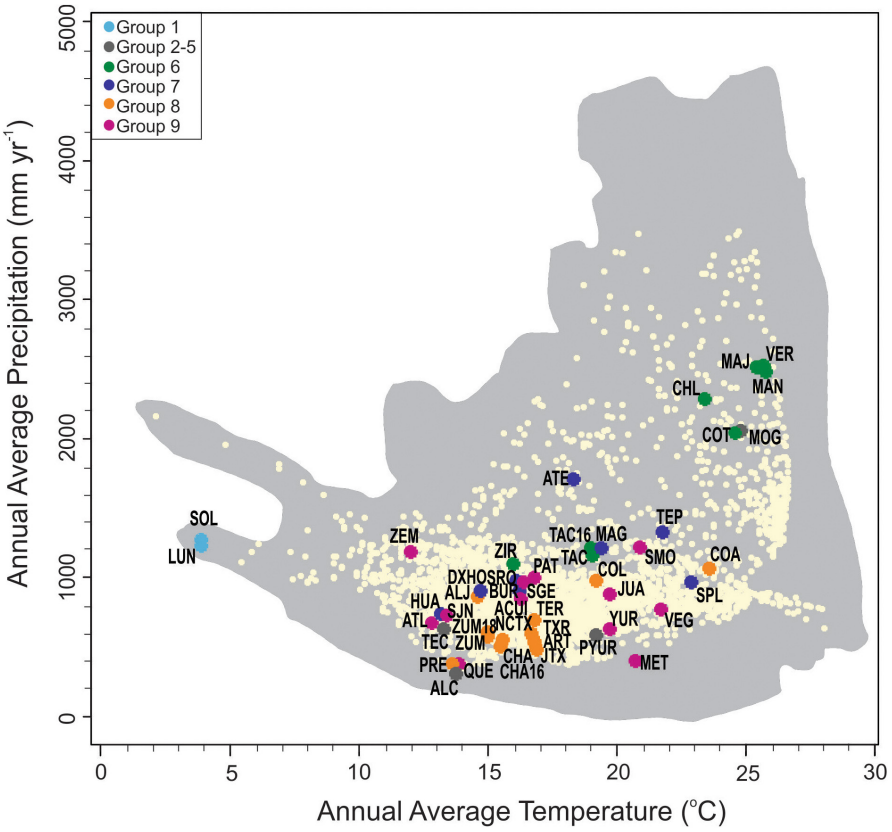

FIGURE 9 Distribution of the study sites along the ecological envelope of the Trans-Mexican Volcanic Belt (TMVB). Grey shaded area represent random points of temperature and precipitation along Mexico and clear dots correspond to random points along the TMVB.

samples in the deep (>20 m) lakes at "Los Tuxtlas" and in Alberca de Tacámbaro (Vázquez & Caballero, 2013). In any case this taxon also seems to have a high dispersal potential as it is one of the most frequently occurring diatoms in freshwater environments around the world (Potapova & Hamilton, 2007). The distributions of these cosmopolitan taxa along the salinity gradient show at least some level of niche conservation, as they have been reported in other regions of the world, including North America, Africa and Australia, with generally similar affinities towards saline or freshwater environments (Fritz et al., 1993; Gasse et al., 1995; Gell, 1997; Wilson et al., 1996). In central Mexico, *N. frustulum* (Groups 8a) and *S. meneghinianus* (formerly *C. meneghiniana*, Group 8b) were most abundant in the higher salinity environments along the TMVB, in accordance with findings from other saline lake surveys around the world (Fritz et al., 1993; Gasse et al., 1995; Gell, 1997; Reed, 1998; Wilson et al., 1996) where these taxa also were characteristic of high salinity environments. The WA optima showed that in central Mexico *N. frustulum* had a higher salinity distribution (hyposaline) than *S. meneghinianus* (subsaline). Besides, *S. meneghinianus* was present in lakes with a higher trophic status (eutrophic or hypertrophic) compared with *N. frustulum* (mesotrophic to eutrophic). However, the remaining six taxa were most abundant in the freshwater lakes along the TMVB, which also was in general agreement with their distribution in other regions of the world (Bicudo et al., 2016; Gasse et al., 1995; Potapova & Hamilton, 2007; Saros et al., 2005; Wilson et al., 1996). In central Mexico, *A. granulata* and *A. granulata* var. *angustissima* (Group 9a) had their highest abundances in freshwater (WA optima ≥ 200 mg L^{-1}) eutrophic lakes, whereas *Achnanthidium mintussimum* (Group 6) also was associated to freshwater (WA optima < 200 mg L^{-1}) eutrophic lakes, but in addition to warmer lake conditions. However, *A. ambigua* (Group 7b) and *D. stelligera* (Group 7a) preferred eutrophic lakes with a lower salinity (~100 mg L^{-1}), whereas *F. crotonensis* (Group 9b) showed an affinity for freshwater lakes (WA optima < 200 mg L^{-1}) with a lower trophic level (mesotrophic). Our data also showed that *A. ambigua* preferred slightly cooler conditions compared to *D. stelligera*.

The studied lakes covered a wide range of climatic conditions which are representative of the ecological envelope of the TMVB. Most interestingly, they covered an altitudinal range of nearly 4,000 m, which gave the opportunity to test whether diatom species richness reduced with increasing altitude as reported in other surveys (Benito, Fritz, Steinitz-Kannan, Vélez, & McGlue, 2018). Our data did not support this hypothesis as there was no relationship between richness and altitude. From our data it seems more likely that other factors common to higher altitude lakes, such as their lower pH or lower nutrient levels, might be determinant (Wang et al., 2011). For example, in our dataset, the two high-altitude lakes in the Nevado de Toluca showed contrasting species richness: Lake La Luna was effectively one of the lakes lower than average richness (6), but it was also the only ultraoligotrophic system and the lake with the lowest pH (6.3) in the dataset, and by contrast, Lake El Sol, a larger, oligotrophic lake, with higher pH (7.2), had an average richness (14).

Our data also showed that there were 13 distinctive diatom metacommunities controlled mostly by lake salinity (TDS), even though temperature (AAT), precipitation (AAP), depth and phosphorus

concentrations (SRP) also were relevant. Lake salinity, TP and lake depth are variables that have been identified in studies worldwide as important ecological controls for diatom distributions (Fritz, 2007; Juggings et al., 2013; Laird & Cumming, 2008). Nevertheless, our results highlight the importance of climatic variables, such as temperature or precipitation, which have been less studied, but that seem to be important controls of diatom species distribution when analysed at relatively large geographical scales (Benito, Fritz, Steinitz-Kannan, Tapia, et al., 2018; Caballero et al., 2019). Temperature, for example, was found as one of the most important factors controlling diatom species distributions in rivers in the United States, when analysed at a nation level, as the differences in climatic conditions between sites became more important than other environmental gradients (Potapova & Charles, 2002).

The 13 distinctive metacommunities that characterised the lacustrine environments in the TMVB were in very close agreement with the beta diversity, which predicted 12 effective diatom assemblages. There was a high species replacement between these metacommunities, reflected in the high Beta diversity turnover component (β_{sim} = 0.97) and also in the length of the CCA axes (>3 units). In the ecological space of the TMVB it is clear that these associations extend across the temperature gradient, from the coldest (Group 1) to the warmest (Group 6b) conditions, allowing for a complete species turnover between them. For the rest of the groups, there is a gradual transition along the climatic space and a partial species replacement. This can be visualised, for example by subgroups 8a (higher salinity) and 8b (lower salinity), where there is a gradual replacement between *N. frustulum*, *S. meneghinianus* and *N. amphibia* as conditions transition from higher to lower salinity. This also means that some species co-occur in more than one group, representing a considerable overlap in geographical distribution. Finally, we also found evidence that regional occupancy was related to niche breath and habitat availability (Heino & Soininen, 2006). The species that showed a low regional occupancy were limited to rarer habitat conditions in the region as the case of groups 1 to 5, 6a and 7a that were formed by one or two lakes with the presence of diatom taxa with narrower niche breaths that did not occur at other sites.

5 | CONCLUSIONS

The taxa in this study that showed a larger regional occupancy were mostly cosmopolitan, planktic or epipelic, motile taxa with high dispersal potential. Their general ecological distribution along the salinity gradient was similar to other regions of the world, pointing to some level of niche conservation. There were few endemic taxa, which unexpectedly were planktic or motile forms with high dispersal potential, suggesting that they were constrained mostly by environmental filtering rather than by dispersal limitations. There was no evidence of an altitude–diversity pattern like that found in other freshwater diatom studies. Instead, it seems more likely that factors such as lake size, salinity, pH, or nutrients might be determinants of species diversity.

This study encompassed the entire climatic envelope of the TMVB region and highlighted the importance of climatic variables in diatom species distribution when relatively broad geographical areas with large climatic gradients (temperature or precipitation) are analysed. The wide range of climatic conditions analysed reflected in a high species turnover driven mainly by lake salinity (TDS) but also related to temperature, precipitation, lake depth and phosphorus concentrations.

AUTHOR CONTRIBUTIONS

Conceptualisation: MC. Data analysis, preparation figures & tables, writing: MC, DA. Developing methods, conducting the research, data interpretation, writing: MC, DA, GV. MC conceptualisation, developing methods, conducting the research, data analysis, data interpretation, writing. DA conducting the research, data analysis, data interpretation, preparation figures & table, writing. GV developing methods, data interpretation, writing.

ACKNOWLEDGMENTS

We thank: Ma. Aurora Armienta and the staff in the Laboratorio de Quimica Análitica, Instituto de Geofisica, UNAM for major anions and SiO_2 analysis; Ariadna Martinez and Daniela Cela from the "Red de Ecología Funcional" laboratory at the Instituto de Ecología, A.C. (INECOL), Xalapa, Mexico, for the nutrients analysis.

FUNDIG INFORMATION

This research is part of grant UANAM-PAPIIT 100820 "Registros Interglaciares del Centro de México". Diana Avendaño thanks the Posgrado de Ciencias de la Tierra, UNAM and CONACyT (CVU 854736) for financial support.

CONFLICT OF INTEREST

The authors of this paper declare that there is no conflict of interest regarding the publication of this manuscript.

DATA AVAILABILITY STATEMENT

The data presented in this work are availabe upon request from the corresponding author and also from the "Diatomeas de México" and "Lagos de Méxcio" data bases at https://datosabiertos.unam.mx/.

ORCID

Caballero Margarita https://orcid.org/0000-0001-5691-0773

REFERENCES

Abell, R., Thieme, M. L., Revenga, C., Bryer, M., Kottelat, M., Bogutskaya, N., Coad, B., Mandrak, N., Contreras, B. S., Bussing, W., Stiassny, M. L. J., Skelton, P., Allen, G. R., Unmack, P., Naseka, A., Ng, R., Sindorf, N., Robertson, J., Armijo, E., … Petry, P. (2008). Freshwater ecoregions of the world: A new map of biogeographic units for freshwater biodiversity conservation. *Bioscience*, *58*(5), 403–414.

Avendaño, D., Caballero, M., & Vázquez, G. (2021). Ecological distribution of *Stephanodiscus niagarae* Ehrenberg in Central Mexico and niche modeling for its Last glacial maximum habitat suitability in

the Nearctic realm. *Journal of Paleolimnology*, *66*, 1–14. https://doi.org/10.1007/s10933-021-00178-w

Baselga, A., & Orme, C. D. L. (2012). Betapart: An R package for the study of beta diversity. *Methods in Ecology and Evolution*, *3*, 808–812. https://doi.org/10.1111/J.2041-210X.2012.00224.X

Battarbee, R. W., Jones, V. J., Flower, R. J., Cameron, N. G., Bennion, H., Carvalho, L., & Juggins, S. (2002). Diatoms. In J. Smol, H. J. Birks, W. Last, R. Bradley, & K. Alverson (Eds.), *Tracking environmental change using Lake sediments. Volume 3: Terrestrial, algal, and siliceous indicators* (pp. 155–202). Springer.

Battarbee, R. W., Mackay, A., Jewson, D., Ryves, D., & Sturm, M. (2005). Differential dissolution of Lake Baikal diatoms: Correction factors and implications for palaeoclimatic reconstruction. *Global and Planetary Change*, *46*(1–4), 75–86.

Benito, X., Fritz, S., Steinitz-Kannan, M., Tapia, P. M., Kelly, M. A., & Lowell, T. V. (2018). Geo-climatic factors drive diatom community distribution in tropical south American freshwaters. *Journal of Ecology*, *106*, 1660–1672. https://doi.org/10.1111/1365-2745.12934

Benito, X., Fritz, S. C., Steinitz-Kannan, M., Vélez, M. I., & McGlue, M. M. (2018). Lake regionalization and diatom metacommunity structuring in tropical South America. *Ecology and Evolution*, *8*(16), 7865–7878.

Bicudo, D. C., Tremarin, P. I., Almeida, P. D., Zorzal-Almeida, S., Wengrat, S., Faustino, S. B., Costa, L. F., Bartozek, E. C., Rocha, A. C., & Bicudo, C. E. (2016). Ecology and distribution of Aulacoseira species (Bacillariophyta) in tropical reservoirs from Brazil. *Diatom Research*, *31*(3), 199–215.

Birks, H. J. B., Line, J. M., Juggins, S., Stevenson, A. C., & Ter Braak, C. J. F. (1990). Diatoms and pH reconstruction. *Philosophical Transactions of the Royal Society of London B: Biological Sciences*, *327*, 263–278.

Caballero, M. (1996). The diatom flora of two acid lakes in Central Mexico. *Diatom Research*, *11*, 227–240. https://doi.org/10.1080/0269249X.1996.9705381

Caballero, M., Lozano-García, S., Ortega-Guerrero, B., & Correa-Metrio, A. (2019). Quantitative estimates of orbital and millennial scale climatic variability in Central Mexico during the last ~40,000 years. *Quaternary Science Reviews*, *205*, 62–75. https://doi.org/10.1016/j.quascirev.2018.12.002

Chao, A., Gotelli, N. J., Hsieh, T. C., Sander, E. L., Ma, K. H., Colwell, R. K., & Ellison, A. M. (2014). Rarefaction and extrapolation with Hill numbers: A framework for sampling and estimation in species diversity studies. *Ecological Monographs*, *84*, 45–67. https://doi.org/10.1890/13-0133.1

Davies, S. J., Metcalfe, S. E., Caballero, M. E., & Juggins, S. (2002). Developing diatom-based transfer functions for central Mexican lakes. *Hydrobiologia*, *467*, 199–213. https://doi.org/10.1023/A:1014971016298

De La Rey, P. A., Roux, H., Van Rensburg, L., & Vosloo, A. (2008). On the use of diatom-based biological monitoring part 2: A comparison of the response of SASS 5 and diatom indices to water quality and habitat variation. *Water SA*, *34*, 61–69. https://doi.org/10.4314/wsa.v34i1.180763

Fritz, S. C. (2007). Salinity and climate reconstruction from diatoms in continental lake deposits. In S. A. Elias (Ed.), *Encyclopedia of quaternary science* (pp. 514–522). Elsevier.

Fritz, S. C., Juggins, S., & Battarbee, R. W. (1993). Diatom assemblages and ionic characterization of lakes of the northern great plains, North America: A tool for reconstructing past salinity and climate fluctuations. *Canadian Journal of Fisheries and Aquatic Sciences*, *50*, 1844–1856. https://doi.org/10.1139/f93-207

Gasse, F., Juggins, S., & Khelifa, L. B. (1995). Diatom-based transfer functions for inferring past hydrochemical characteristics of African lakes. *Palaeogeography, Palaeoclimatology, Palaeoecology*, *117*(1–2), 31–54.

Gell, P. A. (1997). The development of a diatom database for inferring lake salinity, western Victoria, Australia: Towards a quantitative approach for reconstructing past climates. *Australian Journal of Botany*, *45*(3), 389–423.

Haberyan, K. A., Horn, S. P., & Cumming, B. F. (1997). Diatom assemblages from Costa Rican Lakes: An initial ecological assessment. *Journal of Paleolimnology*, *17*, 263–274. https://doi.org/10.1023/A:1007933130319

Hammer, Ø., Harper, D. A. T., & Ryan, P. D. (2001). Past: Paleontological statistics software package for education and data analysis. *Palaeontologia Electronica*, *4*, 1–9.

Heino, J., & Soininen, J. (2006). Regional occupancy in unicellular eukaryotes: A reflection of niche breadth, habitat availability, or size-related dispersal capacity? *Freshwater Biology*, *51*, 672–685. https://doi.org/10.1111/j.1365-2427.2006.01520.x

Hijmans, R. J., Cameron, S. E., Parra, J. L., Jones, P. G., & Jarvis, A. (2005). Very high resolution interpolated climate surfaces for global land areas. *International Journal of Climatology*, *25*, 1965–1978. https://doi.org/10.1002/joc.1276

Hijmans, R. J., Van Etten, J., Sumner, M., Cheng, J., Baston, D., Bevan, A., Bevan, A., Bivand, R., Busetto, L., Canty, M., Fasoli, B., Forrest, D., Ghosh, A., Golicher, D., Gray, J., Greenberg, J. A., Hiemstra, P., Hingee, K., Ilich, A., … Karney, C. (2020). *Package "raster": Geographic data analysis and modeling*. R package version 3.4–5. https://cran.r-project.org/web/packages/raster/index.html

Hill, E. L. (2006). *Quantitative reconstruction of eutrophication histories in central Mexican Lakes*. PhD Thesis, University of Nottingham, UK.

Hill, M. O. (1973). Diversity and evenness: A unifying notation and its consequences. *Ecology*, *54*, 427–432. https://doi.org/10.2307/1934352

Hsieh, T. C., Ma, K. H., & Chao, A. (2016). iNEXT: An R package for rarefaction and extrapolation of species diversity (Hill numbers). *Methods in Ecology and Evolution*, *7*, 1451–1456. R package version 2.0.20. https://doi.org/10.1111/2041-210X.12613

Jost, L. (2007). Partitioning diversity into independent alpha and beta components. *Ecology*, *88*, 2427–2439.

Juggings, S., Anderson, J., Ramstack, H. J., & Heathcote, A. (2013). Reconstructing epilimntic total phosphorus using diatoms: Statistical and ecoogical constraints. *Journal of Paleolimnology*, *49*, 373–390.

Juggins S. (2019). Package "Rioja": Analysis of quaternary science data. R package version 0.9–21. https://cran.r-project.org/web/packages/rioja/index.html

Julius, M. L., & Theriot, E. C. (2010). The diatoms: A primer. In J. P. Smol & E. F. Stoermer (Eds.), *The diatoms: Applications for the environmental and earth sciences* (pp. 8–22). Cambridge University Press.

Kassambara A. & Mundt F. (2020). Package "factoextra": Extract and visualize the results of multivariate data analyses. R packagee version 1.0.7. https://cran.r-project.org/web/packages/factoextra/index.html

Laird, K. R., & Cumming, B. (2008). Diatom-inferred lake level from near-shore cores in a drainage lake from the Experimental Lakes area, northwestern Ontario, Canada. *Journal of Paleolimnology*, *42*, 65–80.

Lobo, E. A., Heinrich, C. G., Schuch, M., Wetzel, C. E., & Ector, L. (2016). Diatoms as bioindicators in Rivers. In J. O. Necchi (Ed.), *River Algae* (pp. 245–271). Springer.

Metcalfe, S. E. (1988). Modern diatom assemblages in Central Mexico: The role of water chemistry and other environmental factors as indicated by TWINSPAN and DECORANA. *Freshwater Biology*, *19*, 217–233.

Morrone, J. J. (2020). A historical perspective of the Mexican transition zone. In J. J. Morrone (Ed.), *The Mexican transition zone* (pp. 69–101). Springer.

Novelo, E., & Tavera, R. (2011). Un panorama gráfico de las algas de agua dulce de México. *Hidrobiológica*, *21*, 333–341.

Novelo E. & Tavera R. (2021). bdLACET Base de datos de algas continentales. *Facultad de Ciencias*, *UNAM*. Retrieved from https://bdlacet.mx; searched on May 20, 2021.

J Oksanen, Gavin L. Simpson, F. Guillaume Blanchet, Roeland Kindt, Pierre Legendre, Peter R. Minchin, R.B. O'Hara, Peter Solymos, M. Henry H. Stevens, Eduard Szoecs, Helene Wagner, Matt Barbour, Michael Bedward, Ben Bolker, Daniel Borcard, Gustavo Carvalho, Michael Chirico, Miquel De Caceres, Sebastien Durand, Heloisa Beatriz Antoniazi Evangelista, Rich FitzJohn, Michael Friendly, Brendan Furneaux, Geoffrey Hannigan, Mark O. Hill, Leo Lahti, Dan McGlinn, Marie-Helene Ouellette, Eduardo Ribeiro Cunha, Tyler Smith, Adrian Stier, Cajo J.F. Ter Braak, James Weedon *et al.* (2019). Package "vegan": Community ecology package. R package version 2.5–5. https://cran.r-project.org/web/packages/vegan/index.html

Oliva, M. G., Lugo, A., Alcocer, J., & Cantoral-Uriza, E. A. (2006). *Cyclotella alchichicana* sp. nov. from a saline mexican lake. *Diatom Research*, *21*, 81–89. https://doi.org/10.1080/0269249X.2006.9705653

Organization for Economic Co-operation and Development (OECD). (1982). *Eutrophication of waters. Monitoring, assessment and control* (p. 152). Organization for Economic Cooperation and Development.

Pérez, L., Lorenschat, J., Massaferro, J., Pailles, C., Sylvestre, F., Hollwedel, W., Brandorff, G. O., Brenner, M., Islebe, G., Lozano, M. D. S., Scharf, B., & Schwalb, A. (2013). Bioindicators of climate and trophic state in lowland and highland aquatic ecosystems of the northern Neotropics. *Revista de Biología Tropical*, *61*, 603–644. https://doi.org/10.15517/RBT.V61I2.11164

Potapova, M., & Charles, D. F. (2002). Benthic diatoms in USA rivers: Distributions along spatial and environmental gradients. *Journal of Biogeography*, *29*, 167–187.

Potapova, M., & Hamilton, P. B. (2007). Morphological and ecological variation within the *Achnanthidium minutissimum* (Bacillariophyceae) species complex. *Journal of Phycology*, *43*, 561–575.

R Development Core Team. (2009). R: A language and environment for statistical computing, *R Foundation for Statistical Computing*. Version 3.6.0. https://www.R-project.org/

Reed, J. (1998). A diatom-conductivity transfer function for Spanish salt lakes. *Journal of Paleolimnology*, *19*(4), 399–416.

Reynolds, C. S. (1999). Non-determinism to Probability, or N:P in the community ecology of phytoplankton. *Archiv für Hydrobiologie*, *146*, 23–35. https://doi.org/10.1127/archiv-hydrobiol/146/1999/23

Saros, J. E., Michel, T. J., Interlandi, S. J., & Wolfe, A. P. (2005). Resource requirements of Asterionella formosa and *Fragilaria crotonensis* in oligotrophic alpine lakes: Implications for recent phytoplankton community reorganizations. *Canadian Journal of Fisheries and Aquatic Sciences*, *62*(7), 1681–1689.

Sathicq, M. B., Gelis, M. M. N., & Cochero, J. (2020). Calculating autoecological data (optima and tolerance range) for multiple species with the 'optimos.Prime' R package. *Austral Ecology*, *45*, 845–850. R package version 0.1.2. https://doi.org/10.1111/AEC.12868

Sigala, I., Caballero, M., Correa-Metrio, A., Lozano-García, S., Vázquez, G., Pérez, L., & Zawisza, E. (2017). Basic limnology of 30 continental waterbodies of the Transmexican Volcanic Belt across climatic and environmental gradients. *Boletín de la Sociedad Geológica Mexicana*, *69*, 313–370. https://doi.org/10.18268/bsgm2017v69n2a3

Smol, J. P. (1981). Problems associated with the use of "species diversity" in paleolimnological studies. *Quaternary Research*, *15*(2), 209–212.

Soininen, J., & Teittinen, A. (2019). Fifteen important questions in the spatial ecology of diatoms. *Freshwater Biology*, *64*(11), 2071–2083.

Stenger-Kovács, C., Buczkó, K., Hajnal, É., & Padisák, J. (2007). Epiphytic, littoral diatoms as bioindicators of shallow lake trophic status: Trophic diatom index for lakes (TDIL) developed in Hungary. *Hydrobiologia*, *589*, 141–154. https://doi.org/10.1007/S10750-007-0729-Z

Ter Braak, C. J. F. (1986). Canonical correspondence analysis: A new eigenvector technique for multivariate direct gradient analysis. *Ecology*, *67*, 1167–1179.

Vázquez, G., & Caballero, M. (2013). The structure and species composition of the diatom communities in tropical volcanic lakes of eastern Mexico. *Diatom Research*, *28*, 77–91. https://doi.org/10.1080/0269249X.2012.739974

Wang, J., Soininen, J., Zhang, Y., Wang, B., Yang, X., & Shen, J. (2011). Contrasting patterns in elevational diversity between microorganisms and macroorganisms. *Journal of Biogeography*, *38*, 595–603. https://doi.org/10.1111/j.1365-2699.2010.02423.x

Whittaker, R. H. (1960). Vegetation of the Siskiyou Mountains, Oregon and California. *Ecological Monographs*, *30*, 279–338. https://doi.org/10.2307/1943563

Wilson, S. E., Cumming, B. F., & Smol, J. P. (1996). Assessing the reliability of salinity inference models from diatom assemblages: An examination of a 219-lake data set from western North America. *Canadian Journal of Fisheries and Aquatic Sciences*, *53*(7), 1580–1594.

SUPPORTING INFORMATION

Additional supporting information can be found online in the Supporting Information section at the end of this article.

How to cite this article: Diana, A., Margarita, C., & Gabriela, V. (2022). Diversity and distribution of lacustrine diatoms along the Trans-Mexican Volcanic Belt. *Freshwater Biology*, *00*, 1–15. https://doi.org/10.1111/fwb.14033

Capítulo VI

6. Respuesta de los conjuntos de diatomeas a la variabilidad climática a escala orbital y milenaria desde el penúltimo máximo glacial en el límite norte del Neotrópico.

(Artículo publicado, citar como: Avendaño, D., Caballero, M., Ortega-Guerrero, B., & Lozano-García, S. (2023). Response of diatom assemblages to orbital-and millennial-scale climatic variability since the penultimate glacial maximum in the northern limit of the Neotropics. *Journal of Quaternary Science*. 1-17. https://doi.org/10.1002/jqs.3507)

Este artículo representa el núcleo del proyecto de investigación. Aquí se describen los principales grupos de diatomeas presentes a lo largo del registro de Chalco, que ayudaron a inferir las condiciones climáticas a partir de promedios ponderados de salinidad y temperatura. En este trabajo también se correlacionaron los datos de diatomeas del núcleo CHA08 con los datos ya publicados del núcleo ChaB (Caballero et al., 2019; Caballero y Ortega-Guerrero 1998) para formar un registro continuo de los últimos 150 mil años.

Resumen:

El lago de Chalco, en el centro de México, tiene un largo registro de diatomeas que brinda una excelente oportunidad para documentar las respuestas bióticas e hidrológicas de este ecosistema a la variabilidad climática a escala orbital y milenaria durante los últimos 150 ka. Se utilizó un análisis de correspondencia sin tendencia para evaluar el recambio ecológico y para identificar asociaciones de especies de diatomeas a lo largo de la secuencia. A escala orbital, los conjuntos de agua dulce: *Stephanodiscus* spp. – pequeñas Fragilariaceae spp. – *Cocconeis placentula* involucraron cambios durante los intervalos más fríos (final del Estadio isotópico (EI) EI6, EI5d, EI2), mientras que los taxones tolerantes a la concentración de sales dominados por especies de los géneros *Cyclotella* y *Stephanocyclus*, en condiciones de mayor evaporación (EI5e, EI5c-a, EI4, EI3, principios del EI1). Las fluctuaciones climáticas a escala milenaria también se identificaron como picos en agua dulce (principalmente por pequeñas Fragilariaecae spp.) o como picos en especies tolerantes a la concentración de sales. Comparativamente, el EI6 y EI5d fueron más fríos (-6 a -7º C) y más húmedos que el EI2 (-4 a -5º C). Por el contrario, durante EI5e y principios del EI1 (11.5 – 6 ka) tuvieron un bajo nivel lacustre y condiciones salinas (+2 a +3º C). Además, el EI5 fue un periodo de intenso cambio climático asociado a un forzamiento orbital de amplia amplitud que favoreció a una sucesión de especies de *Cyclotella y Stephanocyclus (S. meneghinianus, C. tlalocii, C. poyeka, S. quillensis).* Por el contrario, se infirieron cambios de temperatura más pequeños (-1 a +1º C) durante los EI4 y EI3.

Palabras clave: Pleistoceno tardío, Paleoclima, Interglacial(es), Glacial(es), diatomeas.

JOURNAL OF QUATERNARY SCIENCE (2023) 1–17 ISSN 0267-8179. DOI: 10.1002/jqs.3507

JQS Journal of Quaternary Science QRA Quaternary Research Association

Response of diatom assemblages to orbital- and millennial-scale climatic variability since the penultimate glacial maximum in the northern limit of the Neotropics

DIANA AVENDAÑO,[1]* MARGARITA CABALLERO,[2] BEATRIZ ORTEGA-GUERRERO[2] and SOCORRO LOZANO-GARCÍA[3]

[1]Posgrado de Ciencias de la Tierra, Instituto de Geofísica, Universidad Nacional Autónoma de México, Ciudad Universitaria, Ciudad de México, México

[2]Laboratorio de Paleolimnología, Instituto de Geofísica, Universidad Nacional Autónoma de México, Ciudad Universitaria, Ciudad de México, México

[3]Instituto de Geología, Universidad Nacional Autónoma de México, Ciudad Universitaria, Ciudad de México, México

Received 27 July 2022; Revised 17 January 2023; Accepted 27 January 2023

ABSTRACT: Lake Chalco, in Central Mexico, has a long diatom record which provides an excellent opportunity to document the biotic and hydrological responses of this ecosystem to orbital- and millennial-scale climatic variability during the last 150 ka. Detrended correspondence analysis was used to evaluate the ecological turnover and to identify diatom species associations throughout the sequence. Millennial-scale climatic fluctuations were identified as peaks in freshwater (mostly small Fragilariaceae spp.) or as peaks in salt-tolerant species. At orbital scales, species turnover involved changes between freshwater assemblages dominated by *Stephanodiscus* spp. – small Fragilariaceae spp. – *Cocconeis placentula*, present during low-evaporation, cool intervals [late Marine Isotope Stage (MIS)6, MIS5d, MIS2] against salt-tolerant taxa, dominated by *Stephanocyclus* and *Cyclotella* spp., in higher evaporation, higher salinity conditions (MIS5e, MIS5c–a, MIS4, MIS3, early MIS1). Comparatively, MIS6 and MIS5d seem to have been cooler (~ −6 to −7 °C) and wetter than MIS2 (~ – 4 to −5 °C). In contrast, MIS5e and early MIS1 (11.5–6 ka) had similar warmer, low lake level, saline conditions. In addition, MIS5 was a period of intense climatic change associated with wide-amplitude orbital forcing that favored a *Stephanocyclus–Cyclotella* spp. ecological succession (*S. meneghinianus*, *C. tlalocii*, *C. poyeka*, *S. quillensis*). In contrast, smaller temperature changes were inferred during MIS4 and MIS3.

KEYWORDS: diatoms; glacial(s); interglacial(s); Late Pleistocene; paleoclimate

Introduction

Quaternary glacial cycles have been recorded as fluctuations in $\delta^{18}O$ from planktonic foraminifera preserved in deep-sea sediments around the world (Lisiecki & Raymo 2005). Marine Isotope Stages (MISs) reflect shifts between glacial periods, with extensive continental ice cover (even-numbered MISs), and warm interglacial episodes (odd-numbered MISs), with smaller ice extent and high sea levels (Emiliani 1955, Shackleton 1967, Berger et al. 2016). Furthermore, Quaternary glaciations have also been tracked in the $\delta^{18}O$ record from ice cores recovered in Greenland and Antarctica (Grootes & Stuiver 1997, Petit et al. 1999), where millennial-scale rapid warm–cold climatic oscillations were identified (Heinrich 1988, Hemming 2004). In contrast, long, continuous records from continental environments are relatively scarce, particularly for the tropics. However, recent paleoclimate research has highlighted the importance of terrestrial records for tracking biotic responses to Quaternary glaciations, for example ecosystem restructuring, species migrations, and evolutionary processes such as diversification, speciation and extinction (Blois & Hadly 2009, Keith et al. 2009, Blois & Williams 2016, Rull 2020). In addition, there is also evidence pointing to the existence of non-modern analog climates during past glacial cycles, based, for example, on the identification of unusual species associations (non-modern analogs) in terrestrial and aquatic ecosystems (Williams & Jackson 2007, Gonzales et al. 2009, Correa-Metrio et al. 2012, Haberyan & Horn 2022).

The interplay between climatic and biotic changes on continental ecosystems during past glaciations can be tracked in long lacustrine sequences where biologic and non-biologic indicators are preserved along one or more full glacial/interglacial cycles. A good example is the record from Lake Titicaca (ca. 370 ka) in the Andean altiplano (Peru/Bolivia), which showed a diatom species turnover between glacial periods, when freshwater taxa were dominant, and peak interglacial conditions, when benthic–saline species were most abundant (Fritz et al. 2007, 2012). In the northern hemisphere Neotropics there are, however, very few long (>100 ka), continuous lacustrine sequences; they include the records from Lake Fúquene (last ca. 284 ka) in Colombia (Groot et al. 2011), from Lake El Valle (only from 137 to 30 ka), in Panama (Shadik et al. 2017, Cárdenes-Sandí et al. 2015) and from Lake Chalco (last ca. 150 ka and ca. 400 ka) in Central Mexico (Ortega-Guerrero et al. 2020, Martínez-Abarca et al. 2021b).

*Correspondence: Diana Avendaño, as above.
Email: da.avendano.v@ciencias.unam.mx

The record from Lake Chalco is particularly interesting because Central Mexico represents the northern limit of the Neotropics and the transition to the Nearctic realm. Furthermore, during past glaciations, this region had an important role as a corridor of suitable climates (refugia) for the migration of species (Ceballos et al. 2010, Pardi & Graham 2019, Avendaño et al. 2021). The northern hemisphere Neotropics were also centers of species diversification, for example of neotropical birds and freshwater fishes, as well as types of forests (Cracraft & Prum 1988, Albert et al. 2020, Figueroa-Rangel et al. 2020).

The present study therefore constitutes an important contribution to Neotropical paleoecology and paleoclimatology. In this paper we present for the first time the detailed diatom record for the last 150 ka from Lake Chalco, Central Mexico, spanning from late MIS6 to early MIS1. This long diatom record provides an excellent opportunity to document the biotic and hydrological responses of this ecosystem to orbital- and millennial-scale climatic variability during the full last glaciation (MIS5d to MIS2) as well as to compare environmental conditions between the two last glacial maxima (MIS6 and MIS2) and interglacials (MIS5e and MIS1).

Study site and geological setting

The Basin of Mexico (BM) is a hydrologically closed basin located at the central–eastern sector of the Trans-Mexican Volcanic Belt (TMVB) (Ferrari et al. 2012) (Figure 1a,b). Lake Chalco is situated to the southeast of the BM (19°15′N, 98°58′W, 2230 m asl) and is limited by the Sierra Nevada (including the high stratovolcanoes Popocatépetl and Iztaccíhuatl) to the east, the Santa Catarina range to the north and the Sierra Chichinautzin monogenetic volcanic field to the south (Figure 1b,c). The catchment is dominated by volcanic deposits of basaltic to dacitic composition (Arce et al. 2019). The uplift of the Sierra Chichinautzin closed the drainage of the BM around 1.2 Ma, allowing for the establishment of an extensive lake system (Arce et al. 2013). The region is characterized by a temperate (mean annual temperature of 16.8 °C) sub-humid climate with summer rains (annual precipitation 540 mm/a) associated with the northerly position of the Intertropical Convergence Zone, the influence of the trade winds, and the onset of the Mesoamerican monsoon and hurricane seasons (Amador et al. 2006). Occasional rainfalls occur in winter related to the passage of frontal systems. Currently Lake Chalco is a shallow marsh (<3 m depth; Figure 1c), that covers an area of <6 km^2, with alkaline, subsaline and hypertrophic waters (pH = 9 and total dissolved solids = 1097 mg/L) (Avendaño et al. 2021).

Methods

Drilling and core correlation

Several sediment sequences from ancient Lake Chalco have been collected near the depocenter of the lake. In this paper, we present the detailed diatom record of the CHA08 sequence from 17.5 to 122.4 m. Note, however, that in previous works the CHA08 sequence was integrated with the CHA11-VII core, which covers the uppermost 18 m to produce a master sequence from which facies analysis, geochemical, magnetic mineralogy, summary diatom groups and charcoal records have been published previously (Torres-Rodríguez et al. 2015, 2018, 2022, Ortega-Guerrero et al. 2017, 2020, Martínez-Abarca et al. 2021a). In this work, nevertheless, we present the CHA08 sequence and the previously published diatom data from the 26-m-long Cha-B core (Caballero &

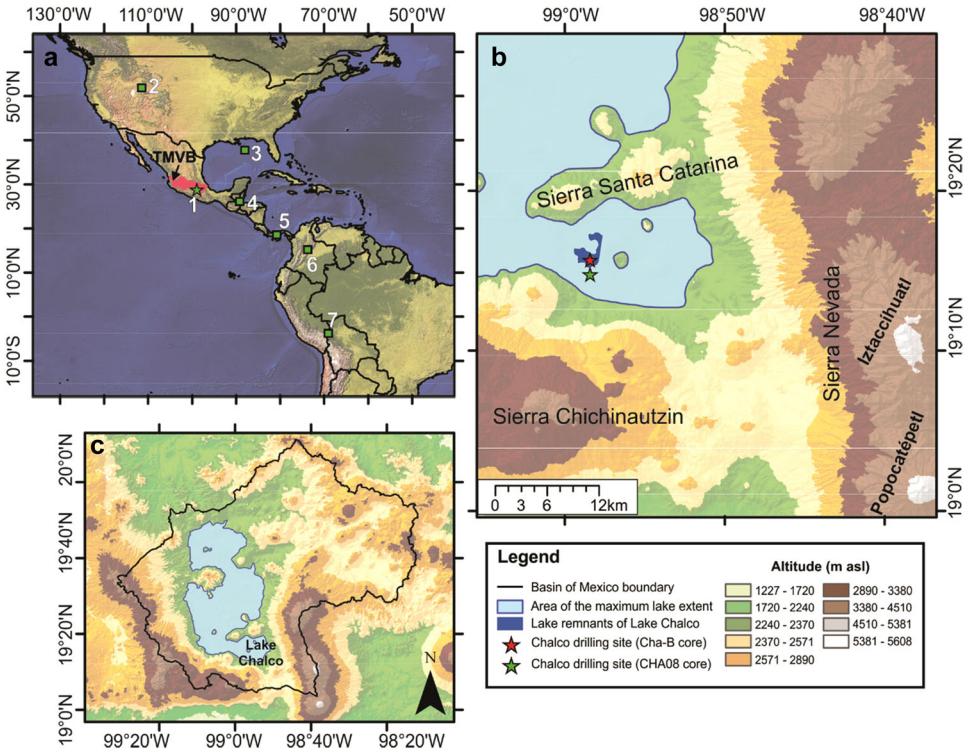

Figure 1. Location maps. (a) Lake Chalco (1) in the Trans-Mexican Volcanic Belt; other sites mentioned in the text: (2) Bear Lake, USA (Jiménez-Moreno et al. 2007); (3) sediment core MD02-2575, Gulf of Mexico (Ziegler et al. 2008); (4) Lake Petén-Itzá, Guatemala (Hodell et al. 2008); (5) El Valle caldera, Panama (Cárdenes-Sandí et al. 2019, Shadik et al. 2017); (6) Lake Fúquene, Venezuela (Groot et al. 2011); (7) Lake Titicaca, Peru/Bolivia (Fritz et al. 2007, 2012). (b) Part of the Basin of Mexico showing the distribution of lacustrine sediments. (c) Lake Chalco sub-basin showing the distribution of lacustrine sediments (light blue), modern-day lake remnant (darker blue) and locations of the Cha-B and CHA08 sequences. [Color figure can be viewed at wileyonlinelibrary.com]

Ortega-Guerrero 1998, Caballero et al. 2019). The overlap between the two sequences was based on the geochronology of the sediments, the diatom stratigraphy and the Tláhuac Tephra. The Cha-B and the CHA11-VII cores were drilled using a modified Livingstone piston corer (more details in Caballero & Ortega-Guerrero 1998 and in Ortega-Guerrero et al. 2017), while the CHA08 cores were drilled using a Shelby corer with inner 1-m-long PVC tubes (more details in Lozano-García et al. 2015, Ortega-Guerrero et al. 2017). Splitting and initial description of the CHA08 cores was carried out in the LacCore Facility of the University of Minnesota.

Diatom analysis

Samples for diatom analysis from the CHA08 sequence were collected approximately every 20 cm between 17.5 and 122.4 m (546 samples). For this, 0.5 g of dry sediment was treated with (10%) HCl, (30%) H_2O_2 and 5 mL of concentrated HNO_3 at 80 °C. We prepared permanently mounted on slides with 200-µL aliquots of the final solution that were air-dried and mounted on a hot plate using Naphrax. Due to the large number of samples, and in order to standardize the sampling effort between them, diatom counts were carried out along a maximum of four transects per sample, aiming to reach a minimum diatom count of 100 valves per sample. However, in several sections of the sequence diatom valves were scarce or badly broken and only in about 50% of the samples were minimum counts of over 100 valves achieved. To extend the temporal coverage we decided to include in our diatom analysis 60 samples where diatom counts were between 75 and 100 valves. Even though this is a small count number, considering the high dominance of the diatom assemblages in most of these samples, these counts were considered to be adequate to track changes in the main taxa present in the samples (Patterson and Fishbein, 1989). Therefore, diatom analysis of the CHA08 sequence was based on a total of 311 samples where diatom counts were above 75 valves. This set of diatom-positive samples had an average spacing of 33 cm and average diatom counts of 290 valves. Fossil diatom counts were performed using a light microscope (Olympus BX50) with a 1000× oil immersion objective. Diatoms were identified based on a specialized literature, including Krammer et al. (1991), Krammer and Lange-Bertalot (1991, 1988, 1986), Gasse (1986) and Spaulding et al. (2021). The total diatom concentration was calculated with the aliquot settling method (Schrader, 1974) and expressed as number of valves per gram of dried sediment (v/gds).

Samples for diatom analysis from the Cha-B core, previously reported by Caballero & Ortega-Guerrero (1998), were based on 203 samples taken every 10 cm with a minimum of 400 valves counted. The Cha-B core covered the most-recent 40 ka and the diatom data were successfully used to generate salinity, temperature and precipitation transfer functions (Caballero et al. 2019). This approach, however, was not possible for the CHA08 core because of the high abundance of diatom taxa that were not present in the modern samples of the training data set.

Statistical analysis

Diatom diagrams for species with >10% abundance in at least one sample from both cores (Cha-B and CHA08) were plotted using the 'rioja' (Juggins, 2019, version 0.9-21) package in R (R Development Core Team, 2009, version 3.6.0). Diatom zonation was based on a Constrained Incremental Sum of Squares (CONISS) cluster analysis (Grimm 1987) also using the 'rioja' package.

A detrended correspondence analysis (DCA) was performed to estimate the species compositional turnover in both sequences (Cha-B and CHA08). The relationships of the DCA axes with environmental gradients was inferred based on modern ecological information stemming mainly from the Central Mexico diatom data set (Avendaño et al. 2021, 2022; Caballero et al. 2019) but other bibliographic references were also used (Gasse & Tekaia 1983, Blinn 1993, Fritz et al. 1993, Gasse et al. 1995). The DCA Axis 1 scores were stratigraphically plotted to infer the environmental changes through time. In addition, the rates of ecological change (RoC) were calculated using the distance between contiguous samples based on the first four DCA axes scores and dividing by time (Correa-Metrio et al. 2014). This analysis was done in the statistical package 'paleoMAS' (Correa-Metrio et al. 2015, version 2.5-5).

Geochronology and sediment description

Throughout this work, calibrated ^{14}C dates are expressed as 'k cal a BP', while dates outside this range are expressed as 'ka'. The Cha-B (Caballero & Ortega-Guerrero 1998) and the CHA08-CHA11-VII (Ortega-Guerrero et al. 2017) sequences have two independent age models. An updated age model for Cha-B core was published by Caballero et al. (2019), estimating an age interval from 5 to 40k cal a BP. The model was constructed with eight calibrated dates from pollen, charcoal, bulk sediment and tephrochronological markers with the 'Bacon' package (Blaauw & Christeny 2011) in R (R Development Core Team 2009) using the IntCal13 calibration curve (Reimer et al. 2013). The tephrochronological age markers used were the Upper Toluca Pumice (UTP) produced by the Nevado de Toluca volcano around 12.4 k cal a BP (Arce et al. 2003) the 'Tutti Frutti' Pumice (TFP), produced by an eruption from the Popocatépetl volcano around 17k cal a BP (Sosa-Ceballos et al. 2012), and the Tláhuac Tephra dated at ~31.4k cal a BP (Herrera Hernández 2011).

The age model for the CHA08-CHA11-VII master sequence was published by Ortega-Guerrero et al. (2017), estimating a basal age of 150 ka. The ages for the first 35 m were based on 14 ^{14}C dates and two tephrostratigraphic age markers (the UTP and the TFT). The deeper part of the sequence is beyond the range of ^{14}C dating, so the chronology was established by one $^{230}Th/U$ date of zircons from a tephra layer at 63.5 m (Torres-Rodríguez et al. 2015) and a tie-point at 106 m, corresponding to the transition from MIS6 to MIS5, dating to 130 ± 3 ka (Ortega-Guerrero et al. 2017, Avendaño et al. 2018). This model was constructed by a P-sequence deposition model (Bronk-Ramsey 2008) using the online version of OxCal 4.2 (Bronk-Ramsey 2009) and the IntCal13 calibration curve (Reimer et al. 2013). The diatom data from the CHA08 sequence from 17.5 to 122.4 m presented in this paper correspond to an age interval of 32–150 ka. Therefore, the full diatom data presented in this paper cover from 5 to 150 ka and the 311 diatom-positive samples from the CHA08 sequence had an average time interval of 391 years.

The CHA08-CHA11-VII master sequence (Ortega-Guerrero et al. 2017) was divided into seven lithostratigraphic units and the Cha-B core stratigraphy correlates with the first three units (Figure 2) (Ortega-Guerrero et al. 2017). Unit 3 represents the overlap between the Cha-B and the CHA08 cores (Figure 3). In Table 1 we present a summary of their main sedimentary characteristics and charcoal accumulation rates (Torres-Rodríguez et al. 2015, 2022, Martínez-Abarca et al. 2021a). The depth scales used for each sequence are independent from each other (CHA08 from 17.5 to 122.4 m, and Cha-B from 0 to 26 m). For this reason, we used the depth of Units 7–3 based

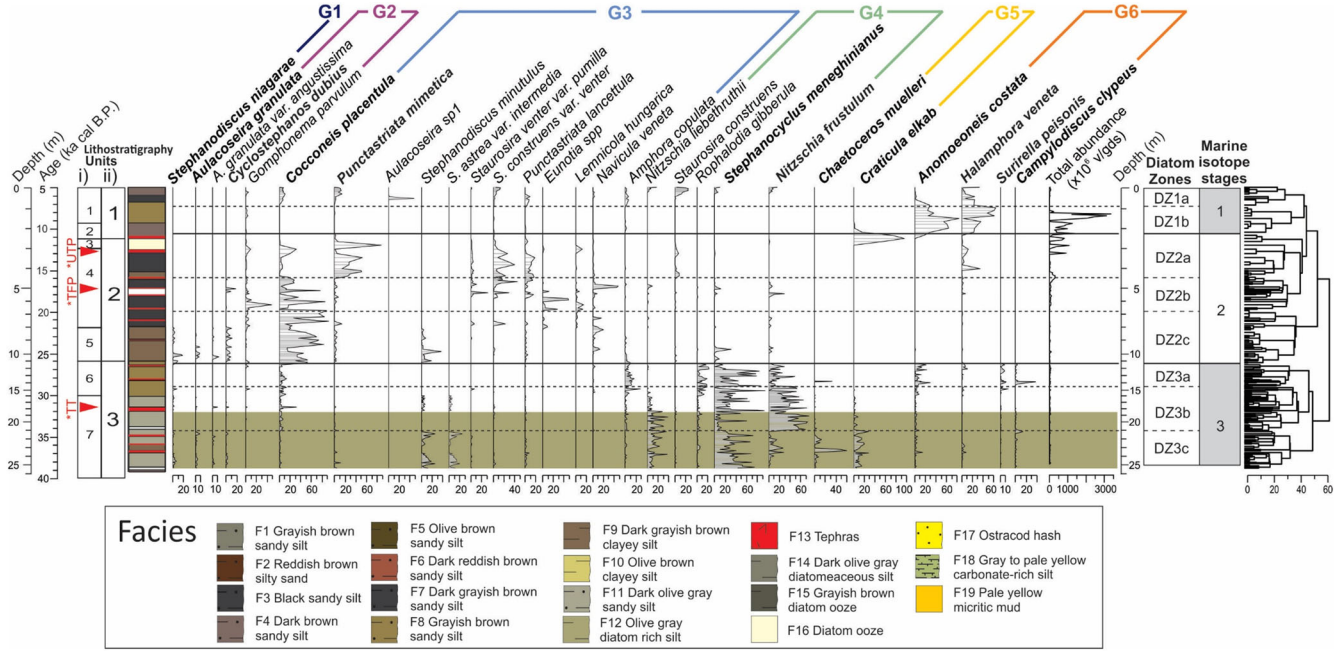

Figure 2. Diatom record of the Cha-B sequence (5–40k cal a BP) from Lake Chalco, central Mexico. The figure shows the original lithostratigraphic units (i) reported in Caballero & Ortega-Guerrero (1998) and their correlation with the units of the CHA08–CHA11-VII master sequence (ii) reported in Ortega-Guerrero et al. (2017). Asterisks show the tephrostratigraphic age markers: UTP = Upper Toluca Pumice, TFP = 'Tutti Frutti' Pumice, TT = Tláhuac Tephra. The shaded area represents the overlap between the CHA08 and the Cha-B sequences.

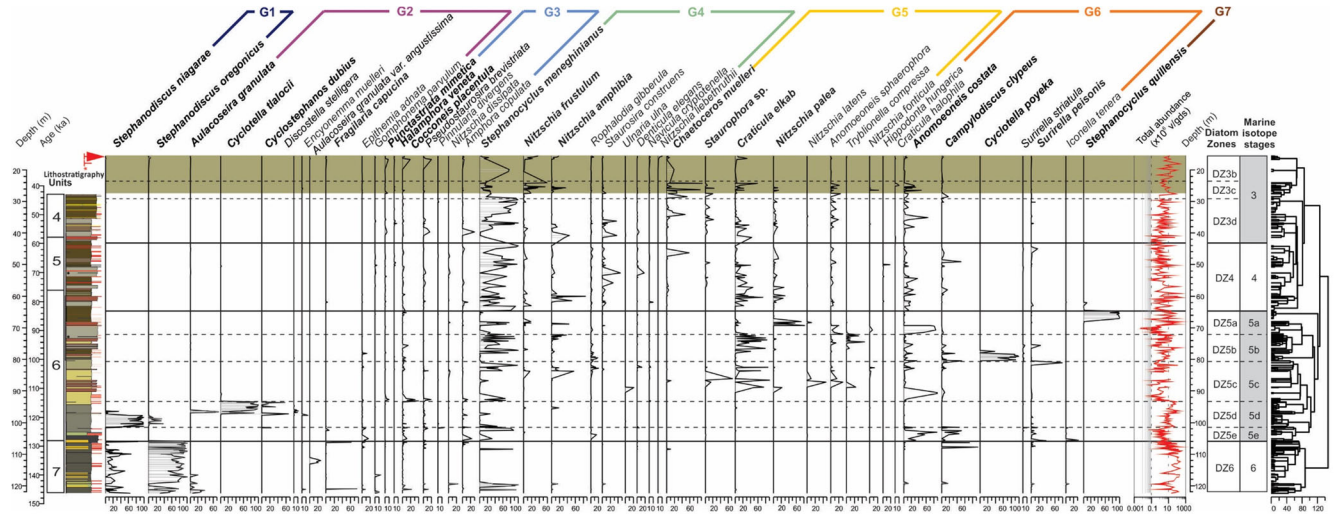

Figure 3. Diatom record of the CHA08 sequence (31–150 ka) from Lake Chalco, central Mexico. The figure shows the stratigraphic units according to Ortega-Guerrero et al. (2017). Asterisks show the tephrostratigraphic age markers: UTP = Upper Toluca Pumice, TFP = 'Tutti Frutti' Pumice, TT = Tláhuac Tephra. Diatom groups are based on Figure 3 and described in Table 2. The shaded area represents the overlap between the CHA08 and the Cha-B sequences. Facies key as in Figure 2. [Color figure can be viewed at wileyonlinelibrary.com]

on the CHA08-CHA11-VII master sequence (Ortega-Guerrero et al. 2017) (122.4–30 m, Figure 3) and for Units 3–1 based on the Cha-B core (Caballero & Ortega-Guerrero 1998) (26–0 m, Figure 2).

Results

Diatom abundance of both sequences ranged from 0 to 3400 × 10^6 v/gds (Figures 2 and 3), with maximum concentrations in the sediments from the Cha-B core dating to the late MIS2 glaciation (termination I, 18–11.5k cal a BP) (Figure 2). The diatom concentration in the CHA08 sediments was generally lower (<300 × 10^6 v/gds). Highest values were in the sediments dating to the late MIS6 glaciation (150–130 ka) while five sections of the core dating to MIS5c, MIS5a and MIS4 had the lowest diatom abundances (92.7–87.2, 86.5–83.6, 70.6–69.4, 53.5–50.7 and 44.5–41.5 m) (Figure 3). Some of these low diatom abundance sections also correlated with mottled sediment intervals, which suggested very low lake levels and occasional subaerial exposure. A total of 108 species in both sedimentary sequences were identified, 86 from CHA08 and 41 from Cha-B, with 19 taxa common to both sequences. Six main diatom zones (DZs) were identified with a total of 16 subzones (Figures 2 and 3). DZ6 to DZ3b correspond to the CHA08 sequence, while DZ3c to DZ1 correspond to the Cha-B sequence. Subzones DZ3b and DZ3c represent the overlap between the Cha-B and CHA08 sequences. Note that the diatom zone numbers along the sequence match perfectly the MIS numbers to which they

Table 1. Main characteristics and charcoal accumulation rates in the sediment units of the Cha-B and CHA08 sequences, from Lake Chalco, Central Mexico.

Lithostratigraphy units	Sedimentological features	Charcoal accumulation rates
1 Cha B 2.5–0.5 m	Massive to faintly bedded silicate grains with calcareous concretions, alkaliphilous and halophilous diatoms, ostracod, and gastropod fragments.	
2 Cha-B 11–2.5 m	Massive alternating with faintly laminated clayey silt with freshwater diatoms. Includes the TFP and the UTP tephras.	Low charcoal particles.
3 Cha-B 26–11 m CHA08 < 28 m	Massive to bedded sandy to clayey organic silts with alkaliphilous diatoms. Includes the Tláhuac Tephra.	Medium to low.
4 CHA08 41.1–28 m	Laminated or bedded silts with abundant biogenic components, which include alkaliphilous and halophilous diatoms, *Chara* sp., ostracods, and calcite, dolomite and gypsum crystals. Massive, mottled intervals show features of occasional subaerial exposure between 44.5 and 36 m	Highest at the top of the unit
5 CHA08 57.5–41.1 m	Laminated or bedded silts with abundant biogenic components, which include alkaliphilous and halophilous diatoms. Massive, mottled intervals show features of occasional subaerial exposure between 53.5 and 50.7 m.	Medium to high
6	93.3–57.5 m – Massive, calcareous clayey silt with biogenic components which include *Chara* sp., *Phacotus*, ostracod valves, alkaliphilous and halophilous diatoms. Massive mottled intervals give evidence of occasional subaerial exposure between 75.5 and 62.5 m.	Variable to high
CHA08	103.2–93.3 m – Laminated diatom ooze (*Stephanodiscus* spp. clear laminae) and silt with minor calcareous components (dark laminae).	High to medium
106–57.5 m	106–103.3 m – Calcareous dark grayish brown sandy silt with ostracodes, and alkaliphilous–halophilous diatoms.	High
7 CHA08 122.4–106 m	Laminated diatom ooze (*Stephanodiscus* spp., clear laminae) and silt with minor calcareous components (dark laminae), with 13 layers (2–5 cm thick) of pale yellow micritic mud formed by calcite, siderite, dolomite and minor amounts of clays.	Low

correspond according to the age models, facilitating sequence interpretation and correlation with orbital-scale events. Therefore in the discussion as well as in Figures 6–8, and in Table 2, the MIS terminology is used, as it is interchangeable with the diatom zones. Therefore, the MIS boundaries could be different from those used in previous studies in Chalco (Ortega-Guerrero et al. 2017, 2020, Martínez-Abarca et al. 2021a, Lozano-García et al. 2022, Chávez-Lara et al. 2022a, 2022b).

Twenty-one diatom taxa were very abundant along the Chalco record, reaching abundances of ≥50% in at least one sample (Figures 2 and 3); these taxa are illustrated in Figures 4 and 5. One of these taxa has recently been transferred to *Stephanocyclus meneghinianus* (Kützing) Kulikovskiy, Genkal et Kociolek (2022) (Figure 4i). This taxon, formerly identified as *Cyclotella meneghinana*, is part of a group of four Cyclotelloid diatoms present in the CHA08 sequence and reported by Avendaño & Caballero (2022a). From detailed analysis of the Cyclotelloid taxa in this publication we realize that the recognition of the genus *Stephanocyclus* implies that another of the Cyclotelloid species in the Chalco record should also be transferred to this genus, as already recognized by Stoermer & Julius (2003): *Stephanocyclus quillensis* comb. nov. (Basinonm: *Cyclotella quillensis* L.W. Bailey, 1922: Diatoms from the Quill Lakes, Saskatchewan, and from Airdrie, Alberta. *Contributions to Canadian Biology* 11: 159, pl. I: Figure 1) (Figure 4b). This taxon shares with other *Stephanocyclus* species the presence of central fultoportulae with three satellite pores, a robust rimoportula, mantle rimoportula present on most ribs and open marginal alveoli (Battarbee et al. 1984, Häkansson 2002, Avendaño et al. 2022a). The other two Cyclotelloid taxa reported by Avendaño et al. (2022a) have complex marginal chambers (Figure 4c,d), and therefore remain in *Cyclotella*.

Seven ecological diatom groups reflecting distinctive environmental conditions were identified based on the DCA (Figure 6a). Along DCA Axis 1 (eigenvalue = 0.89, axis length 6.3) *Stephanodiscus* spp. are distributed towards the far left (negative values), in contrast to *Stephanocyclus quillensis* that is present towards the far right of the diagram (positive values). *Stephanodiscus* spp. are freshwater taxa (Fritz et al. 1993, Avendaño et al. 2021) an ecological affinity that is also shared by the other taxa with negative scores on Axis 1, which include: *Aulacoseira granulata*, *Cyclostephanos dubius*, *Cocconeis placentula* and *Fragilaria capucina* (Fritz et al. 1993, Wilson et al. 1996, Chaffin et al. 2012, Ramírez-Nava et al. 2022). On the other hand, *Stephanocyclus quillensis* thrives in high-salinity environments (7.2–102.8 g/L in Dakota Lakes) (Battarbee et al. 1984, Fritz et al. 1993), and other taxa with positive scores on Axis 1 also share an affinity for high-salinity environments, such as *Chaetoceros muelleri*, *Campylodiscus clypeus*, *Anomoeoneis costata*, *Stephanocyclus meneghinianus* and *Nitzschia frustulum* (Fritz et al. 1993, Blinn 1993, Wilson et al. 1996, Saros & Fritz 2000). These ecological affinities show that DCA Axis 1 reflects a salinity gradient. In this way, the diatom groups that plot on the negative side of DCA Axis 1 (Groups 1–3) represent freshwater assemblages [total dissolved solids (TDS) < 500 mg/L) while the groups on the positive side of DCA Axis 1 (Groups 4–7) represent subsaline (TDS = 500–3000 mg/L), hyposaline (TDS = 3000–20 000 mg/L) and mesosaline (TDS = 20 000–50 000 mg/L) environments (Figure 6a). The main factor that controls salinity in tropical regions is variations in evaporation (Hecky & Kilham 1973, Padisák & Naselli-Flores 2021).

Table 2. Diatom assemblages present in the Lake Chalco stratigraphic sequence as identified in the DCA species plot. Ecological preferences are based on specialized literature and in the central Mexico diatom data set (Avendaño et al. in review, Avendaño et al. 2021, Caballero et al. 2019). Bold text indicates diatoms with abundance >50%.

Ecological group	Species	Code	Ecology	Marine Isotopic Stages
1	***Stephanodiscus oregonicus*** (Ralfs) Håkansson 1986	**SteOre**	Freshwater planktonic taxa in cold (<15 °C), nutrient-rich (↑N), deep waters.	6
	Stephanodiscus niagarae Ehrenberg 1845	**SteNia**		5d
2	***Cyclotella tlalocii*** Avendaño & Caballero 2022	**CylTla**	Freshwater planktonic taxa in cool (<20 °C) nutrient-rich conditions.	5d
	Aulacoseira granulata (Ehrenberg) Simonsen 1979	**AulGra**		
	Cyclostephanos dubius (Hustedt) Round 1988	**CycDub**		
	Gomphonema parvulum (Kützing) Kützing 1849	GomPar		
	Fragilaria capucina Desmazières 1830	**FraCap**		
	Aulacoseira granulata var. *angustissima* (O.Müller) Simonsen 1979	AulAng		
	Epithemia adnata (Kützing) Brébisson 1838	EpiAdn		
	Discostella stelligera (Cleve & Grunow) Houk & Klee 2004	DisSte		
	Encyonema muelleri (Hustedt) Mann 1990	EncMue		
3	***Cocconeis placentula*** Ehrenberg 1838	**CocPla**	Freshwater facultative planktonic and benthic taxa in cool (~8–17 °C), shallow, waters.	2
	Punctastriata mimetica Morales 2005	**PunMim**		
	Amphora copulata (Kützing) Schoeman & Archibald 1986	AmpCop		
	Pseudostaurosira brevistriata (Grunow) Williams & Round 1988	PseBre		
	Staurosira construens var. *venter* (Ehrenberg) Hamilton 1992	StaCnv		
	Stephanodiscus minutulus (Kützing) Cleve & Möller 1882	SteMin		
	Navicula veneta Kützing 1844	NavVen		
	Punctastriata lancettula (Schumann) Hamilton & Siver 2008	SirPnc		
	Eunotia spp	EunSpp		
	Staurosira venter var. *pumilla* (Grunow) Kingston 2000	StaCpu		
	Aulacoseira sp1	Aulsp1		
	Nitzschia dissipata (Kützing) Rabenhorst 1860	NtzDis		
	Stauroneis kriegeri Patrick 1945	StaKri		
	Pinnularia divergens Smith 1853	PinDiv		
4	***Stephanocyclus meneghinianus*** (Kützing) Kulikovskiy, Genkal & Kociolek 2022	**CylMen**	Subsaline planktonic to epiphytic taxa in nutrient-rich (↑P), warm (16–20 °C) environments.	3 4
	Nitzschia frustulum (Kützing) Grunow 1880	**NtzFru**		
	Nitzschia amphibia Grunow 1862	**NtzAmp**		
	Nitzschia liebethruthii Rabenhorst 1864	NtzLie		
	Rhopalodia gibberula (Ehrenberg) Otto Müller 1895	RhoGla		
	Staurosira construens Ehrenberg 1843	StaCon		
	Stephanodiscus astrea var. *intermedia* Fricke 1901	SteAst		
	Denticula elegans Kützing 1844	DenEle		
	Ulnaria ulna (Nitzsch) Compère 2001	UlnUln		
	Navicula cryptotenella Lange-Bertalot 1985	NavCla		
5	***Craticula elkab*** (O.Müller ex O.Müller) Lange-Bertalot, Kusber & Cocquyt 2007	**CraElk**	Hyposaline facultatively planktonic and benthic taxa, in nutrient-rich environments. High pH (~9) and sodium carbonate to sodium chloride dominated lakes.	5c, 5b-a 4
	Chaetoceros muelleri Lemmermann 1898	**ChaMue**		3
	Nitzschia palea (Kützing) Smith 1856	**NtzPal**		1
	Anomoeoneis sphaerophora Pfitzer 1871	AnoCap		
	***Staurophora* sp** Mereschkowsky 1903	**Stasp**		
	Tryblionella compressa (Bailey) Poulin 1990	TriCom		
	Nitzschia latens Hustedt 1949	NtzLat		
	Nitzschia fonticola (Grunow) Grunow 1881	NtzFon		
	Hippodonta hungarica (Grunow) Lange-Bertalot, Metzeltin & Witkowski 1996	HipHun		
	Craticula halophila (Grunow) Mann 1990	CraHal		
6	***Anomoeoneis costata*** (Kützing) Hustedt 1959	**AnoCos**	Hyposaline benthic taxa. High pH (>8) in sodium carbonate to sodium chloride dominated, shallow lakes.	5e, 5c-a
	Cyclotella poyeka Avendaño & Caballero 2022	**CylPoy**		4
	Campylodiscus clypeus (Ehrenberg) Ehrenberg ex Kützing 1844	**CamCly**		3 1
	Halamphora veneta (Kützing) Levkov 2009	**HmpVen**		
	Surirella peisonis Pantocsek 1902	**SurPei**		
	Iconella tenera (W.Gregory) Ruck & Nakov 2016	IcoTen		
	Surirella striatula Turpin 1828	SurStr		
7	***Stephanocyclus quillensis*** com. nov.	**CylQui**	Hyposaline planktonic taxa characteristic of sodium chloride dominated lakes.	5a

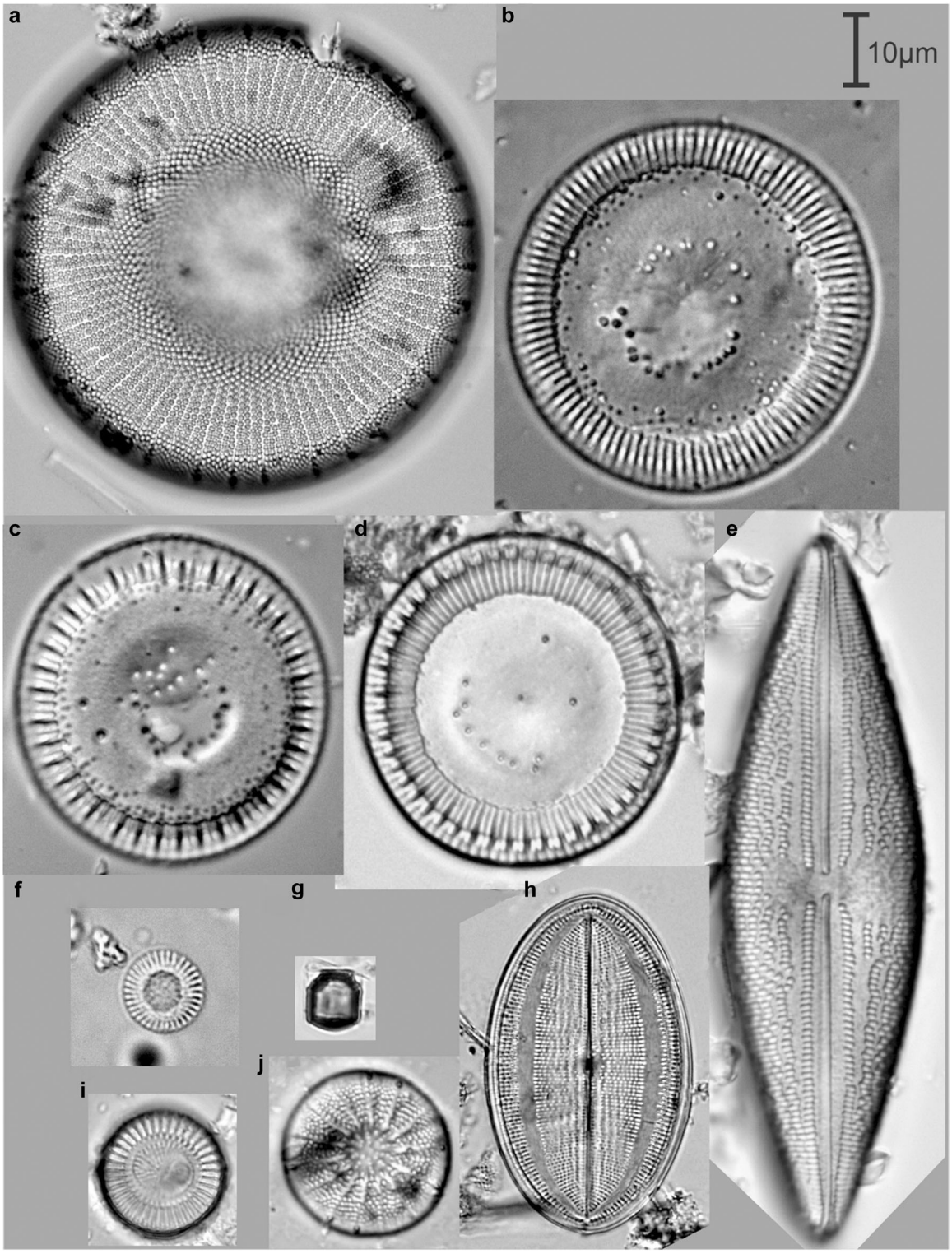

Figure 4. Plate showing 10 of the 21 high-abundance diatom taxa (>50% in at least one sample) in the record from Lake Chalco, central Mexico. (a) *Stephanodiscus niagarae*, (b) *Stephanocyclus quillensis*, (c) *Cyclotella poyeka*, (d) *Cyclotella tlalocii*, (e) *Anomoeoneis costata*, (f) *Cyclostephanos dubius*, (g) *Chaetoceros muelleri*, (h) *Cocconeis placentula*, (i) *Stephanocyclus meneghinianus*, (j) *Stephanodiscus oregonicus*.

Therefore, we consider that this is the main environmental driver behind the salinity gradient represented by DCA Axis 1. The DCA Axis 1 scores have a range of 4 standard deviations, indicating that there is a complete species turnover along the sedimentary sequence (Correa-Metrio et al. 2014) between the freshwater taxa (Groups 1–3) and the subsaline (Group 4) to hyposaline and mesosaline taxa (Groups 5–7). The DCA Axis 1 vs. DCA Axis 2 sample plot (Figure 6b) shows that species turnover follows the diatom zonation, which as mentioned before also represents the MISs, showing an ecological transition from freshwater environments dominating during the cooler, lower evaporation conditions in MIS6, MIS5d and MIS2 (negative side of DCA Axis 1) to saline environments during the higher evaporation, warmer conditions in MIS5e, MIS5c, MIS5b, MIS5a, MIS4, MIS3 and MIS1.

The transitions in the salinity of the lake with time are evident when the DCA1 sample scores and the diatom groups are plotted against the age of the sediments (Figure 7a–c). The rate of change in the CHA08 sequence remains low except for key moments, for example at the transition from MIS6 to

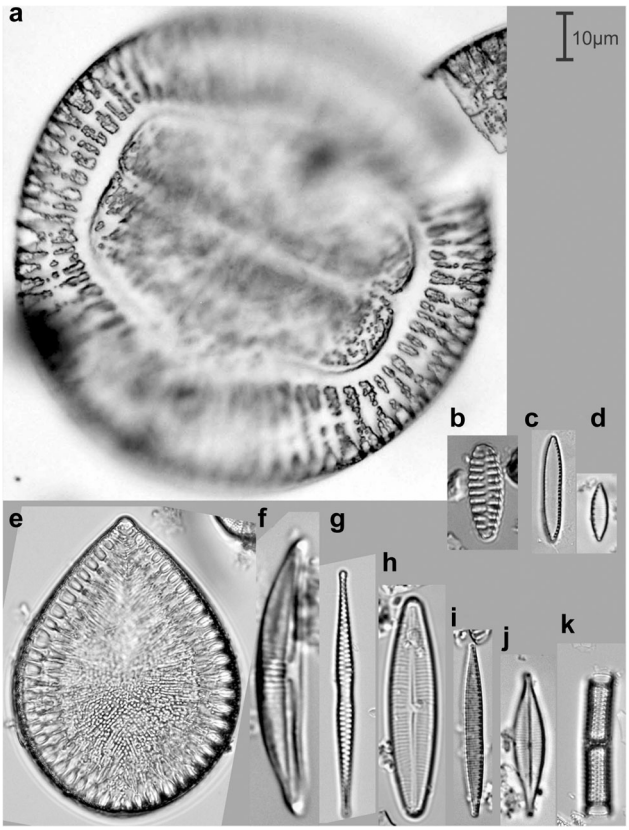

Figure 5. Plate showing 11 of the 21 high-abundance diatom taxa (>50% in at least one sample) in the record from Lake Chalco, central Mexico. (a) *Campylodiscus clypeus*, (b) *Punctastriata mimetica*, (c) *Nitzschia palea*, (d) *Nitzschia frustulum*, (e) *Surirella peisonis*, (f) *Halamphora veneta*, (g) *Fragilaria capucina*, (h) *Staurophora* sp., (i) *Nitzschia amphibia*, (j) *Craticula elkab*, (k) *Aulacoseira granulata*.

MIS5e, MIS5e to 5d, or MIS5c to MIS5b (Figure 7d). Along the Cha-B sequence values are higher at the end of MIS3, at the transition between the last glacial maximum and termination I (ca. 18k cal a BP) and at ca. 5k cal a BP (mid-Holocene). The difference in the rates of change during MIS3 between the CHA08 (5 samples/m) and Cha-B (8 samples/m) cores is due to the sample resolution, which was higher in the Cha-B sequence.

Discussion

Ecological interpretation of the diatom groups

The detailed ecological preferences of the diatom groups identified by the DCA are presented below and in Table 2. The diatom group succession along the whole Chalco sequence is presented in Figure 7.

Group 1: Stephanodiscus spp.

This assemblage is dominated by two planktonic taxa in the genus *Stephanodiscus*, *Stephanodiscus oregonicus* and *Stephanodiscus niagarae*. Avendaño et al. (2021) proposed that Central Mexico acted as glacial refugium for *Stephanodiscus niagarae*, which in its modern distribution occurs mostly in freshwater bodies with circumneutral pH and high nutrient levels in northern USA and Canada, in contrastingly cooler climatic conditions compared to Central Mexico (Theriot & Stoermer 1984, Fritz et al. 1993, Reavie et al. 2014a). While *Stephanodiscus oregonicus* is absent in the modern diatom data set from Central México, *Stephanodiscus niagarae* was present only in low-evaporation, cool environments at altitudes above 2500 m asl, in freshwater with high nutrient concentrations (particularly high nitrogen). The temperature optimum for *Stephanodiscus niagarae* in Mexican lakes is ~15 to 14 °C (Avendaño et al. 2021, Avendaño et al. 2022b), while the water temperature in Lake Erie, where *Stephanodiscus niagarae* is abundant, ranges from 4 to 10 °C (Burns et al. 2005, Lashaway & Carrick 2010, Reavie et al. 2014b, 2014a), supporting the interpretation that this species prefers realtively cool water conditions. This diatom assemblage is therefore consistent with freshwater conditions, nitrogen-rich waters and low-evaporation environments associated with relatively cool temperatures during late MIS6, 150–130 ka (DZ6), and during the first part of early MIS5d, 123–117 ka (DZ5d). Similar conditions are also suggested by the presence of *Stephanodiscus niagarae* in the sediments from the last glacial maximum during MIS2, 26–22k cal a BP (DZ2c).

Group 2: Aulacoseira granulata, Cyclostephanos dubius, Cyclotella tlalocii and Fragilaria capucina

This group includes planktonic freshwater diatoms that thrive in nutrient-rich systems (Bradshaw & Anderson 2003). *Aulacoseira granulata* thrives in eutrophic environments (Bicudo et al. 2016, Ramírez-Nava et al. 2022), while *Cyclostephanos dubius* is a good indicator of phosphorous-rich waters (Bradshaw & Anderson, 2003). The diatom species in this assemblage reflect low-evaporation, freshwater environments with high nutrients, a well-mixed water column and low light availability during the latter part of MIS5d. However, *Aulacoseira granulata* is also present in minor proportions in the sediments dating to MIS6 (DZ6) and MIS2 (DZ2). Two short intervals of *Fragilaria capucina* were present in sediments dating to MIS6 (146 and 132 ka) which probably suggest short periods of warming, as this species had a preference for the warmer conditions in the Central Mexico training set (Avendaño et al. 2022b). *Cyclotella tlalocii* is a fossil taxon exclusive to Lake Chalco, but its scores on DCA Axis 1 show its association with other freshwater taxa, suggesting that its optimum distribution lies within the freshwater spectrum.

Group 3: Small Fragilariaceae spp. and Cocconeis placentula

This group includes facultative planktonic and epiphytic, freshwater taxa. The small Fragilariaceae spp., especially *Punctastriata mimetica* and *Pseudostaurosira brevistriata*, are tychoplanktonic taxa tolerant of low temperatures as they are common in temperate and alpine regions (Anderson 2000, Schmidt et al. 2004, Vélez-Agudelo et al. 2017). This agrees with the presence of this group of taxa, particularly of *Pseudostaurosira brevistriata* in high mountain lakes of Central Mexico (Zawisza et al. 2008, Avendaño et al. 2022b). *Cocconeis placentula* is an epiphytic freshwater taxon reported in nutrient-rich lakes, especially with high phosphorous (Van Dam et al. 1994; Avendaño et al. 2022b). This association has low abundances in the older sediments from Lake Chalco, with only a few isolated peaks along the sequence, the largest in sediments dating to MIS5c (DZ5c) and MIS5d (DZ3d). The tolerance to cooler conditions of the small Fragilariaceae taxa suggests that these short-term peaks could indicate rapid cooling intervals such as Heinrich events. This assemblage becomes dominant in the sediments dating to MIS2 (DZ2) where *Cocconeis placentula* shows its highest abundances during the last glacial maximum (27–18k cal a BP, DZ2c and DZ2b), while the small Fragilariaceae spp. dominated in the sediments dating to termination I (18–11.5k cal a BP, DZ2a).

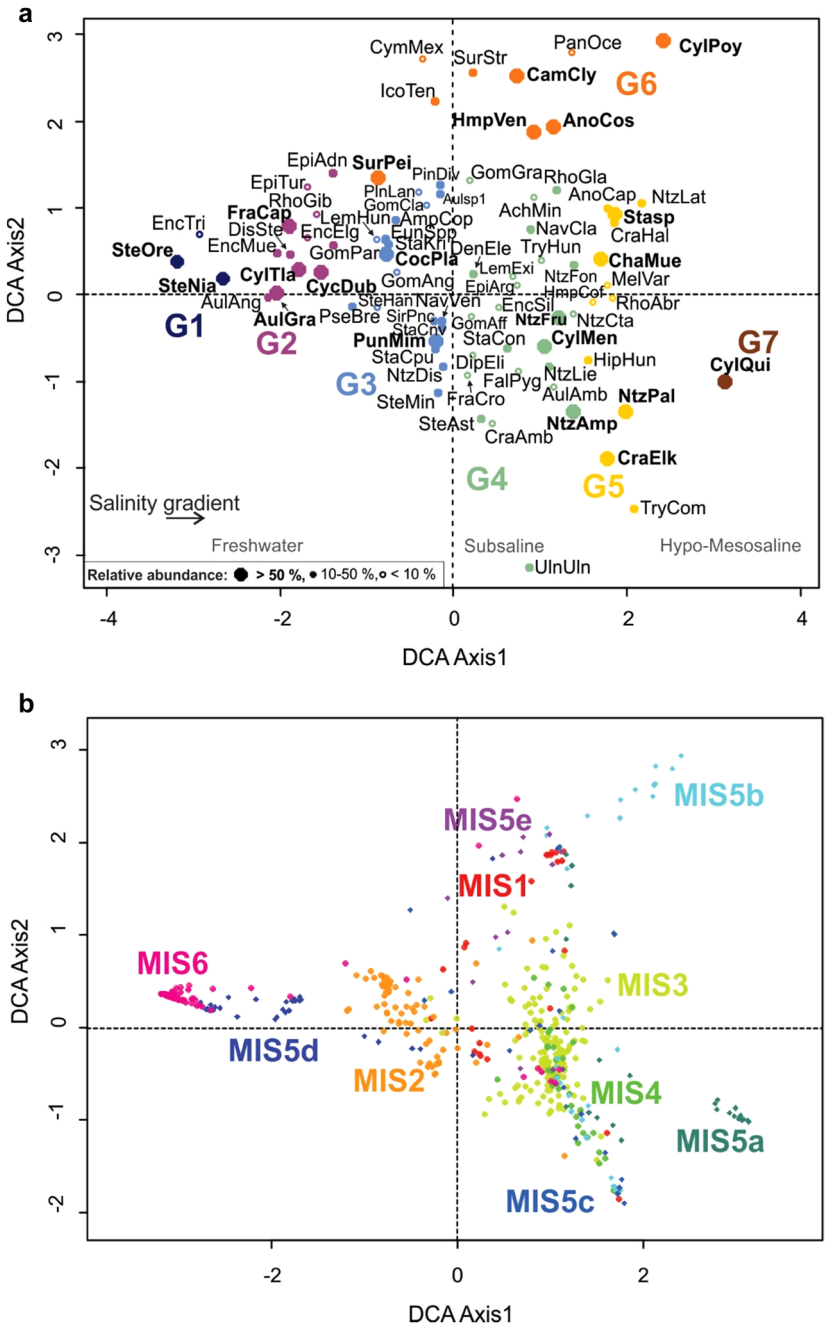

Figure 6. Detrended correspondence analysis (DCA) of the diatom taxa in the record (150–5 ka) from Lake Chalco (CHA08 and Cha-B cores), central Mexico. (a) Scatter plot of DCA species. High-abundance species (> 50% in at least one sample) are in bold type. (b) Scatter plot of DCA samples. The full names of the species with a relative abundance >10% and their codes are listed in Table 1. [Color figure can be viewed at wileyonlinelibrary.com]

Group 4: Nitzschia amphibia, Stephanocyclus meneghinianus and Nitzschia frustulum

This group is dominated by alkaliphilous, planktonic *Stephanocyclus meneghinianus* and periphytic taxa including *Nitzschia amphibia*, *N. frustulum*, *Epithemia gibberula*, *Staurosira construens*, *Denticula elegans*, *Nitzschia liebethruthii* and *Navicula cryptotenella*. *Nitzschia amphibia* has a preference for nutrient-rich waters with high phosphorous concentrations and a salinity optimum in the range from fresh to subsaline (~166–612 mg/L) in Central Mexico (Davies et al. 2002; Avendaño et al. 2022b) and mostly subsaline in lakes of the USA (Fritz et al. 1993). *Stephanocyclus meneghinianus* has a similar ecology with a salinity optimum from fresh to hyposaline levels in Central Mexico and also in other North American lakes (Blinn, 1993; Fritz et al. 1993; Avendaño et al. 2022b). On the other hand, *Nitzschia frustulum* has a higher salinity tolerance than *Stephanocyclus meneghinianus* and *Nitzschia amphibia*, which ranges from subsaline to mesosaline in Central Mexico and other North American lakes (Fritz et al. 1993; Avendaño et al. 2022b). The salinity ranges of *Nitzschia amphibia*, *Stephanocyclus meneghinianus* and *Nitzschia frustulum* represent a transition to higher salinity conditions (from freshwater to mesosaline) associated with increasing evaporation and/or temperature. This group indicates the presence of higher evaporation, warmer conditions leading to higher water salinity than previously. This assemblage dominates along large sections of the sequence, mostly in sediments dating to MIS4 and MIS3 (DZ4 and DZ3), but it is also shows peaks in sections of MIS5 (DZ5).

Group 5: Craticula elkab, Chaetoceros muelleri, Nitzschia palea and Staurophora sp.

This group includes benthic taxa (*Craticula elkab, Staurophora* sp., *N. palea)* and halophilous planktonic to tychoplanktonic forms such as *Chaetoceros muelleri. Crati-*

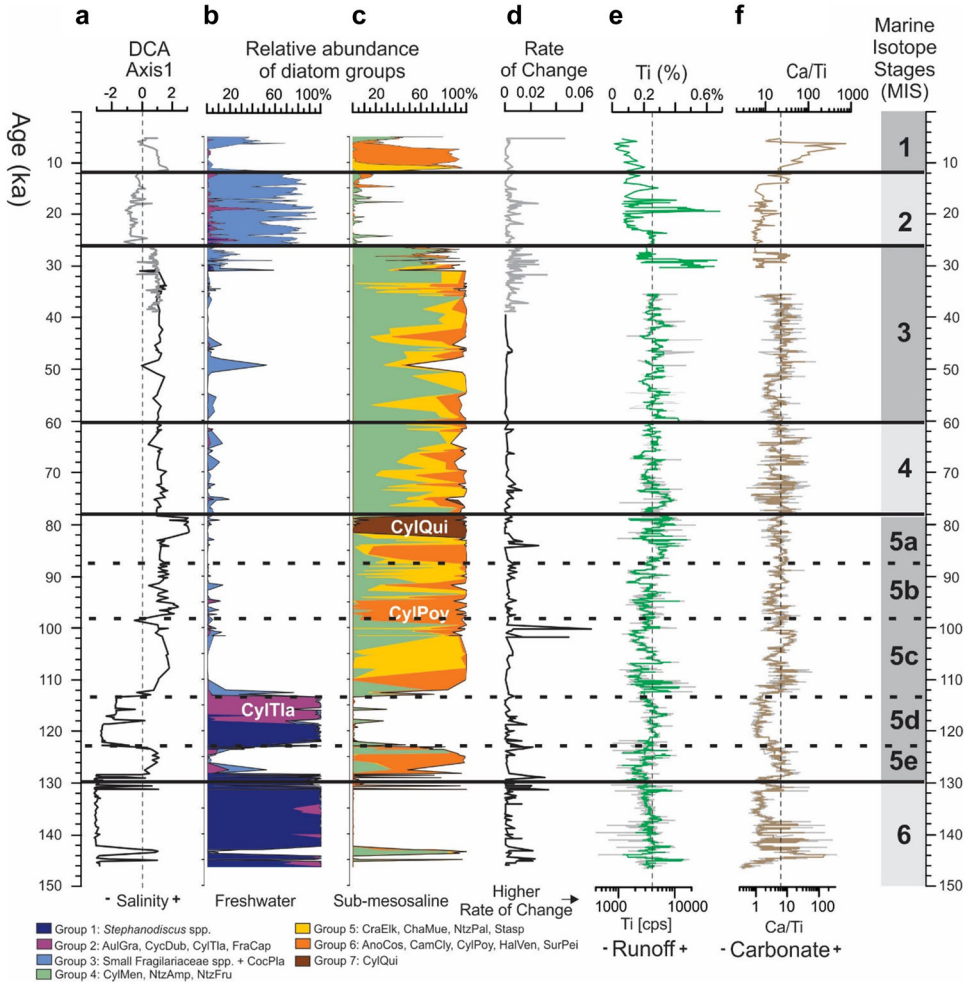

Figure 7. Multiproxy diagram from 150 to 5 ka of the Lake Chalco record, eastern-central Mexico. (a) Detrended correspondence analysis (DCA) Axis 1 sample scores for the CHA08 (black) and Cha-B (grey) cores. (b) Freshwater assemblages (Groups 1–3) from the CHA08 sequence. (c) Freshwater assemblages (Groups 1–3) from the Cha-B sequence. (d) High-salinity assemblages (Groups 4–7) from the CHA08 sequence. (e) High-salinity assemblages (Groups 4–7) from the Cha-B sequence. (f) Rates of change from CHA08 (black) and Cha-B (grey) sequences. (g) Titanium (Ti) values as counts per second (cps) for the CHA08 sequence (Martínez-Abarca et al. 2021a) and as percentages (%) for the CHA11-VII sequence (Lozano-García et al. 2015, Caballero et al. 2019). Dotted line represents average value. (h) Ca/Ti ratios for the CHA08 (Ortega-Guerrero et al. 2020) and CHA11-VII (Lozano-García et al. 2015) cores. Dotted line represents average value. The shaded area is the overlap between the CHA08 and Cha-B sequences. CylTla = *Cyclotella tlalocii*, CylPoy = *Cyclotella poyeka*, CylQui = *Stephanocyclus quillensis*. [Color figure can be viewed at wileyonlinelibrary.com]

cula elkab is tolerant of high alkalinity conditions in sodium carbonate waters (Gasse et al. 1995), while *Chaetoceros muelleri* has a strong chloride association in hyposaline to mesosaline lakes (Fritz et al. 1993, Saros & Fritz 2000). *Craticula elkab* is found in modern populations and fossil records of African lakes accompanied by *Stephanocyclus meneghinianus* and *Nitzschia frustulum*; in Africa, these species thrive in alkaline waters with pH > 9 (Hecky & Kilham 1973). A similar *Craticula elkab* and *Chaetoceros muelleri* association was observed in Central Mexico only in Lake Piscina de Yuriria, characterized by a sodium carbonate ionic dominance, high nutrient level (eutrophic–hypertrophic) and a pH of 9.4 (Hill 2006, Holmes et al. 2016, Avendaño et al. 2021). This assemblage reflects high evaporation probably associated with warm conditions and low precipitation. This group, therefore, reflects higher alkalinity and salinity (hyposaline to mesosaline) conditions, in waters dominated by sodium carbonate and even sodium chloride. This assemblage is most abundant in sediments dating to MIS5c (102–108 ka, DZ5c), and is also present during MIS5b, MIS5a (DZ5b–5a), MIS4 (DZ4), MIS3 (DZ3) and the early part of MIS1 (11.5k cal a BP, DZ1b).

Group 6: Campylodiscus clypeus, Anomoeoneis costata, Cyclotella poyeka, Halamphora veneta and Surirella peisonis

This assemblage is characterized by benthic halophilous taxa (*Campylodiscus clypeus* and *Anomoeoneis costata*) that have a preference for sodium carbonate sulfate-dominated habitats (Blinn 1993; Saros and Fritz 2000). *Campylodiscus clypeus* – *Anomoeoneis costata* assemblages were observed in saline lakes of East Africa (Carvalho et al. 1995, Poulíčková & Jahn 2007). These benthic species have a salinity optimum from subsaline to hyposaline and an alkaline pH range (8–10) (Gasse & Tekaia 1983, Fritz et al. 1993, Gasse et al. 1995). *Surirella peisonis* is common in brackish, soda lakes of the USA and Europe (Kusel-Fetzmann 1979, Schmid 1979, 1995, Fritz 1990, Fritz et al. 1993). In the diatom dataset from Central Mexico (n = 46 lakes) *Anomoeoneis costata* and *Campylodiscus clypeus* were present in hyposaline lakes; however *S. peisonis* was absent (Avendaño et al. 2022b). *Halamphora veneta* is a common species that thrives in shallow waters with abundant aquatic vegetation in carbonate-rich, subsaline environments of Mexico (Novelo et al. 2007; Caballero et al. 2015, Avendaño et al. 2022b), whereas in lakes from the USA its salinity ranges includes hyposaline to mesosaline

environments (Fritz et al. 1993). *Cyclotella poyeka* is a fossil species from Lake Chalco. Even though we do not know its ecology, its association with *Anomoeoneis costata*, *Anomoeoneis sphaerophora* and *Campylodiscus clypeus* and its position in the DCA diagram indicate that it was also a salt-tolerant variety, but as with most centric taxa, it is likely that it had a planktonic habit. This group is associated with very shallow lake levels of high salinity (hyposaline to mesosaline), with sodium carbonate to sodium chloride ionic dominance. The low lake levels and high salt concentration together suggests high evaporation and warm conditions. This association was dominant in the sediments from Lake Chalco dating to MIS5 and early MIS1, specifically during MIS5e (130–123 ka, DZ5e), early MIS5c (113–100 ka, base of DZ5c), early MIS5b (98–94 ka, base of DZ5b), early MIS5a (84–88 ka, base of DZ5a) and also early MIS1 (10–6k cal a BP, DZ1b). Less important peaks were also present along MIS4 and MIS3 (DZ4 and DZ3).

Group 7: Stephanocyclus (Cyclotella) quillensis

This group is formed only by planktonic *Stephanocyclus quillensis*. This taxon is present in saline lakes with sodium chloride – sulfate ionic dominance in semi-arid climates of the USA and Canada (Battarbee et al. 1984, Salm et al. 2009). According to salinity optimum estimations, *Stephanocyclus quillensis* lives in a range between hyposaline and hypersaline conditions (Battarbee et al. 1984, Fritz et al. 1993). *Stephanocyclus quillensis* is morphologically very similar to *Cyclotella alchichicana* which only lives in hyposaline sodium chloride Lake Alchichica in Central Mexico (Oliva et al. 2006; Avendaño et al. 2022b). There are very few reports of *Stephanocyclus quillensis* in Mexico, and these include reports from calcareous springs in La Huasteca (Cantoral-Uriza 1997, Montejano et al. 2000) and the lower Pánuco River (Montejano et al. 2004), but these observations would need to be corroborated because they do not match the ecological distribution of this species which thrives in saline ecosystems. Furthermore, this species was absent from the Central Mexico diatom dataset (Caballero et al. 2019; Avendaño et al. 2022b), showing that it is not a common taxon in the modern environments in Mexico. This assemblage represents the highest salinity levels in the record and sodium chloride-dominated waters. However, as in the case of *Stephanodiscus niagarae*, the present distribution of this species is in lakes from more northerly regions in Canada and northern USA, which points to the possibility that its presence in Central Mexico was favored by at least seasonally cooler conditions than present. This species was only observed in sediments dating to late MIS5a (83–78 ka, top of DZ5a).

Diatom species ecological turnover during last 150 ka in Lake Chalco and its paleoenvironmental implications:

The DCA Axis 1 scores (Figure 7a) and the diatom groups (Figure 7b,c) plotted against the age of the sediments allow us to visualize the environmental changes in Lake Chalco through time and to compare them with the geochemical record from the CHA08 – CHA11-VII sequence (Ti and Ca/Ti, Figure 7e,f) and with other key records in this hemisphere (Figure 8a–d). These selected records include the Greenland (GRIP) $\delta^{18}O$ record (Johnsen et al. 1997), the Bear Lake warm-arid pollen record (Jiménez-Moreno et al. 2007), the sea surface temperature (SST) reconstruction from the Gulf of México (Ziegler et al. 2008) and the Lake Fúquene arboreal pollen-based temperature reconstruction (Groot et al. 2011) (location of sites is shown in Figure 1a).

Changes in the diatom assemblages in the Chalco sequence during the last 150 ka show a robust relationship with hemispheric glacial and interglacial conditions ultimately driven by orbital forcing (Figure 8g,h). A complete species turnover is recorded in Chalco between a dominance of freshwater taxa (Groups 1–3, Axis 1 negative scores) during glacial periods (MIS6, MIS5e and MIS2) and alkaline, salt-tolerant taxa (Groups 4–7, Axis 1 positive scores) during warmer intervals, with a high salinity association (Group 6) present during the peak of the last two interglacials (MIS5e and early MIS1). A similar diatom replacement during the glacial–interglacial cycles was observed in Lake Titicaca (Figure 1a), where freshwater taxa increased during the glacial intervals, whereas salt-tolerant species were most abundant during the peak of the interglacials (Fritz et al. 2007). Both Lake Chalco and Lake Titicaca show ecosystem rearrangements that follow orbital-scale climate changes. This reorganization of the diatom community between freshwater and salt-tolerant taxa could be a useful tool to identify boundaries between previous glacial maxima when analyzing other long lacustrine sequences from the Basin of Mexico that have been recovered recently (Lozano-García et al. 2017, Brown et al. 2019, Ortega-Guerrero et al. 2022).

Furthermore, the Lake Chalco diatom record is also sensitive to millennial-scale events. Temperature reconstruction on the Cha-B core (Caballero et al. 2019) revealed cooling events during MIS2 associated with Heinrich stadials 0–2. In the CHA08 sequence, peaks in freshwater diatoms from Group 3 during MIS5–MIS3 denote rapid reductions in salinity and probably also in temperature. In contrast, peaks in the abundance of hyposaline diatoms from Group 6 show periods of higher salinity and evaporation, possibly during climatic oscillation towards warmer conditions. The most important cooling events show a good correspondence with Heinrich stadials and a correlation is proposed in Figure 8.

The three main time windows when Lake Chalco showed freshwater environments (MIS6, MIS5d and MIS2) were times of minima in spring and summer insolation (Figure 8h) and of less seasonal climates. The Lake Chalco diatom record gives the unique opportunity to compare the environmental conditions during these three cool events, which include the two last glacial maxima and their terminations during MIS6 and MIS2. As mentioned before these intervals were dominated by freshwater taxa, but while MIS6 was dominated by Group 1 (*Stephanodiscus* spp.), MIS5d shows a transition from Group 1 (*Stephanodiscus* spp.) to Group 2 (*Aulacoseira granulata* – *Cyclotella tlalocii*) and MIS2 was dominated by diatom Group 3, with a transition from *Cocconeis placentula* during the Last Glacial Maximum (LGM) to the small Fragilariaceae spp. assemblage during Termination I (TI). These diatom associations suggest that lake levels were different between them. The DCA Axis 1 scores, the planktonic habitat of the *Stephanodiscus* taxa, and the presence of laminated sediments during both MIS6 and MIS5d (Ortega-Guerrero et al. 2017, Avendaño et al. 2018) support the interpretation of a deeper lake compared to the LGM in MIS2, when epiphytic *Cocconeis placentula* was dominant and the titanium signal points to generally low surface runoff (Figure 7e). This could be related to drier conditions during MIS2, even though changes in the basin morphometry should also be considered, as sediment accumulation could explain a shallower lake environment during MIS2. The known ecology of *Stephanodiscus niagarae*, a species that migrated to Central Mexico from the northern USA during glacial episodes, allows us to speculate that MIS6

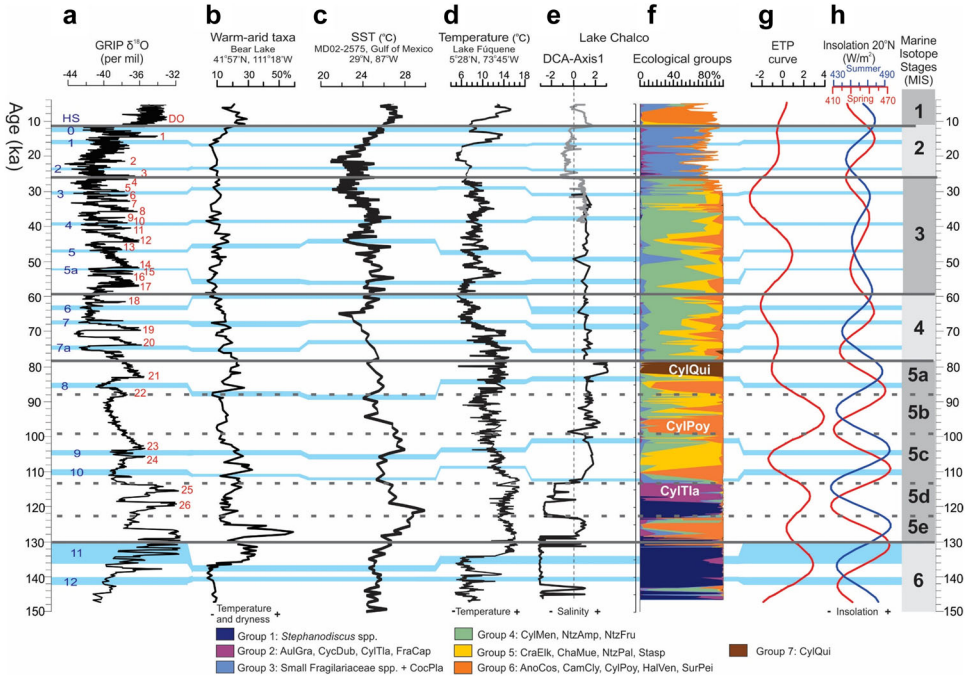

Figure 8. Comparison of selected regional temperature records with the DCA Axis 1 scores and diatom groups from Lake Chalco. (a) Oxygen isotopes ($\delta^{18}O$) of the GRIP ice core (Johnsen et al. 1997); the Dansgaard Oescher events (DO) are numbered in red, while Heinrich events (HS) are shaded and numbered in blue. (b) Warm-arid taxa from Bear Lake, USA (Jiménez-Moreno et al. 2007). (c) Sea Surface temperature (SST) reconstruction from sediment core MD02-2575, Gulf of Mexico (Ziegler et al. 2008). (d) Arboreal pollen-based temperature reconstruction from Lake Fúquene, Venezuela (Groot et al. 2011). (e) Detrended correspondence analysis (DCA) Axis 1 plotted against the age of the sediments (black line = CHA08, grey line = ChaB core). (f) Diatom ecological groups from the CHA08 and ChaB cores. Diatom groups are detailed in Table 1. (g) Integrated orbital forcing eccentricity + tilt + precession (ETP) curve (Laskar et al. 2004). (h) Spring (red line) and summer (blue line) insolation for 20 N (Berger & Loutre, 1991). CylTla = *Cyclotella tlalocii*, CylPoy = *Cyclotella poyeka*, CylQui = *Stephanocyclus quillensis*. [Color figure can be viewed at wileyonlinelibrary.com]

and the first part of MIS5d were also somewhat cooler than MIS2. A temperature reduction of about 6–7 °C is possible considering the optimal distribution of this species in the Great Lakes area. This last estimate is in line with the cooling of 7.5–8 °C based on the pollen records from Lake Valle in Panama (Cárdenes-Sandí et al. 2019) and Lake Fúquene in Colombia (Groot et al. 2011). In contrast, the temperature drop during MIS2 in Lake Chalco, based on pollen and diatom transfer functions, indicate a maximum cooling during the LGM of ~4–5 °C (Correa-Metrio et al. 2013, Caballero et al. 2019). The idea of cooler conditions with higher humidity and a deeper lake during MIS6 agrees with the larger area of the Nexcoalango glaciers dating to MIS6 compared to the Hueyatlaco-1 moraines dating to MIS2 at nearby Iztaccíhuatl volcano (Figure 1c) (Vázquez-Selem & Heine 2011).

Termination II (TII) is related to an increase in spring and summer insolation and warming temperature trends in the hemispheric records starting at around 135 ka (Figure 8). At Lake Chalco TII is an unstable interval with high rates of change. An intense warming (peak in Group 6 diatoms) is recorded at about 131 ka followed by a return to glacial-stage conditions (Group 1 diatoms) from ca. 130 to 129 ka, after which the warmer environments of MIS5e (Group 6 diatoms) were established. This cool reversal is also a feature of regional temperature records (Figure 8b–d), but is particularly evident in the Bear Lake pollen (Jiménez-Moreno et al. 2007) (Figure 8b). This reversal has been interpreted as comparable to the Younger Dryas cooling during TI (Riboulleau et al. 2014, Moseley et al. 2015), and has also been associated with the entrance of cool waters to the North Atlantic from the Laurentide Ice Sheet (Nicholl et al. 2012). In contrast, during TI the diatom-based temperature reconstructions from Chalco (Caballero et al. 2019) showed a rapid warming of about 2–3 °C after 16k cal a BP (Bølling/Allerød), but a relatively mild cooling (~−1.5 °C) during the Younger Dryas reversal (~12k cal a BP) that differs from the return to full glacial conditions during the cool reversal in TII.

The diatom record from Chalco shows a return to low-evaporation, glacial-stage conditions and a deep, freshwater lake (diatom Group 1 and laminated sediments) at the beginning of MIS5d, when spring insolation was at a minimum (Figure 8h). However, after 118 ka, as spring insolation increased (Figure 8h), the lake transitioned to less cool conditions, dominated by diatom Group 2, which included *Cyclotella tlalocii*. Nevertheless, cool, freshwater environments continued until the end of MIS5d, and the lake remained deeper than during MIS2. In the Bear Lake pollen record (Jiménez-Moreno et al. 2007), and in the SST data from the Gulf of Mexico (Ziegler et al. 2008) a sharp cooling during MIS5d is also recorded (Figures 1a and 8b,c), even though the arboreal pollen from Lake Fúquene only shows a slight decrease in temperature (Groot et al. 2011) (Figures 1a and 8d). During the last two interglacial stages (MIS5e and early MIS1) the diatom assemblages in Lake Chalco were similar (diatom Group 6), suggesting that in both cases there was an increase in evaporation, probably associated with warming, a salinity increase and a reduction of the lake level associated with maxima in summer insolation (Figure 8h). Even though it is generally considered that MIS5e was the warmest interval of the last 800 ka (Masson-Delmotte et al. 2010, Turney & Jones 2010), the record from Lake Chalco shows similar conditions during MIS5e and the early part of MIS1 (11.5–6 ka). The diatom-based temperature reconstruction for Chalco shows that the early Holocene was 2–3 °C warmer than present (Caballero et al. 2019); this is a plausible reconstruction for MIS5e temperatures given the similar diatom assemblages. Temperature estimates for MIS5e of around 2 °C above present have been proposed based on the Lake Valle (Cárdenes-Sandí et al. 2019) and the Lake Fúquene (Groot et al. 2011) pollen data. Warmer than present conditions and

an expansion of the Atlantic warm pool during MIS5e are also supported by the SST reconstruction from the Gulf of Mexico (Ziegler et al. 2008) (Figure 8c). In addition, paleosol records form Yucatán give evidence of drier and hotter climates (Valera-Fernández et al. 2020) while corals and relict mangrove systems in the Gulf of Mexico record a sea level up to 9 m higher (Blanchon et al. 2009, Aburto-Oropeza et al. 2021). However, moisture conditions during MIS5e are contrasting between records; in the Cariaco Basin (11°N), off the coasts of Venezuela (Figure 1a), in Lake Valle caldera (8°N), in Panamá, and Lake Fúquene (5°N) in Colombia, relatively wet or similar-to-present conditions were recorded (Groot et al. 2011, Riboulleau et al. 2014, Shadik et al. 2017, Cárdenes-Sandí et al. 2019). In contrast, at Chalco (19°N), in Central Mexico, and in Lake Titicaca (15°S), in Perú–Bolivia, the last interglacial stage was dry (Fritz et al. 2007, 2012). It has been proposed that during the warmer conditions of MIS5e the average position of the Intertropical Convergence Zone (ITCZ) migrated northwards (Nikolova et al. 2013, Riboulleau et al. 2014). Nevertheless, the record from Chalco suggests that the evaporative pressure of warmer climates exceeded any increase of precipitation that could have been associated with a larger Atlantic warm pool and a more northerly position of the ITCZ. Furthermore, the latitudinal distribution of the records that show interglacial wet conditions suggest that the average location of the ITCZ during MIS5e was probably 5–10°N, which is similar to its typical latitudinal location at present (Waliser & Somerville 1994).

Wide amplitude changes in insolation and a strong orbital forcing shown by the eccentricity + tilt + precession (ETP) curve (Figure 8g) dominated during MIS5, leading to the extreme climate conditions during MIS5e and MS5d that have already been discussed. However, during the rest of MIS5 (MIS5c to 5a) there are also periods with high rates of change associated with shifts between the diatoms in Group 4 (subsaline) and the salt-tolerant diatoms in Groups 5–7 (hyposaline), which point to frequent changes in salinity and lake level. In addition, the peaks in dominance of salt-tolerant *Cyclotella poyeka* and *Stephanocyclus quillensis* were recorded during MIS5b and MIS5a, which occurred at extremes in the insolation parameters, minima in spring insolation in the first case and a peak summer insolation and seasonality in the second case (Figure 8g,h). Late MIS5a, when *Stephanocyclus quillensis* was dominant, was also a period of high fire activity around the lake (Torres-Rodríguez et al. 2015, 2022, Martínez-Abarca et al. 2021a). Non-modern analog climates with cooler winters and warmer summers during MIS5a could explain the peak in *Stephanocyclus quillensis*, a species that today lives in saline lakes of Canada and northern USA.

The transition to MIS4 marks a reduction in lake salinity and a small increase in lake level in Chalco, with a lower abundance of the salt-tolerant diatoms from Groups 5 and 6, particularly after 70 ka, and the predominance of the lower salinity diatoms from Group 4. This represents a reduction in evaporation and probably also in temperature, to similar-to-modern values. In the modern environments of Lake Chalco, the diatom assemblage is also dominated by Group 4 diatoms, mainly *Stephanocyclus meneghinianus*, even though there are species reflecting recent anthropogenic pollution, such as *Thalassiosira* aff. *duostra*, that had never been recorded previously (Buendía-Flores et al. 2019, Avendaño et al. 2021). The transition into MIS3 in Chalco showed a persistence of the environmental conditions during MIS4, with relatively small evaporation and temperature changes until the marked cooling recorded at the onset of MIS2 (27 ka), when freshwater environments returned. The transfer function for the Cha-B sequence shows that temperature was similar-to-modern during late MIS3 (− 1 to +1 °C, Caballero et al. 2019). Compared to MIS5, during MIS4 and MIS3 there was a reduced intensity in the orbital forcing as the ETP and insolation curves show (Figure 8g,h), which might explain the small changes in evaporation and temperature recorded at Chalco during these intervals. The Lake Fúquene record (Figure 5d) shows a temperature reduction at 70 ka, and small changes at the MIS4 to MIS3 transition (Groot et al. 2011). In addition, the pollen record from Lake Petén-Itzá also agrees with nearly uniform temperatures during MIS4 and MIS3 (Correa-Metrio et al. 2012) even though the reconstructed temperature is 3 °C lower than present. In this lake, however, magnetic susceptibility (Hodell et al. 2008) shows important variations in moisture availability between MIS4 and MIS3 that are not recorded at Chalco, with wetter conditions during MIS4 and the beginning of MIS3 and drier conditions during the rest of MIS3.

The Lake Chalco diatom record allowed the identification of different biotic–climate responses during the last 150 ka, such as the freshwater species turnover during the low-evaporation, cooler phases in the record or the southward migration of species like *Stephanodiscus niagarae* during the coolest intervals. Furthermore, the Chalco record also shows that rapid climatic shifts during MIS5 were favorable for the ecological displacement of *Cyclotella* species of different salinity tolerances. The rapid climatic shifts during MIS5, driven by high-amplitude fluctuations in orbital forcing, show an ecological succession that started with *Cyclotella tlalocii* during MIS5d and followed with salt-tolerant *Cyclotella poyeka* and *Stephanocyclus quillensis* during MIS5b and MIS5a. Each of these species appeared in the record for a short time and then disappeared (Figure 5f), as they were displaced by other taxa during periods of rapid climate change (Davis 1984, Keith et al. 2009). The presence in the record from Lake Chalco of species that are unusual or absent in the modern environments from Central Mexico (non-modern analog assemblages) confirms the existence of non-analog climatic conditions particularly during MIS6 and MIS5.

Conclusions

The diatom sequence of Lake Chalco provides a continuous record of salinity changes during the last 150 ka that responded mostly to orbitally controlled evaporation and associated temperature changes, but that also recorded millennial-scale climatic oscillations.

The diatom record showed an ecological turnover from freshwater environments during the low-evaporation, cool intervals (MIS 6, MIS5d and MIS 2) to saline environments during times of higher evaporation (MIS5e, MIS5c–5a, MIS4, MIS3 and early MIS1). This turnover can be simplified as an alternation of *Stephanodiscus* spp. versus *Stephanocyclus*–*Cy-Cyclotella* spp. that could reveal the boundaries of previous glacial–interglacial periods in long sequences from the Basin of Mexico.

MIS6 was cooler (possibly −6 to −7 °C) and wetter than MIS2 (~ − 4 to −5 °C) implying that neither glacial maxima were perfect analogs. MIS5d was initially as cool as MIS6, and it remained cooler and wetter than MIS2. In contrast, MIS5e and early MIS1 had similar high-evaporation, warm and dry conditions estimated to be ~2–3 °C warmer than present. In contrast, MIS4 and MIS3 reflected only small changes in salinity and therefore temperature is estimated to be similar-to-modern.

MIS5 was a period of intense climatic change associated with wide-amplitude orbital forcing that favored a *Stephano-*

cyclus–Cyclotella spp. assemblage of taxa with different salinity affinity (*Stephanocyclus meneghinianus*, *Cyclotella tlalocii*, *Cyclotella poyeka*, *Stephanocyclus quillensis*). These species rapidly disappeared from the record as they were displaced by other taxa during periods of rapid climate change.

Acknowledgments. This research was funded by DGAPA-PAPIIT-IN100820 'Registros interglaciares del centro de México' and DGAPA-IV-100215 'Cambio Climático y Medio Ambiente en la historia del lago de Chalco'. Diana Avendaño thanks the Posgrado de Ciencias de la Tierra, UNAM and CONACyT (CVU 854736) for financial support. We also thank Teresa Mercado Serón for her help with initial diatom counts of a section of the sequence, and Jorge Salgado for his assistance with diatom sample preparation.

Conflict of Interest—The authors declare no conflict of interest.

Author contribution—Writing-original draft, conceptualization, data curation, preparation figures & tables: D.A., M.C. Conducting the research, supervision, writing-review & editing: M.C., S.L.G., B.O.G. Funding acquisition: M.C., S.L.G. Methodology: D.A., M.C., S.L.G., B.O.G.

Data availability statement

The data that support the findings of this study are available from corresponding author upon reasonable request and also from "Registros Paleoambientales de México" data bases at https://datosabiertos.unam.mx/IGL:PALEOMEX:CHA08.

Abbreviations. BM, Basin of Mexico; CONISS, Constrained Incremental Sum of Squares; cps, counts per second; CylTla, *Cyclotella tlalocii*; CylPoy, *Cyclotella poyeka*; CylQui, *Stephanocyclus quillensis*; DCA, detrended correspondence analysis; DO, Dansgaard–Oescher events; DZ, diatom zones; ETP, eccentricity + tilt + precession curve; HS, Heinrich events; ITCZ, Intertropical Convergence Zone; LGM, Last Glacial Maximum; MIS, Marine Isotope Stage; SST, sea surface temperature; TMVB, Trans-Mexican Volcanic Belt; TFP, 'Tutti Frutti' Pumice; TT, Tláhuac Tephra; TI, Termination I; TII, Termination II; TDS, Total dissolved solids; UTP, Upper Toluca Pumice; USA, United States of America.

References

Aburto-Oropeza O., Burelo-Ramos C.M., Ezcurra E., Ezcurra P., Henriquez C.L., Vanderplank S.E. & Zapata F. (2021) Relict inland mangrove ecosystem reveals Last Interglacial sea levels. *Proceedings of the National Academy of Sciences* 118, 1–8.

Albert J.S., Tagliacollo V.A. & Dagosta F. (2020) Diversification of Neotropical Freshwater Fishes. *Annual Review of Ecology, Evolution and Systematics* 51, 27-53.

Amador J.A., Alfaro E.J., Lizano O.G. & Magaña V.O. (2006) Atmospheric forcing of the eastern tropical Pacific: A review. *Progress in Oceanography* 69, 101–142.

Anderson N.J. (2000) Miniview: Diatoms, temperature and climatic change. *European Journal of Phycology* 35, 307–314.

Arce J.L., Layer P.W., Lassiter J.C., Benowitz J.A., Macías J.L. & Ramírez-Espinosa J. (2013) 40Ar/39Ar dating, geochemistry, and isotopic analyses of the quaternary Chichinautzin volcanic field, south of Mexico City: Implications for timing, eruption rate, and distribution of volcanism. *Bulletin of Volcanology* 75, 1–25.

Arce J.L., Layer P.W., Macías J.L., Morales-Casique E., García-Palomo A., Jiménez-Domínguez F.J., Benowitz J. & Vásquez-Serrano A. (2019) Geology and stratigraphy of the Mexico Basin (Mexico City), central Trans-Mexican Volcanic Belt. *Journal of Maps* 15, 320–332. Taylor and Francis Ltd.

Arce J.L., Macías J.L. & Vázquez-Selem L. (2003) The 10.5 ka Plinian erupion of Nevado de Toluca volcano, Mexico: Stratigraphy and hazard implications. *Geological Society of America Bulletin* 115, 230–248.

Avendaño D. & Caballero M. (2022a) *Cyclotella* (Bacillariophyceae) species present in sediments dating to Marine Isotope Stage 5 from Lake Chalco, central Mexico, with special reference to two new species: *Cyclotella poyeka* and *Cyclotella tlalocii*. *Diatom Research* 36, 323–344.

Avendaño D., Caballero M. & Vázquez G. (2022b) Diversity and distribution of lacustrine diatoms along the Trans-Mexican Volcanic Belt. *Freshwater Biology* 1–15. https://doi.org/10.1111/fwb.14033

Avendaño D., Caballero M. & Vázquez G. (2021) Ecological distribution of *Stephanodiscus niagarae* Ehrenberg in central Mexico and niche modelling for its last glacial maximum habitat suitability in the Nearctic realm. *Journal of Paleolimnology* 66, 1–14.

Avendaño D., Caballero M., Ortega-Guerrero B., Lozano-García S. & Brown E. (2018) Environmental conditions at the end of the Isotopic Stage 6 (IS 6: > 130000 years) in the center of Mexico: Characterization of a section of laminated sediments from Lake Chalco. *Revista Mexicana de Ciencias Geologicas* 35, 168–178.

Battarbee R.W., Keister C.M. & Bradbury J.P. (1984) The frustule morphology and taxonomic relationship of *Cyclotella quillensisProceedigns of the 7th International Diatom Symposium* Bailey. In: pp. 173–184. Philadelphia.

Berger B., Crucifix M., Hodell D.A., Mangili C., McManus J.F., Otto-Bliesner B., Pol K., Raynaud D., Skinner L.C., Tzedakis P.C., Wolff E.W., Yin Q.Z., Abe-Ouchi A., Barbante C., Brovkin V., Cacho I., Capron E., Ferretti P., Ganopolski A., Grimalt J.O., Hönisch B., Kawamura K.A., Landais A., Margari V., Martrat B., Masson-Delmotte V., Mokeddem Z., Parrenin F., Prokopenko A.A., Rashid H., Schulz M. & Vazquez Riveiros N. (2016) Interglacials of the last 800,000 years. *Reviews of Geophysics* 54(1), 162-219.

Berger A., & Loutre M.F. (1991) Insolation values for the climate of the last 10 million of years. *Quaternary Science Reviews,* 10(4), 297–317, https://doi.org/10.1016/0277-3791(91)90033-Q

Bicudo, D.C., Tremarin, P.I., Almeida, P.D., Zorzal-Almeida, S., Wengrat, S., Faustino, S.B., Costa L., Bartozek E., Rocha A. Bicudo C. & Morales, E.A. (2016) Ecology and distribution of *Aulacoseira* species (Bacillariophyta) in tropical reservoirs from Brazil. *Diatom Research*, 31(3), 199-215.

Blaauw M. & Christeny J.A. (2011) Package 'rbacon': Age-Depth Modelling using Bayesian Statistics. https://cran.r-project.org/web/packages/rbacon/index.html

Blanchon P., Eisenhauer A., Fietzke J. & Liebetrau V. (2009) Rapid sea-level rise and reef back-stepping at the close of the last interglacial highstand. *Nature* 458, 881-884.

Blinn D.W. (1993) Diatom community structure along physicochemical gradients in saline lakes. *Ecology* 74, 1246–1263.

Blois J.L. & Hadly E.A. (2009) Mammalian response to Cenozoic climatic change. *Annual Review of Earth and Planetary Sciences* 37, 181–208.

Blois J.L. & Williams J.E. (2016) Quaternary Biogeography and Climate Change. *Encyclopedia of Evolutionary Biology* In: Kliman R. (Ed.) pp. 395-405. Academic Press.

Bradshaw E.G. & Anderson N.J. (2003) Environmental factors that control the abundance of *Cyclostephanos dubius* (Bacillariophyceae) in danish lakes, from seasonal to century scale. *European Journal of Phycology* 38, 265–276.

Bronk-Ramsey C. (2009) Bayesian Analysis of Radiocarbon Dates. *Radiocarbon* 51, 337–360.

Bronk-Ramsey C. (2008) Deposition models for chronological records. *Quaternary Science Reviews* 27, 42–60.

Brown E.T., Caballero M., Cabral Cano E., Fawcett P.J., Lozano-García S., Ortega B., Pérez L., Schwalb A., Smith V., Steinman B.A., Stockhecke M., Valero-Garcés B., Watt S., Wattrus N.J., Werne J.P., Wonik T., Myrbo A.E., Noren A.J., O'Grady R., Schnurrenberger D., Abarca R.M., Beltrán A.O., Caballero C., Cappio L., Cossio R., Ferland T., Hesse K., Kallmeyer J., Kumar D., Leon S.G., Martínez I., Noriega C.A., Preusser F., Rawson H., Soler A.M., Sosa-Nájera S., Villeda D.A. & Zeeden C. (2019) Scientific drilling of Lake Chalco, Basin of Mexico (MexiDrill). *Scientific Drilling* 26, 1–15.

Buendía-Flores M., Tavera R., Novelo E. & Espinosa-Matias S. (2019) Floristic composition and diversity of benthic diatoms of Lake Chalco, Mexico. *Revista Mexicana de Biodiversidad* 90, 1–18.

Burns N.M., Rockwell D.C., Bertram P.E., Dolan D.M. & Ciborowski J.J.H. (2005) Trends in temperature, Secchi depth and dissolved oxygen depletion rates in the central basin of Lake Erie, 1983–2002. *Journal of Great Lakes Research* 31, 35–49.

Caballero M., Lozano-García S., Ortega-Guerrero B. & Correa-Metrio A. (2019) Quantitative estimates of orbital and millennial scale climatic variability in central Mexico during the last ~40,000 years. *Quaternary Science Reviews* 205, 62–75.

Caballero M. & Ortega-Guerrero B. (1998) Lake Levels since about 40,000 Years Ago at Lake Chalco, near Mexico City. *Quaternary Research* 50, 69–79.

Caballero N., Nass Y. & Téllez B.G. (2015) Diatomeas como indicadoras paleoambientales en la formación Río Negro, Provincia de río Negro, Argentina. *Revista Brasileira de Paleontologia* 18, 443–454.

Cantoral-Uriza E. (1997) Diatomeas (Bacillariophyceae) de ambientes Loticos en la Cuenca baja de la Huasteca Potosina. Ph.D. Thesis, Universidad Nacional Autónoma de México, Mexico.

Cárdenes-Sandí G.M., Shadik C.R., Correa-Metrio A., Gosling W.D., Cheddadi R. & Bush M.B. (2019) Central American climate and microrefugia: A view from the last interglacial. *Quaternary Science Reviews* 205, 224–233.

Carvalho L.R., Cox E.J., Fritz S.C., Juggins S., Sims P.A., Gasse F. & Battarbee R.W. (1995) Standardizing the taxonomy of saline lake Cyclotella spp. *Diatom Research* 10, 229–240.

Ceballos G., Arroyo-Cabrales J. & Ponce E. (2010) Effects of Pleistocene environmental changes on the distribution and community structure of the mammalian fauna of Mexico. *Quaternary Research* 73, 464–473.

Chaffin, J.D., Mishra, S., Kuhaneck, R.M., Heckathorn, S.A., & Bridgeman, T.B. (2012) Environmental controls on growth and lipid content for the freshwater diatom, *Fragilaria capucina*: a candidate for biofuel production. *Journal of Applied Phycology*, 24(5), 1045–1051.

Chávez-Lara C.M., Lozano-García S., Ortega-Guerrero B., Caballero M., Avendaño D., & Brown E.T. (2022a) An ostracod-based record of paleoecological conditions during MIS6 and MIS5, from Lake Chalco, Basin of Mexico. *Journal of Paleoliminology* 67, 359–373.

Chávez-Lara C.M., Lozano-García S., Ortega-Guerrero B., Avendaño D., & Caballero M. (2022b) A Late Pleistocene (MIS4-MIS2) palaeohydrological reconstruction from Lake Chalco, Basin of Mexico. *Journal of South American Earth Sciences* 119, 103944.

Correa-Metrio A., Urrego D.H., Cabrera K.R. & Bush M.B. (2015) Package 'paleoMAS': Paleoecological Analysis. R package version 2.5-5. https://cran.microsoft.com/snapshot/2017-08-01/web/packages/paleoMAS/index.html

Correa-Metrio A., Dechnik Y., Lozano-García S. & Caballero M. (2014) Detrended correspondence analysis: A useful tool to quantify ecological changes from fossil data sets. *Boletín de la Sociedad Geológica Mexicana* 66, 135–143.

Correa-Metrio A., Bush M.B., Cabrera K.R., Sully S., Brenner M., Hodell D.A., Escobar J. & Guilderson T. (2012) Rapid climate change and no-analog vegetation in lowland Central America during the last 86,000 years. *Quaternary Science Reviews* 38, 63–75.

Cracraft J. & Prum R.O. (1988) Patterns and processes of diversification-speciation and historical congruence in some neotropical birds. *Evolution* 42, 603–620.

Davies S.J., Metcalfe S.E., Caballero M.E. & Juggins S. (2002) Developing diatom-based transfer functions for Central Mexican lakes. *Hydrobiologia* 467, 199–213.

Davis M.B. (1984) Climatic Instability, Time, Lags, and Community Disequilibrium. *Ecology, Evolution and Behavior* In: Diamond J.M. & Case T.J. (Eds.), pp. 269–284. Harper and Row, New York.

Emiliani C. (1955) Pleistocene temperatures. *The Journal of geology* 63, 538–578.

Ferrari L., Orozco-Esquivel T., Manea V. & Manea M. (2012) The dynamic history of the Trans-Mexican Volcanic Belt and the Mexico subduction zone. *Tectonophysics* 522–523, 122–149.

Figueroa-Rangel B.L., Olvera-Vargas M., Lozano-García S., Islebe G., Torrescano N., Sosa-Najera S., Castillo-Batista A.P. Del, Figueroa-Rangel B.L., Olvera-Vargas M., Castillo-Batista A.P. Del, Lozano-García S., Sosa-Najera S, Islebe G. & Torrescano N (2020) Forests Diversity in the Mexican Neotropics: A Paleoecological *Neotropical Diversification: Patterns and Processes* In: Rull V. & Carnaval A.C. (Eds.), pp. 449–473. Springer Nature Switzerland.

Fritz S.C. (1990) Twentieth-century salinity and water-level fluctuations in Devils Lake, North Dakota: Test of a diatom-based transfer function. *Limnology and Oceanography* 35(8), 1771–1781.

Fritz S.C., Baker P.A., Tapia P., Spanbauer T. & Westover K. (2012) Evolution of the Lake Titicaca basin and its diatom flora over the last ~370,000 years. *Palaeogeography, Palaeoclimatology, Palaeoecology* 317–318, 93–103.

Fritz S.C., Baker P.A., Seltzer G.O., Ballantyne A., Tapia P., Cheng H. & Edwards R.L. (2007) Quaternary glaciation and hydrologic variation in the South American tropics as reconstructed from the Lake Titicaca drilling project. *Quaternary Research* 68, 410–420.

Fritz S.C., Juggins S. & Battarbee R.W. (1993) Diatom assemblages and ionic characterization of Lakes of the northern great plains, North America: A tool for reconstructing past salinity and climate fluctuations. *Canadian Journal of Fisheries and Aquatic Sciences* 50, 1844–1856.

Gasse F. (1986) East African diatoms: Taxonomy, Ecological Distribution. Bibliotheca Diatomologica, Stuttgart, Germany.

Gasse F., Juggins S. & Khelifa L. Ben. (1995) Diatom-based transfer functions for inferring past hydrochemical characteristics of African lakes. *Palaeogeography, Palaeoclimatology, Palaeoecology* 117, 31–54.

Gasse F. & Tekaia F. (1983) Transfer functions for estimating paleoecological conditions (pH) from East African diatoms. *Hydrobiologia* 103, 85–90.

Gonzales L.M., Williams J.W. & Grimm E.C. (2009) Expanded response-surfaces: a new method to reconstruct paleoclimates from fossil pollen assemblages that lack modern analogues. *Quaternary Science Reviews* 28, 3315–3332.

Grimm E.C. (1987) CONISS: a FORTRAN 77 program for stratigraphically constrained cluster analysis by the method of incremental sum of squares. *Computers & Geosciences* 13, 13–35. Pergamon.

Groot M.H.M., Bogotá R.G., Lourens L.J., Hooghiemstra H., Vriend M., Berrio J.C., Tuenter E., Van Der Plicht J., Van Geel B., Ziegler M., Weber S.L., Betancourt A., Contreras L., Gaviria S., Giraldo C., González N., Jansen J.H.F., Konert M., Ortega D., Rangel O., Sarmiento G., Vandenberghe J., Van Der Hammen T., Van Der Linden M. & Westerhoff W. (2011) Ultra-high resolution pollen record from the northern Andes reveals rapid shifts in montane climates within the last two glacial cycles. *Climate of the Past* 7, 299–316.

Grootes P.M. & Stuiver M. (1997) Oxygen 18/16 variability in Greenland snow and ice with 10-3- to 105-year time resolution. *Journal of Geophysical Research: Oceans* 102, 26455–26470.

Haberyan K.A. & Horn S.P. (2022) An ecological anallysis of lacustrine diatoms in Costa Rica. *Hydrobiologia* 850, 537–563. https://doi.org/10.1007/s10750-022-05099-x

Häkansson H. (2002) A compilation and evaluation of species in the general *Stephanodiscus, Cyclostephanos* and *Cyclotella* with a new genus in the family Stephanodiscaceae, *Diatom Research*, 17:1, 1-139. https://doi.org/10.1080/0269249X.2002.9705534

Hecky R.E. & Kilham P. (1973) Diatoms in alkaline, saline lakes: Ecology and Geochemical implications. *Limnology and Oceanography* 18, 54–71.

Heinrich H. (1988) Origin and Consequences of Cyclic Ice Rafting in the Northeast Atlantic Ocean During the Past 130,000 Years. *Quaternary Research* 29, 142–152.

Hemming S.R. (2004) Heinrich events: Massive late Pleistocene detritus layers of the North Atlantic and their global climate imprint. *Reviews of Geophysics* 42, 1–43.

Herrera Hernández D. (2011) *Estratigrafía y análisis de facies de los sedimentos lacustres del Cuaternario tardío de la Cuenca de Chalco, México*. Master Thesis, Universidad Nacional Autónoma de México, Mexico City.

Hill E. L. (2006) *Quantitative Reconstruction of Eutrophication Histories in Central Mexican Lakes*. Ph.D. Thesis, University of Nottingham, United Kingdom.

Hodell D.A., Anselmetti F.S., Ariztegui D., Brenner M., Curtis J.H., Gilli A., Grzesik D.A., Guilderson T.J., Müller A.D., Bush M.B., Correa-Metrio A., Escobar J. & Kutterolf S. (2008) An 85-ka record of

climate change in lowland Central America. *Quaternary Science Reviews* 27, 1152–1165.

Holmes J.A., Metcalfe S.E., Jones H.L. & Marshall J.D. (2016) Climatic variability over the last 30 000 years recorded in La Piscina de Yuriria, a Central Mexican crater lake. *Journal of Quaternary Science* 31, 310–324.

Jiménez-Moreno G., Scott Anderson R. & Fawcett P.J. (2007) Orbital- and millennial-scale vegetation and climate changes of the past 225 ka from Bear Lake, Utah-Idaho (USA). *Quaternary Science Reviews* 26, 1713–1724.

Johnsen S.J., Clausen H.B., Dansgaard W., Gundestrup N.S., Hammer C.U., Andersen U., Andersen K.K., Hvidberg C.S., Dahl-Jensen D., Steffensen J.P., Shoji H., Sveinbjörnsdóttir Á. E., White J., Jouzel J. & Fisher D. (1997) The δ 18 O record along the Greenland Ice Core Project deep ice core and the problem of possible Eemian climatic instability. *Journal of Geophysical Research: Oceans* 102, 26397–26410.

Juggins S. (2019) *Package "rioja": Analysis of Quaternary Science Data*. R package version 0.9-21. https://cran.r-project.org/web/packages/rioja/index.html

Keith S.A., Newton A.C., Herbert R.J.H., Morecroft M.D. & Bealey C.E. (2009) Non-analogous community formation in response to climate change. *Journal for Nature Conservation* 17, 228–235.

Krammer K. & Lange-Bertalot H. (1991) 2/4. Bacillariophyceae. 4. Teil: Achnanthaceae. Kritische Ergänzungen zu Navicula (Lineolatae) und Gomphonema. *Sübwasserflora von Mitteleuropa* In: Ettl H., Gerloff J., Heynig H. & Mollenhauer D. (Eds.), p. 437. G. Fischer Verlag, Stuttgart-Jena.

Krammer K., Lange-Bertalot H., Håkansson H. & Nörpel M. (1991) 2/3 Bacillariophyceae. 3. Teil: Centrales, Fragilariaceae, Eunotiaceae. *Sübwasserflora von Mitteleuropa* In: Ettl H., Gerloff J., Heynig H. & Mollenhauer D. (Eds.), p. 576. G. Fischer Verlag, Stuttgart-Jena.

Krammer K. & Lange-Bertalot H. (1986) 2/1. Bacillariophyceae. 1. Teil: Naviculaceae. *Sübwasserflora von Mitteleuropa* In: Ettl H., Gerloff J., Heynig H. & Mollenhauer D. (Eds.), p. 876. G. Fischer Verlag, Stuttgart, Germany.

Krammer K. & Lange-Bertalot H. (1988) 2/2. Bacillariophyceae. 2. Teil: Bacillariaceae, Epithemiaceae, Surirellaceae. *Sübwasserflora von Mitteleuropa* In: Ettl H., Gerloff J., Heynig H. & Mollenhauer D. (Eds.), p. 596 184 Tafeln mit 1914 Figuren. G. Fischer Verlag, Stuttgart-New York.

Kusel-Fetzmann E. (1979) The algal vegetation of Neusiedlersee. In: *Neusiedlersee: The Limnology of a Shallow Lake in Central Europe* pp. 71–202.

Lashaway A.R. & Carrick H.J. (2010) Effects of light, temperature and habitat quality on meroplanktonic diatom rejuvenation in Lake Erie: implications for seasonal hypoxia. *Journal of Plankton Research* 32, 479–490.

Laskar J., Robutel P., Joutel F., Gastineau M., Correia A., Levrard B. (2004) A long-term numericalsolution for the insolation quantities of the Earth Astron. *Astrophys* 428, 261–285.

Lisiecki L.E. & Raymo M.E. (2005) A Pliocene-Pleistocene stack of 57 globally distributed benthic δ 18O records. *Paleoceanography* 20, 1–17.

Lozano-García S., Torres-Rodríguez E., Figueroa-Rangel B., Caballero M., Sosa-Nájera S., Ortega-Guerrero B., & Acosta-Noriega C. (2022) Vegetation history of a Mexican Neotropical basin from the late MIS 6 to early MIS 3: The pollen record of Lake Chalco. *Quaternary Science Reviews* 297, 107830.

Lozano-García S., Sosa-Nájera S., Pérez L., Acosta C., Brown E.T., Stockhecke M., Steinman B., Wattrus N., Ortega B., Caballero M., Cabral-Cano E., Caballero C., Soler A.M., Arciniega A., Martínez I., Cossio R., Vergara-Huerta F., Werne J., Kumar D., Ferland T., Fawcett P.J., Schwalb A., Garcés B.L.V., Schnurrenberger D., O'grady R., Noren A., Myrbo A., Bücker M., Wonik T., Watt S. & Valero-Garcés B.L. (2017) Perforación profunda en el lago de Chalco: reporte técnico. *Boletín de la Sociedad Geológica Mexicana* 69, 299–311.

Lozano-García S., Ortega-Guerrero B., Roy P.D., Beramendi-Orosco L., & Caballero M. (2015) Climatic variability in the northern sector of the American tropics since the latest MIS 3. *Quaternary Research* 69, 299–311.

Martínez-Abarca L.R., Lozano-García S., Ortega-Guerrero B., Chávez-Lara C.M., Torres-Rodríguez E., Caballero M., Brown E.T., Sosa-Nájera S., Acosta-Noriega C. & Sandoval-Ibarra V. (2021a) Environmental changes during MIS6-3 in the Basin of Mexico: A record of fire, lake productivity history and vegetation. *Journal of South American Earth Sciences* 109, 103231.

Martínez-Abarca L.R., Ortega-Guerrero B., Lozano-García S., Caballero M., Valero-Garcés B., McGee D., Brown E.T., Stockhecke M. & Hodgetts A.G.E. (2021b) Sedimentary stratigraphy of Lake Chalco (Central Mexico) during its formative stages. *International Journal of Earth Sciences* 110, 2519–2539.

Masson-Delmotte V., Stenni B., Pol K., Braconnot P., Cattani O., Falourd S., Kageyama M., Jouzel J., Landais A., Minster B., Barnola J. M., Chappellaz J., Krinner G., Johnsen S., Röthlisberger R., Hansen J., Mikolajewicz U. & Otto-Bliesner B. (2010) EPICA Dome C record of glacial and interglacial intensities. *Quaternary Science Reviews* 29, 113–128.

Montejano G., Cantoral-Uriza E.A. & Carmona-Jiménez J. (2004) Algas de ambientes lóticos en la cuenca baja del río Pánuco. *Biodiversidad de la Sierra Madre Oriental* In: Luna I., Morrone J.J. & Espinosa D. (Eds.), pp. 111–126. Las prensas de Ciencias, Universidad Nacional Autónoma de México, México.

Montejano G., Carmona-Jimenez J. & Cantoral-Uriza E.A. (2000) Algal communities from calcareous springs in La Huasteca, central México: A syntesis. *Aquatic Ecosystems of Mexico* In: Munawar M., Lawrence S.G., Munawar I.F. & Malley D.F. (Eds.), pp. 135–149. Backhuys, Leiden.

Moseley G.E., Spötl C., Cheng H., Boch R., Min A. & Edwards R.L. (2015) Termination-II interstadial/stadial climate change recorded in two stalagmites from the north European Alps. *Quaternary Science Reviews* 127, 229–239.

Nicholl J.A.L., Hodell D.A., Naafs B.D.A., Hillaire-Marcel C., Channell J.E.T. & Romero O.E. (2012) A Laurentide outburst flooding event during the last interglacial period. *Nature Geoscience* 5, 901–904.

Nikolova I., Yin Q., Berger A., Singh U.K. & Karami M.P. (2013) Climate of the Past Geoscientific Instrumentation Methods and Data Systems The last interglacial (Eemian) climate simulated by LOVE-CLIM and CCSM3. *Clim. Past* 9, 1789–1806.

Novelo E., Tavera R. & Ibarra C. (2007) *Bacillariophyceae from karstic wetlands in Mexico*. Biblioteca Diatomologica. Cramer, Stuttgart.

Oliva M.G., Lugo A., Alcocer J. & Cantoral-Uriza E.A. (2006) *Cyclotella alchichicana* sp. nov. from a saline mexican lake. *Diatom Research* 21, 81–89.

Ortega-Guerrero B., García S., Cruz, G., Salinas C., Caballero M., Reyes I., & Cabalelro L. (2022) Estratigrafía del Holoceno y Pleistoceno Superior del Lago de Xochimilco, centro de México. *Revista Mexicana de Ciencias Geológicas*. 39(2), 167-178.

Ortega-Guerrero B., Avendaño D., Caballero M., Lozano-García S., Brown E.T., Rodríguez A., García B., Barceinas H., Soler A.M. & Albarrán A. (2020) Climatic control on magnetic mineralogy during the late MIS 6- Early MIS 3 in Lake Chalco, central México. *Quaternary Science Reviews* 230, 106163.

Ortega-Guerrero B., Lozano-García S., Herrera-Hernández D., Caballero M., Beramendi-Orosco L., Bernal J.P., Torres-Rodríguez E. & Avendaño D. (2017) Lithostratigraphy and physical properties of lacustrine sediments of the last ca. 150 kyr from Chalco basin, central México. *Journal of South American Earth Sciences* 79, 507–524.

Padisák J. & Naselli-Flores L. (2021) Phytoplankton in extreme environments: importance and consequences of habitat permanency. *Hydrobiologia* 848, 157–176.

Pardi M.I. & Graham R.W. (2019) Changes in small mammal communities throughout the late Quaternary across eastern environmental gradients of the United States. *Quaternary International* 530–531, 80–87.

Patterson R.T. & Fishbein E. (1989) Re-examination of the statistical methods used to determine the number of point counts needed for micropaleontological quantitative research. *Journal of Paleontology* 63(2), 245–248.

Petit J.R., Jouzel J., Raynaud D., Barkov N.I., Barnola J.-M., Basile I., Bender M., Chappellaz J., Davisk M., Delaygue G., Delmotte M., Kotlyakov V.M., Legrand M., Lipenkov V.Y., Lorius C., Pé L., Ritz C.,

Saltzmank E. & Stievenard M. (1999) Climate and atmospheric history of the past 420,000 years from the Vostok ice core, Antarctica. *Nature* 399, 429–436.

Poulíčková A. & Jahn R. (2007) *Campylodiscus clypeus* (Ehrenberg) Ehrenberg ex Kützing: Typification, morphology and distribution. *Diatom Research* 22, 135–146.

R Development Core Team. (2009) R: a Language and Environment for Statistical Computing, *R Foundation for Statistical Computing*. Version 3.6.0. https://www.R-project.org/

Ramírez-Nava, M., Caballero, M., & Avendaño, D. (2022) Variabilidad morfológica y distribución ecológica de especies del género *Aulacoseira* (Bacillariophyceae) en cuerpos de agua del centro de México. *Revista Mexicana de Biodiversidad*, 93, e934197.

Reavie E.D., Barbiero R.P., Allinger L.E. & Warren G.J. (2014a) Phytoplankton trends in the Great Lakes, 2001-2011. *Journal of Great Lakes Research* 40, 618–639.

Reavie E.D., Heathcote A.J. & Shaw Chraïbi V.L. (2014b) Laurentian Great Lakes phytoplankton and their water quality characteristics, including a diatom-based model for paleoreconstruction of phosphorus. *PLoS ONE* 9(8), e104705.

Reimer P.J., Bard E., Bayliss A., Beck J.W., Blackwell P.G., Ramsey C.B., Buck C.E., Cheng H., Edwards R.L., Friedrich M., Grootes P.M., Guilderson T.P., Haflidason H., Hajdas I., Hatté C., Heaton T.J., Hoffmann D.L., Hogg A.G., Hughen K.A., Kaiser K.F., Kromer B., Manning S.W., Niu M., Reimer R.W., Richards D.A., Scott E.M., Southon J.R., Staff R.A., Turney C.S.M. & Plicht J. van der. (2013) IntCal13 and Marine13 Radiocarbon Age Calibration Curves 0–50,000 Years cal BP. *Radiocarbon* 55, 1869–1887.

Riboulleau A., Bout-Roumazeilles V. & Tribovillard N. (2014) Controls on detrital sedimentation in the Cariaco Basin during the last climatic cycle: Insight from clay minerals. *Quaternary Science Reviews* 94, 62–73.

Rull V. (2020) Organisms: adaption, extinction, and biogeographical reorganizations. In: *Quaternary Ecology, Evolution, and Biogeography* pp. 35–73.

Salm C.R., Saros J.E., Fritz S.C., Osburn C.L. & Reineke D.M. (2009) Phytoplankton productivity across prairie saline lakes of the Great Plains (USA): a step toward deciphering patterns through lake classification models. *Canadian Journal of Fisheries and Aquatic Sciences* 66, 1435–1448.

Saros J.E. & Fritz S.C. (2000) Changes in the growth rates of saline-lake diatoms in response to variation in salinity, brine type and nitrogen form. *Journal of Plankton Research* 22, 1071–1083.

Schmid A. (1995) Salt tolerance of diatoms of Neusiedlersee (Austria): A model study for palaeolimnological interpretations. *Landscapes and Life: studies in honour of Urve Miller* In: Robertson A.M., Risberg J. & Hicks S. (Eds.), pp. 463–470. PACT.

Schmid A. (1979) Influence of environmental factors on the development of the valve in diatoms. *Protoplasma* 99, 99–115.

Schmidt R., Kamenik C., Lange-Bertalot H. & Klee R. (2004) *Fragilaria* and *Staurosira* (Bacillariophyceae) from sediment surfaces of 40 lakes in the Austrian Alps in relation to environmental variables, and their potential for palaeoclimatology. *Journal of Limnology* 63(2), 171-189.

Schrader H.J. (1974. Proposal for a standarised method of cleaning diatom-bearing deep-sea and land-exposed marine sediments. *Nova Hedwigia Beih.* 45, 403-409.

Shackleton N. (1967) Oxygen Isotope Analyses and Pleistocene Temperatures Re-assessed. *Nature* 215, 15–17.

Shadik C.R. Cárdenes-SAndí G.M. Correa-Metrio, A. Edwards, R.L., Min, A. & Brush M.B. (2017) Glacial and interglacials in the Neotropics: a 130, 000-year diatom record from central Panama. *Journal of Paleolimnology*, 58, 497–510.

Sosa-Ceballos G., Gardner J.E., Siebe C. & Macías J.L. (2012) A caldera-forming eruption ~ 14,100 ^{14}C yr BP at Popocatépetl volcano, México: Insights from eruption dynamics and magma mixing. *Journal of Volcanology and Geothermal Research* 213–214, 27–40.

Spaulding S.A., Potapova M.G., Bishop I.W., Lee S.S., Gasperak T.S., Jovanoska E., Furey P.C. & Edlund M.B. (2021) 'Diatoms.org': supporting taxonomists, connecting communities. *Diatom Research* 36, 291–304.

Theriot E.C. & Stoermer E.F. (1984) Principal component analysis of character variation in Stephanodiscus niagarae Ehrenb.: Morphological variation related to Lake Trophic status. In: *7th International Diatom Symposium* pp. 97–111. Otto Koeltz Science Publishers, Koenigstein.

Torres-Rodríguez E., Figueroa-Rangel B.L., Lozano-García S., Ortega-Guerrero B., Caballero-Miranda M. & Herrejon-Serrano A. (2022) Charcoal morphotypes and potential fuel types from a Mexican lake during MIS 5a and MIS 3. *Journal of South American Earth Sciences* 115, 103724.

Torres-Rodríguez E., Lozano-García S., Caballero-Miranda M., Ortega-Guerrero B., Sosa-Nájera S. & Debajyoti-Roy P. (2018) Pollen and non-pollen palynomorphs of Lake Chalco as indicators of paleolimnological changes in high-elevation tropical central Mexico since MIS 5. *Journal of Quaternary Science* 33, 945–957.

Torres-Rodríguez E., Lozano-García S., Roy P., Ortega B., Beramendi-Orosco L., Correa-Metrio A. & Caballero M. (2015) Last Glacial droughts and fire regimes in the central Mexican highlands. *Journal of Quaternary Science* 30, 88–99.

Turney C.S.M. & Jones R.T. (2010) Does the Agulhas Current amplify global temperatures during super-interglacials? *Journal of Quaternary Science* 25, 839–843.

Valera-Fernández D., Solleiro-Rebolledo E., López-Martínez R.A., Pi-Puig T., Salgado-Garrido H. & Cabadas-Báez H. (2020) Quaternary carbonates on the coast of the Yucatan Peninsula and the island of Cozumel, Mexico: Paleoenvironmental implications. *Journal of South American Earth Sciences* 102, 102670.

Van Dam H., Mertens A. & Sinkeldam J. (1994) A coded checklist and ecological indicator values of freshwater diatoms from The Netherlands. *Netherlands Journal of Aquatic Ecology 28*, 117–133. Kluwer Academic Publishers.

Vázquez-Selem L. & Heine K. (2011) Late Quaternary Glaciation in Mexico. *Developments in Quaternary Science* In: Ehlers J., Gibbard P.L. & Hughes P.D. (Eds.), pp. 849–861.

Vélez-Agudelo C., Espinosa M., Fayó R. & Isla F. (2017) Modern diatoms from a temperate river in South America: the Colorado River (North Patagonia, Argentina). *Diatom Research* 32, 133–152.

Waliser D.E. & Somerville R.C.J. (1994) Preferred Latitudes of the Intertropical Convergence Zone. *Journal of Atmospheric Sciences* 51, 1619–1639.

Williams J.W. & Jackson S.T. (2007) Novel climates, no-analog communities, and ecological surprises. *Frontiers in Ecology and the Environment* 5(9), 475-482.

Wilson S.E., Cumming, B.F., & Smol, J.P. (1996) Assessing the reliability of salinity inference models from diatom assemblages: an examination of a 219-lake data set from western North America. *Canadian Journal of Fisheries and Aquatic Sciences*, 53(7), 1580-1594.

Ziegler M., Nürnberg D., Karas C., Tiedemann R. & Lourens L.J. (2008) Persistent summer expansion of the Atlantic Warm Pool during glacial abrupt cold events. *Nature Geoscience* 1, 601–605.

Zawisza E., Cuna E., Caballero M., Ruiz-Fernandez A.C., Szeroczynska K., Woszczyk M., & Zawiska I. (2008) Environmental changes during the last millennium recorded in subfossil Cladocera, diatoms and sediments geochemistry from Lake El Sol (Central Mexico). *Geological Quarterly* 61, 81–90.

Capítulo VII

7. Síntesis: Discusión final y conclusiones.

Este proyecto de tesis representa un acercamiento a la distribución ecológica de las diatomeas, confirmando su facultad como indicadoras para inferir cambios climáticos del pasado. Específicamente, para hacer inferencias de cambios climáticos durante los últimos 150 mil años (Cuaternario tardío).

La primera parte de esta tesis (Ortega-Guerrero et al. 2020) permitió conocer de forma general el cambio de las asociaciones de diatomeas y a partir de un enfoque multiproxy inferir las variaciones climáticas pasadas. En el capítulo II (Ortega-Guerrero et al. 2020) se realizó una primera clasificación de las asociaciones de diatomeas del registro de Chalco reconociendo cuatro grupos: *Stephanodiscus* spp., pequeñas Fragilareaceae, alcalíphilas y halophilas, identificadas con los estudios previos del sitio de estudio (Caballero et al. 2019). La distribución casi opuesta de las *Stephanodiscus* spp. y pequeñas Fragilareaceae respecto a los taxones alcalífilos y halófilos permitió inferir cambios en el nivel del lago, asociando a las *Stephanodiscus* spp. y pequeñas Fragilareaceae a condiciones de agua dulce y un lago relativamente profundo, mientras que las especies alcalífilas y halófilas se relacionan con un lago somero. Además, se observa una correlación entre la suma de las especies alcalífilas y halófilas con los análisis geoquímicos de Ca/Ti. Esta relación entre ambos proxies permite asociar el origen de los carbonatos a ambientes de condiciones secas y alta evaporación, ya que en dichos ambientes la concentración de sales tiende a incrementarse (Hardie et al. 1978, Haberzettl et al. 2007), coincidiendo con la presencia de las especies alcalífilas y halófilas. Los minerales magnéticos en los sedimentos están controlados por minerales ferromagnéticos de baja coercitividad (Bh<125 mT), posiblemente retenidos por Ti-magnetita/maghemita detrítica parcialmente oxidada. Además, los procesos de meteorización o diagenéticos han alterado en diferentes grados la población mineral detrítica de baja coercitividad por oxidación parcial de las Ti-magnetitas (vía maghemitización). Además, la presencia de tefras en el registro no muestra correlación precisa con los cambios en el registro de diatomeas, quizá debido a que los eventos volcánicos son demasiado puntuales para ser comparados con la resolución temporal de las muestras. Sin embargo, se podría analizar el efecto que tiene de la presencia de las tefras analizando de manera puntual muestras de diatomeas antes, durante y después de varios eventos volcánicos. En las muestras analizadas que coincidieron con alguna tefra se observó una baja concentración de diatomeas, lo cual puede ser debido a que la presencia del material volcánico diluye la concentración de diatomeas.

La interpretación multiproxy (Ortega-Guerrero et al. 2020) señala el principal cambio ambiental en todos los parámetros analizados después de *ca*. 130 ka, al comienzo del último interglacial y durante todo el EI5. La mayor concentración magnética y la mayor coercitividad, junto con un mayor contenido de carbonatos y la presencia de diatomeas alcalífilas y halófilas sugieren que se produjo una mayor oxidación de Ti-magnetitas durante los periodos secos, disminuyendo la amplitud de estos cambios en el EI4 (71-57 ka) y la primera parte del EI3 (57-35 ka). Así mismo, se observó una correlación entre las variaciones en los parámetros analizados con las oscilaciones climáticas a escala orbital en la primera parte del registro. La baja insolación de verano y primavera, así como la menor estacionalidad inhibieron la evaporación, favoreciendo los niveles altos del lago durante el EI6. Mientras que en el EI5 la correlación entre los máximos en la insolación de primavera y verano, y las condiciones más secas se observaron *ca.* 130-122 y 112-100 ka. La combinación de condiciones húmedo-frío/seco-caliente están relacionados con la transición global glacial/interglacial desde el EI6 hasta el subestadio 5e, lo que implica una fuerte influencia de la excentricidad. Sin embargo, durante la última glaciación entre 144-88 ka los cambios de insolación inducidos por la precesión controlaron la precipitación.

En la segunda parte que conforma esta tesis se identificaron diferentes respuestas de las diatomeas a los cambios climáticos del Cuaternario en el registro de Chalco. Debido a que las características particulares del nicho ecológico de una especie es lo que determina la forma en que dicha especie va a responder al cambio climático (Rue, 2020). En la investigación del capítulo III (Avendaño et al. 2021) se analizó el modelo de nicho ecológico de *Stephanodiscus niagarae* y la transferencia de su nicho al último máximo glacial. Se concluyó que esta especie es un indicador de ambientes ricos en nutrientes (mesotrófico-hipertrófico) con tendencia a la limitación por fósforo y de periodos fríos en México debido al desplazamiento latitudinal al sur de esta especie durante los periodos glaciales, confirmándose la existencia de un refugio glacial en el centro de México. Potencialmente, *S. niagarae* puede contribuir a reconstrucciones paleoclimáticas como marcador estratigráfico para periodos glaciales anteriores (Avendaño et al. 2021). Por ejemplo, los registros largos de Chalco (Lozano et al. 2019) y Xochimilco (Ortega-Guerrero et al. 2022) que abarcan varios ciclos glaciales. Además, se sugiere que *Stephanodiscus oregonicus* puede tener un nicho ecológico parecido a *S. niagarae* ya que ambas especies están presentes durante el EI6 y una parte del EI2.

En el capítulo IV (Avendaño & Caballero 2022), se lleva a cabo la descripción taxonómica de las especies del género *Cyclotella* y recientemente *Stephanocyclus* (género actualizado en 2022), que fueron dominantes durante las condiciones más cálidas del EI5-3, especialmente, en los sedimentos del EI5 se observó una alternancia dominada por estas cuatro especies de *Cyclotella* y *Stephanocyclus*. Este estudio (Avendaño & Caballero 2022) permitió conocer a detalle las estructuras que conforman dichos géneros, lo cual hizo posible la identificación de dos nuevas especies (*C. tlalocii* y *C. poyeka*). Prasad & Nienow (2006) plantean que las especies del género *Cyclotella* que poseen cámaras marginales complejas

(alveolos complejos) se encuentran en ambientes marinos, zonas costeras o prosperan en ecosistemas con altos niveles de salinidad. Sin embargo, las especies identificadas en este estudio son epicontinentales. Una de ellas posiblemente asociada a condiciones de agua dulce, ya que se encontró asociada con *Cyclostephanos dubius* y *Aulacoseira granulata*, especies que tienen una preferencia por ambientes de agua dulce y altas concentraciones de nutrientes. En cambio, *Cyclotella poyeka* puede estar asociada a condiciones de mayor salinidad, ya que se encontró con *Anomoeoneis costata, Rophalodia gibberula*, especies asociadas a condiciones salobres. *Stephanocyclus quillensis* y *S. meneghinianus* son especies conocidas por su tolerancia a la salinidad (Fritz et al., 1993) y que además se diferencian taxonómicamente de las dos especies nuevas porque presentan cámaras marginales sencillas (alveolos sencillos). *Stephanocyclus meneghinianus* está presente en varios intervalos del registro de Chalco, por el contrario, *C. tlalocii*, *C. poyeka* y *S. quillensis* dominan únicamente en un periodo corto dentro del EI5 (118 – 112 ka, 98 – 94 ka, 84 – 75 ka, respectivamente). Además, se observó que algunos de los especímenes de *Stephanocyclus quillensis* muestran una transición morfológica a *C. alchichicana* (ausencia de fultoportulae marginales en algunas costas) por lo que se sugiere que *S. quillensis* de Chalco es el posible ancestro de la especie endémica, *C. alchichicana*. Por otro lado, la aparición de las especies de *Cyclotella* indica que los cambios morfológicos, las cámaras marginales complejas, es otro tipo de respuesta que pueden presentar las especies como respuesta de adaptación al cambio climático. Sin embargo, el que estas especies se observen en un periodo de tiempo único dentro del registro sugiere que las condiciones fueron diferentes a los otros estadios isotópicos, evidenciando la presencia de comunidades no análogas a las modernas. En cambio, es diferente a lo que se observó con *Stephanodiscus niagarae*, quien también se ha observado en el EI6, subestadio 5d y EI2, así como en las etapas formativas del lago de Chalco (Martínez-Abarca et al. 2021b) y posiblemente pueda estar presente en diferentes secciones laminadas del registro (Brown et al. 2019).

Al realizar reconstrucciones paleoclimáticas un obstáculo que suele presentarse en ellas cuando abarcan decenas o cientos de miles de años, es el encontrarse con especies que no han sido identificadas previamente, lo cual dificulta las inferencias de las condiciones climáticas y fisicoquímicas del medio donde se encontraban. Para resolver esta dificultad se infirió la ecología de *C. poyeka* y *C. tlalocii* con base en las preferencias ecológicas de las especies con que estuvieron presentes. No obstante, la presencia de especies fósiles es un impedimento para realizar estimaciones cuantitativas como funciones de transferencia, para los momentos en que dominaron (Avendaño & Caballero 2022).

Las especies del género *Cyclotella* reportadas por Bradbury (1971) para el lago de Texcoco tienen una distribución estratigráfica similar a las especies encontradas en el registro de Chalco, por lo que se sugiere que la secuencia de Chalco se podría usar para correlacionar al primero. Esta conjetura también puede aplicarse al registro del Lago de Xochimilco (Ortega-Guerrero et al. 2022) debido a la cercanía de los lagos.

En el capítulo V (Avendaño et al. 2023a), para reafirmar el potencial de las diatomeas en las reconstrucciones paleoambientales y usarlas como referencia para éste y futuros

estudios, se analizaron los índices de diversidad y se realizaron análisis multivariados de las poblaciones modernas en 49 muestras de sedimento superficial provenientes de 46 lagos ubicados en la Faja Volcánica Transmexicana (FVTM). Los taxones de diatomeas modernas mostraron una mayor ocupación regional. En su mayoría fueron cosmopolitas, planctónicos o epipélicos, móviles con un alto potencial de dispersión. Hubo pocos taxones endémicos, que inesperadamente eran formas planctónicas o móviles con un alto potencial de dispersión, lo que sugiere que estaban restringidos principalmente por algún factor ambiental más que por las limitaciones de dispersión. No hubo evidencia de un patrón altitud-diversidad como el encontrado en otros estudios de diatomeas de agua dulce. En cambio, parece más probable que factores como el tamaño del lago, la salinidad, el pH o los nutrientes puedan ser determinantes de la diversidad de las especies. El análisis de las poblaciones modernas de diatomeas mostró un recambio total de las especies controlado principalmente por la salinidad, sin embargo, otras variables relacionadas fueron la temperatura, precipitación, profundidad y concentración de fósforo. Además, la distribución ecológica de las especies observadas en los lagos de la FVTM a lo largo del gradiente de salinidad apunta a un nivel de conservación de nichos entre diferentes regiones geográficas como el resto de Norteamérica y África. Así mismo, este estudio (Avendaño et al. 2023a) destacó la importancia de las variables climáticas en la distribución de especies de diatomeas cuando se analizan áreas geográficas relativamente amplias (como la FVTM) con grandes gradientes climáticos (temperatura o precipitación). Debido a que la salinidad y temperatura fueron las variables más importantes en el recambio ecológico de las especies, se desarrollaron óptimos de ambas variables mediante el método de promedios ponderados. Estas estimaciones de temperatura y salinidad permiten realizar reconstrucciones cuantitativas en momentos de enfriamiento o calentamiento.

Al comparar las asociaciones de diatomeas modernas (Capítulo V, Avendaño et al. 2023a) con las fósiles (Capítulo VI, Avendaño et al. 2023b) se observó que las poblaciones de diatomeas fósiles no están totalmente representadas en la base de datos de las poblaciones modernas de la FVTM. En el registro de Chalco hay 21 especies dominantes (abundancia > 50%). Quince de ellas se encuentran en ambas bases de datos (moderna y fósil), de las cuales cinco especies (*Aulacoseira granulata, Craticula elkab*, *Nitzschia frustulum Punctastriata mimetica* y *Stephanocyclus meneghinianus)* son abundantes (abundancia > 10%); mientras que las otras diez especies (*Anomoeoneis costata, Chaetoceros muelleri*, *Campylodiscus clypeus, Cocconeis placentula, Cyclostephanos dubius*, *Fragilaria capucina, Halamphora veneta*, *Nitzschia amphibia*, *N. palea* y *Stephanodiscus niagarae*) tienen una abundancia menor al 10%. Las seis especies que no están presentes en la base de datos moderna son: *Cyclotella poyeka, C. tlalocii*, *Surirella peisonis y Saurophora* sp. *Stephanodiscus oregonicus, Stephanocyclus quillensis*, esta discrepancia en la estructura ecológica de las diatomeas implica que las condiciones climáticas de los últimos 150 mil años tuvieron la suficiente magnitud para generar cambio en las comunidades a nivel regional.

Los mayores cambios en la sucesión ecológica de las diatomeas se dieron entre las especies de agua dulce *Stephanodiscus* spp. – pequeñas Fragilariaceae spp. – *Cocconeis placentula* contra las especies tolerantes a las sales dominadas por los géneros *Cyclotella* y *Stephanocyclus* spp. El periodo en que se observaron las variaciones de las anteriores asociaciones de diatomeas fue de los eventos fríos (final del EI6, EI5d, EI2) a eventos de alta evaporación (EI5e, EI5c-a, EI4, EI3, principios del EI1), estos cambios se caracterizan por ser variaciones a escala orbital (Avendaño et al. 2023b).

El alcance de este trabajo permitió evidenciar que incluso entre momentos glaciales no existen analogías absolutas o determinantes. Por ejemplo, en el caso de los máximos glaciales, el EI6 tuvo un mayor enfriamiento (-6 a -7°C) y fue más húmedo que el EI2 (~ -4 a -5 °C). Durante el EI6, los registros de polen en Petén Itzá y la vegetación tipo C_4 en calcretas de la costa de Yucatán y Cozumel señalan condiciones de aridez durante el PMG (Valera-Fernández et al. 2020a, 2020b, Cruz Silva 2018), mientras que en este trabajo (Avendaño et al. 2023b) se indica que las condiciones fueron húmedas, posiblemente implicando que las tendencias de humedad fueron opuestas entre el centro y sureste del país. La disminución de la temperatura ocasionó un desplazamiento de la ZCIT al sur, esto propició que las zonas de alta presión (Pacífico Norte y Bermuda) dominaran (Cheng et al. 2019), disminuyendo la presencia de lluvias al sureste del país. Además, el desplazamiento al sur de los vientos del este pudo causar que el transporte de humedad del Atlántico al mar del Caribe se modificara, igualmente, el debilitamiento de la Circulación Meridional del Atlántico pudo suscitar una reducción del vapor de agua, debilitando el flujo de bajo nivel del Caribe. La fuente de humedad en la zona centro del país pudo asociarse a frentes fríos, los cuales debieron ser más intensos que en el EI2. Lo cual pudo deberse a que el glaciar del Illinois (EI6) tuvo una mayor extensión al sur que el glaciar del Wisconsin (EI2) (Forman & Pierson 2002; Obrochta et al. 2014). Asimismo, el desplazamiento al sur de los vientos del oeste pudo favorecer la entrada de humedad en la zona centro del país.

Por otro lado durante interglaciales como el EI5e, las estimaciones de temperatura en Panamá sugieren que fue entre 1 a 2º C más cálido que en la actualidad (Cárdenes-Sandí et al. 2019); se esperaba que a partir de las asociaciones de diatomeas presentes sería posible indicar una diferencia climática entre ambos interglaciales (EI5e vs. EI1). Sin embargo, las asociaciones de diatomeas fueron similares durante ambos periodos, mostrando que en ambos eventos las condiciones fueron cálidas y secas estimando un calentamiento de 2 a 3°C mayor a la actualidad. Durante el último interglacial (EI5e) se vuelven a observar tendencias opuestas de las condiciones climáticas entre el centro y sureste del país, teniendo climas cálido-húmedos en la península de Yucatán (Cruz Silva 2018), mientras que el presente trabajo indica que en el centro de México las condiciones fueron cálidas y secas. Valera-Fernández et al. (2020a, 2020b) sugieren a partir de la composición isotópica de $\delta^{13}C$ en calcretas de la costa de Yucatán, que los climas fueron cálidos donde las tasas de evaporación superaron a las de precipitación. En la zona del sureste las principales fuentes de lluvia

pudieron ser ocasionadas por el desplazamiento al norte de la ZCIT, así como por el flujo de bajo nivel del Caribe, sin embargo, estos climas cálidos debieron ocasionar que el flujo de humedad que llegara al centro del país se evaporara debido al balance negativo, provocando una gran reducción en el nivel lacustre de Chalco.

Al comienzo de la última glaciación (EI5d), se observó un enfriamiento en el presente trabajo (Avendaño et al. 2023b) y en el registro de Petén-Itzá (Cruz Silva 2018). El registro de Chalco sugiere que el subestadio 5d inicialmente era tan frío como el EI6 y se mantuvo más frío y húmedo que EI2 (Avendaño et al. 2023b). Después del enfriamiento del subestadio 5d, las condiciones fueron variables en los registros paleoclimáticos del país señalando un ligero incremento de la temperatura de la península de Yucatán, aunque este cambio no determinó un remplazo completo de las comunidades vegetales, mientras que hacia el final del EI5 el espectro polínico señala condiciones frías y secas (Cruz Silva 2018). Al este del país, el registro de paleosuelos en Veracruz indica condiciones húmedas asociadas a suelos arcillosos con alto grado de meteorización de los minerales primarios durante los subestadios 5c-a (Solleiro-Rebolledo et al. 2022). Al sureste del país las condiciones de sequía pudieron deberse al desplazamiento al sur de la ZCIT. Además, las variaciones de temperatura superficial en el Océano Pacífico tropical, así como en el mar del Caribe y las variaciones en la Circulación meridional del Atlántico pudieron ocasionar fluctuaciones en el transporte de las masas de humedad hacia la zona sureste, este y noroeste del país (Bereither et al. 2012). Las condiciones de humedad que se observaron en el registro de Veracruz (Solleiro-Rebolledo et al. 2022) no concuerdan con las condiciones secas en el lago de Chalco (Avendaño et al. 2023b, Martínez-Abarca et al. 2021a), por lo que se sugiere que los climas cálidos en el centro de México debieron ocasionar que el flujo de humedad, proveniente del Golfo de México hacia la zona centro del país, se evaporara generando un balance negativo y provocando una gran reducción en el nivel lacustre de Chalco.

Durante los periodos glaciales (EI6, EI2) y los interglaciales (EI5e, EI1) se pudo percibir un recambio total de las diatomeas. En contraste, durante los EI4 y EI3 no se observaron las variaciones que se esperaban. Se pensaba que el EI4 sería un evento de agua dulce, mientras que el EI3 un evento de agua salobre; pero solamente ocurrieron pequeñas variaciones en la temperatura (-1 a +1°C), que se estima fueron similares a las condiciones modernas. Sin embargo, para el EI4 las condiciones que se observaron en el registro de Babícora (Roy et al. 2013) y sur de Estados Unidos (Li et al. 2004; Brook et al. 2006) sugieren climas húmedos, en cambio en la zona centro, este y sureste del país, los registros de Cuitzeo, Texcoco, Veracruz, Petén Itzá y el presente trabajo infieren condiciones secas (Badbury et al. 1971; Israde-Alcántara et al. 2002, 2010; Hodell et al. 2008; Cruz Silva 2018). Thompson & Anderson (2000) proponen que la gran humedad en el norte del país se debió al desplazamiento al sur de la zona de alta presión del Pacífico norte, facilitando la presencia de lluvias. El desplazamiento al sur de los vientos del este, así como el debilitamiento de la Circulación Meridional del Atlántico (Bereiter et al. 2012) pudieron ocasionar una reducción

del vapor de agua, disminuyendo las fuentes de precipitación provenientes del mar Caribe y Golfo de México. Las diferencias de temperatura entre el sureste y centro de México se pudieron deber a una variación en la altitud (Caballero et al. 2019).

Por otra parte, durante el EI3 los registros de Babícora, Cuitzeo, Pátzcuaro y Zacapu sugieren condiciones de humedad (Bradbury 2000, Israde-Alcántara et al. 2002, 2010, Ortega et al. 2002) tanto en la zona norte como al oeste de México, lo cual puede estar asociado con el restablecimiento del monzón Norteamericano. El registro de Texcoco (Bradbury et al. 1971) y el presente trabajo (Avendaño et al. 2023b) sugieren principalmente condiciones cálidas y secas. Sin embargo, otros registros del centro de México como el registro de Cuitzeo y Tlaxcala, el lago de Cuitzeo indica las condiciones de temperatura y humedad aumentaron ligeramente, favoreciendo un lago más profundo (Israde-Alcántara et al. 2002, 2010), en Tlaxcala se propone la presencia ecosistemas de humedades más extendidos que en la actualidad (Sedov et al., 2009). En cambio, en otros registros como los paleosuelos del Nevado de Toluca observaron fluctuaciones húmedas-secas (Sedov et al. 2003),

Así como en el lago de Tecocomulco que en al inicio (entre 50 – 42 ka cal AP) se presentan condiciones asociadas a un cuerpo de agua profundo y las comunidades vegetales establecen climas fríos y húmedos entre, pero después (entre 42 – 37 ka cal AP) las condiciones fluctúan reduciendo el nivel del lago y la vegetación indica climas ligeramente cálidos (Caballero et al. 1999)y también en el valle de Teotihuacán, donde los suelos se formaron en paisajes boscosos estables y húmedos que hacia el final del EI3 apuntan a climas estacionales (Solleiro-Rebolledo et al. 2011). Los registros del occidente sugieren una humedad más estable que los del oriente, lo que puede estar asociado con las fuentes de humedad provenientes del Golfo de México o el Pacífico tropical. Además, la resolución de las muestras permitió observar durante el EI4 y EI3 cambios rápidos en las asociaciones de diatomeas, similares a los observados en el registro de Petén Itzá (Hodell et al. 2008; Pérez et al. 2021). Caballero et al. (2019) observan tendencias climáticas similares entre ambos registros durante los eventos Heinrich (HS) 3-1, del mismo modo durante el HS6-4 se observan las mismas tendencias. Por ejemplo, en el evento HS6 y HS4, el registro de Petén Itzá (Pérez et al. 2021) indica que las condiciones fueron cálidas y secas, mientras el pico de pequeñas Fragilariaceae junto con los conjuntos *Stephanocyclus meneghinianus, Nitzschia frustulum* y *N. amphibia* señalan que también las condiciones fueron secas. Estas condiciones se pudieron deber al desplazamiento al sur de la ZCIT. Durante el HS5a las especies de ostrácodos en el registro de Petén Itzá indican condiciones ligeramente cálidas, lo cual coincide con el pico de pequeñas Fragilariaceae y la presencia de *Craticula elkab, Chaetoceros muellerii, Nitzschia palea* y *Staurophora* sp.

Durante el EI2, en la zona norte del país se infieren condiciones de humedad debido a la presencia de los lagos en Babícora y San Felipe (Roy et al. 2013, Ortega-Guerrero et al. 1999). Estas condiciones se pudieron asociar a los frentes fríos y la entrada de humedad por los vientos del oeste. Tanto en los registros glaciares de los volcanes del Nevado de Toluca,

Ajusco, Tancítaro, Malinche, Cofre de Perote (Vázquez-Selem & Heine 2011; Vázquez-Selem & Lachniet 2017) como los registros lacustres de Pátzcuaro (Bradbury 2000) y Chignahuapan (Caballero et al. 2002) indican una mayor humedad al oriente y occidente del país comparado con la zona central (Caballero et al. 2010). Aunque el registro de paleosuelos en Veracruz sugiere un suelo poco desarrollado con abundantes carbonatos pedogénicos, indicando climas secos (Solleiro-Rebolledo et al. 2022). Además, el registro de Petén Itzá indica un lago profundo, climas relativamente húmedos y la presencia comunidades vegetales no análogas a las modernas (Hodell et al. 2008). El desplazamiento al sur de la ZCIT pudo propiciar que los vientos del oeste llevaran humedad a la zona centro-oeste de la FVTM (Bradbury 2000), mientras que una menor estacionalidad y la presencia de frentes fríos pudieron llevar humedad a la zona sureste del país (Hodell et al. 2008). Las asociaciones de diatomeas del registro de Chalco mostraron un cambio a condiciones de agua dulce, además se presentó una sucesión ecológica de *Cocconeis placentula* a las pequeñas Fragilariaceae hacia el último máximo glacial (UMG), sugiriendo un incremento del nivel del lago en el UMG (Caballero et al. 2019, Avendaño et al. 2023b). Caballero et al. (2019) observan un patrón bimodal con dos episodios fríos y secos en el UMG, el primer pulso está asociado con el HS2 (24-23 ka cal. A P) y el segundo ca. 20-19 ka cal AP. Estos autores proponen que los contrastes estacionales, así como la baja insolación a principios y en la deglaciación del EI2 pueden explicar las condiciones húmedas en los registros de paleosuelos en Tlaxcala (Sedov et al. 2009), Teotihuacán (Solleiro-Rebolledo et al. 2006, 2011) y el Nevado de Toluca (Sedov et al. 2001). Además, en los registros de Petén-Itzá y Chalco se observaron condiciones similares de rápidos enfriamientos y condiciones secas asociados a los eventos HS2-0 que pudieron estar asociados al desplazamiento al sur de la ZCIT (Caballero et al. 2019).

Referencias

ARCE, J.L., LAYER, P.W., LASSITER, J.C., BENOWITZ, J.A., MACÍAS, J.L., RAMÍREZ-ESPINOSA, J. (2013). 40Ar/39Ar dating, geochemistry, and isotopic analyses of the quaternary Chichinautzin volcanic field, south of Mexico City: Implications for timing, eruption rate, and distribution of volcanism. *Bull. Volcanol.* 75, 1–25. https://doi.org/10.1007/s00445-013-0774-6

AVENDAÑO, D., CABALLERO, M., ORTEGA-GUERRERO, B., LOZANO-GARCÍA, S., BROWN, E., (2018). Environmental conditions at the end of the Isotopic Stage 6 (IS 6: > 130000 years) in the center of Mexico: Characterization of a section of laminated sediments from Lake Chalco. *Rev. Mex. Ciencias Geol.* 35, 168–178. https://doi.org/10.22201/cgeo.20072902e.2018.2.649

AVENDAÑO D., CABALLERO M. & VÁZQUEZ G. (2021). Ecological distribution of *Stephanodiscus niagarae* Ehrenberg in central Mexico and niche modeling for its last glacial maximum habitat suitability in the Nearctic realm. *Journal of Paleolimnology* 66: 1–14. https://doi.org/10.1007/s10933-021-00178-w

AVENDAÑO D. & CABALLERO M. (2022). *Cyclotella* (Bacillariophyceae) species present in sediments dating to Marine Isotope Stage 5 from Lake Chalco, central Mexico, with special reference to two new species: *Cyclotella poyeka* and *Cyclotella tlalocii*. *Diatom Research* 36: 323–344. https://doi.org/10.1080/0269249X.2021.2010808

AVENDAÑO D., CABALLERO M. & VÁZQUEZ G. (2023a). Diversity and distribution of lacustrine diatoms along the Trans-Mexican Volcanic Belt. *Freshwater Biology*. 68:391-405. https://doi.org/10.1111/fwb.14033

AVENDAÑO D., CABALLERO M. ORTEGA-GUERRERO B., & LOZANO-GARCÍA S. (2023b). Response of diatom assemblages to orbital and millennial-scale climatic variability since the penultimate glacial maximum in the Northern limit of the Neotropics. *Journal of Quaternary Science*. 00: 1-17. https://doi.org/10.1002/jqs.3507

ABURTO-OROPEZA O., BURELO-RAMOS C. M., EZCURRA E., EZCURRA P., HENRIQUEZ C. L., VANDERPLANK S. E. & ZAPATA F. (2021). Relict inland mangrove ecosystem reveals Last Interglacial sea levels. *Proceedings of the National Academy of Sciences* 118: 1–8.

ANDERSON, P., BENNIKE, O., BIGELOW, N., BRIGHAM-GRETTE, J., DUVALL, M., EDWARDS, M., FRÉCHETTE, B., FUNDER, S., JOHNSEN, S., KNIES, J., KOERNER, R., LOZHKIN, A., MARSHALL, S., MATTHIESSEN, J., MACDONALD, G., MILLER, G., MONTOYA, M., MUHS, D., OTTO-BLIESNER, B., OVERPECK, J., REEH, N., SEJRUP, H.P., SPIELHAGEN, R., TURNER, C., VELICHKO, A., (2006). Last Interglacial Arctic warmth confirms polar amplification of climate change. *Quat. Sci. Rev.* 25, 1383–1400. https://doi.org/10.1016/j.quascirev.2006.01.033

BARLOW, M., NIGAM, S., & BERBERY, E. H. (1998). Evolution of the North American monsoon system. *Journal of Climate*, *11*(9), 2238-2257.

BERGER B., CRUCIFIX M., HODELL D. A., MANGILI C., MCMANUS J. F., OTTO-BLIESNER B., POL K., RAYNAUD D., SKINNER L. C., TZEDAKIS P. C., WOLFF E. W., YIN Q. Z., ABE-OUCHI A., BARBANTE C., BROVKIN V., CACHO I., CAPRON E., FERRETTI P., GANOPOLSKI A., GRIMALT J. O., HÖNISCH B., KAWAMURA K. A., LANDAIS A., MARGARI V., MARTRAT B., MASSON-DELMOTTE V., MOKEDDEM Z., PARRENIN F., PROKOPENKO A. A., RASHID H., SCHULZ M. & VAZQUEZ RIVEIROS N. (2016). Interglacials of the last 800,000 years. *Reviews of Geophysics* 54(1):162-219. https://doi.org/10.1002/2015RG000482

BIRKS H.J.B. (2012). Overview of numerical methods in paleolimnology. En: Birks H. J. B., Lotter A. L., Juggins S., Smol J. P. (eds). Tracking Environmental Change Using Lake Sediments. Springer, London. pp19–92.

BLANCHON P., EISENHAUER A., FIETZKE J. & LIEBETRAU V. (2009). Rapid sea-level rise and reef back-stepping at the close of the last interglacial highstand. *Nature* 458:881-884.

BRADBURY, J. P. (2000). Limnologic history of Lago de Pátzcuaro, Michoacán, México for the past 48,000 years: impacts of climate and man. *Palaeogeography, Palaeoclimatology, Palaeoecology*, 163(1-2), 69-95.

BRADBURY, J. P. (1971). Paleolimnology of Lake Texcoco, Mexico. Evidence from diatoms 1. *Limnology and Oceanography*, *16*(2), 180-200.

BROWN, E.T., CABALLERO, M., CABRAL CANO, E., FAWCETT, P.J., LOZANO-GARCÍA, S., ORTEGA, B., PÉREZ, L., SCHWALB, A., SMITH, V., STEINMAN, B.A., STOCKHECKE, M., VALERO-GARCÉS, B., WATT, S., WATTRUS, N.J., WERNE, J.P., WONIK, T., MYRBO, A.E., NOREN, A.J., O'GRADY, R., SCHNURRENBERGER, D., ABARCA, R.M., BELTRÁN, A.O., CABALLERO, C., CAPPIO, L., COSSIO, R., FERLAND, T., HESSE, K., KALLMEYER, J., KUMAR, D., LEON, S.G., MARTÍNEZ, I., NORIEGA, C.A., PREUSSER, F., RAWSON, H., SOLER, A.M., SOSA-NÁJERA, S., VILLEDA, D.A., ZEEDEN, C., (2019). Scientific drilling of Lake Chalco, Basin of Mexico (MexiDrill). *Sci. Drill.* 26, 1–15. https://doi.org/10.5194/sd-26-1-2019

CABALLERO, M. (1997). Reconstrucción paleolimnológica del Lago de Chalco, México, durante el último máximo glaciar-El registro de diatomeas entre 34,000 y 15,000 años AP. *Revista Mexicana de Ciencias Geológicas*, *14*(1), 91-100.

CABALLERO, M., LOZANO-GARCÍA, S., ORTEGA-GUERRERO, B., & CORREA-METRIO, A. (2019). Quantitative estimates of orbital and millennial scale climatic variability in central Mexico during the last ∼40,000 years. *Quat. Sci. Rev.* 205, 62–75. https://doi.org/10.1016/j.quascirev.2018.12.002

CABALLERO, M., LOZANO-GARCÍA, S., VÁZQUEZ-SELEM, L., & ORTEGA-GUERRERO, B. (2010). Evidencias de cambio climático y ambiental en registros glaciares y cuancas lacustres del centro de México durante el último máximo glaciar. *Boletín la Soc. Geológica Mex*. 62, 359–377.

CABALLERO, M., ORTEGA, B., VALADEZ, F., METCALFE, S., MACIAS, J. L., & SUGIURA, Y. (2002). Sta. Cruz Atizapán: a 22-ka lake level record and climatic implications for the late Holocene human occupation in the Upper Lerma Basin, Central Mexico. *Palaeogeography, Palaeoclimatology, Palaeoecology*, 186 (3-4), 217-235.

CABALLERO, M., LOZANO, S., ORTEGA, B., URRUTIA, J., & MACIAS, J. L. (1999). Environmental characteristics of Lake Tecocomulco, northern Basin of Mexico, for the last 50,000 years. *Journal of Paleolimnology*, *22*(4).

CABALLERO, M., & ORTEGA GUERRERO, B. (1998). Lake Levels since about 40,000 Years Ago at Lake Chalco, near Mexico City. *Quat. Res*. 50, 69–79. https://doi.org/https://doi.org/10.1006/qres.1998.1969

CABALLERO-RODRÍGUEZ D., CORREA-METRIO A. (2017). Métodos cuantitativos para la reconstrucción paleoambiental. En: Paleobioindicadores lacustres neotropicales. Pérez L., Massaferro J., Correa-Metrio A., & Rubio K. (Eds.) México: *CONACYT*. pp.205-219

CÁRDENES-SANDÍ, G.M., SHADIK, C.R., CORREA-METRIO, A., GOSLING, W.D., CHEDDADI, R., BUSH, M.B., (2019). Central American climate and microrefugia: A view from the last interglacial. *Quat. Sci. Rev*.

205, 224–233. https://doi.org/10.1016/j.quascirev.2018.12.021

CASTILLO, R. R., & MORÁN, T. G. (1989). Comportamiento hidrodinámico del sistema acuífero de la subcuenca de Chalco, México. *Geofísica Internacional*, *28*(2), 207-217.

CEBALLOS G, ARROYO-CABRALES J, PONCE E (2010) Effects of Pleistocene environmental changes on the distribution and community structure of the mammalian fauna of Mexico. *Quat Res* 73:464–473. https://doi.org/10.1016/j.yqres.2010.02.006

CHENG H., SPRINGER G. S., SINHA A., HARDT B. F., YI L., LI H., TIAN Y., LI X., ROWE H., KATHAYAT G., NING Y. & EDWARDS, R. L. (2019). Eastern North American climate in phase with fall insolation throughout the last three glacial-interglacial cycles. *Earth and Planetary Science Letters*, *522*, 125-134.

COOK, K. H., & VIZY, E. K. (2010). Hydrodynamics of the Caribbean low-level jet and its relationship to precipitation. *Journal of Climate*, *23*(6), 1477-1494

CORREA-METRIO, A., BUSH, M., LOZANO-GARCÍA, S., & SOSA-NÁJERA, S. (2013). Millennial-scale temperature change velocity in the continental northern neotropics. *PLoS One* 8, e81958. https://doi.org/10.1371/journal.pone.0081958

CORREA-METRIO A., BUSH M. B., CABRERA K. R., SULLY S., BRENNER M., HODELL D. A., ESCOBAR J. & GUILDERSON T. (2012). Rapid climate change and no-analog vegetation in lowland Central America during the last 86,000 years. *Quaternary Science Reviews* 38: 63–691 75.

CRUZ SILVA (2018) Historia de la vegetación de la península de Yucatán durante los últimos dos ciclos interglacial-glacial del Pleistoceno. Master thesis. Posgrado en Ciencias Biológicas, UNAM.

DANSGAARD, W., JOHNSEN, S.J., CLAUSEN, H.B., DAHL-JENSEN, D., GUNDESTRUP, N., HAMMER, C.U., & OESCHGER, H. (1984). North Atlantic Climatic Oscillations Revealed by Deep Greenland Ice Cores. *Clim. Process. Clim. Sensit*. 29, 288–298. https://doi.org/10.1029/GM029P0288

DÍAZ-RODRÍGUEZ, J. A. (2006). Los suelos Volcánico-lacustres de la ciudad de México. *Revista Internacional de Desastres Naturales, Accidentes e Infraestructura Civil*, *6*, 44.

EMILIANI, C. (1955). Pleistocene temperatures. *The Journal of Geology*, 63(6), 538-578.

FISCHER, H., WAHLEN, M., SMITH, J., MASTROIANNI, D. & DECK, B., (1999). Ice Core Records of Atmospheric CO_2 Around the Last Three Glacial Terminations. *Science* (80) 283, 1712–1714.

FRITZ S. C., BAKER P. A., TAPIA P., SPANBAUER T. & WESTOVER K. (2012). Evolution of the Lake Titicaca basin and its diatom flora over the last ~370,000 years. *Palaeogeography, Palaeoclimatology, Palaeoecology* 317–318: 93–103.

FRITZ S. C., BAKER P. A., SELTZER G. O., BALLANTYNE A., TAPIA P., CHENG H. & EDWARDS R. L. (2007). Quaternary glaciation and hydrologic variation in the South American tropics as reconstructed from the Lake Titicaca drilling project. *Quaternary Research* 68: 410–420.

GARCÍA ÁMARO, E. (2004). Modificaciones al Sistema de Clasificación Climática de Köppen. México, D.F., México: Instituto de Geografía, UNAM.

GARCÍA-MARTÍNEZ, I. M., & BOLLASINA, M. A. (2020). Sub-monthly evolution of the Caribbean Low-Level Jet and its relationship with regional precipitation and atmospheric circulation. *Climate Dynamics*, *54*,

4423-4440.

GRAHAM, R. W. (2005). Quaternary mammal communities: relevance of the individualistic response and non-analogue faunas. *The Paleontological Society Papers*, *11*, 141-158.

GROOT, M.H.M., BOGOTÁ, R.G., LOURENS, L.J., HOOGHIEMSTRA, H., VRIEND, M., BERRIO, J.C., TUENTER, E., VAN DER PLICHT, J., VAN GEEL, B., ZIEGLER, M., WEBER, S.L., BETANCOURT, A., CONTRERAS, L., GAVIRIA, S., GIRALDO, C., GONZÁLEZ, N., JANSEN, J.H.F., KONERT, M., ORTEGA, D., RANGEL, O., SARMIENTO, G., VANDENBERGHE, J., VAN DER HAMMEN, T., VAN DER LINDEN, M., & WESTERHOFF, W. (2011). Ultra-high resolution pollen record from the northern Andes reveals rapid shifts in montane climates within the last two glacial cycles. *Clim. Past* 7, 299–316. https://doi.org/10.5194/cp-7-299-2011

GOCHIS, D. J., BRITO-CASTILLO, L., & SHUTTLEWORTH, W. J. (2006). Hydroclimatology of the North American Monsoon region in northwest Mexico. *Journal of Hydrology*, *316*(1-4), 53-70.

GUO R. (2021). Cross-border environmental pollution and human health. In: Cross-Border Resource Management Fourth edition (ed. Guo R.) Elsevier. Amsterdam https://doi.org/10.1016/B978-0-323-91870-1.00010-0

HABERZETTL T., CORBELLA H., FEY M., JANSSEN S., LÜCKE A., MAYR C., OHLENDORF C., SCHÄBITZ F., SCHLESER G.H., WILLE M., WULF S & ZOLITSCHKA B. (2007). Lateglacial and Holocene wet--dry cycles in southern Patagonia: chronology, sedimentology and geochemistry of a lacustrine record from Laguna Potrok Aike, Argentina. Holocene 17, 297-310. https://doi.org/10.1177/0959683607076437

HANSEN., J. & SATO, M. (2012). Paleoclimate implications for Human-Made Climate Change. En: Berger, A., Mesinger, F., y Sijacki, D. (eds), Climate change: inferences from paleoclimate and regional aspects. Springer, Vienna, 21-49.

HARDIE L., SMOOT J.P & EUGSTER H.P. (1978). Saline lakes and their teposits: a sedimentological approach. En: Modern an Ancient Lake Sediments. Matter A. & Tucker M. E. (eds). The International Association of Sedimentologist. Blackwell Sccientific Publications, pp. 7-41.

HARRISON, S.P. & SANCHEZ GOÑI M.F. (2010). Global patterns of vegetation response to millennial-scale variability and rapid climate change during the last glacial period. *Quat. Sci. Rev.* 29, 2957–2980. https://doi.org/10.1016/j.quascirev.2010.07.016

HEINRICH, H. (1988) Origin and Consequences of Cyclic Ice Rafting in the Northeast Atlantic Ocean During the Past 130,000 Years. *Quaternary Research*, 29, pp. 142–152. https://doi.org/10.1016/0033-5894(88)90057-9

HODELL D. A., ANSELMETTI F. S., ARIZTEGUI D., BRENNER M., CURTIS J. H., GILLI A., GRZESIK D. A., GUILDERSON T. J., MÜLLER A. D., BUSH M. B., CORREA-METRIO A., ESCOBAR J. & KUTTEROLF S. (2008). An 85-ka record of climate change in lowland Central America. *Quaternary Science Reviews* 27: 1152–1165.

IMBRIE, J., HAYS, J. D., MARTINSON, D. G., MCINTYRE, A., MIX, A. C., MORLEY, J. J., PISIAS N.G., PRELL W.L. & SHACKLETON, N. J. (1984). The orbital theory of Pleistocene climate: support from a revised chronology of the marine $\delta^{18}O$ record. In: Milankovitch and Climate, Part I. Berger A. L. et al. (eds.) pp. 269-305.

ISRADE ALCÁNTARA, I., GARDUÑO-MONROY, V. H., & ORTEGA MURILLO, R. (2002). Paleoambiente lacustre del Cuaternario tardío en el centro del lago de Cuitzeo. *Hidrobiológica*, 12(1), 61-78.

ISRADE ALCÁNTARA, I., VELÁZQUEZ-DURÁN, R., LOZANO GARCÍA, M., BISCHOFF, J., DOMÍNGUEZ VÁZQUEZ, G., & GARDUÑO MONROY, V. H. (2010). Evolución Paleolimnológica del Lago Cuitzeo, Michoacán durante el Pleistoceno-Holoceno. *Boletín de la Sociedad Geológica Mexicana*, 62(3), 345-357.

JACKSON, S. T., WEBB, R. S., ANDERSON, K. H., OVERPECK, J. T., WEBB III, T., WILLIAMS, J. W., & HANSEN, B. C. (2000). Vegetation and environment in eastern North America during the last glacial maximum. *Quaternary Science Reviews*, *19*(6), 489-508.

JIMÉNEZ-MORENO, G., SCOTT ANDERSON, R. & FAWCETT, P. J. (2007) Orbital- and millennial-scale vegetation and climate changes of the past 225 ka from Bear Lake, Utah-Idaho (USA), *Quaternary Science Reviews*, 26(13–14) https://doi.org/10.1016/j.quascirev.2007.05.001.

JOHNSEN S. J., CLAUSEN H. B., DANSGAARD W., GUNDESTRUP N. S., HAMMER C. U., ANDERSEN U., ANDERSEN K. K., HVIDBERG C. S., DAHL-JENSEN D., STEFFENSEN J. P., SHOJI H., SVEINBJÖRNSDÓTTIR Á. E., WHITE J., JOUZEL J. & FISHER D. (1997). The $\delta^{18}O$ record along the Greenland Ice Core Project deep ice core and the problem of possible Eemian climatic instability. *Journal of Geophysical Research: Oceans* 102: 26397–26410.

KEITH S. A., NEWTON A. C., HERBERT R. J. H., MORECROFT M. D. & BEALEY C. E. 2009. Non-analogous community formation in response to climate change. *Journal for Nature Conservation* 17: 228–235.

KÖHLER, P., BINTANJA, R., FISCHER, H., JOOS, F., KNUTTI, R., LOHMANN, G., & MASSON-DELMOTTE, V. (2010). What caused Earth's temperature variations during the last 800,000 years? Data-based evidence on radiative forcing and constraints on climate sensitivity. *Quaternary Science Reviews*, *29*(1-2), 129-145.

KHURSEVICH, G. K., KARABANOV, E. B., PROKOPENKO, A. A., WILLIAMS, D. F., KUZMIN, M. I., & FEDENYA, S. A. (2001). Biostratigraphic significance of new fossil species of the diatom genera *Stephanodiscus* and *Cyclotella* from Upper Cenozoic deposits of Lake Baikal, Siberia. *Micropaleontology*, *47*(1), 47-71.

KULIKOVSKIY, M., GENKAL, S., MALTSEV, Y., GLUSHCHENKO, A., KUZNETSOVA, I., KAPUSTIN, D., GUSEV E., MARTYNENKO N. & KOCIOLEK, J. P. (2022). Resurrection of the diatom genus *Stephanocyclus* (Coscinodiscophyceae: Stephanodiscaceae) on the basis of an integrated molecular and morphological approach. *Fottea*, *22*(2), 181-191.

LACHNIET, M.S. & VAZQUEZ-SELEM, L. (2005). Last Glacial Maximum equilibrium line altitudes in the circum-Caribbean (Mexico, Guatemala, Costa Rica, Colombia, and Venezuela). *Quat. Int.* 138–139, 129–144. https://doi.org/10.1016/j.quaint.2005.02.010

LISIECKI, L. E. & RAYMO, M. E. (2005). A Pliocene-Pleistocene stack of 57 globally distributed benthic $\delta^{18}O$ records, *Paleoceanography*. American Geophysical Union, 20(1), pp. 1–17. https://doi.org/10.1029/2004PA001071.

LISIECKI, L.E., & STERN, J. V. (2016). Regional and global benthic δ18O stacks for the last glacial cycle. *Paleoceanography* 31, 1368–1394. https://doi.org/10.1002/2016PA003002

LOZANO-GARCÍA, S., TORRES-RODRÍGUEZ, E., FIGUEROA-RANGEL, B., CABALLERO, M., SOSA-NÁJERA, S., ORTEGA-GUERRERO, B., & ACOSTA-NORIEGA, C. (2022). Vegetation history of a Mexican Neotropical basin from the late MIS 6 to early MIS 3: The pollen record of Lake Chalco. *Quaternary Science Reviews*, *297*, 107830.

LOZANO-GARCÍA, S., SOSA-NÁJERA, S., PÉREZ, L., ACOSTA, C., BROWN, E.T., STOCKHECKE, M., STEINMAN, B.,

WATTRUS, N., ORTEGA, B., CABALLERO, M., CABRAL-CANO, E., CABALLERO, C., SOLER, A.M., ARCINIEGA, A., MARTÍNEZ, I., COSSIO, R., VERGARA-HUERTA, F., WERNE, J., KUMAR, D., FERLAND, T., FAWCETT, P.J., SCHWALB, A., GARCÉS, B.L.V., SCHNURRENBERGER, D., O´GRADY, R., NOREN, A., MYRBO, A., BÜCKER, M., WONIK, T., WATT, S., VALERO-GARCÉS, B.L., (2017). Perforación profunda en el lago de Chalco: reporte técnico. *Boletín la Soc. Geológica Mex*. 69, 299–311.

MAGAÑA, V., AMADOR, J. A., & MEDINA, S. (1999). The midsummer drought over Mexico and Central America. *Journal of Climate*, *12*(6), 1577-1588.

MARTÍNEZ-ABARCA, L.R., LOZANO-GARCÍA, S., ORTEGA-GUERRERO, B., CHÁVEZ-LARA, C.M., TORRES-RODRÍGUEZ, E., CABALLERO, M., BROWN, E.T., SOSA-NÁJERA, S., ACOSTA-NORIEGA, C., & SANDOVAL-IBARRA, V., (2021a). Environmental changes during MIS6-3 in the Basin of Mexico: A record of fire, lake productivity history and vegetation. *J. South Am. Earth Sci.* 109. https://doi.org/10.1016/j.jsames.2021.103231

MARTÍNEZ-ABARCA, L.R., ORTEGA-GUERRERO, B., LOZANO-GARCÍA, S., CABALLERO, M., VALERO-GARCÉS, B., MCGEE, D., BROWN, E.T., STOCKHECKE, M., & HODGETTS, A.G.E., (2021b). Sedimentary stratigraphy of Lake Chalco (Central Mexico) during its formative stages. Int. J. Earth Sci. 110, 2519–2539. https://doi.org/10.1007/s00531-020-01964-z

MASSON-DELMOTTE, V., STENNI, B., POL, K., BRACONNOT, P., CATTANI, O., FALOURD, S., KAGEYAMA, M., JOUZEL, J., LANDAIS, A., MINSTER, B., BARNOLA, J.M., CHAPPELLAZ, J., KRINNER, G., JOHNSEN, S., RÖTHLISBERGER, R., HANSEN, J., MIKOLAJEWICZ, U., & OTTO-BLIESNER, B. (2010). EPICA Dome C record of glacial and interglacial intensities. *Quat. Sci. Rev*. 29, 113–128. https://doi.org/10.1016/j.quascirev.2009.09.030

MCMANUS J. F., FRANCOIS R., GHERARDI J. M., KEIGWIN L. D., & BROWN-LEGER S. (2004). Collapse and rapid resumption of Atlantic meridional circulation linked to deglacial climate changes. *nature*, *428*(6985), 834-837.

METCALFE, S. E. (1992). *Changing environments of the Zacapu Basin, central Mexico: A diatom-based history spanning the last 30,000 years* (Vol. 48). School of Geography, University of Oxford.

METCALFE, S. E., BARRON, J. A., & DAVIES, S. J. (2015). The Holocene history of the North American Monsoon:'known knowns' and 'known unknowns' in understanding its spatial and temporal complexity. *Quaternary Science Reviews*, *120*, 1-27.

METCALFE, S., SAY, A., BLACK, S., MCCULLOCH, R., & O'HARA, S. (2002). Wet conditions during the last glaciation in the Chihuahuan Desert, Alta Babicora Basin, Mexico. *Quaternary Research*, 57(1), 91-101.

METCALFE, S. E., O'HARA, S. L., CABALLERO, M., & DAVIES, S. J. (2000). Records of Late Pleistocene–Holocene climatic change in Mexico—a review. *Quaternary Science Reviews*, *19*(7), 699-721.

MILANKOVITCH, M. (1941). Kanon der Erdbestrahlung und seine Anwendung auf das Eiszeitenproblem. *R. Serbian Acad. Spec. Publ.* 133, 1–633.

MUHS, D.R., SIMMONS, K.R., & STEINKE, B. (2002). Timing and warmth of the Last Interglacial period: new U-series evidence from Hawaii and Bermuda and a new fossil compilation for North America, *Quaternary Science Reviews. 21*(12-13), 1355-1383.

ORTEGA-GUERRERO B., GARCÍA S., CRUZ, G., SALINAS C., CABALLERO M., REYES I., & CABALLERO L. (2022). Estratigrafía del Holoceno y Pleistoceno Superior del Lago de Xochimilco, centro de México. *Revista Mexicana de Ciencias Geológicas*. 39(2):167-178.

ORTEGA-GUERRERO B., AVENDAÑO D., CABALLERO M., LOZANO-GARCÍA S., BROWN E., RODRÍGUEZ A., GARCÍA B., BARCEINAS H., SOLER A. M. & ALBARRÁN A. (2020). Climatic control on magnetic mineralogy during the late MIS 6 - early MIS 3 in Lake Chalco, central Mexico. *Quaternary Science Reviews 230*, 106163. https://doi.org/10.1016/j.quascirev.2020.106163

ORTEGA-GUERRERO, B., LOZANO-GARCÍA, S., HERRERA-HERNÁNDEZ, D., CABALLERO, M., BERAMENDI-OROSCO, L., BERNAL, J.P., TORRES-RODRÍGUEZ, E., AVENDAÑO, D. (2017). Lithostratigraphy and physical properties of lacustrine sediments of the last ca. 150 kyr from Chalco basin, central México. *J. South Am. Earth Sci.* 79, 507–524. https://doi.org/10.1016/j.jsames.2017.09.003

ORTEGA-GUERRERO B., VÁZQUEZ, G., CABALLERO, M., ISRADE, I., LOZANO-GARCÍA, S., SCHAAF, P., & TORRES, E. (2010). Late Pleistocene: Holocene record of environmental changes in lake Zirahuen, Central Mexico. *Journal of Paleolimnology*, *44*, 745-760.

ORTEGA-GUERRERO, B., LOZANO GARCÍA, M., CABALLERO, M., & HERRERA HERNÁNDEZ, D. A. (2015). Historia de la evolución deposicional del lago de Chalco, México, desde el MIS 3. *Boletín de la Sociedad Geológica Mexicana,* 67(2), 185-201.

ORTEGA-GUERRERO, B., CABALLERO, C., LOZANO, S., ISRADE, I., & VILACLARA, G. (2002). 52 000 years of environmental history in Zacapú basin, Michoacán, Mexico: the magnetic record. *Earth and Planetary Science Letters,* 202(3-4), 663-675.

GUERRERO, B. O., THOMPSON, R., & FUCUGAUCHI, J. U. (2000). Magnetic properties of lake sediments from Lake Chalco, central Mexico, and their palaeoenvironmental implications. *Journal of Quaternary Science: Published for the Quaternary Research Association*, *15*(2), 127-140.

ORTEGA-GUERRERO, B., CABALLERO MIRANDA, M., LOZANO GARCÍA, S., & DE LA O VILLANUEVA, M. (1999). Palaeoenvironmental record of the last 70,000 yr in San Felipe Basin, Sonora desert, Mexico: Preliminary results. *Geofisica Internacional* 38(3), 1-11.

ORTIZ ZAMORA, D. D. C., & ORTEGA GUERRERO, M. A. (2007). Origen y evolución de un nuevo lago en la planicie de Chalco: implicaciones de peligro por subsidencia e inundación de áreas urbanas en Valle de Chalco (Estado de México) y Tláhuac (Distrito Federal). *Investigaciones geográficas*, (64), 26-42.

OSTER, J. L., IBARRA, D. E., WINNICK, M. J., & MAHER, K. (2015). Steering of westerly storms over western North America at the Last Glacial Maximum. *Nature Geoscience*, *8*(3), 201-205.

PAILLÈS, C., SYLVESTRE, F., TONETTO, A., MAZUR, J. C., & CONROD, S. (2020). New fossil genus and new extant species of diatoms (Stephanodiscaceae, Bacillariophyceae) from Pleistocene sediments in the Neotropics (Guatemala, Central America): adaptation to a changing environment?. *European Journal of Taxonomy*, *726*, 1-23.

PARDI MI, GRAHAM RW (2019) Changes in small mammal communities throughout the late Quaternary across eastern environmental gradients of the United States. *Quat Int* 530–531:80–87. https://doi.org/10.1016/j.quaint.2018.05.041

PRASAD A. K., & NIENOW J. A. (2006). The centric diatom genus *Cyclotella*, (Stephanodiscaceae: Bacillariophyta) from Florida Bay, USA, with special reference to *Cyclotella choctawhatcheeana* and

Cyclotella desikacharyi, a new marine species related to the *Cyclotella striata* complex. *Phycologia*, *45*(2), 127-140.

PÉREZ, L., CORREA-METRIO, A., COHUO, S., GONZÁLEZ, L. M., ECHEVERRÍA-GALINDO, P., BRENNER, M., CURTIS J. KUTTEROLF S., STOCKHECKE M., SCHENK F., BAUERSACHS T., & SCHWALB, A. (2021). Ecological turnover in neotropical freshwater and terrestrial communities during episodes of abrupt climate change. *Quaternary Research*, *101*, 26-36.

RAYMO, M.E. (1997). The timing of major climate terminations. *Paleoceanography* 12, 577–585. https://doi.org/10.1029/97PA01169

RIVEIROS, N. V., TOUCANNE, S., RODRIGUES, T., LANDAIS, A., NAUGHTON, F., & GOÑI, M. F. S. (2022). Definition of the Last Glacial Cycle marine stages and chronology. In *European Glacial Landscapes*. (ed. Palacios D., García-Ruiz J., Hughes P. D. & Andrés N.) pp. 171-173. Elsevier. Amsterdam https://doi.org/10.1016/B978-0-12-823498-3.00023-6

ROY, P. D., QUIROZ-JIMÉNEZ, J. D., PÉREZ-CRUZ, L. L., LOZANO-GARCÍA, S., METCALFE, S. E., LOZANO-SANTACRUZ, R., LÓPEZ-BALBIAUX N., SÁNCHEZ-ZAVALA J.L. & ROMERO, F. M. (2013). Late Quaternary paleohydrological conditions in the drylands of northern Mexico: a summer precipitation proxy record of the last 80 cal ka BP. *Quaternary Science Reviews*, *78*, 342-354.

ROY, P. D., CABALLERO M., LOZANO R., ORTEGA B., LOZANO S., PI T., ISRADE I. & MORTON O. (2010). Geochemical record of Late Quaternary paleoclimate from lacustrine sediments of paleo-lake San Felipe, western Sonora Desert, Mexico. Journal of South American Earth Sciences. 29: 586-596.

SÁNCHEZ-GOÑI, M. F. & HARRISON, S. P. (2010). Millennial-scale climate variability and vegetation changes during the Last Glacial: Concepts and terminology. *Quaternary Science Reviews*, *29*(21-22), 2823-2827.

SEDOV S., SOLLEIRO-REBOLLEDO E., TERHORST B., SOLÉ J., FLORES-DELGADILLOM. D. L., WERNER G., & POETSCH T. (2009). The Tlaxcala basin paleosol sequence: a multiscale proxy of middle to late Quaternary environmental change in central Mexico. *Revista mexicana de ciencias geológicas*, *26*(2), 448-465.

SEDOV S., SOLLEIRO-REBOLLEDO E., MORALES-PUENTE P., ARIAS-HERREÌA A., VALLEJO-GÒMEZ E., & JASSO-CASTAÑEDA C. (2003). Mineral and organic components of the buried paleosols of the Nevado de Toluca, Central Mexico as indicators of paleoenvironments and soil evolution. *Quaternary International*, *106*, 169-184.

SERVICIO METEOROLÓGICO NACIONAL, MÉXICO (2023). Información obtenida el 18 de enero de 2023 de https://smn.conagua.gob.mx/es/climatologia/informacion-climatologica/informacion-estadistica-climatologica Estación Tláhuac – 9051. Datos de 1981-2010.

SHADIK C. R. CÁRDENES-SANDÍ G. M. CORREA-METRIO, A. EDWARDS, R. L., MIN, A. & BRUSH M. B. (2017). Glacial and interglacials in the Neotropics: a 130, 000-year diatom record from central Panama. *Journal of Paleolimnology*, 58: 497–510.

SHACKLETON, N. J. (1969). The last interglacial in the marine and terrestrial records. *Proceedings of the Royal Society of London. Series B. Biological Sciences*, *174*(1034), 135-154.

SHACKLETON, N.J., FERNANDA SÁNCHEZ-GOÑI, M., PAILLER, D., LANCELOT, Y., 2003. Marine Isotope Substage 5e and the Eemian Interglacial. *Glob. Planet. Change* 36, 151–155. https://doi.org/10.1016/S0921-8181(02)00181-9

SHACKLETON, N.J. & OPDYKE, N.D. (1973). Oxygen isotope and paleomagnetic stratigraphy of equatorial Pacific Core V28-238: oxygen isotope temperatures and ice volume on a 10^5 year and 10^6 year scale. *Quaternary Research*, **3**, 39-55, https://doi.org/10.1016/0033-5894(73)90052-5

SOLLEIRO-REBOLLEDO, E., SEDOV, S., TERHORST, B., LÓPEZ-MARTÍNEZ, R., DÍAZ-ORTEGA, J., DÍAZ-HERNÁNDEZ, Y., VALERA-FERNÁNDEZ D., CABADAS-BÁEZ H. & TSUKAMOTO, S. (2022). Late Quaternary paleosols and landscape evolution in dune systems of Veracruz at the Gulf of Mexico coast. *Quaternary International*, *618*, 70-86. https://doi.org/10.1016/j.quaint.2021.05.016

SOLLEIRO-REBOLLEDO E., SYCHEVA S., SEDOV S., DE TAPIA E. M., RIVERA-URIA, Y., SALCIDO-BERKOVICH C. & KUZNETSOVA A. (2011). Fluvial processes and paleopedogenesis in the Teotihuacan Valley, México: Responses to late Quaternary environmental changes. *Quaternary International*, *233*(1), 40-52.

SOLLEIRO-REBOLLEDO E., SEDOV S., DE TAPIA E. M., CABADAS H., GAMA-CASTRO J., & VALLEJO-GÓMEZ E. (2006). Spatial variability of environment change in the Teotihuacan Valley during the Late Quaternary: Paleopedological inferences. *Quaternary International*, *156*, 13-31.

STERN, J. V., LISIECKI, L.E., (2014). Termination 1 timing in radiocarbon-dated regional benthic $\delta^{18}O$ stacks. *Paleoceanogr. Paleoclimatology* 29, 1127–1142. https://doi.org/10.1002/2014PA002700

THOMPSON, R. S., & ANDERSON, K. H. (2000). Biomes of western North America at 18,000, 6000 and 0 14C yr BP reconstructed from pollen and packrat midden data. *Journal of Biogeography*, *27*(3), 555-584.

TIWARI, M., SINGH, A. K., & SINHA, D. K. (2015). Stable isotopes: Tools for understanding past climatic conditions and their applications in chemostratigraphy. In *Chemostratigraphy* (ed. Ramkumar Mu). Elsevier, Amsterdam. pp. 65-92

TORRES-RODRÍGUEZ, E., FIGUEROA-RANGEL, B.L., LOZANO-GARCÍA, S., ORTEGA-GUERRERO, B., CABALLERO-MIRANDA, M., & HERREJON-SERRANO, A., (2022). Charcoal morphotypes and potential fuel types from a Mexican lake during MIS 5a and MIS 3. *J. South Am. Earth Sci.* 115. https://doi.org/10.1016/j.jsames.2022.103724

TORRES-RODRÍGUEZ, E., LOZANO-GARCÍA, S., CABALLERO-MIRANDA, M., ORTEGA-GUERRERO, B., SOSA-NÁJERA, S., & DEBAJYOTI-ROY, P. (2018). Pollen and non-pollen palynomorphs of Lake Chalco as indicators of paleolimnological changes in high-elevation tropical central Mexico since MIS 5. *Journal of Quaternary Science*, *33*(8), 945-957.

TORRES-RODRÍGUEZ, E., LOZANO-GARCÍA, S., ROY, P., ORTEGA, B., BERAMENDI-OROSCO, L., CORREA-METRIO, A., & CABALLERO, M., (2015). Last Glacial droughts and fire regimes in the central Mexican highlands. *J. Quat. Sci.* 30, 88–99. https://doi.org/10.1002/jqs.2761

TURNEY, C.S.M., & JONES, R.T. (2010). Does the Agulhas Current amplify global temperatures during super-interglacials? *J. Quat. Sci.* 25, 839–843. https://doi.org/10.1002/jqs.1423

VALADEZ, F., OLIVA, G., VILACLARA, G., CABALLERO, M., & RODRÍGUEZ, D. C. (2005). On the presence of *Stephanodiscus niagarae* Ehrenberg in central Mexico. *Journal of Paleolimnology*, *34*(2), 147.

VALERA-FERNÁNDEZ D., SOLLEIRO-REBOLLEDO E., LÓPEZ-MARTÍNEZ R. A., PI-PUIG T., SALGADO-GARRIDO H. & CABADAS-BÁEZ H. (2020a). Quaternary carbonates on the coast of the Yucatan Peninsula and the island of Cozumel, Mexico: Paleoenvironmental implications. *Journal of South American Earth Sciences* 102:102670.

VALERA-FERNÁNDEZ, D., CABADAS-BÁEZ, H., SOLLEIRO-REBOLLEDO, E., LANDA-ARREGUÍN, F. J., & SEDOV, S. (2020b). Pedogenic carbonate crusts (calcretes) in karstic landscapes as archives for paleoenvironmental reconstructions–A case study from Yucatan Peninsula, Mexico. *Catena*, *194*, 104635.

VÁZQUEZ-SELEM, L. & HEINE, K. (2011). Late Quaternary glaciation in Mexico, En: *Quaternary glaciations-extent and chronology*, Ehlers, J., Ehlers, J., Gibbard, P.L., Hughess, P.D. (eds.), Amsterdam, Elsevier, 849-861.

WALTARI, E., HIJMANS, R. J., PETERSON, A. T., NYÁRI, A. S., PERKINS, S. L., & GURALNICK, R. P. (2007). Locating Pleistocene refugia: comparing phylogeographic and ecological niche model predictions. *PLoS one*, *2*(7), e563.

WARKEN SF. SCHOLZ D., SPÖTL C., JOCHUM K.P., PAJÓN J. M., BAHR A. & MANGINI A. (2019). Caribbean hydroclimate and vegetation history across the last glacial period. *Quaternary Science Reviews*, *218*, 75-90.

WILLIAMS J. W. & JACKSON S. T. (2007). Novel climates, no-analog communities, and ecological surprises. *Frontiers in Ecology and the Environment* 5(9):475-482.

YIM, S. Y., WANG, B., LIU, J., & WU, Z. (2014). A comparison of regional monsoon variability using monsoon indices. *Climate dynamics*, *43*, 1423-1437.

ZIEGLER M., NÜRNBERG D., KARAS C., TIEDEMANN R. & LOURENS L. J. (2008). Persistent summer expansion of the Atlantic Warm Pool during glacial abrupt cold events. *Nature Geoscience* 1: 601–605.